Seismic Analysis of Telecommunication Towers Mounted on Building Rooftops

by

Rola Assi

May 2006

Department of Civil Engineering and Applied Mechanics

McGill University, Montreal, Canada

A thesis submitted to the Faculty of Graduate Studies and Research at McGill University in partial fulfillment of the requirements for the degree of Doctor of Philosophy

Your file Votre référence
ISBN: 978-0-494-25090-7
Our file Notre référence
ISBN: 978-0-494-25090-7

Abstract

This thesis deals with the assessment of seismic accelerations in buildings and the seismic analysis of components installed on building rooftops, with special focus on operational telecommunition towers during and after earthquake shaking.

First, acceleration data recorded during the 1999 Chi Chi earthquake from 11 instrumented buildings located in Taiwan were studied. Fundamental building periods were extracted by system identification and compared to those evaluated according to the equations proposed in the 2005 edition of the National Building Code of Canada (NBCC). Next, rooftop acceleration spectra and time histories were evaluated using 3-D finite element building models; three models of instrumented buildings were calibrated using accelerograms from the Chi Chi earthquake and the fourth model is a building located in downtown Montreal. The building models were subjected to 44 historical strong motion accelerograms and 30 synthetic accelerograms compatible with the target uniform hazard spectra specified in NBCC 2005 for Montreal. Based on both the experimental and numerical results, a maximum rooftop acceleration amplification of 4 is proposed for low/medium rise buildings and 3 for flexible high-rise buildings ($T > 1.7$ s).

In the second stage, a simplified method for the prediction of seismic shear forces and overturning moments at the base of self-supporting steel lattice telecommunication towers mounted on building rooftops is presented. The proposed method involves the estimation of four parameters: the rooftop seismic acceleration, the mass distribution profile of the tower along its height, the maximum acceleration amplification at the tower top, and the fundamental sway mode shape of the tower on a rigid base. The method was validated by means of numerical results of nine generated building-tower combinations

composed of three towers assumed to be mounted on three of the building models studied in the first stage of the research. The building-tower combinations were subjected to the same sets of earthquake records used for the prediction of accelerations. It was found the proposed method yields conservative results in all the cases analyzed.

In addition, the empirical component force amplification factor for telecommunication towers as proposed in the NBCC 2005 was compared to the factors evaluated for the towers of the 16 building-tower combinations. Improved component force amplification factors based on rational analysis are proposed.

Sommaire

La recherche présentée dans cette thèse traite de l'évaluation des accélérations sismiques dans les bâtiments et de l'analyse sismique des composants installés sur les toits de bâtiments, en particulier les pylônes de télécommunication qui doivent demeurer fonctionnels durant et après le séisme.

Dans une première étape, des accélérations enregistrées lors du tremblement de terre de Chi Chi en 1999 dans 11 bâtiments instrumentés et situés à Taiwan ont été étudiées. Les périodes fondamentales de ces bâtiments ont été extraites des enregistrements et comparées à celles évaluées selon les équations de l'édition 2005 du Code national du bâtiment canadien (CNBC). Aussi, les historiques des accélérations et les accélérations spectrales ont été évalués au toit en utilisant des simulations numériques avec des modèles d'éléments finis en 3-D générés et calibrés par les accélérogrammes du Chi Chi pour trois des bâtiments instrumentés à Taiwan et un bâtiment situé à Montréal. Les modèles des bâtiments ont été soumis à 44 accélérogrammes réels et 30 synthétiques compatibles avec les spectres de l'aléa sismique du CNBC 2005 pour Montréal. En se basant sur les résultats expérimentaux et numériques, une valeur de 4 est suggérée pour l'amplification de l'accélération au toit pour les bâtiments rigides à faible ou moyenne hauteur, et 3 pour les bâtiments élevés ($T > 1.7$ s).

En seconde étape, l'auteure présente une méthode simplifiée pour la prédiction des forces de cisaillement et des moments de renversement sismiques à la base des pylônes de télécommunication autoporteurs montés sur des toits de bâtiments. La méthode proposée nécessite l'évaluation de quatre paramètres: l'accélération sismique au toit, le profil de masse du pylône, l'amplification maximale de l'accélération au sommet du pylône, et la

forme du mode de vibration fondamental du pylône sur base rigide. La méthode proposée a été validée à l'aide de modèles numériques de neuf combinaisons bâtiment-pylône soumises aux mêmes accélérogrammes utilisés en première partie. On a trouvé que la méthode proposée est conservatrice pour tous les cas étudiés.

Finalement, le facteur empirique d'amplification de force des composants pour les pylônes de télécommunication, tel que proposé dans le CNBC 2005, a été comparé aux facteurs évalués pour les pylônes de 16 combinaisons bâtiment-pylône. En se basant sur ces analyses rationnelles, l'auteure propose des facteurs améliorés pour l'amplification de force sismique des pylônes de télécommunication installés sur les toits de bâtiments.

Statement of Original Contributions

To the author's best knowledge, the original contributions of this research include:

- The study of seismic floor acceleration demands in buildings based on a combined use of recorded accelerations in instrumented buildings and the results of numerical simulations.
- The use of system identification techniques to study the accelerations in 11 buildings and compute their fundamental periods.
- The generation of detailed three-dimensional linear finite element models of four existing buildings having geometries ranging from simple to quite complex. Three of these modeled buildings are located in Taiwan and their models were calibrated using recorded accelerograms during the 1999 Chi Chi earthquake. These models are deemed reasonably accurate to represent the seismic behavior of existing buildings during earthquake shaking.
- The evaluation of seismic component force amplification factors for rooftop telecommunication towers based on rational analysis.
- The development of a simple method for the prediction of seismic acceleration profiles for telecommunication towers mounted on building rooftops.
- The development of a simplified method for the prediction of seismic shear forces and overturning moments at the base of a telecommunication tower mounted on a building rooftop. It is the first time that such a method has been developed.

Acknowledgments

The author would like to express her deep appreciation and gratitude to many people involved in this research project, particularly to:

Professor Ghyslaine McClure, for her skillful guidance, valuable suggestions, constant support, patience, and continuous encouragement throughout this research. This work would have never been completed without such supervision.

Professor George Yao, for his help in providing the data for the buildings studied and his substantial assistance during my stay in Taiwan. His guidance in data processing is greatly appreciated.

The entire Staff of the Department of Civil Engineering and Applied Mechanics at McGill University, especially Dr William Cook and the secretaries.

The graduate students in the Department of Architecture at National Cheng Kung University in Taiwan, their help in ambient vibration tests and in the collection of buildings' data are greatly appreciated.

The Lebanese National Council for Scientific Research, the Natural Sciences and Engineering Research Council of Canada, and the National Science Council of Taiwan for their financial support.

Most of all, my parents for their continuous support and constant encouragement during my stay in Canada and throughout my studies at McGill.

Table of Contents

Abstract i
Sommaire iii
Statement of Original Contributions v
Acknowledgments vi
Table of Contents vii
List of Figures x
List of Tables xiv
Nomenclature xviii

Chapter 1
Introduction 1
1.1 Background and problem definition 1
1.2 Research objectives 3
1.3 Research approach 3
1.4 Thesis organization 4

Chapter 2
Literature Review 7
2.1 Definition and general review of the seismic performance of operational and functional components in buildings 7
2.2 Types of OFCs 11
2.3 Classification of OFCs 11
2.4 Codes for seismic design of OFCs 13
2.5 Historical review of provisions of the National Building Code of Canada 14
2.6 Correction for forces on tops of buildings 26
2.7 CSA S832-01: Guideline for seismic risk reduction of operational and functional components (OFCs) of buildings 28

2.8 International Building Code (IBC) and NEHRP 2000 recommended provisions for seismic regulations of new buildings 29
2.9 Method proposed in TM 5-809-10-1: Seismic design guideline for essential buildings 33
2.10 Previous research on seismic acceleration amplification in buildings 35
2.11 Seismic provisions in Standards and Codes of practice for telecommunication towers 42
2.12 Previous research to determine seismic forces for towers mounted on tops of buildings 49
2.13 Summary 53

Chapter 3

Data Processing and System Identification 54
3.1 Instrumentation of buildings located in Taiwan 54
3.2 Characteristics of the instrumented buildings used in this study 55
3.3 Data processing 57
3.4 System identification techniques 60
3.5 Analysis of the Chi Chi records 67
3.6 Frequency domain analysis 84
3.7 Comparison of building periods extracted from the Chi Chi records with the values suggested in the NBCC 2005 87
3.8 Conclusions 89

Chapter 4

Finite Element Models of Building/Tower Systems and Rooftop Accelerations 90
4.1 Geometric properties of the buildings and towers 91
4.2 Modeling assumptions 99
4.3 Method of analysis 107
4.4 Earthquake records 110
4.5 Amplification of rooftop accelerations 114
4.6 Conclusions 129

Chapter 5

Proposed Simplified Method of Seismic Analysis of Rooftop Towers 130

5.1 Component force amplification factor A_r for telecommunication towers of the building-tower combinations 130

5.2 Prediction of forces at the building-tower interface 147

5.3 A simplified method for calculating seismic base shear forces and overturning moments at a building-tower interface 167

5.4 Summary 193

Chapter 6

Summary and Conclusions 194

6.1 Seismic floor acceleration demands 194

6.2 Simplified method for seismic analysis of telecommunication towers mounted on building rooftops 195

6.3 Research limitations 196

6.4 Recommendations for future work 197

References 199

Appendix A 211

Appendix B 223

Appendix C 235

Appendix D 252

Appendix E 268

List of Figures

Figure 2-1 Damage to library stacks during the 1999 Chi Chi earthquake (Source G.C. Yao) 10
Figure 2-2 Damage to pipes during the 1999 Chi Chi earthquake (Source G.C. Yao) .. 10
Figure 2-3 Component force amplification factor according to NBCC 2005 25
Figure 2-4 Design Magnification Factor versus the period ratio (After US Army 1986)34
Figure 2-5 Example of approximate floor response spectra 34
Figure 2-6 Amplification of seismic accelerations from the grade level to the rooftop. 35
Figure 3-1 Effect of Hanning window on DFT 59
Figure 3-2 Ideal single input/output linear system 62
Figure 3-3 Random signal 64
Figure 3-4 Input/output relationship with noise at the output 65
Figure 3-5 Amplification of horizontal accelerations in CHYBA9 68
Figure 3-6 Amplification of horizontal accelerations in CHYBA4 69
Figure 3-7 Amplification of horizontal accelerations in CHYBA5 70
Figure 3-8 Amplification of horizontal accelerations in TCUBA0 71
Figure 3-9 Amplification of horizontal accelerations in TCUBAA 72
Figure 3-10 Amplification of horizontal accelerations in CHYBA0 73
Figure 3-11 Amplification of horizontal accelerations in TCUBA6 74
Figure 3-12 Amplification of horizontal accelerations in TCUBA2 75
Figure 3-13 Amplification of horizontal accelerations in TCUBA4 76
Figure 3-14 Amplification of horizontal accelerations in CHYBA7 77
Figure 3-15 Amplification of horizontal accelerations in TAPBA7 78
Figure 3-16 Peak floor acceleration amplification profiles for the 11 buildings studied in principal horizontal directions X and Y 79
Figure 3-17 Number of stories versus the rooftop acceleration amplification ratio (A_{roof}/A_g) 83
Figure 3-18 The rooftop acceleration amplification versus the building periods 86
Figure 4-1 Isometric and facade elevation views of the CHYBA9 building 94
Figure 4-2 Isometric and facade elevation views of the CHYBA4 building 95

Figure 4-3 Free field and ground level accelerograms of CHYBA4 in the directions U1 and U2 95
Figure 4-4 Isometric and facade elevation views of the TCUBAA building 96
Figure 4-5 Free field and ground level accelerograms of TCUBAA in the directions U1 and U2 97
Figure 4-6 Isometric view of the 2020 University building in Montreal 97
Figure 4-7 3-D finite element model of the CHYBA9 building 102
Figure 4-8 3-D finite element model of the CHYBA4 building 103
Figure 4-9 3-D finite element model of the TCUBAA building 103
Figure 4-10 3-D finite element model of the 2020 University building 104
Figure 4-11 Tower base 105
Figure 4-12 Close-up of the tower base 105
Figure 4-13 Finite element meshes of the generated tower models 106
Figure 4-14 Mean 5% damped elastic acceleration response spectra for the sets of High a/v and 2%/50 years normalized to 1g 119
Figure 4-15 Mean 5% damped elastic acceleration response spectra for the sets of Medium a/v and 10%/50 years normalized to 1g 119
Figure 4-16 Mean 5% damped elastic acceleration response spectra for the sets of Low a/v and 50%/50 years normalized to 1g 120
Figure 4-17 UHS proposed in NBCC 2005 and computed 5% damped average absolute acceleration response spectra for 2%/50 years 121
Figure 4-18 UHS proposed in NBCC 2005 and computed 5% damped elastic average acceleration response spectra for 10%/50 years 122
Figure 4-19 UHS proposed in NBCC 2005 and computed 5% damped elastic average acceleration response spectra for 50%/50 years 122
Figure 4-20 Computed 5% damped elastic acceleration response spectra for the set High a/v. (a) Without normalization (b) Normalized to 1g 123
Figure 4-21 Computed 5% damped elastic acceleration response spectra for the set Medium a/v. (a) Without normalization (b) Normalized to 1g 124
Figure 4-22 Computed 5% damped elastic acceleration response spectra for the set Low a/v. (a) Without normalization (b) Normalized to 1g 125

Figure 5-1 A_r for CHYBA9 in the U1 direction 132
Figure 5-2 A_r for CHYBA9 in the U2 direction 132
Figure 5-3 A_r for CHYBA4 in the U1 direction 133
Figure 5-4 A_r for CHYBA4 in the U2 direction 133
Figure 5-5 A_r for TCUBAA in the U1 direction 134
Figure 5-6 A_r for TCUBAA in the U2 direction 134
Figure 5-7 A_r for 2020 University in the U1 direction 135
Figure 5-8 A_r for 2020 University in the U2 direction 135
Figure 5-9 Concept of the proposed simplified method 168
Figure 5-10 Mode shapes of TC2 tower projected on the U1 direction 170
Figure 5-11 Mode shapes of TC2 tower projected on the U2 direction 170
Figure 5-12 Mode shapes of TC3 tower projected on the U1 direction 171
Figure 5-13 Mode shapes of TC3 tower projected on the U2 direction 171
Figure 5-14 Mode shapes of TC4 tower projected on the U1 direction 172
Figure 5-15 Mode shapes of TC4 tower projected on the U2 direction 172
Figure 5-16 Proposed and calculated tower acceleration amplification factors versus T_p/T for stiff buildings 175
Figure 5-17 Acceleration amplification profiles of TC2 mounted on CHYBA9 - U1 direction 176
Figure 5-18 Acceleration amplification profiles of TC2 mounted on CHYBA9 - U2 direction 176
Figure 5-19 Acceleration amplification profiles of TC3 mounted on CHYBA9 - U1 direction 177
Figure 5-20 Acceleration amplification profiles of TC3 mounted on CHYBA9 - U2 direction 177
Figure 5-21 Acceleration amplification profiles of TC4 mounted on CHYBA9 - U1 direction 178
Figure 5-22 Acceleration amplification profiles of TC4 mounted on CHYBA9 - U2 direction 178
Figure 5-23 Acceleration amplification profiles of TC2 mounted on CHYBA4 - U1 direction 179

Figure 5-24 Acceleration amplification profiles of TC2 mounted on CHYBA4 - U2 direction........ 179
Figure 5-25 Acceleration amplification profiles of TC3 mounted on CHYBA4 - U1 direction........ 180
Figure 5-26 Acceleration amplification profiles of TC3 mounted CHYBA4 - U2 direction........ 180
Figure 5-27 Acceleration amplification profiles of TC4 mounted on CHYBA4 - U1 direction........ 181
Figure 5-28 Acceleration amplification profiles of TC4 mounted on CHYBA4 - U2 direction........ 181
Figure 5-29 Acceleration amplification profiles of TC2 mounted on 2020 University - U1 direction........ 182
Figure 5-30 Acceleration amplification profiles of TC2 mounted on 2020 University - U2 direction........ 182
Figure 5-31 Acceleration amplification profiles of TC3 mounted on 2020 University - U1 direction........ 183
Figure 5-32 Acceleration amplification profiles of TC3 mounted on 2020 University - U2 direction........ 183
Figure 5-33 Acceleration amplification profiles of TC4 mounted on 2020 University - U1 direction........ 184
Figure 5-34 Acceleration amplification profiles of TC4 mounted on 2020 University - U2 direction........ 184

List of Tables

Table 2-1 Seismic design check recommendations of CSA S37-01 (CSA 2001 a) 44

Table 3-1 Characteristics of the 11 instrumented buildings 56

Table 3-2 Rooftop acceleration amplification 81

Table 3-3 Comparison of building periods from the Chi Chi earthquake versus previous events 85

Table 3-4 Comparison of building periods extracted from the Chi Chi records and calculated with the NBCC 2005 formulas 88

Table 4-1 Geometric properties of the telecommunication towers 98

Table 4-2 Comparison of existing building and generated model for CHYBA9 100

Table 4-3 Comparison of existing building and generated model for CHYBA4 100

Table 4-4 Comparison of existing building and generated model for TCUBAA 101

Table 4-5 Natural periods of the buildings from FE models 102

Table 4-6 Dynamic properties of the towers 106

Table 4-7 Earthquake records classified according to their a/v ratio 112

Table 4-8 Characteristics of M-R scenarios considered for Montreal 113

Table 4-9 Rooftop acceleration amplification for CHYBA9 115

Table 4-10 Rooftop acceleration amplification for CHYBA4 115

Table 4-11 Rooftop acceleration amplification for TCUBAA 116

Table 4-12 Rooftop acceleration amplification for 2020 University 116

Table 4-13 Comparison of rooftop peak and spectral accelerations for the CHYBA9 building 126

Table 4-14 Comparison of rooftop peak and spectral accelerations for the CHYBA4 building 126

Table 4-15 Comparison of rooftop peak and spectral accelerations for the TCUBAA building 127

Table 4-16 Comparison of rooftop peak and spectral accelerations for the 2020 University building 127

Table 5-1 A_r factors for the TC1, TC2, TC3, and TC4 towers mounted on the CHYBA9 building calculated according to NBCC 2005 136

Table 5-2 A_r factors for CHYBA9-TC1 ... 136
Table 5-3 A_r factors for CHYBA9-TC2 ... 137
Table 5-4 A_r factors for CHYBA9-TC3 ... 137
Table 5-5 A_r factors for CHYBA9-TC4 ... 138
Table 5-6 A_r factors for the TC1, TC2, TC3, and TC4 towers mounted on the CHYBA4 building calculated according to NBCC 2005 ... 138
Table 5-7 A_r factors for CHYBA4-TC1 ... 139
Table 5-8 A_r factors for CHYBA4-TC2 ... 139
Table 5-9 A_r factors for CHYBA4-TC3 ... 140
Table 5-10 A_r factors for CHYBA4-TC4 ... 140
Table 5-11 A_r factors for the TC1, TC2, TC3, and TC4 towers mounted on the TCUBAA building calculated according to NBCC 2005 ... 141
Table 5-12 A_r factors for TCUBAA-TC1 ... 141
Table 5-13 A_r factors for TCUBAA-TC2 ... 142
Table 5-14 A_r factors for TCUBAA-TC3 ... 142
Table 5-15 A_r factors for TCUBAA-TC4 ... 143
Table 5-16 A_r factors for the TC1, TC2, TC3, and TC4 towers mounted on the 2020 University building calculated according to NBCC 2005 ... 143
Table 5-17 A_r factors for 2020 University-TC1 ... 144
Table 5-18 A_r factors for 2020 University-TC2 ... 144
Table 5-19 A_r factors for 2020 University-TC3 ... 145
Table 5-20 A_r factors for 2020 University-TC4 ... 145
Table 5-21 Shear forces for the combination CHYBA9-TC1 ... 150
Table 5-22 Shear forces for the combination CHYBA9-TC2 ... 150
Table 5-23 Shear forces for the combination CHYBA9-TC3 ... 151
Table 5-24 Shear forces for the combination CHYBA9-TC4 ... 151
Table 5-25 Shear forces for the combination CHYBA4-TC1 ... 153
Table 5-26 Shear forces for the combination CHYBA4-TC2 ... 153
Table 5-27 Shear forces for the combination CHYBA4-TC3 ... 154
Table 5-28 Shear forces for the combination CHYBA4-TC4 ... 154
Table 5-29 Shear forces for the combination 2020 University-TC1 ... 155

Table 5-30 Shear forces for the combination 2020 University-TC2 156
Table 5-31 Shear forces for the combination 2020 University-TC3 156
Table 5-32 Shear forces for the combination 2020 University-TC4 157
Table 5-33 Ratio M/V for CHYBA9-TC1 160
Table 5-34 Ratio M/V for CHYBA9-TC2 160
Table 5-35 Ratio M/V for CHYBA9-TC3 161
Table 5-36 Ratio M/V for CHYBA9-TC4 161
Table 5-37 Ratio M/V for CHYBA4-TC1 162
Table 5-38 Ratio M/V for CHYBA4-TC2 162
Table 5-39 Ratio M/V for CHYBA4-TC3 163
Table 5-40 Ratio M/V for CHYBA4-TC4 163
Table 5-41 Ratio M/V for 2020 University-TC1 164
Table 5-42 Ratio M/V for 2020 University-TC2 164
Table 5-43 Ratio M/V for 2020 University-TC3 165
Table 5-44 Ratio M/V for 2020 University-TC4 165
Table 5-45 Summary of results for M/V ratio for all building-tower combinations 166
Table 5-46 Calculated tower acceleration amplification factors for TC2 on 3 buildings 174
Table 5-47 Calculated tower acceleration amplification factors for TC3 on 3 buildings 174
Table 5-48 Calculated tower acceleration amplification factors for TC4 on 3 buildings 174
Table 5-49 Proposed tower acceleration amplification factors for stiff buildings......... 175
Table 5-50 Validation of the simplified method for CHYBA9-TC2............................ 188
Table 5-51 Validation of the simplified method for CHYBA9-TC3............................ 188
Table 5-52 Validation of the simplified method for CHYBA9-TC4............................ 189
Table 5-53 Validation of the simplified method for CHYBA4-TC2............................ 189
Table 5-54 Validation of the simplified method for CHYBA4-TC3............................ 190
Table 5-55 Validation of the simplified method for CHYBA4-TC4............................ 190
Table 5-56 Validation of the simplified method for 2020 University-TC2.................. 191
Table 5-57 Validation of the simplified method for 2020 University-TC3.................. 191

Table 5-58 Validation of the simplified method for 2020 University-TC4 192

Nomenclature

A	=	acceleration ratio
A_0	=	shear area of the cantilever section at the base (fixed end)
A_g	=	peak ground acceleration
A_r	=	component force amplification factor
A_{roof}	=	peak acceleration at the rooftop level
A_x	=	height factor
C	=	constant appropriate for the part or portion of the building being considered (Equation 2.1)
C	=	constant function of the type of construction (Equation 2.3)
C	=	OFC consequence rating score (Equation 2-18)
$[C]$	=	viscous damping matrix (Equation 4-1)
C_a	=	constant equivalent to the design spectral acceleration at short period
C_d	=	deflection amplification factor to apply to the calculated elastic deflection
C_{nr}	=	coefficients of the viscous damping matrix C
C_p	=	seismic coefficient for mechanical/electrical equipment
C_{pi}	=	basic horizontal seismic coefficient for a part at level i in NZS 4203:1992 (Equation 2-30)
D_p	=	design relative seismic displacement for a component
D_s	=	dimension of the lateral-force resisting system in the direction parallel to the applied forces, in ft
EI_0	=	flexural rigidity at the base of the structure
F	=	foundation factor
F_a	=	acceleration-based site coefficient
F_p	=	seismic design force centered at the component's center of gravity

F_{sz} = lateral seismic force induced at level z of the tower

F_t = portion of the building base shear to be concentrated at the top of the structure

F_v = velocity-based site coefficient

GA_0 = shear rigidity at the base of the structure

H = total height of the structure, in m

H (Ω) = transfer function

I, I_E = importance factor for the building

I_p = component importance factor (Equation 2-21)

I_p = importance factor for the structure (Equation 2-30)

[K] = diagonal stiffness matrix

[M] = diagonal mass matrix

M_{demand} = overturtning moment calculated in the numerical simulations in SAP 2000

$M_{calculated}$ = overturtning moment calculated according to the proposed simplified method

M_{JMA} = Japan meteorological agency scale for the earthquake magnitude

M_L = local magnitude of the earthquake

M_S = surface wave magnitude of the earthquake

N = number of stories above ground of a building

R = measure of the estimated intensity of earthquake forces that may occur in the area considered in NBCC 1953-1965 (Equation 2-4)

R = seismic regionalization factor in NBCC 1970 (Equation 2-5)

R = seismic risk rating score in CSA S832-01 (Equation 2-18)

R_d = energy dissipation capacity of the structure

R_o = force overstrength factor

R_p = component response factor

R_p = risk factor for the part in NZS 4203:1992 (Equation 2-30)

R_q = reduction factor to account for the effect of ductility on the primary lateral force resisting system, associated with mode q

$R_{xx}(t)$ = autocorrelation function of the input record

$R_{yy}(t)$ = autocorrelation function of the output record

$R_{xy}(t)$ = cross-correlation function of the input and output records

RB = factor depending on the type of structural system in CSA S832-01 (Equation 2-19)

RG = factor depending on the characteristics of ground motion and soil conditions in CSA S832-01 (Equation 2-19)

RS = seismic rating score factor in CSA S832-01 (Equation 2-19)

S = factor related to the total number of stories N of the building (Equation 2-4)

S_a = spectral acceleration

$S_a(0.2)$ = spectral response acceleration value at a period of 0.2 s

S_1 = maximum spectral response acceleration at a period of 1.0 s

S_{D1} = design spectral response acceleration at a period of 1.0 s

S_{DS} = design spectral response acceleration at short period

S_p = horizontal force factor for part or portion of a structure (Equation 2-11)

S_p = structural performance factor in NZS 4203:1992 (Equation 2-30)

S_s = maximum spectral response acceleration at short period

$S_a(T)$ = spectral acceleration at the period T

$S_{xx}(\Omega)$ = power spectral density function of $R_{xx}(t)$

$S_{yy}(\Omega)$ = power spectral density function of $R_{yy}(t)$

$S_{xy}(\Omega)$ = cross-spectral density function of $R_{xy}(t)$

T, T_a = fundamental period of the building in seconds

$T_{1,2,3}$	=	first, second, and third periods of vibration of the structure in seconds
$T_{building}$	=	natural period of vibration of the building
T_p	=	fundamental period of the component in seconds
T_q	=	natural period of vibration associated with mode q
T_{tower}	=	natural period of vibration of the telecommunication tower
U1	=	longitudinal direction of the building model
U2	=	transverse direction of the building model
V	=	OFC seismic vulnerability related to its probability of failure in CSA S832-01 (Equation 2-18)
V, V_s	=	lateral seismic action or force on a part or portion of the structure, known as base shear
$V_{calculated}$	=	base shear force calculated according to the proposed simplified method
V_{demand}	=	base shear force calculated in the numerical simulations in SAP 2000
V_x	=	shear force distribution along x
W	=	total reactive weight of the structure including machinery and other fixed concentrated loads
W_p	=	weight of the component
WF	=	weight factor in CSA S832-01 (Equation 2-19)
X	=	height of upper support attachment at level x as measured from the base (Equation 2-25)
X	=	longitudinal direction of the existing building
$X(\Omega)$	=	Fourier Transform of the input motion x(t)
Y	=	height of lower support attachment at level y as measured from the base (Equation 2-25)
Y	=	transverse direction of the existing building
$Y(\Omega)$	=	Fourier Transform of the response y(t)

Z	=	seismic zone factor in NZS 4203:1992 (Equation 2-30)
a	=	peak horizontal ground acceleration
$a(x)$	=	unknown acceleration profile along the tower height
a_p	=	component amplification factor
$a_{rooftop}$	=	rooftop seismic acceleration
f_1	=	fundamental frequency of the structure
h, h_n	=	average roof height of the structure above the base
h_i, h_x, h_{sx}, h_z	=	height from the base of structure to level i, x, or z
i	=	number designating the level under consideration
k_e	=	seismic force distribution exponent (Equation 2-38)
l	=	tower's height
$m(x)$	=	mass of the tower at position x measured from the tower base
n	=	number designating the uppermost level of the structure
$n(t)$	=	extraneous noise
$q_n(t)$	=	modal coordinate associated with mode n
$\{u(t)\}$	=	vector containing the relative displacements with respect to the moving base
$\{u_n(t)\}$	=	modal displacement response associated with mode n
u	=	vector containing the relative displacements with respect to the moving base, and is function of time t
$\dot{u}$	=	vector containing the relative velocities with respect to the moving base, and is function of time t
$\ddot{u}$	=	vector containing the relative accelerations with respect to the moving base, and is function of time t
$\ddot{u}_g$	=	base acceleration (uniform at all support points)
v	=	peak horizontal ground velocity
w_i, w_z	=	portion of total gravity load (w) assigned to level i or z

ω_n	=	circular frequency associated with mode n
x(t)	=	input signal
y(t)	=	ouput signal
z	=	height in the structure of the point of attachment of the component
δ_{xA}	=	deflection at building level x of structure A, determined by an elastic analysis
δ_{yA}	=	deflection at building level y of structure A, determined by an elastic analysis
δ_{yB}	=	deflection at building level y of structure B, determined by an elastic analysis
Δ_{aA}	=	allowable story drift for structure A
Δ_{aB}	=	allowable story drift for structure B
Γ_q	=	participation factor for mode q
ϕ_n	=	n^{th} mode shape of the structure
Φ_q^n	=	amplitude of mode q at level n
$\xi_{n,q}$	=	critical damping ratio associated with mode n or q
ι	=	influence vector
μ	=	average value
σ	=	standard deviation
ν	=	zonal velocity ratio, dimensionless
BSSC	=	Building Seismic Safety Council
CSA	=	Canadian Standards Association
DFT	=	Discrete Fourier Transform
Famos	=	Fast analysis and monitoring of signals
FEMA	=	Federal Emergency Management Agency
FFT	=	Fast Fourier Transform
IBC	=	International Building Code

IMC	=	Integrated Measurement and Control
MDOF	=	Multi-Degree-of-Freedom
NBCC	=	National Building Code of Canada
NEHRP	=	National Earthquake Hazards Reduction Program
NTT	=	Nippon Telegraph and Telephone Corporation
NZS	=	New Zealand Standard
PGA	=	Peak Ground Acceleration
PGV	=	Peak Ground Velocity
PRA	=	Peak Roof Acceleration
SDOF	=	Single-Degree-of-Freedom
SRSS	=	Square Root of the Sum of the Squares
TF	=	Transfer Function
TSMIP	=	Taiwan Strong Motion Instrument Program
UBC	=	Uniform Building Code
UHS	=	Uniform Hazard Spectra

Chapter 1
Introduction

1.1 Background and problem definition

A review of the current state of knowledge in seismic design of operational and functional components of buildings (OFCs) as reflected in codes, standards, and guidelines currently in use in Canada and the United States can be found in Assi (2003). These design provisions achieve a good balance between simplicity and rationality. Further research, however, has identified some deficiencies of these provisions. During an earthquake, the OFCs are subjected to seismic motion that is filtered through the supporting structure, while the acceleration at the building's base is amplified along the building's height. The increase of acceleration along the building's height is accounted for in code provisions through the height amplification factor. One of the major deficiencies of code provisions is that the height factor used in the design methods for OFCs neglects the influence of the structural behavior of their supporting building. The 2005 edition of the National Building Code of Canada (NRC/IRC 2005) assumes that seismic accelerations increase linearly along a building's height and reach a maximum amplification of 3 at rooftop level.

On the other hand, current seismic provisions in codes and standards for self-supporting steel lattice telecommunication towers relate to structures on the ground and are not specific for towers on building rooftops. The design of telecommunication towers on the ground is typically controlled by extreme wind, ice and wind combinations, and restrictive serviceability limits (CSA 2001 a; TIA/EIA 222-G 2005); therefore, in cold regions, most codes and standards are concerned with exteme wind and ice loads. However, when the tower supports heavy attachments at the upper level, or in the case of uneven distribution of rigidity and/or mass, or when the tower is erected on top of a building, it becomes necessary to check its seismic response in areas prone to earthquakes. At present, designers are left without much guidance on how to evaluate earthquake effects on telecommunication towers erected on building rooftops. Moreover, the 2005 edition of the NBCC treats telecommunication towers mounted on building rooftops as acceleration-sensitive OFCs and proposes an empirical component force amplification factor of 2.5 when the properties of the tower and building are not known. This factor and the base shear formula presented in Chapter 2 need revision based on rational analysis. No provisions are presently available for the estimation of overturning moments at the base of these towers.

The shortcomings in the code provisions for the estimation of accelerations in buildings and the lack of adequate simplified provisions for seismic analysis of telecommunication towers on rooftops have motivated this research. The main objectives of the research and an overview of its approach are summarized in the following sections.

1.2 Research objectives

The objectives of this research are:

- To gain insight into in-structure peak floor acceleration demands during earthquakes for common buildings, especially at rooftop level.
- To verify the Canadian code recommendations for estimating floor acceleration demands and seismic base shear forces for OFCs that are acceleration-sensitive.
- To propose a simplified method for seismic analysis of self-supporting steel lattice telecommunication towers mounted on building rooftops, in addition to improving the NBCC recommendations regarding the component force amplification factor for these towers.

1.3 Research approach

The first and second aforementioned research objectives are achieved by combining the experimental results for accelerations measured in existing instrumented buildings and the numerical results for accelerations obtained from finite element models of the same buildings. Through research collaboration with Professor George C. Yao from the Department of Architecture of National Cheng Kung University in Tainan City, Taiwan, the author of the present study was given access to and analyzed 11 existing instrumented buildings having records from the 1999 Chi Chi earthquake in Taiwan. Each of these buildings was instrumented with 20 to 28 sensors. The detailed description of the buildings, processing of the measured records, and a discussion of the results are given in Chapter 3. In addition, 3-D numerical models of four existing buildings, three in Taiwan and one in Montreal, were generated using the software SAP 2000 (Wilson and

Habibullah 2003). Seismic numerical simulations were carried out on these models, using several historical earthquake records and artificial earthquakes compatible with the target Unifrom Hazard Spectra of the 2005 edition of the NBCC (NRC/IRC 2005) for the city of Montreal. Detailed description of the numerical models, earthquake records, and a discussion of the results are presented in Chapter 4. In the light of the results presented in Chapters 3 and 4, trends relating the ground and rooftop accelerations are identified, and suggestions for improvement of current building code recommendations are proposed.

The third research objective is achieved through numerical simulations performed on generated finite element models of building-tower combinations. The detailed methodology used for the development of the simplified method for seismic analysis of self-supporting steel lattice telecommunication towers mounted on building rooftops is presented in Chapter 5. The component force amplification factor of the towers was determined for each building-tower combination, which allowed a better understanding of the dynamic behavior of rooftop towers, thus resulting in proposed simplified seismic design recommendations.

1.4 Thesis organization

Chapter two: A literature review is presented. Code provisions and recent research conducted to predict seismic accelerations along a building's height are presented, followed by a review of current codes, standards, and research conducted for seismic analysis of telecommunication towers. The historical development of the Canadian code provisions for the computation of seismic base shear forces and displacement demands for OFCs is also outlined.

Chapter three: Strong motion analysis techniques that can be applied to recorded accelerations from past earthquakes are presented. The non-parametric system identification technique is summarized. Recorded accelerations during the Chi Chi earthquake that occurred in Taiwan at 17:47 GMT on September 20, 1999 (01:47 AM on September 21 Taiwan time) are studied. Results of seismic acceleration amplification of 11 instrumented buildings located in different parts of Taiwan are presented and discussed.

Chapter four: The finite element models of the buildings and towers used in this research and generated in the commercial software SAP 2000 v.8.2.3 (Wilson and Habibullah 2003) are described. The buildings were subjected to two sets of earthquakes: one set is composed of 30 artificial records compatible with the target Uniform Hazard Spectra (UHS) of the 2005 edition of the NBCC for the city of Montreal, and the second set is composed of 44 historical records from different events classified according to the ratio of peak ground acceleration to peak ground velocity (a/v). The results of horizontal acceleration amplification at the building rooftops are discussed.

Chapter five: The results of numerical simulations for the finite element models of the building-tower combinations subjected to the same earthquake sets used in Chapter 4 are presented. The acceleration profiles along the towers mounted on the building rooftops are discussed. In addition, the base shear forces and overturning moments at the building-tower interface resulting from the different numerical simulations are presented. These results are compared to values computed from a proposed simplified method based on the prediction of the seismic horizontal acceleration at the tower base, the prediction of the horizontal acceleration amplification at the tower top, the evaluation of the fundamental sway mode of the tower on rigid base, and the mass distribution of the tower along its height.

Chapter six: In this chapter, the salient findings, main assumptions, limitations, and conclusions of the research are highlighted. In addition, suggestions for relevant future work are summarized.

For completeness, five appendices are also included. The first appendix includes the architectural plans and instrumentation schemes of the 11 Taiwanese buildings. The second appendix includes the transfer functions of these buildings as calculated with the software Famos (IMC 2000). The third appendix includes the 20 lowest natural frequencies of the generated buildings and towers, and the corresponding first three mode shapes for each building and tower. The fourth appendix includes the detailed calculation of seismic base shear forces and overturning moments at the base of the TC2, TC3, and TC4 towers assumed to be mounted on the CHYBA9 building, resulting from the generated models and the proposed simplified method, and corresponding to the records of UHS at 2% exceedance in 50 years. The fifth appendix includes the acceleration amplification profiles along the TC2, TC3, and TC4 towers assumed to be mounted on the CHYBA9 building, corresponding to each individual record applied separately to both main orthogonal horizontal directions of the building.

Chapter 2
Literature Review

This research is motivated by a desire to improve current code recommendations pertaining to acceleration-sensitive operational and functional components (OFCs) encountered in common and essential buildings and, particularly, the design provisions for self-supporting steel lattice telecommunication towers mounted on building rooftops. The development of the seismic provisions for OFCs in the National Building Code of Canada is reviewed first, followed by a review of the provisions provided in other North American codes and guidelines. Relevant research concerning the prediction of seismic floor accelerations in buildings is discussed next, followed by a review of the current seismic provisions for telecommunication towers. Finally, literature documenting the seismic analysis of telecommunication towers mounted on building rooftops is summarized.

2.1 Definition and general review of the seismic performance of operational and functional components in buildings

A building is made up of various components that can be divided into two groups: structural components and operational and functional components. According to CSA S832-01 (CSA 2001 b), OFCs are systems and elements housed in or attached to the floors, roofs, and walls of a building or an industrial facility, but they are not part of the main or intended load-bearing structural system. However, these components may contribute to the structural integrity of the building, depending on their location, type of construction, and method of fastening. Like structural components, OFCs may be subjected to large seismic forces and must be designed to safely resist these forces.

Some of the alternative names for OFCs are: non-structural components or elements, secondary systems, building attachments, and nonbuilding components. According to Chen and Soong (1988), secondary systems can be classified into non-structural secondary systems and structural secondary systems. For the latter type, there is concern not only about the seismic behavior of the component, but also about its interaction with the primary structural system.

OFCs represent a high percentage of the total capital economic investment for buildings and their failure during an earthquake can disrupt the function of the building and pose a significant safety risk to building occupants as well; therefore, these components are far from being secondary in importance.

In fact, the development of seismic design provisions for OFCs has lagged behind that for primary structures. It is recognized that considerable progress has been made over the last two decades in the seismic analysis of structural systems, resulting in substantial improvement in seismic analysis, design, and construction of buildings, bridges, and other industrial facilities (Filiatrault et al. 2001 a). Structural earthquake engineering having reached a fair level of maturity, the research focus now includes also the seismic performance of secondary systems attached to primary structures. A review of typical damages sustained in recent earthquakes (Soong 1990; McKevitt et al. 1995; Phipps 1997; McGavin and Gates 1998; Kao et al. 1999; Naeim 1999, 2000; Filiatrault et al. 2001 a, b) highlights the fact that the poor performance of non-structural components, equipment, and functional systems is the greatest contributor to damage, losses, and business interruption in many essential and critical facilities. The vulnerabilities of non-structural components in modern buildings were not explicitely exposed until the 1964 Alaska and 1971 San Fernando earthquakes (Reitherman 1997). It then became clear that damage to non-structural elements not only can result in major economic losses, but also can pose a threat to life safety, even when structural damage is not significant. It should be stressed that, in moderate earthquakes, damage to critical equipment and contents may be far more important than damage to the structural framework, and earthquakes of moderate intensity are more frequent than earthquakes of high intensity. Therefore, a need was identified to design and construct buildings with better OFC performance during earthquakes.

Figures 2-1 and 2-2 show examples of the non-structural damage that occurred during the 1999 Chi Chi earthquake in two of the buildings studied in this research.

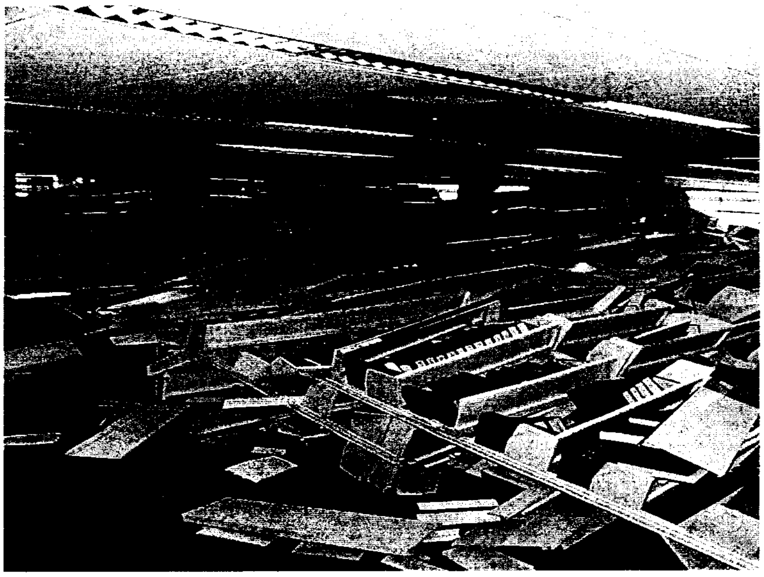

Figure 2-1 Damage to library stacks during the 1999 Chi Chi earthquake (Source G.C. Yao)

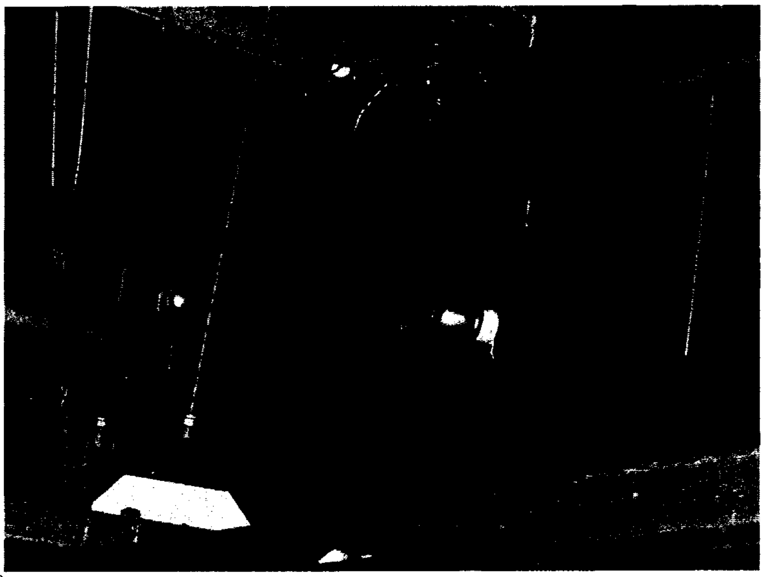

Figure 2-2 Damage to pipes during the 1999 Chi Chi earthquake (Source G.C. Yao)

2.2 Types of OFCs

Operational and functional components of buildings can generally be divided into three sub-categories according to Villaverde (1997) and CSA S832-01 (CSA 2001 b):

- Architectural components, internal and external, such as cladding, interior partition walls, ceilings, light fixtures, and others.
- Building services, including mechanical and electrical systems, such as electrical power distribution systems, heating, ventilation, cooling systems, fire protection systems, telecommunications, and others.
- Building contents, such as furniture, supplies, computer systems, record storage, racks, shelving, and others.

2.3 Classification of OFCs

From a structural perspective, OFCs can be classified into either acceleration-sensitive, when their design is controlled by the prediction of the seismic input force, or deformation-sensitive, when their design is controlled by the supporting structure's displacement, typically the measured interstory drift. In fact, many components are classified as both deformation and acceleration-sensitive (BSSC 2001; Naeim 2001). In this study, we are mainly interested in acceleration-sensitive components; however, the NBCC seismic provisions for both acceleration and deformation-sensitive components are presented for completeness.

2.3.1 Acceleration-sensitive OFCs

Acceleration-sensitive OFCs include most of the electrical and mechanical equipment. These components are vulnerable to excessive shaking, shifting, and overturning if anchorage or bracing is inadequate. Any interaction with stiff elements such as walls and the structural system has to be taken into account so that the capacity of the structural system is not impaired by the behavior or failure of these elements. This requirement is reflected in the provisions of all past editions of the NBCC.

2.3.2 Deformation-sensitive components

The failure of deformation-sensitive components, which include most of the architectural components and building services, such as ducts, trays, and various line services, is caused either by excessive interstory displacement or drift, or incompatible stiffness between the building structure and the component, or interaction between adjacent structural systems and OFCs. A good seismic performance of deformation-sensitive components can be obtained by implementing two general design strategies (Naeim 1989):

- An isolation approach, in which elements are provided with sufficient separation from the structure so that the deformation of the structure will not produce stress on the element.
- A deformation approach, in which the elements are designed to be able to undergo the required deformation of the supporting structure. This can be achieved either by controlling the interstory drift of the supporting structure, or by designing the component to accommodate the expected displacements without damage.

2.4 Codes for seismic design of OFCs

The review of codes and recommended provisions, in terms of lateral force and displacement, is intended to illustrate the variation in seismic design requirements for OFCs among different codes of practice.

Architectural, mechanical, and electrical systems, building contents, and components permanently attached to structures, including attachments and nonbuilding components that are supported by other structures, must meet the requirements presented in the following sections.

In general, the lateral seismic force, V, to which an OFC is subjected is higher than a comparative force used for the design of the structural system for many reasons (SEAOC 1999; Tauby et al. 1999), among them the following:

- The accelerations acting on elements or their supports higher up within a building are greater than at ground level because of the dynamic response of the structure to earthquake ground motion.
- If an element is flexible or flexibly supported, its dynamic response may be amplified.
- Some elements and supports lack the energy-absorbing properties of ductile structures and may hence fail in a brittle manner.
- Poor design or lack of design of anchorage and restraint can lead to connection failure; therefore, attachment failure should be minimized.

2.5 Historical review of provisions of the National Building Code of Canada

Seismic design practices in Canada and in other countries have evolved significantly over the past fifty years. The first edition of the NBCC was developed in 1941 (NRC/IRC 1941) and contained seismic provisions only in an appendix, based on concepts presented in the 1937 United States Uniform Building Code (UBC) (Heidebrecht 2003). Specific provisions for seismic design of structural and non-structural components in buildings and essential facilities were first introduced in the 1953 edition. In all editions of the NBCC, the provisions concerning the OFCs are given in Part 4 of the Code for design, with Commentary J as a specialized supplement.

In the following sections, the evolution of the provisions and recommendations of the NBCC concerning seismic hazard, force, and displacement are presented, starting from the 1953 edition until the 2005 edition.

2.5.1 NBCC provisions for the editions from 1953 to 1965

Within the 1953, 1960, and 1965 editions of the NBCC (NRC/IRC 1953, 1960, 1965), the seismic zoning maps divided the country into four seismic zones (labeled 0, 1, 2, 3) based on qualitative assessment of historical earthquake activity.

2.5.1.1 Seismic force requirements

In these editions, portions of a building or structure should be designed to resist a minimum horizontal force, V, given in Equations 2-1 to 2-4:

$$V_{1953,1960} = CW \qquad 2\text{-}1$$

$$V_{1965} = kW \quad (2\text{-}2)$$

$$k = RCIFS \quad (2\text{-}3)$$

$$S = \frac{0.25}{9+N} \quad (2\text{-}4)$$

Where:

V : lateral seismic force in pounds.

C : numerical constant given in Table 4.1.2 of Part 4 of the NBCC, appropriate for the part or portion of the building being considered (Equation 2.1).

W: total dead load, including machinery and other fixed concentrated loads.

R : measure of the estimated intensity of earthquake forces that may occur in the area considered.

C : numerical constant function of the type of construction (Equation 2.3).

I : importance factor of the building, equal to 1.3 or 1.0, depending on the building's use and occupancy.

F : foundation factor, equal to 1.5 for buildings on highly compressible soil and 1.0 for all other soil types.

S : factor related to the total number of stories, N, of the building (Equation 2-4).

It should be noted that the parameters C and k in Equations 2-1 and 2-2 cover only the architectural components, towers, and tanks. It is also worth mentioning that starting from the 1965 edition, rational dynamic analysis was mentioned as an alternative to equivalent simple static analysis for earthquake-resistant design.

2.5.1.2 Seismic displacement requirements

In the early editions of the NBCC, there were no provisions related to displacements.

2.5.2 Provisions of the 1970 edition of the NBCC

The 1970 edition of the NBCC (NRC/IRC 1970 a, b) introduced more refined seismic maps dividing the country into four zones (labeled 0, 1, 2, 3), based on expected ground accelerations having a return period of 100 years. The new maps were based on the analysis of past earthquakes known or recorded throughout the country between 1899 and 1963.

2.5.2.1 Seismic force requirements

In this edition, building parts and their anchorage should be designed for a minimum lateral force, V, given in Equation 2-5:

$$V_{1970} = \frac{1}{4} R C_p W_p \tag{2-5}$$

Where:

R : seismic regionalization factor that is a measure of the seismic activity and risk in the area considered.

C_p : horizontal force factor for part or portion of a structure, varying between 0.2 and 2.0.

W_p : weight of a part or portion of a structure, such as cladding partitions and appendages.

In the 1970 edition, the commentary states that machinery and electrical/mechanical equipment mounted within buildings should be designed to withstand the forces that arise from the seismic response of the structure, but no more specific provisions are given.

2.5.2.2 Seismic displacement requirements

In the 1970 edition of the NBCC, it was recommended in the commentary to limit the interstory drift of the building to $0.005h_s$, where h_s is the story height. It was further suggested to multiply the deflections obtained from an elastic analysis using lateral forces by a factor of 3, to account for inelastic deformations at very high load levels.

2.5.3 Provisions of the 1975 and 1980 editions of the NBCC

The seismic zoning maps of the 1975 and 1980 editions of the NBCC (NRC/IRC 1975 a, b; 1980 a, b) are the same as those used in the 1970 edition.

2.5.3.1 Seismic force requirements

In these editions, building parts and their anchorage are required to be designed for a minimum lateral force, V, given in Equation 2-6:

$$V_{1975,1980} = AS_pW_p \qquad \text{2-6}$$

Where:

A : acceleration ratio, also called assigned horizontal design acceleration, is assumed constant over each seismic zone, and is equal to the ratio of the specified maximum horizontal ground acceleration to the acceleration due to gravity.

S_p : horizontal force factor for part or portion of a structure as given in Table 4.1.9.C, varying between 2.0 and 25.

W_p : weight of the component.

It is in the 1975 edition that specific S_p factors for machinery and electrical/mechanical equipment mounted within buildings were first introduced.

2.5.3.2 Seismic displacement requirements

The same recommendations as those of the 1970 edition applied.

2.5.4 Provisions of the 1985 edition of the NBCC

In the 1985 edition of the NBCC (NRC/IRC 1985 a, b), new seismic zoning maps were introduced, dividing the country into seven acceleration and velocity related zones (zones 0 to 6). The contour maps of maximum horizontal acceleration and maximum horizontal velocity on rock or firm ground were based on a probability of exceedance of 10% in 50 years, i.e. a probability of 0.0021 per annum, corresponding to a return period of 475 years, instead of a return period of 100 years as in the previous editions. This was a very important increase in design earthquake hazard level.

2.5.4.1 Seismic force requirements

In this edition, building parts and their anchorage should be designed for a minimum lateral force, V, given in Equation 2-7:

$$V_{1985} = vS_pW_p \qquad 2\text{-}7$$

Where:

v : zonal velocity ratio. It is the specified maximum zonal horizontal ground velocity expressed as a ratio to 1m/s.

S_p : horizontal force factor for part or portion of a structure as given in Table 4.1.9.D, varying between 0.9 and 11.

W_p : weight of the component.

2.5.4.2 Seismic displacement requirements

The same recommendations as those of the 1970 edition applied.

2.5.5 Provisions of the 1990 edition of the NBCC

The ground acceleration and velocity zoning maps of the 1990 edition of the NBCC (NRC/IRC 1990 a, b) are the same as those used in the 1985 edition.

2.5.5.1 Seismic force requirements

According to this edition, buildings parts and their anchorage should be designed for a minimum lateral force, V, given in Equation 2-8:

$$V_{1990} = vS_pW_p \qquad 2\text{-}8$$

Where:

v : zonal velocity ratio as defined in the 1985 edition.

S_p : horizontal force factor for part or portion. For architectural components, values of S_p should conform to Table 4.1.9.D, varying between 0.7 and 6.5, while for mechanical/electrical equipment, S_p is equal to $C_pA_rA_x$, where:

C_p : seismic coefficient for mechanical/electrical equipment, as given in Table 4.1.9.E. It varies from 0.7 to 1.5.

A_r : response force amplification factor to account for the type of attachment of mechanical/electrical components.

= 1.0 for rigid components that are rigidly connected to the supporting structure.

= 2.0 for flexible components or flexibly mounted components located on ground level.

= 4.5 for all other cases.

A_x : amplification factor at level x to account for the variation of the response of mechanical/electrical equipment according to their elevation in the building; A_x is equal to $(1+ h_x/h_n)$.

h_x : elevation at level x of the building.

h_n : elevation of the highest level in the building.

W_p : weight of the component.

In the 1990 edition of the NBCC, a distinction was made between the seismic force demand of architectural and mechanical/electrical components. Also, the height factor, A_x, was introduced for the mechanical/electrical components only.

2.5.5.2 Seismic displacement requirements

In this edition of the NBCC, it was recommended to limit the largest interstory drift at any level based on the lateral deflections obtained from linear elastic analysis, to $0.01h_s$ for post-disaster buildings, and $0.02\ h_s$ for all other buildings. It should be noted that this requirement was far less restrictive than the limit of $0.005\ h_s$ introduced in 1970. The lateral deflections obtained from an elastic analysis should be multiplied by R to give realistic values of anticipated deflections. R is a ductility factor that reflects the capacity of the structure to dissipate energy through inelastic behavior. Values of R vary between 1.0 and 4.0.

2.5.6 Provisions of the 1995 edition of the NBCC

The 1995 edition of the NBCC (NRC/IRC 1995 a, b) is still currently in use as several municipalities have not yet approved the recent 2005 edition of the NBCC. The seismic provisions for parts and portions are given in Section 4.1.9.1.15. This edition specifies the same design earthquake hazard level and zoning maps as in the 1985 edition.

2.5.6.1 Seismic force requirements

The provisions of the 1995 edition of the NBCC provide distinct force requirements for architectural components (Equation 2-9), and for mechanical and electrical equipment (Equation 2-10).

According to this edition, parts of buildings and their anchorage should be designed for a lateral force, V, given in Equations 2-9 and 2-10:

$$V_{1995,architectural} = vIS_pW_p \tag{2-9}$$

$$V_{1995,mechanial/electrical} = vIC_pA_rA_xW_p \tag{2-10}$$

Where:

v : zonal velocity ratio as defined in the 1990 edition.

I : importance factor for the structure. It is equal to 1.5 for post-disaster buildings, 1.3 for schools, and 1.0 for all other buildings.

S_p : horizontal force factor for architectural part or portion of a building and its anchorage, should conform to Table 4.1.9 D. It varies between 0.7 and 6.5.

= $C_pA_rA_x$ for mechanical/electrical equipment, where:

C_p : seismic coefficient for mechanical / electrical equipment, given in Table 4.1.9.1.E. It varies between 0.7 and 1.5.

A_r : response amplification factor to account for type of attachment of mechanical/ electrical equipment.

= 1.0 for rigid components that are rigidly connected and for non-brittle pipes and ducts.

= 1.5 for components located on the ground level that are flexible or flexibly connected except for non-brittle pipes and ducts.

= 3.0 for all other cases.

A_x : equal to $1.0 + (h_x/h_n)$.

W_p : weight of the component.

It should be indicated that importance factor I, which applied before for the main structure, was introduced for the first time in 1995 for mechanical/electrical equipment.

2.5.6.2 *Seismic displacement requirements*

The same recommendations as those of the 1990 edition applied.

2.5.7 Provisions of the 2005 edition of the NBCC

The specification of seismic hazard in the 2005 edition of the NBCC (NRC/IRC 2005) has changed significantly from the previous editions of the Code. It now takes the form of Uniform Hazard Spectra (UHS) at specific geographical locations (Adams and Atkinson 2003) in order to provide a more uniform margin of collapse, thus resulting in a more consistent and uniform seismic level of protection throughout the country. The provisions of this edition are based on seismic hazard values having a probability of exceedance of 2% in 50 years, which correponds to a return period of 2500 years. As was the case in 1985, this is a very important additional increase in seismic hazard level.

2.5.7.1 *Seismic force requirements*

The provisions of the 2005 edition of the NBCC use the same force requirements for architectural components and for mechanical and electrical equipment. Elements and components of buildings and their connections should be designed for a lateral force, V, given in Equation 2-11 :

$$V_{2005} = 0.3 F_a S_a(0.2) I_E S_p W_P \qquad \text{2-11}$$

Where:

0.3 F_a S_a (0.2) represents the input ground acceleration to the building with:

F_a : acceleration-based site coefficient. It is a function of site class and $S_a(0.2)$, and it varies between 0.7 and 1.4.

$S_a(0.2)$: spectral response acceleration value at a period of 0.2 s.

I_E : importance factor for the building, equal to 1.0 for normal use and occupancy, 1.3 for highly important structures, and 1.5 for post-disaster facilities.

S_p : horizontal force factor for part or portion of a building and its anchorage, varying between 0.7 and 4.0.

$= C_pA_rA_x/R_p$, with:

C_p : component factor. It takes into account the risk to life safety associated with failure of the component and/or release of contents. It may vary between 0.7 and 1.5. C_p is equal to 1.0 for towers.

A_r : component force amplification factor. It represents the dynamic amplification of the component relative to the position of its attachment to the building structure. It is function of the ratio of the fundamental period of the component (T_p) and the fundamental period of the structure (T), as shown in Figure 2-3. In case the ratio of the periods is not known, values are suggested for various component types; a factor of 2.5 is suggested for towers.

A_x : height factor. It considers the linear amplification of accelerations along the height of the building and is equal to $(1+ 2h_x/h_n)$, in which h_n is the total height of the building and h_x is the floor elevation where the component is located.

R_p : component response modification factor. It represents the energy-absorption capacity of the element and its attachment. It may vary from 1.25 to 5, and is equal to 2.5 for towers.

W_p : weight of the component.

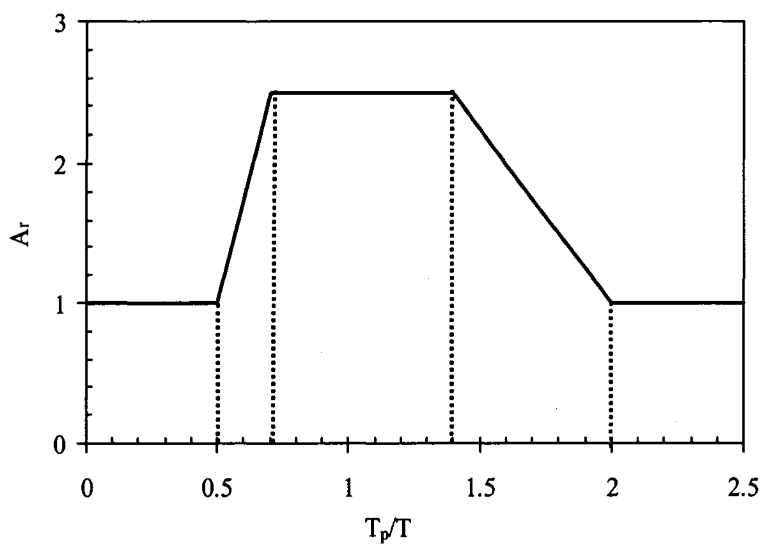

Figure 2-3 Component force amplification factor according to NBCC 2005

2.5.7.2 Seismic displacement requirements

The 2005 edition of the NBCC suggests limiting the largest interstory drift at any level, based on the lateral deflections obtained from linear elastic analysis, to $0.01h_s$ for post-disaster buildings, 0.02 h_s for schools, and 0.025 h_s for all other buildings. The lateral deflections obtained from an elastic analysis should be multiplied by the factor R_dR_o/I_E to give realistic values of anticipated deflections, where R_o is the force overstrength factor and R_d represents the energy dissipation capacity of the structure.

2.5.8 Comments on the NBCC provisions: 2005 edition versus 1995 edition

There are a number of differences between the 1995 and 2005 editions of the NBCC. Among others, the NBCC 1995 did not account for the soil type, the near-fault effect, and the variation of acceleration along the building height for the architectural components. Moreover, the component response modification factor R was only implicitly accounted for. Also, the acceleration amplification with elevation in the 2005 edition ranges from 1.0 at ground level to 3.0 at roof level, while in the 1995 edition, the acceleration amplification with elevation ranged from 1.0 at ground level to only 2.0 at roof level. Therefore, the 2005 code provisions bring more stringent requirements for equipment located at higher elevations in a building.

Also, in the 2005 edition of the NBCC, situations where dynamic analysis is needed as a substitute for the simplified static method of analysis are identified more precisely.

2.6 Correction for forces on tops of buildings

For buildings having long periods, the contribution of higher modes to the response of the building becomes more important, thus resulting in higher accelerations and forces in the top stories. In the simplified static method presented in the NBCC, this effect is accounted for by specifying an equivalent concentrated force F_t applied at the top of the building. Accordingly, components located on building rooftops should be subjected to higher seismic forces as well, although related code provisions apply to the primary structure only.

2.6.1 Editions 1970 through 1985 of the NBCC

In the 1970, 1975, 1980, and 1985 editions of the NBCC, the additional concentrated force to consider at the tops of buildings is given in Equations 2-12 to 2-14:

$$F_t = 0.004V(h_n / D_s)^2 \qquad 2\text{-}12$$

$$F_t \leq 0.15V \qquad 2\text{-}13$$

$$F_t = 0 \quad \text{if} \quad h_n/D_s \leq 3 \qquad 2\text{-}14$$

Where:

F_t : portion of V to be concentrated at the top of the structure.

V : lateral seismic action or force on a part or portion of the structure, known as base shear.

h_n : height of the building above the base.

D_s : dimension of the lateral-force resisting system in the direction parallel to the applied forces.

2.6.2 Editions 1990 through 2005 of the NBCC

In the 1990, 1995, and 2005 editions of the NBCC, the additional concentrated force to consider at the tops of buildings is given in Equations 2-15 to 2-17:

$$F_t = 0.07TV \qquad 2\text{-}15$$

$$F_t \leq 0.25V \qquad 2\text{-}16$$

$$F_t = 0 \quad \text{if} \quad T \leq 0.7\text{s} \qquad 2\text{-}17$$

T : fundamental period of the building in seconds.

2.7 CSA S832-01: Guideline for Seismic Risk Reduction of Operational and Functional Components (OFCs) of Buildings

The objectives of the CSA S832-01 guideline (CSA 2001 b) are to provide information and methodology to identify the OFCs whose failure modes and consequences due to earthquakes may require mitigation, and to suggest design approaches to achieve adequate mitigation.

The recommended approach to risk assessment is to determine the risk rating for each OFC, and to establish a ranking of high, moderate, or low, based on the numerical seismic risk rating score, R, given in Equation 2-18. This rating is determined as the product of the OFCs' seismic vulnerability related to probability of failure, V, and the consequences of failure, C, related to the probability of resultant death, injury, or loss of building functionality if failure/malfunction occurs. The methodology is outlined in Clause 6.2 of the guideline.

$$R = V \times C \qquad \text{2-18}$$

V is determined from Table 2 of the guideline and is calculated according to Equation 2-19:

$$V = RG \times RB \times \frac{\sum (RS \times WF)}{10} \qquad \text{2-19}$$

RG depends on the characteristics of the ground motion and soil conditions, expressed as the product of the zonal velocity, v, and foundation factor, F, as defined in the 1995 edition of NBCC. RB depends on the type of structural system of the building.

RS and WF are the rating score and the weight factor, respectively. Values of both RS and WF are functions of vulnerability parameters, including: the type of restraint, the overturning effects of the OFC, the adequacy of gap for the effect of impact/pounding for displacement-sensitive OFCs, the flexibility of the component and its position within the building.

The factor C given in Equation 2-20 is known as the consequence rating score, and is determined according to Table 3 of the guideline.

$$C = \sum RS \qquad \text{2-20}$$

RS is a function of two consequence parameters: the impact on life safety resulting from the malfunction or failure of the OFC during or immediately after an earthquake, and the functionality of the component. Functionality is important if the component is required for post-disaster functions or for immediate occupancy after the earthquake.

2.8 International Building Code (IBC) and NEHRP 2000 recommended provisions for seismic regulations of new buildings

According to the IBC (IBC 2000) and NEHRP 2000 (BSSC 2001), the architectural, mechanical, electrical, and other non-structural components in structures should be designed or constructed to resist the equivalent static forces and displacements given in Equations 2-21 to 2-27.

The interaction effects between the structure and the supported component should be considered when the weight of the component exceeds 25% of the weight of the supporting structure.

2.8.1 Seismic force requirements

The seismic design force provisions of the NEHRP 2000 (BSSC 2001) were taken from the 1997 NEHRP seismic provisions (BSSC 1997), which in turn had evolved from those of the 1994 NEHRP that were based on strength design (Soong et al. 1993; Bachman and Drake 1994, 1995; Drake and Bachman 1995, 1996). The principal contributor to these provisions is the Building Seismic Safety Council (BSSC).

Seismic force, F_p, according to the NEHRP 2000 (BSSC 2001), is determined according to Equations 2-21 to 2-23:

$$F_p = \frac{0.4 a_p S_{DS} W_p}{\frac{R_p}{I_p}}\left(1 + 2\frac{z}{h}\right) \qquad \text{2-21}$$

$$F_{p\max} = 1.6 S_{DS} I_p W_p \qquad \text{2-22}$$

$$F_{p\min} = 0.3 S_{DS} I_p W_p \qquad \text{2-23}$$

Where:

F_p : seismic design force applied at the component's center of gravity and distributed relative to the component's mass distribution.

a_p : component amplification factor, varying between 1.0 and 2.5.

S_{DS} : design spectral acceleration at short period. It reflects the seismicity of the site including soil amplification effects. It is obtained from the maximum earthquake ground motion maps, reduced by a factor of 2/3. The 2/3 factor accounts for the margin of performance as the buildings are assumed to have a margin of collapse of 1.5, so that the deterministic earthquake results are equal to 2/3*1.5 = 1.0.

W_p : component reactive weight.

R_p : component response factor, varying between 1.0 and 5.0. R_p considers both the overstrength and deformability of the component and its attachment.

I_p : component importance factor, equal to either 1.0 or 1.5. It represents the life-safety importance of the component and the hazard exposure importance of the structure. This factor indirectly accounts for the functionality of the component or structure by requiring the design for a higher force level.

z : height in the structure of the point of attachment of the component.

h : average roof height of the structure relative to the grade level.

It is noted that the effect of the natural period of the supporting structure is not taken into account in these provisions. In addition, a minimum value of F_p is set to assure a minimal seismic design force, while a maximum value of F_p is set to assure that the multiplication of the individual factors does not yield an unreasonably high design force.

2.8.2 Seismic displacement requirements

For two connection points on the same structure, A, or the same structural system, one on level x and the other on level y, the relative seismic displacement, D_p, is determined in accordance with Equation 2-24:

$$D_p = \delta_{xA} - \delta_{yA} \qquad \text{2-24}$$

D_p is not required to be greater than the value given in Equation 2-25:

$$D_p = X - Y\left(\frac{\Delta_{aA}}{h_{sx}}\right) \qquad \text{2-25}$$

For two connection points on separate structures A and B or separate structural systems, one at level x and the other at level y, D_p should be determined according to Equation 2-26:

$$D_p = |\delta_{xA}| - |\delta_{yB}| \qquad \text{2-26}$$

D_p is not required to be greater than the value given in Equation 2-27:

$$D_p = \frac{X\Delta_{aA}}{h_{sx}} + \frac{Y\Delta_{aB}}{h_{sx}} \qquad \text{2-27}$$

Where:

D_p : relative seismic displacement that the component must be designed to accommodate.

δ_{xA} : deflection at building level x of structure A, determined by an elastic analysis and multiplied by the C_d factor.

C_d : deflection amplification factor to increase the calculated elastic deflection to the total deflection anticipated in the post-elastic response range.

δ_{yA} : deflection at building level y of structure A, determined by an elastic analysis and multiplied by the C_d factor.

δ_{yB} : deflection at building level y of structure B, determined by an elastic analysis and multiplied by the C_d factor.

X : height of upper support attachment at level x as measured from the base.

Y : height of lower support attachment at level y as measured from the base.

Δ_{aA} : allowable story drift for structure A.

Δ_{aB} : allowable story drift for structure B.

h_{sx} : story height below level x used in the definition of the allowable drift, Δ_a.

Δ_a/h_{sx} : allowable drift index.

2.9 Method proposed in TM 5-809-10-1: Seismic design guideline for essential buildings

The US Departments of the Army, Navy and Air Force (1986) propose in guideline TM 5-809-10-1 an approximate procedure to determine the seismic forces to be applied to non-structural components in essential buildings.

For rigid components, the total design force representing earthquake effects is equal to the product of the component's weight and the maximum design acceleration. The latter is determined from the maximum floor or roof acceleration of the building and from a design response spectrum based on 2% damping. Therefore, a standard modal analysis of the building is performed to determine the periods and mode shapes for the significant modes of the building. The acceleration at each floor is calculated separately for each mode, as the product of the spectral acceleration of the mode times its participation factor. The minimum design acceleration is determined by taking the square root of the sum of the squares (SRSS) of the maximum floor acceleration for each mode considered.

For components that are flexible or flexibly supported, the modal story acceleration is amplified by a magnification factor to account for resonance between the component and the building when the ratio of their natural periods is equal or close to one. The magnification factor, varying between 1 and 7.5 as shown in Figure 2-4, depends on the ratio of the period of vibration of the non-structural element to that of the supporting building, T_p/T. The peak is broadened for ratios of 1± 0.2 to account for the uncertainty in evaluating the periods. The guideline gives a procedure to create a response spectrum for the component for the specific building considered, giving the spectral acceleration as a function of the component's fundamental period, as shown in Figure 2-5.

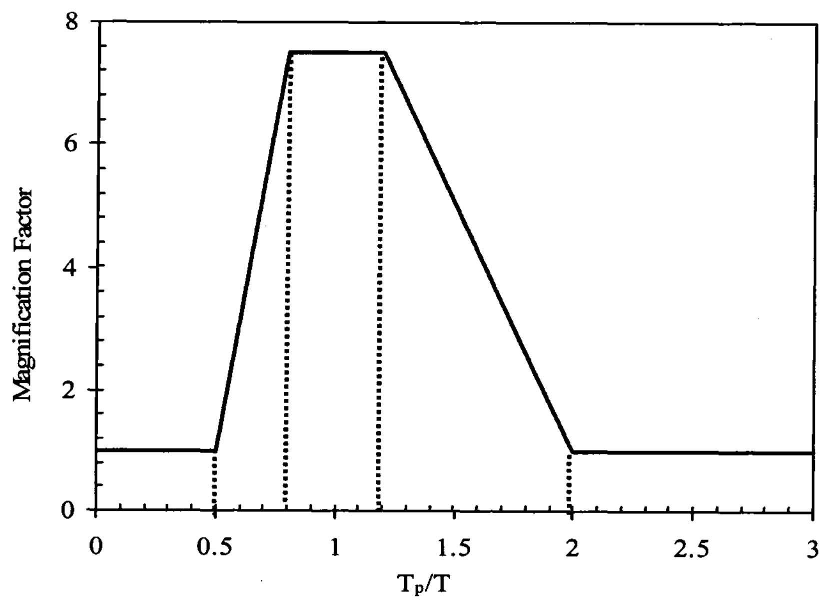

Figure 2-4 Design magnification factor versus the period ratio (After US Army 1986)

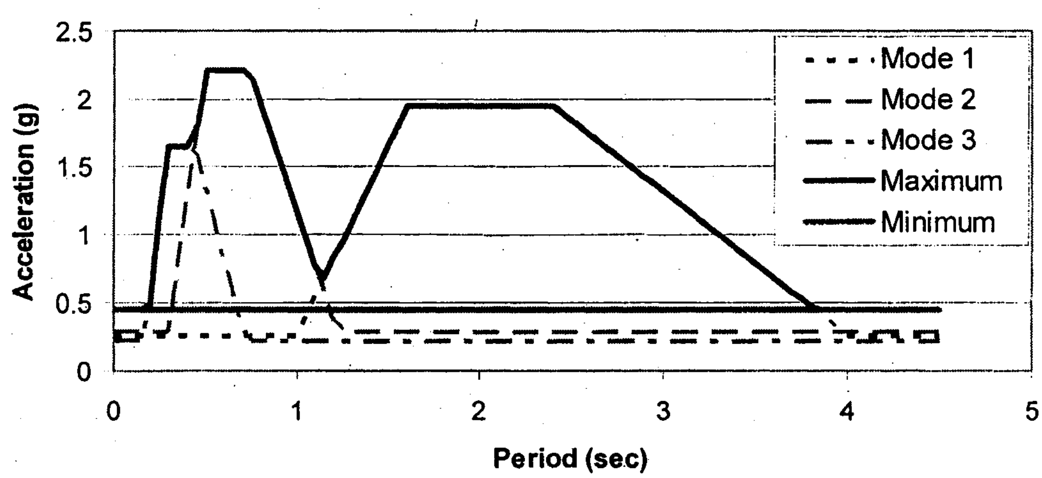

Figure 2-5 Example of approximate floor response spectra (After US Army 1986)

2.10 Previous research on seismic acceleration amplification in buildings

The concept of linearly increasing horizontal accelerations with floor elevation, illustrated in Figure 2-6, was originally suggested by engineers on the basis of statistical analyses of observed data. Some linear elastic multistory buildings were used to justify general, yet simple relationships for various recorded values (Sato et al. 1984; Hiramatsu et al. 1988).

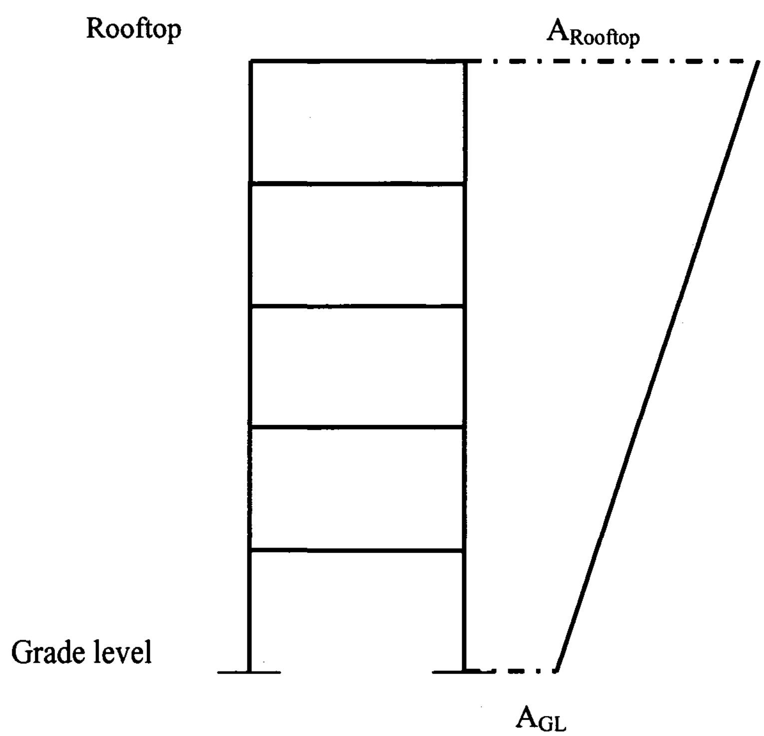

Figure 2-6 Amplification of seismic accelerations from the grade level to the rooftop

To evaluate forces on non-structural components, Singh et al. (1993) studied the provisions of the 1991 NEHRP and proposed a simplified approach using only the first mode of the supporting building and a more rigorous approach considering the first few dominant modes. These procedures served later as a basis for the 1994 NEHRP provisions. This rigorous method incorporates the dynamic characteristics of the supporting structure as well as those of the non-structural components. Moreover, they proposed simplified procedures for calculating the frequencies, mode shapes, and modal properties for calculating the seismic coefficients.

Bachman and Drake (1994, 1995) and Drake and Bachman (1995, 1996) examined more than 400 recorded structural acceleration data sets for buildings subjected to large Californian earthquakes collected between the 1971 San Fernando earthquake and the 1994 Northridge earthquake. Their study revealed that buildings typically exhibit a sharp increase in floor acceleration response near the top of the structure, especially if the structure is flexible. It was further observed that a reasonable maximum for the rooftop acceleration is four times the input ground acceleration. Following this study, the elimination of the period effect from the 1994 NEHRP provisions was proposed. The shortcomings of this study are due to the structures' fundamental periods being computed using the approximate formulas proposed in the 1994 UBC, and records from two orthogonal principal directions being averaged. This last assumption may have obscured some of the results since the structural system may be different in both principal directions and consequently affect the response of the buildings.

Recently, the linear distribution of accelerations adopted in the most current provisions has been severely criticized by practicing engineers. Kehoe and Freeman (1998) carried out a dynamic analysis of a limited number of buildings assuming that non-structural elements are rigidly attached to the framework of the structure. They found that for buildings with higher mode effects, the floor accelerations are relatively constant over most of the building height. These results are consistent with those found by Soong et al. (1993) for very flexible buildings.

Lam et al. (1998) presented a simplified procedure for estimating peak floor accelerations for multistory buildings subjected to earthquakes. They recommended determining the effective peak floor acceleration at the rooftop by multiplying the effective peak acceleration at the ground level by a factor of 3.0 for elastic structures, and by a factor of 1.5 for structures undergoing post-elastic ductile behavior. For the design of rigidly attached components, the authors assumed that design force is simply the product of the peak acceleration and the component mass, while the acceleration amplification of flexible and flexibly supported components was outside the scope of their study.

Marsantyo et al. (1998, 2000) performed both experimental and analytical work to gain insight into the horizontal acceleration responses of non-structural systems mounted on a structural framework during earthquakes. They concluded that in the case of components mounted on fixed-base structures, the maximum acceleration amplification occurs at the condition of resonance between the structure and the non-structural systems, and/or at the condition of resonance between the predominant period of the ground excitation and the main structure's fundamental period. The comparison of the generated force coefficients to the provisions stipulated in the 1997 Uniform Building Code (ICBO 1997) and those of the 1997 Building Center of Japan indicated that these codes were inadequate when the primary structure remains elastic with little damping. Moreover, they demonstrated that building equipment and contents equipped with a base isolation system and those mounted on the floors of a base-isolated main structure experience significantly reduced acceleration responses. Therefore, base isolation can be used as an alternative solution in case sufficient damping cannot be achieved.

Using the 1992 New Zealand loading standard NZS 4203, Rodriguez et al. (2000, 2002) proposed a method based on modal superposition modified to account for inelastic response in order to evaluate the seismic design coefficients for rigid parts and diaphragms in regular buildings. They performed parametric nonlinear time-history dynamic analyses for three-, six- and twelve-story cantilevered wall structures. The analyses included both elastic and inelastic responses for different levels of ductility, types of hysteresis loops, and two input ground motions. The number of levels, a contribution factor due to the first sway mode, and a reduction factor associated with structural ductility were considered. They proposed their 'First Mode Reduced' method, where the floor acceleration A_n^q corresponding to mode q at the uppermost level of the building can be formulated according to Equation 2-28:

$$A_n^q = \Gamma_q \Phi_n^q \frac{S_a(T_q, \xi_q)}{R_q} \qquad \text{2-28}$$

Where:

Γ_q : participation factor for mode q.

Φ_q^n : amplitude of mode q at level n.

S_a : spectral acceleration.

R_q : reduction factor to account for the effect of ductility on the primary lateral force resisting system, associated with mode q.

T_q : natural period of vibration of the structure, associated with mode q.

ξ_q : damping ratio of the structure, associated with mode q.

The modal accelerations of Equation 2-28 were then combined using the SRSS technique. For simplification, it was assumed that ductility affects only the accelerations associated with the first mode of the response, and therefore $R_q = 1$ for $q > 1$. R_1 is obtained from the ratio of base overturning moments obtained from the nonlinear time-history analysis and the elastic analysis. The acceleration at level n is given by Equation 2-29:

$$A_n^q = \sqrt{\left[\Gamma_1 \Phi_n^1 \frac{S_a(T_1, \xi_1)}{R_1}\right]^2 + \sum_{q=2}^{r} \left[\Gamma_q \Phi_n^q S_a(T_q, \xi_q)\right]^2} \qquad 2\text{-}29$$

A drawback of this method is that it is cumbersome for common design; therefore, the authors presented a simplified equation to calculate the horizontal design force for a rigid part or diaphragms, F_{ph}, given in Equation 2-30:

$$F_{ph} = S_p \times R_p \times Z \times C_{pi} \times W_p \qquad 2\text{-}30$$

Where:

S_p : structural performance factor in NZS 4203:1992.

R_p : risk factor for the part in NZS 4203:1992.

Z : seismic zone factor in NZS 4203:1992.

C_{pi} : basic horizontal seismic coefficient for a part at level i in NZS 4203:1992.

W_p : reactive weight of a part or diaphragm.

Based on raw data from a previous study by Bachman and Drake (1995), Searer and Freeman (2002) proposed an upper bound simplified equation for horizontal accelerations where the height effect was neglected. For rigid components not supported at the rooftop, the design force should be evaluated according to Equation 2-31:

$$F_p = 1.4 \times C_a \times I_p \times W_p \qquad \text{2-31}$$

Where:

C_a : factor equivalent to the design spectral acceleration at short period, S_{DS}, in current building codes. It is a function of the soil type and the seismic zone factor. It is given in Table 104-9 of the SEAOC Blue book (SEAOC 1999).

I_p : importance factor. It is equal to 1.0 for standard occupancy structures, and 1.5 for essential and hazardous facilities and special occupancy structures.

W_p : weight of the component.

For rigid components supported at the rooftop, the design force should be increased according to Equation 2-32 to account for the increased accelerations experienced at the roof level due to the effects of higher modes:

$$F_p = 2.0 \times C_a \times I_p \times W_p \qquad \text{2-32}$$

The horizontal force calculated in Equations 2-31 and 2-32 should be doubled for the design of flexible components to account for potential resonance amplification.

There has also been relevant recent work at Stanford University (Miranda and Taghavi 2005; Taghavi and Miranda 2005) concerning the estimation of seismic demands for acceleration-sensitive components attached to conventional buildings that respond elastically or remain practically elastic when subjected to small and moderate earthquakes. The dynamic characteristics of the buildings were approximated by using an equivalent uniform continuum cantilever that consists of a combination of a flexural beam and a shear beam. The method proposed by Miranda and Taghavi (2005) is based on simplified analytical models and takes into account the contribution of the lowest three sway modes of vibration of a building. The method yields rapid estimation of floor acceleration demands with only three parameters: the fundamental period of vibration of the building, a damping ratio characteristic of the building, and a non-dimensional parameter α_0 (Equation 2-33) that reflects the degree of participation of overall flexural and shear deformations in the building. For buildings with reduction in stiffness along the height that do not deflect laterally like flexural beams, an additional parameter is introduced consisting of the ratio of the lateral stiffness at the top of the structure to the lateral stiffness at the bottom of the structure (EI_{top}/EI_0).

$$\alpha_0 = H\left(\frac{GA_0}{EI_0}\right)^{1/2} \qquad \text{2-33}$$

Where:

GA_0 : equivalent shear rigidity at the base of the structure.

EI_0 : equivalent flexural rigidity at the base of the structure.

H : total height of the structure.

The mode shapes and modal participation factors of the buildings were computed from the continuum cantilever model, assuming uniform mass and stiffness along the building height. The authors showed that the reduction in lateral stiffness and mass along the height has a negligible effect on the modal participation factors and mode shapes for buildings deforming like flexural beams. They also proposed approximate equations to compute mode shapes, natural periods, and modal participation factors for buildings with non-uniform stiffness and significant shear deformations. The method does not address torsional deformations and is targeted at relatively regular buildings.

2.11 Seismic provisions in standards and codes of practice for telecommunication towers

A review of available research and information resources shows that most of the published work on the analysis of steel lattice telecommunication towers is devoted to analysis under wind and ice loads. In the following section, the current provisions available in some design codes and standards for the seismic analysis and design of telecommunication towers are reviewed. In a survey of earthquake performance of telecommunication towers (Schiff 1999), it was concluded that tall broadcast towers and large building-supported microwave towers are the most vulnerable to earthquakes, but none of these towers has been a direct threat to life safety during an earthquake. The main issue for telecommunication towers is their functionality during or immediately after an earthquake.

2.11.1 CSA S37-01: Antennas, towers and antenna supporting structures

The 2001 edition of the Canadian standard CSA S37-01: Antennas, towers and antenna supporting structures (CSA 2001 a) introduced a new appendix (Appendix M) which addresses earthquake-resistant design of both self-supporting and guyed lattice telecommunication towers. However, this appendix is not a mandatory part of the standard. It states that unlike buildings for which life safety is of foremost concern, the target performance level for telecommunication towers depends on the tower's economic value and the function of the structure; therefore, the owner decides the appropriate performance level among the following: life safety, interrupted serviceability, and continuous serviceability. The life safety performance level ensures a minimum level of protection for towers located in areas of human occupancy, with special attention paid to towers supported by buildings. The interrupted serviceability performance level is for towers that should be able to quickly resume service following an earthquake. Finally, the continuous serviceability performance level is for towers that should remain fully functional during and after an earthquake.

In this research, the focus is on towers having continuous or interrupted serviceability performance levels. These performance levels imply that the global response of the tower should remain elastic during the seismic shaking. Appendix M also recommends performing a frequency analysis of the tower in order to allow identification of the tower's sensitive frequency range. Past earthquake records have typical frequencies in the range 0.1-10 Hz, with a concentration in the 0.3-3 Hz range for horizontal motion, while the vertical motion involves a higher frequency band. Nevertheless, in the case of building-mounted towers, the frequency content of the input earthquake is modified and filtered according to the dynamic characteristics of the supporting building. Table 2-1 summarizes the type of seismic analysis that is recommended in Appendix M of the CSA S37-01 standard. As indicated in Table 2-1, at least a static design check is recommended for rooftop towers located in moderate seismic zones and with life safety and interrupted serviceability performance levels. However, no specific guidance is available for such a static design verification. For the continuous serviceability performance level, in moderate and high seismic zones, a dynamic check for all tower types is recommended. Appendix M further recommends adopting the provisions of the NBCC 1995 concerning the direction of the seismic input and load combinations.

Table 2-1 Seismic design check recommendations of CSA S37-01 (CSA 2001 a)

Level of Seismicity	Life Safety	Interrupted Serviceability	Continuous Serviceability
Low Seismicity	No seismic check necessary	No seismic check necessary	No seismic check necessary
Moderate Seismicity	Static check for building-supported towers	Static check for building-supported towers and irregular towers (geometry/mass) Dynamic check for masts of height 300 m and more	Dynamic check for all tower types
High Seismicity	Static check for all free standing towers of height 50 m and more and masts from 50 m to 150 m	Static check for all free standing towers and masts up to 150 m	Dynamic check for all tower types
	Dynamic check for masts of height 150m and more	Dynamic check for masts of height 150m and more	

2.11.2 TIA/EIA-222-G: Structural standard for antenna supporting structures and antennas

The increased awareness of seismic risk in the last decade has encouraged the American Electrical and Telecommunication Industries Association to formulate seismic provisions for antenna structures in its TIA/EIA-222-G standard (2005). This standard provides seismic design provisions for self-supporting and guyed antenna towers on the ground, or mounted on building rooftops or other supporting structures. The design provisions apply only for ultimate strength limit state conditions, i.e. not for serviceability limit states. The earthquake effects may be ignored when the total seismic base shear is less than 50% of the total horizontal wind load without ice, and for category I structures that represent a low hazard to human life and damage to property in the event of failure.

The maximum earthquake ground motion should be taken as the motion of probability of exceedance of 2% in 50 years. The design spectral response acceleration should be calculated at short period, S_{DS}, and at 1 second, S_{D1}, assuming 5% of critical viscous damping in all structures. This standard proposes four methods to calculate the earthquake loads: the equivalent lateral force procedure that will be summarized below, the equivalent modal analysis procedure, the full modal analysis procedure, and time-history analysis.

2.11.2.1 Equivalent lateral force procedure

According to the TIA 222 G standard, the total seismic force, V_s, is obtained from Equations 2-34 and 2-35:

$$V_s = \frac{S_{DS} WI}{R} \tag{2-34}$$

$$V_s \le \frac{f_1 S_{D1} WI}{R} \tag{2-35}$$

When Equation 2-35 is used, V_s should not be less than the values given in Equations 2-36 and 2-37:

$$V_s = 0.044\, S_{DS}\, WI \tag{2-36}$$

$$V_s = \frac{0.5 S_1 WI}{R} \qquad \text{for } S_1 \ge 0.75 \tag{2-37}$$

Where:

S_{DS} : design spectral response acceleration at short period, equal to 2/3 F_a S_S.

W : total weight of the structure including appurtenances.

I : importance factor, equal to either 1.0 or 1.5 depending on whether the structure's failure represents a substantial hazard or a high hazard to human life and damage to property, respectively.

R : force modification factor, to account for post-elastic response.

= 3.0 for lattice self-supporting structures.

= 2.5 for lattice guyed masts.

= 1.5 for tubular pole structures.

f_1 : fundamental sway frequency of the structure.

S_{D1} : design spectral response acceleration at a period of 1.0 s, equal to 2/3 F_v S_1.

S_s : maximum considered earthquake spectral response acceleration at short period.

S_1 : maximum considered earthquake spectral response acceleration at a period of 1.0 s.

F_a : acceleration-based site coefficient, depends on site class and spectral response acceleration at short period.

Fv : velocity-based site coefficient, depends on site class and spectral response acceleration at 1.0 s.

2.11.2.2 Vertical distribution of the lateral seismic force V_s

The standard provides a methodology for the vertical distribution of the lateral seismic shear forces determined from Equations 2-34 to 2-37. The lateral seismic force, F_{sz}, induced at any level z, is determined from Equation 2-38:

$$F_{sz} = \frac{w_z . h_z^{k_e}}{\sum_{i=1}^{n} w_i . h_i^{k_e}} V_s \qquad 2\text{-}38$$

Where :

V_s : total seismic shear force.

w_z : portion of total gravity load (w) assigned to level z.

h_z : height from the base of structure to level z.

k_e : seismic force distribution exponent, equal to 1.0 for structures having a fundamental frequency of 2.0 Hz or higher, and 2.0 for structures having a fundamental frequency of 0.4 Hz or less. For structures with a fundamental frequency between 2.0 Hz and 0.4 Hz, k_e should be taken as 2.0 or determined by linear interpolation between 1.0 and 2.0. Alternatively, k_e may be set equal to 2.0 for any structure.

n : number designating the uppermost level of the structure with regard to the distribution of gravity loads.

i : number designating the level under consideration.

w_i : portion of total gravity load (w) assigned to level i.

h_i : height from the base of structure to level i.

2.11.2.3 Towers supported on buildings or other supporting structures

For towers less than or equal to 100 ft in height, with no mass or stiffness irregularities and supported on buildings or other supporting structures, the earthquake loads determined according to the equivalent lateral force procedure presented in the previous sections should be multiplied by an amplification factor, A_s, equal to 3.0. This amplification factor stands for the building height amplification factor at rooftop level as suggested in the IBC (IBC 2000) and the 2005 edition of the NBCC (NRC/IRC 2005). Essentially, the towers are considered as rigid acceleration-sensitive non-structural components. However, as will be shown in the subsequent chapters, the response of telecommunication towers is much affected by the response of the supporting structure. The TIA 222 G standard recommends considering the dynamic interaction between the tower and the supporting structure for towers with mass or stiffness irregularities and those over 100 ft in height. In such cases, rational methods that account for the dynamic characteristics of the structures should be used to determine the earthquake loads;

however, earthquake loads should not be less than 80% of those determined from Equations 2-34 to 2-38.

2.11.3 Australian standard AS 3995: Design of steel lattice towers and masts

The Australian standard AS 3995-1994 (Standards Association of Australia 1994) provides some guidance for earthquake design in its Appendix C, which is not mandatory. It states that steel lattice towers and masts are less sensitive to earthquake loads than most other types of structures. A note of caution is given for self-supporting towers of more than 100 m in height with significant mass concentrations, which may be subjected to seismic base shear forces and overturning moments approaching those induced by the ultimate wind loads. However, no specific guidance on how to estimate the tower seismic response is given. It is also suggested that the vertical component of ground motion be considered and that footing ties be provided in case of soft soils for freestanding towers and tall guyed steel masts, depending on the local seismicity. The Australian standard does not address the case of towers mounted on building rooftops.

2.12 Previous research to determine seismic forces for towers mounted on tops of buildings

To perform an adequate seismic design of telecommunication equipment, it is necessary to evaluate seismic forces realistically. Because the design of towers on the ground is usually controlled by ice and wind loads, research on the seismic response of these towers has not been abundant.

One of the first publications discussing earthquake effects on antenna-supporting lattice towers was authored by Konno and Kimura (1973). The study collected information on tower mode shapes, natural frequencies, and damping properties for microwave antennas erected on the roofs of buildings owned by the Nippon Telegraph and Telephone Corporation (NTT). The case study of an instrumented tower mounted on a building rooftop during the 1968 Off-Tokachi earthquake was presented. The collected data were analyzed and compared with results obtained from simplified stick models of the tower alone and of the coupled tower-building system, assuming a viscous damping ratio of 1%. The study concluded that steel towers erected on building rooftops are likely to show resonant phenomena with the building over a wide range of frequencies during an earthquake, and that seismic forces resulting from strong earthquakes might exceed wind forces. These numerical results were validated by observations of local damage and permanent deformations at the tower base following the earthquake. It was also found that the viscous damping coefficient of the coupled system tends to increase with the lengthening period of vibration, while in the case of the tower alone, the damping coefficient is not affected by the period. The response of the coupled tower-building system varies with the period and mass ratios of the tower to the building, and reaches a maximum when the fundamental periods of the tower and building come close to each other. The acceleration response becomes larger as the fundamental period of the coupled system decreases, but as the period increases, the displacement response tends to grow larger.

Sato et al. (1984) analyzed the data of strong-motion accelerographs in selected buildings owned by the Nippon Telegraph and Telephone Public Corporation in Japan. In this study, the authors evaluated the natural periods of the buildings, the acceleration amplification ratios along the height of the buildings, and the acceleration response spectra of the building floors. In addition, they studied the input seismic force to be assumed for the design of appendages. A maximum acceleration amplification of 4 at the rooftop was deemed appropriate. A drawback of the study is that the average amplification was calculated for the two main horizontal directions.

Hirumatsu et al. (1988) reported the continuation of the investigation of the seismic response of NTT telecommunication equipment mounted on building rooftops. A building having a steel lattice tower on its rooftop was used in the study. The building framework was equipped with 7 sensors, the building telecom equipment with 16 sensors, and the tower itself with 2 sensors. The historical records of 6 earthquakes were studied. In general, the results agreed with the earlier observations of Sato et al. (1984).

There have been unofficial reports of tower damage incurred during the 1994 Northridge earthquake, involving mostly localized damages in the vicinity of antenna mounts (Madugula ed. 2002). Similar localized damages were reported by Pierre (1995) following a visit to Japan after the Hanshin Awaji (Kobe, Japan) earthquake that occurred on January 17, 1995.

Kanazawa and Hirata (2000) apply the classical seismic response spectrum method for the analysis of secondary systems considering the dynamic interactions between the primary and secondary structures, and the transient response effects. As a first step, the floor response spectrum to be used as seismic input to the secondary system is evaluated using the specified design spectra at the ground level; the second step consists of applying the modal combination rule to evaluate the maximum response of the secondary systems, using the relative acceleration response spectra from the seismic input given by the first step. To illustrate their proposed method, the researchers performed time-history simulations on a building-tower model. A similar approach was developed at McGill University by Khedr (1998) and Khedr and McClure (2000) for steel lattice towers on firm ground and subjected to both horizontal and vertical earthquake accelerations; however, their method is not applicable to towers mounted on rooftops or other flexible supporting structures.

In a preliminary study, McClure et al. (2004) used numerical simulations to explore the correlation between the building accelerations and the maximum seismic base shear as well as the base overturning moment of towers mounted on building rooftops. This study was the precursor of the research reported in this thesis.

2.13 Summary

In this chapter, a review of code provisions for seismic design of operational and functional components of buildings and for steel lattice telecommunication towers has been presented. The provisions of the National Building Code of Canada were presented, starting from the first edition in 1941 to 2005, as well as the relevant provisions of other codes and guidelines, including the CSA S832-01 guideline, the CSA S37-01 standard, the IBC, the TIA/EIA-222-G standard, the Australian AS 3995 code, and the US Army TM 5-809-10-1 guideline.

In light of present and past research related to the estimation of acceleration amplification along a building's height and the seismic design of telecommunication towers mounted on a building rooftop, it can be concluded that OFCs in general, and telecommunication towers in particular, have received only modest attention from the research community despite the potential importance of damage to them during earthquakes. In fact, earthquake effects on these components have often been ignored.

Chapter 3
Data Processing and System Identification

This chapter describes the analyses and results of recorded accelerations from the 1999 Chi Chi earthquake for 11 instrumented buildings located in different regions of Taiwan. First, the building properties and instrumentation schemes are presented. Secondly, processing of data and system identification techniques that were used to extract the modal properties of the buildings are described. Two classes of system identification techniques are identified: parametric and non-parametric techniques. The dynamic formulation of the non-parametric system identification technique used in the study is summarized. Thirdly, the maximum acceleration profiles of recorded accelerations along the building heights are presented and the results are discussed. Finally, different parameters that could affect the acceleration amplification in buildings are identified and further discussed.

3.1 Instrumentation of buildings located in Taiwan

The 11 buildings used in this research form part of the Taiwan Strong Motion Instrument Program (TSMIP), operated by the National Weather Bureau and Ministry of Transportation and Communications in Taiwan. High quality force-balanced accelerometers with maximum capacity +/-2g were installed in the buildings starting from 1992 (Shin 2000). The buildings were extensively instrumented with a sufficient number of sensors to permit a realistic dynamic analysis of the buildings and system identification. The buildings are located in different regions of Taiwan, at a distance larger than 70 km from the epicenter of the 1999 Chi Chi earthquake, so the seismic waves that reached these buildings were much attenuated, corresponding to an earthquake of moderate intensity. The peak input ground accelerations recorded at the building sites range between 0.015g and 0.07g.

3.2 Characteristics of the instrumented buildings used in this study

The buildings used in this study did not suffer any structural damage, except for some minor cracking of partition walls; nonetheless, they suffered considerable non-structual damage resulting in substantial economic losses. Therefore, the building structural frameworks were assumed to remain elastic, or practically elastic, with time-invariant properties. Moreover, most of the buildings are erected on sand or cohesive soil and supported on rigid foundations. Consequently, soil-structure interaction was assumed to be negligible. Characteristic features of the buildings, including location, geometric properties, and structural lateral load resisting system, are summarized in Table 3-1 where the buildings are classified according to the number of stories.

LLRS refers to the dominant lateral load resisting system of the building. Dual is a combination of shear walls and reinforced concrete frame system, SRC is a system composed of steel frames with concrete covered columns, and R.C. refers to a reinforced concrete frame system. Buildings range from low-rise to high-rise; TAPBA7 is the second highest building in Taiwan, with 57 stories above ground. Most of the buildings are reinforced concrete structures, and they are of relatively recent construction, not older than 26 years. Architectural plans of elevations, ground and rooftop floors of the buildings are presented in Appendix A.

Table 3-1 Characteristics of the 11 instrumented buildings

Building ID	Location	Year of construction	Use	LLRS	No. of stories above ground	Height (m)
CHYBA9	Tainan	1980	Telecom	Dual	4	20
CHYBA4	Jia-Yi	1983	Hospital	Dual	6	24.2
CHYBA5	Hsin-Yen	1984	Hospital	R.C.	6	23
TCUBA0	Zhungli	1994	Library	R.C.	8	32.2
TCUBAA	Hsinchu	1996	Library	R.C.	8	30.4
CHYBA0	Tainan	1989	Office	Dual	8	30.4
TCUBA6	Hsinchu	1991	Residential	R.C.	14	42.6
TCUBA2	Miaoli	1992	Residential	R.C.	17	56.1
TCUBA4	Tao-Yuan	1994	Office	SRC	17	62.9
CHYBA7	Tainan	1995	Residential	Dual	24	75
TAPBA7	Taipei	1993	Office	SRC	57	205.3

3.3 Data processing

The recorded raw data need to be adjusted before being studied. The data processing consists of several steps including: the baseline correction in order to obtain a zero mean value for the accelerations; this is done by subtracting the mean of all values from each value of the records. The frequency components outside the range of interest and dominated by noise are removed by applying a bandpass filter. The high-pass and low-pass cutoff frequencies used in filtering vary from one building to another depending on the geographical location of the building and the sensitivity of the sensors; typical low-pass cutoff frequencies vary between about 0.1 and 0.5 Hz, while high-pass cutoff frequencies lie between 15 and 50 Hz. The high-pass and low-pass cutoff frequencies considered for the buildings in Taiwan are 0.2 Hz and 30 Hz, respectively. The sensors located at different levels within each building are linked to a central recorder providing a constant start time; therefore, the sensors are triggered simultaneously and the accelerograms are assumed to be synchronized without any further processing. In order to reduce the spiky appearance of the accelerograms and suppress noise, smoothing of records over three points was used. Smoothing consists of computing the weighted average of three adjacent data values. Due to the time limitation of the recorded signal coupled with the assumption of periodicity of the sample waveform, an undesirable phenomenon called leakage occurs. Leakage is the presence of spurious components near the sinusoid spectrum where a nonzero value appears in the transform at a frequency f because of the presence of a sinusoid at a different frequency f_0 (Bloomfield 2000). To reduce leakage, a Hanning window w(t) is imposed to the time signal x (t) prior to the Fourier Transform. This window for N points is basically a cosine shaped weighting function (bell shaped) that forces the beginning and end of the sample interval to be heavily weighted to zero and is equal to $w(t) = 0.5\times(1-\cos(2\times\pi\times t/T))$. This is generally useful for signals that do not satisfy periodicity requirements for the FFT process. After applying the window to the time signal x (t), it becomes x'(t), where x'(t) is equal to the product x(t)w(t). This process is used with an overlap of 50% for the windows, with 1024 points inside each window. Overlapping is intended to produce smoother spectra. Figure 3-1 illustrates conceptually the effect of the Hanning window on the DFT of the modified signal. The accelerograms were processed using the signal analysis software Famos (Fast analysis and monitoring of signals) version 3.2 (IMC 2000).

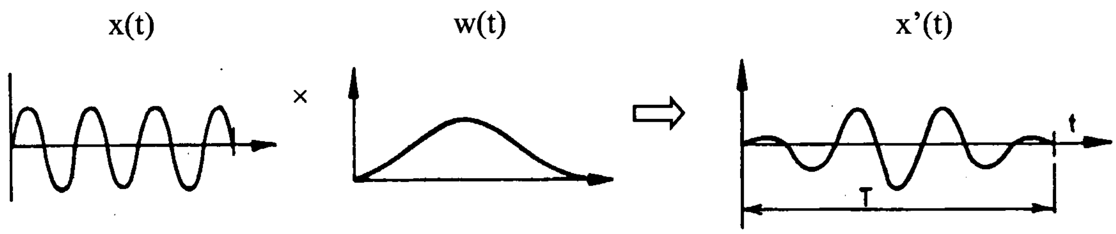

a) Effect of windowing in the time domain

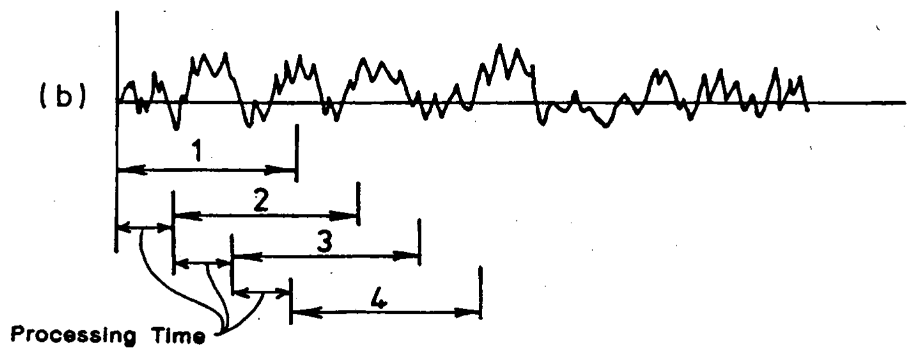

b) Overlapping

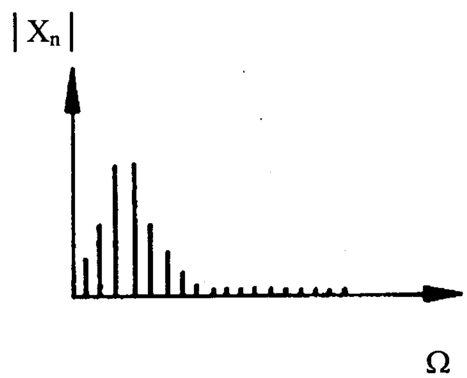

c) Spectrum having leakage before applying the Hanning window

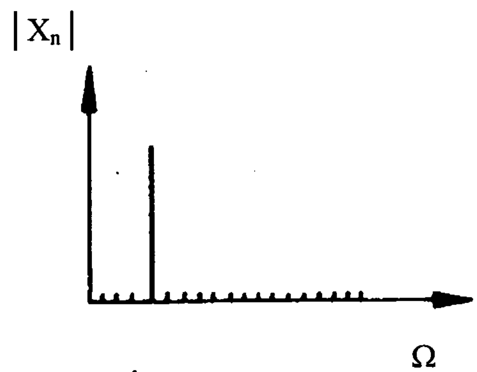

d) Ideal spectrum after applying the Hanning window

Figure 3-1 Effect of Hanning window on DFT (After Ewins 2000)

3.4 System identification techniques

3.4.1 Objectives of system identification

Instrumented buildings undergoing seismic shaking represent large-scale experiments that offer the opportunity to study the vibrational behavior of these buildings. The objective of system identification is to estimate the modal properties and damping ratios of a structure given the input seismic loadings represented by the free-field or grade level recordings and the output records represented by the rooftop records. This can be achieved by deducing a model of a real system represented by a transfer function between the output and the input (Beck 1978). In addition, system identification allows the calibration of numerical models of the instrumented structures for further studies and analysis, as will be discussed in Chapter 4. There are three kinds of system identification techniques:

- Non-parametric, time-invariant: this is used in this study.
- Non-parametric, time-variant.
- Parametric, time-variant.

The time-invariant system identification technique is used for elastic or nearly elastic structures with properties not changing over time, while the time-variant technique is used for structures whose properties (stiffness, damping or mass) vary with time.

Non-parametric methods are commonly used in engineering practices for their simplicity in identifying the frequencies of the structures. However, these approaches may not be suitable for problems that require high-frequency resolution and/or for situations where nonlinear behavior is dominant. On the other hand, the parametric methods are more suitable for problems with closely-spaced modes, non-proportional damping, and for situations where a large number of modes are required to describe the structural response. Approaches in system identification can be further classified into two main groups: the frequency-domain methods and the time-domain methods.

3.4.2 Non-parametric time-invariant system identification technique

In this study, the non-parametric time-invariant system identification technique in the frequency domain was used (Cooley and Tukey 1965; Bendat and Piersol 2000; Ewins 2000). This technique is based on Fourier analysis and assumes that the unknown parts of the system are functions rather than parameters (Beck 1978). The system is treated as a "black box", since the objective is to determine a functional relationship between the input and output without any prior information about the system. The transfer function $H(\Omega)$ given in Equation 3-1 describes the alteration of the frequency content of the records through the elastic structure by using a single input x(t), and a single output y(t). The transfer function of an ideal linear system is illustrated in Figure 3-2. For a constant-parameter linear system, the transfer function, $H(\Omega)$, is a function of the frequency characteristics of the system, and is not a function of either the time or the system excitation. If the system is nonlinear, the transfer function will also be a function of the applied input (Bendat and Piersol 2000).

$$H(\Omega) = \frac{Y(\Omega)}{X(\Omega)} \Leftrightarrow System\ \Pr operties = \frac{\text{Re}sponse}{Input} \qquad 3\text{-}1$$

Where:

$H(\Omega)$: frequency response or transfer function linking the quantities x(t) and y(t).

$X(\Omega)$: Fourier Transform of the input motion x(t).

$Y(\Omega)$: Fourier Transform of the response y(t).

$$x(t) \longrightarrow \boxed{H(\Omega)} \longrightarrow y(t)$$

Figure 3-2 Ideal single input/output linear system

Mathematical formulation of H (Ω)

The frequency response function or transfer function, $H(\Omega)$, is calculated as the ratio of the Fourier Transform of the output signal to that of the input signal (Equation 3-1). However, for a transient problem such as seismic excitation, both the input x(t) and the response y(t) are not periodic and are described by random processes. It is not possible to consider the random signals as periodic with infinite period because the inherent properties of random signals cause them to violate the Dirichlet conditions that guarantee existence and convergence of the Fourier Transform. Consequently, the standard Fast Fourier Transform algorithm cannot be applied directly to the random excitation and response signal. Thereby, $H(\Omega)$ is usually computed from the power spectral density functions $S_{xx}(\Omega)$ and $S_{yy}(\Omega)$, and the cross-spectral density function $S_{xy}(\Omega)$ of the input and output signals, which are the Fourier Transforms of the autocorrelation functions $R_{xx}(t)$ and $R_{yy}(t)$, and the cross-correlation function $R_{xy}(t)$, respectively. Figure 3-3 shows a typical random signal f(t) with its autocorrelation function $R_{ff}(\tau)$ that satisfies convergence requirement of the Fourier Transform, and the spectral density function $S_{ff}(\Omega)$. For a random signal f(t), the autocorrelation function

$R_{ff}(\tau)$ is defined as the average value of the product $f(t).f(t+\tau)$ computed along the time axis. $R_{xx}(t)$ and $R_{yy}(t)$ and $R_{xy}(t)$ are given in Equations 3-2 to 3-4:

$$R_{xx}(\tau) = \lim_{T\to\infty}\frac{1}{T}\int_0^T x(t)x(t+\tau)dt \qquad 3\text{-}2$$

$$R_{yy}(\tau) = \lim_{T\to\infty}\frac{1}{T}\int_0^T y(t)y(t+\tau)dt \qquad 3\text{-}3$$

$$R_{xy}(\tau) = \lim_{T\to\infty}\frac{1}{T}\int_0^T x(t)y(t+\tau)dt \qquad 3\text{-}4$$

The autocorrelation and power spectral density functions are related through the Fourier integrals given in Equations 3-5 to 3-7 (Clough and Penzien 1994):

$$S_{xx}(\Omega) = \frac{1}{2\pi}\int_{-\infty}^{\infty} R_{xx}(\tau)e^{-iw\tau}d\tau \qquad 3\text{-}5$$

$$S_{yy}(\Omega) = \frac{1}{2\pi}\int_{-\infty}^{\infty} R_{yy}(\tau)e^{-iw\tau}d\tau \qquad 3\text{-}6$$

$$S_{xy}(\Omega) = \frac{1}{2\pi}\int_{-\infty}^{\infty} R_{xy}(\tau)e^{-iw\tau}d\tau \qquad 3\text{-}7$$

(a)

(b)

(c)

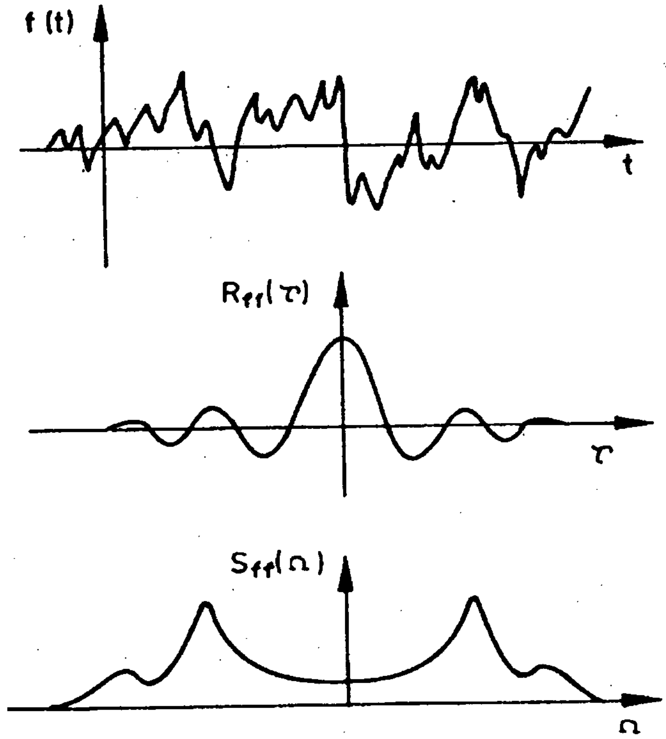

Figure 3-3 Random signal

(a) Time-history (b) Autocorrelation function (c) Power spectral density function

(After Ewins 2000)

Using the spectral density functions, H(Ω) can be computed in two ways according to Equations 3-8 and 3-9 (Bendat and Piersol 2000):

$$S_{yy}(\Omega) = H(\Omega)S_{xx}(\Omega) \qquad 3\text{-}8$$

$$S_{xy}(\Omega) = H(\Omega)S_{xx}(\Omega) \qquad 3\text{-}9$$

Equations 3-8 and 3-9 provide the basis for calculating the transfer function H(Ω) for the system. A good estimate of the transfer function is achieved in ideal situations when no extraneous noise exists at input and/or output points, and when the system has no time-varying or nonlinear characteristics. Equation 3-8 is a real-valued relation and is known as the input/output auto-spectrum relation, while Equation 3-9 is a complex-valued relation and is known as the input/output cross-spectrum relation. In order to calculate the transfer function, Equations 3-8 and 3-9 can be rewritten as:

$$|H_1(\Omega)|^2 = \frac{S_{yy}(\Omega)}{S_{xx}(\Omega)} \tag{3-10}$$

$$|H_2(\Omega)|^2 = \frac{|S_{xy}(\Omega)|^2}{S^2{}_{xx}(\Omega)} \tag{3-11}$$

$|H(\Omega)|$ is known as the gain factor. The two estimates of the transfer function should be theoretically equal. However, in practice, the input and/or output records are contaminated by noise. The gain factor given in Equation 3-10 is a biased estimate for all cases, while the gain factor given in Equation 3-11 is a biased estimate for cases where extraneous noise is present at the input, but will be an unbiased estimate for cases where extraneous noise is present at the output only. Accordingly, the model with extraneous noise present at the output illustrated in Figure 3-4 was adopted in this study.

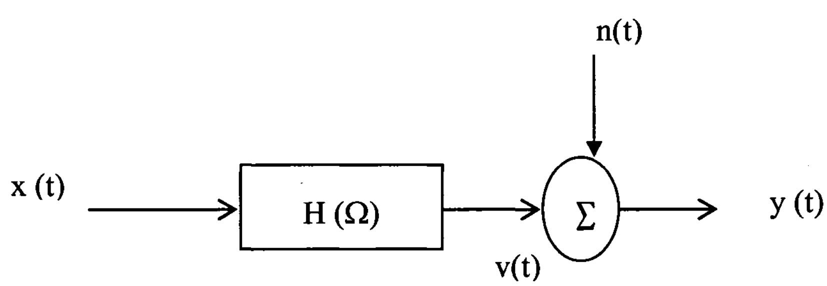

Figure 3-4 Input/output relationship with noise at the output
y(t) = v(t) + n(t), v(t) is the true output signal and n(t) is the extraneous noise
(After Bendat and Piersol 2000)

3.4.3 Non-parametric time-variant system identification

The non-parametric time-variant system identification technique is essentially similar to the previous approach, except that in order to identify the variation of parameters in time, a window smaller than the total duration of the record is moved in time. The size of the window is selected to be a function of the fundamental period of the building.

3.4.4 Parametric system identification

In this technique, a particular mathematical form is chosen to describe the essential features of the input-output relation of the system, but certain parameters must be assigned values before the model is completely specified. Some of the parameters must be estimated from the input and output of the system. The model of the structure is initially converted to an equivalent model in the discrete time domain. The identification is performed by finding the values of the parameters which produce a least-squares match over the specified frequency range between the unsmoothed, complex-valued, finite Fourier series transformation of the acceleration response and that calculated for the model. More explanation and details about the parametric system identification technique can be found in Beck (1978) and McVerry (1979). This technique was not used in this study because the simpler non-parametric system identification technique based on the frequency-domain approach is deemed suitable for this resarch.

3.5 Analysis of the Chi Chi records

Acceleration records of the accelerographs installed in the buildings were analyzed in both the time domain and the frequency domain.

3.5.1 Variation of acceleration profiles along building height

Peak floor accelerations were obtained from the processed accelerograms. The amplification of floor accelerations at the different instrumented levels of each building is shown in the graphs of Figures 3-5 to 3-15. A_x is the height amplification factor and is equal to the ratio of acceleration at elevation h_x and the acceleration at grade level. Also shown are the acceleration amplification profiles suggested in the 2005 edition of the NBCC (NRC/IRC 2005) and the IBC (IBC 2000), ($1+ 2h_x/h_n$, continuous line), and the profile suggested by the 1997 UBC (ICBO 1997), ($1 + 3h_x/h_n$, dashed line). On these graphs, the reference input acceleration was taken as the free field acceleration if available, or the acceleration at grade level. Free field records are available for only 5 of the 11 buildings, namely CHYBA4, CHYBA5, CHYBA0, TCUBAA, and TCUBA0. The results for all buildings in principal directions X and Y are summarized in Figure 3-16, using normalized elevations. X and Y are the longitudinal and transverse geometric horizontal directions of the buildings, respectively.

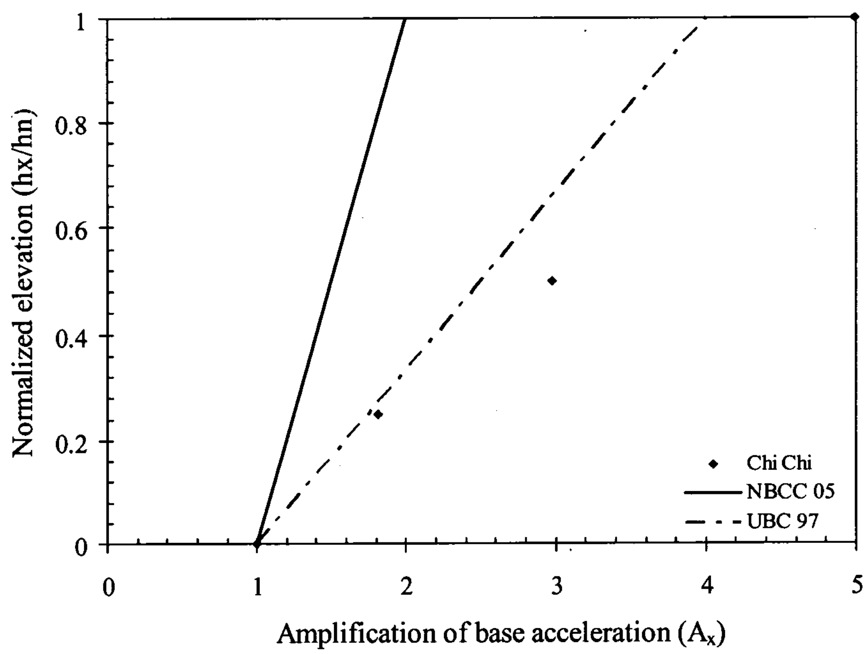

(a) X-direction

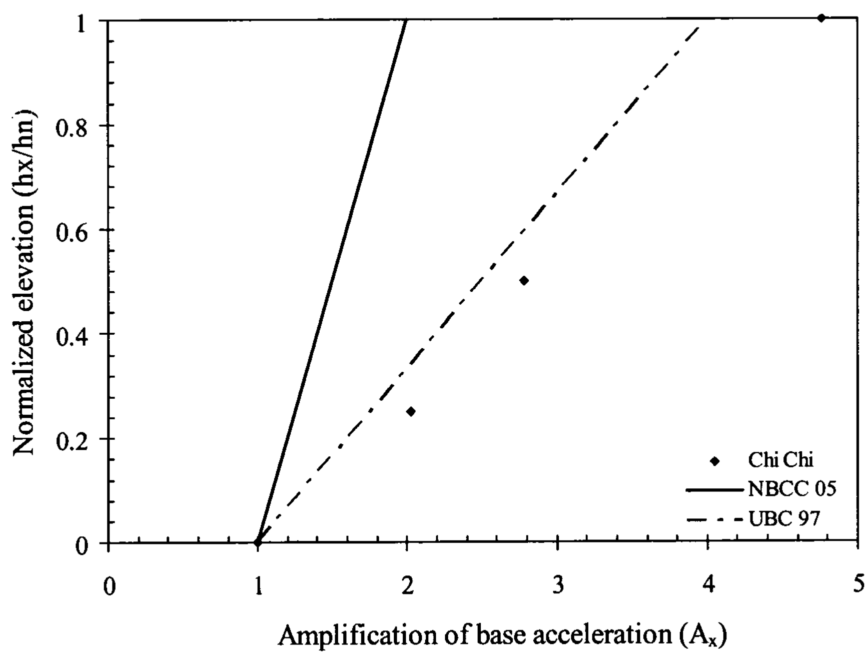

(b) Y-direction

Figure 3-5 Amplification of horizontal accelerations in CHYBA9
(a) X-direction (b) Y-direction

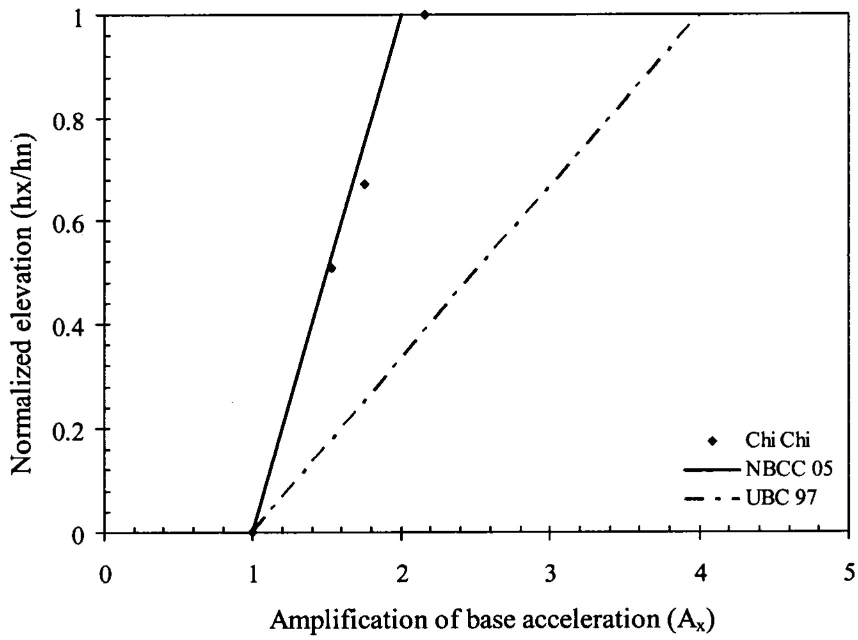

(a) X-direction

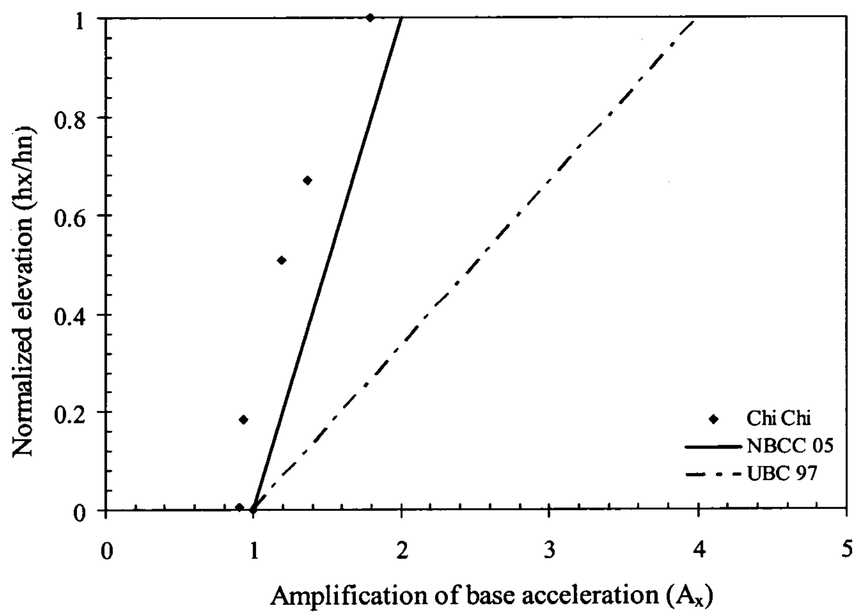

(b) Y-direction

Figure 3-6 Amplification of horizontal accelerations in CHYBA4
(a) X-direction (b) Y-direction

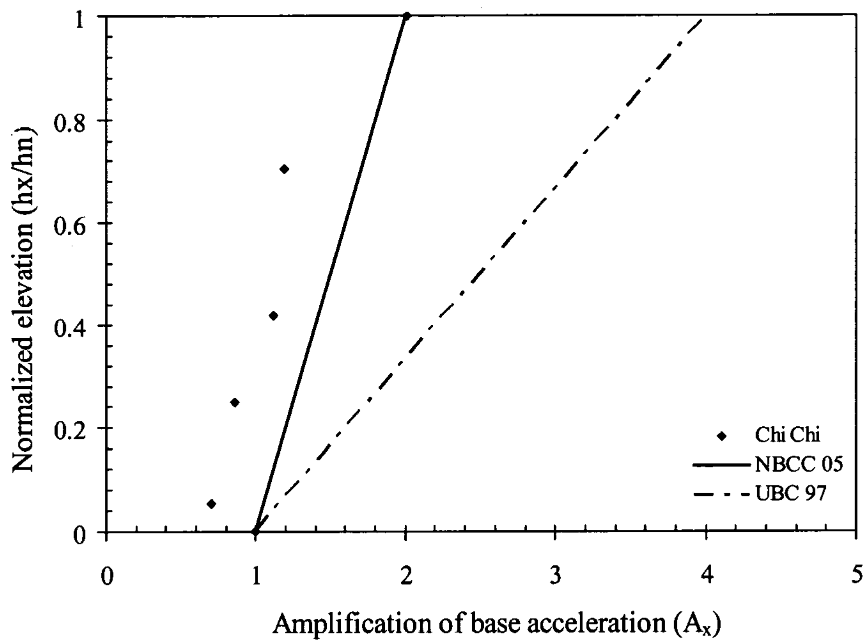

(a) X-direction

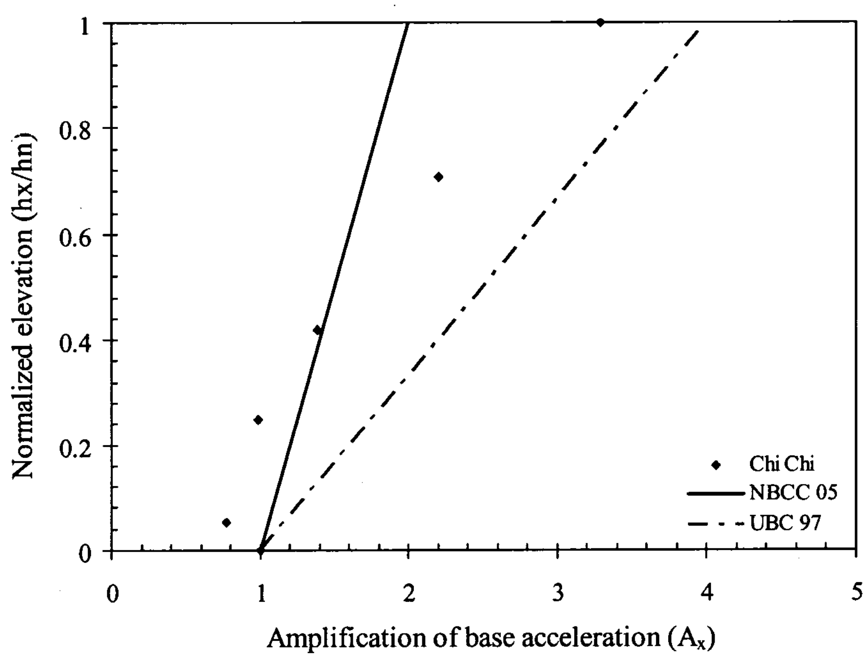

(b) Y-direction

Figure 3-7 Amplification of horizontal accelerations in CHYBA5
(a) X-direction (b) Y-direction

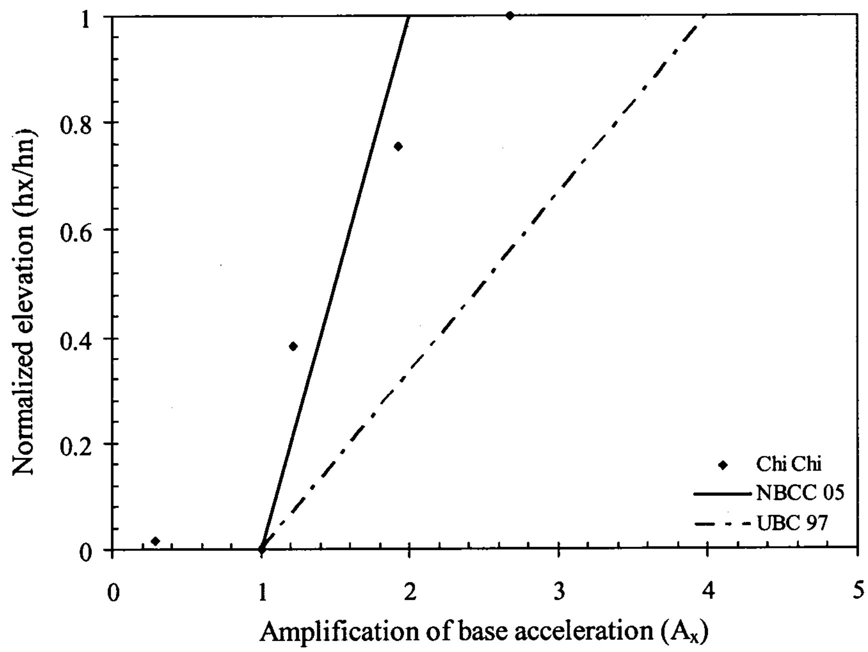

(a) X-direction

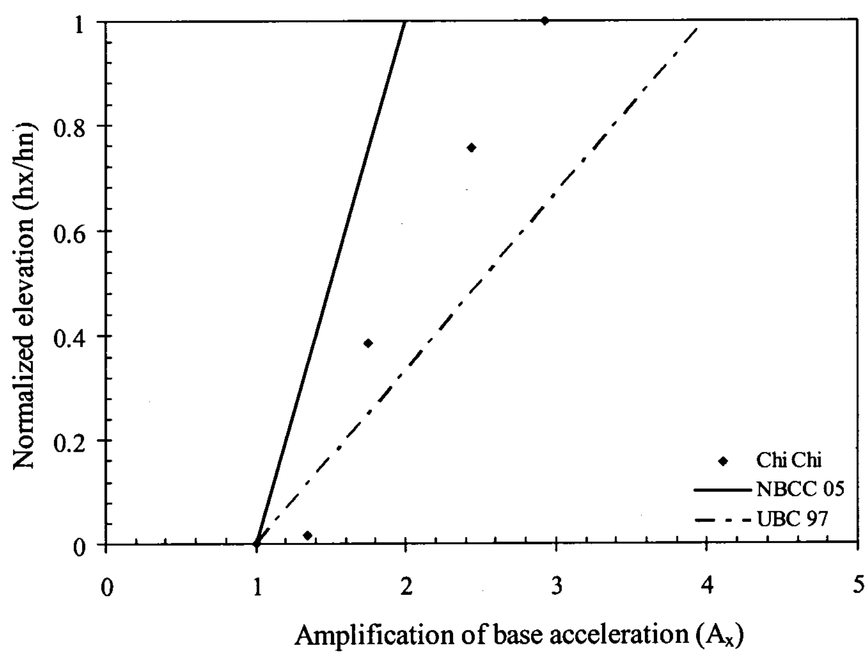

(b) Y-direction

Figure 3-8 Amplification of horizontal accelerations in TCUBA0
(a) X-direction (b) Y-direction

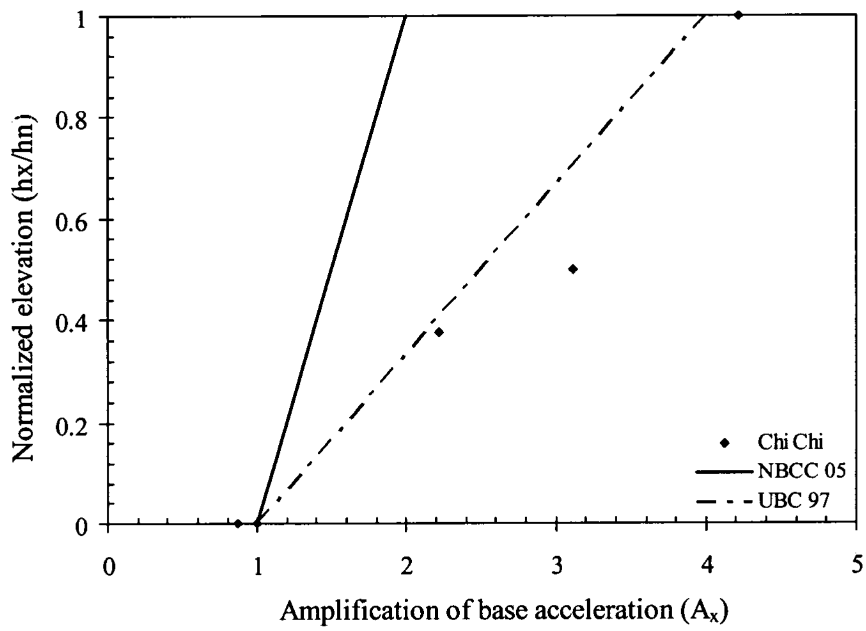

(a) X-direction

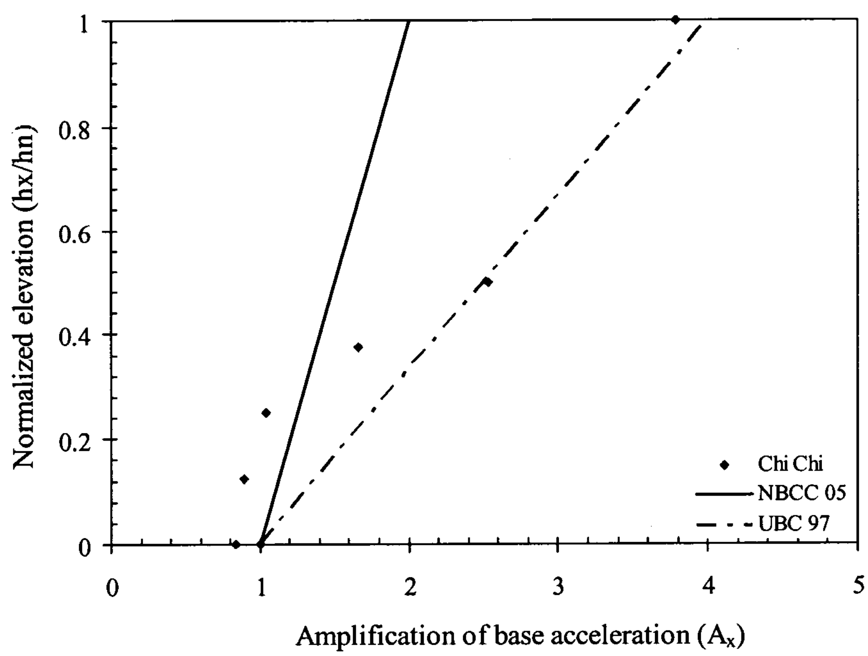

(b) Y-direction

Figure 3-9 Amplification of horizontal accelerations in TCUBAA
(a) X-direction (b) Y-direction

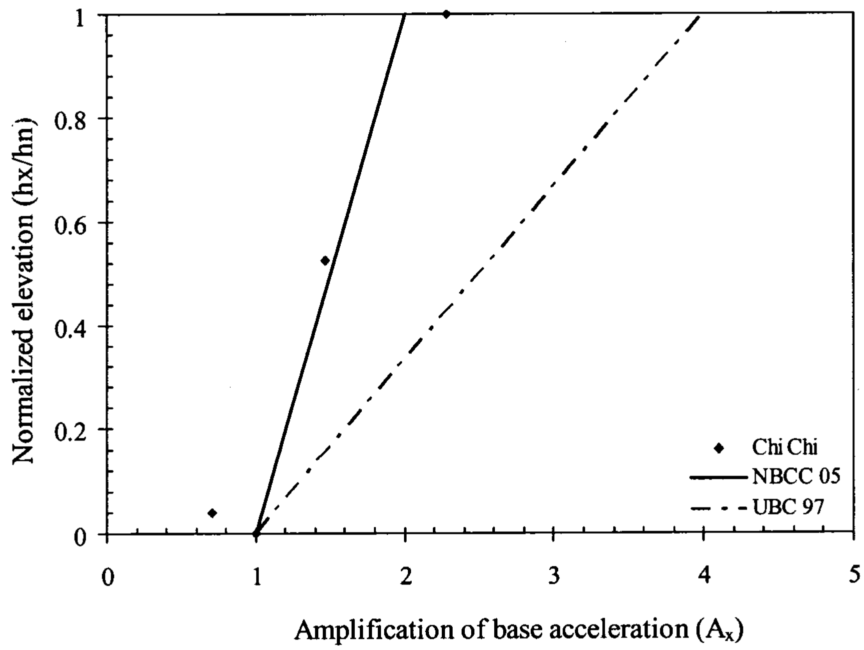

(a) X-direction

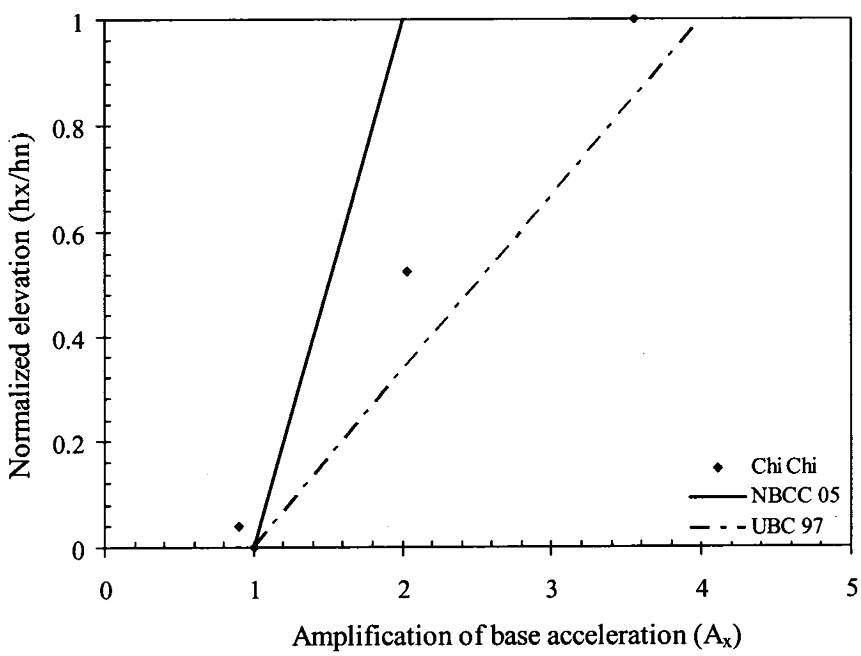

(b) Y-direction

Figure 3-10 Amplification of horizontal accelerations in CHYBA0
(a) X-direction (b) Y-direction

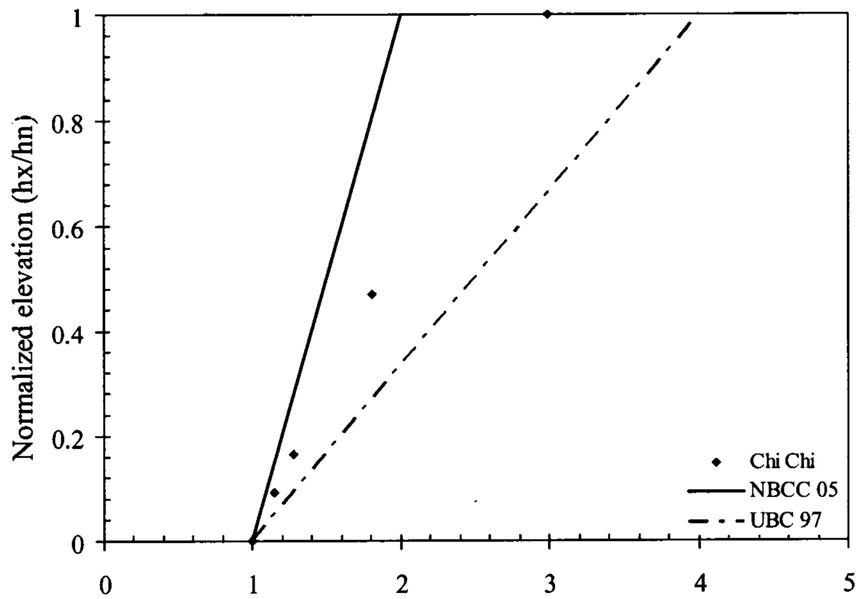

Amplification of base acceleration (A_x)

(a) X-direction

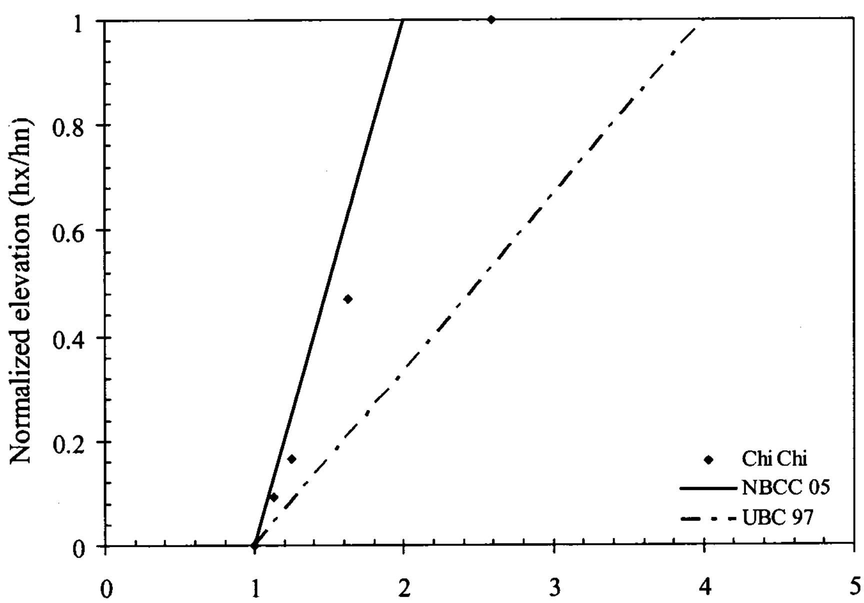

Amplification of base acceleration (A_x)

(b) Y-direction

Figure 3-11 Amplification of horizontal accelerations in TCUBA6
(a) X-direction (b) Y-direction

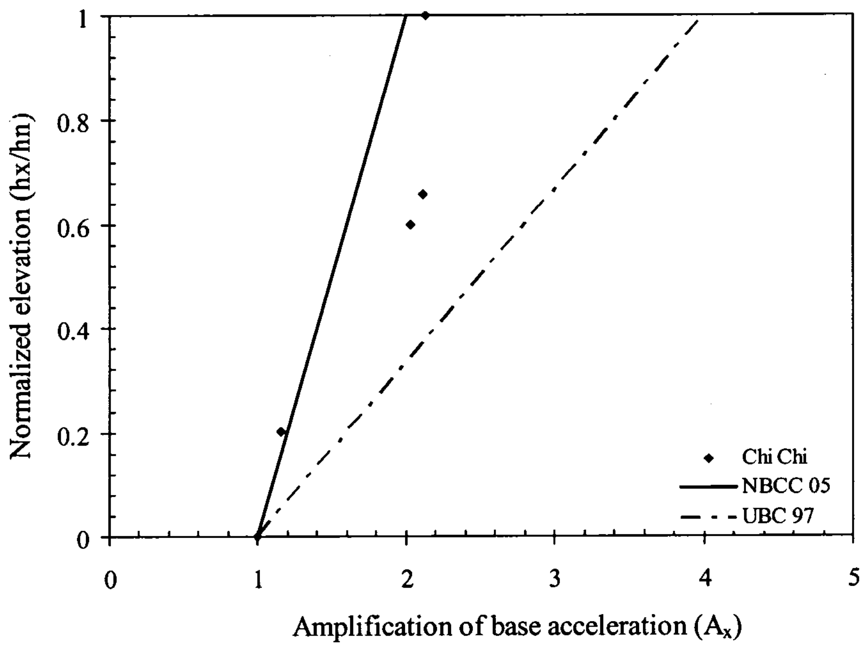

(a) X-direction

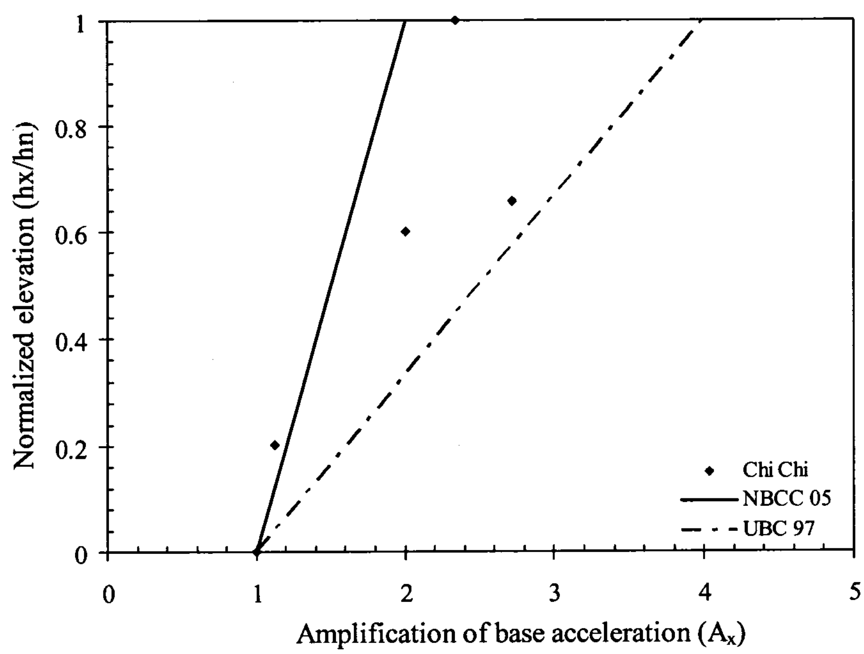

(b) Y-direction

Figure 3-12 Amplification of horizontal accelerations in TCUBA2
(a) X-direction (b) Y-direction

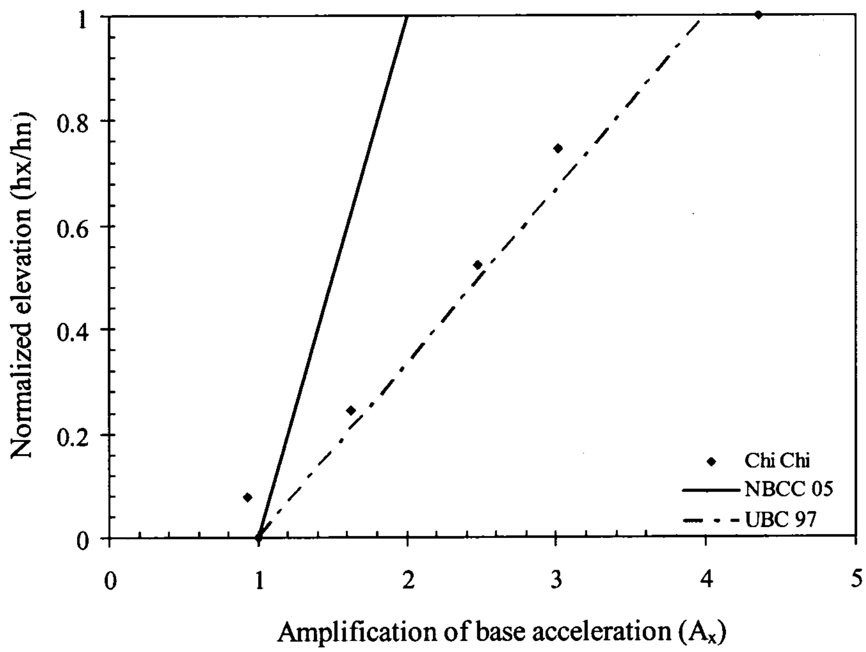

(a) X-direction

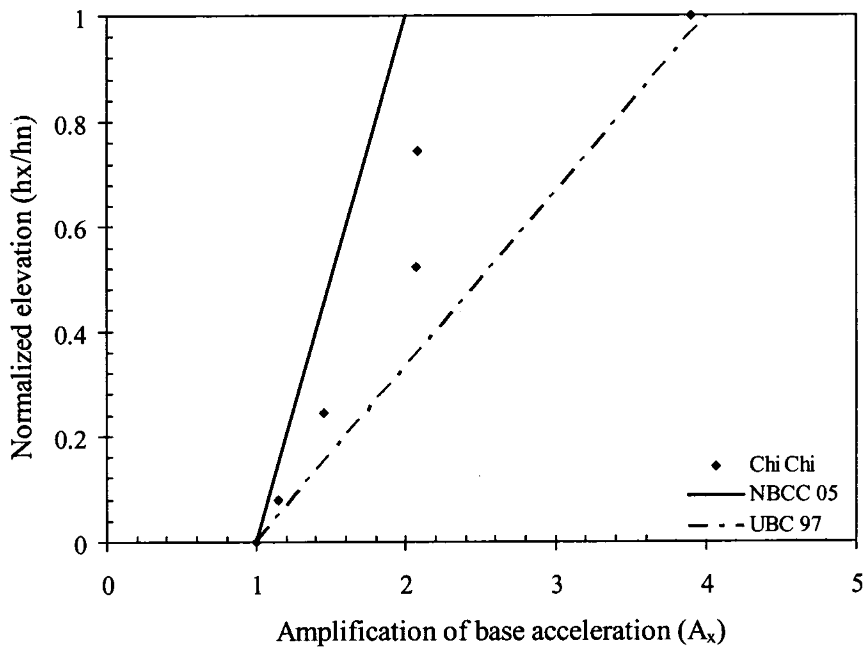

(b) Y-direction

Figure 3-13 Amplification of horizontal accelerations in TCUBA4
(a) X-direction (b) Y-direction

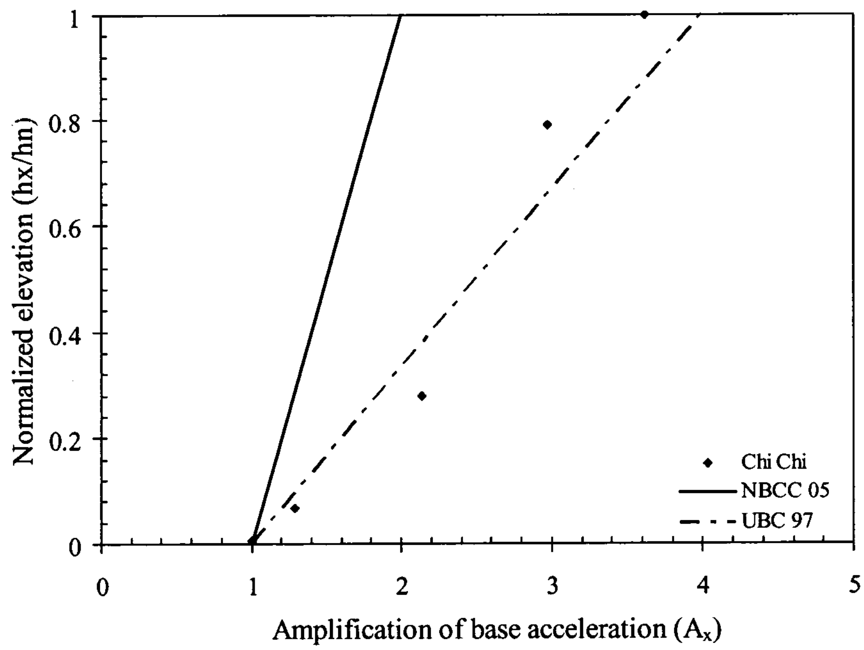

(a) X-direction

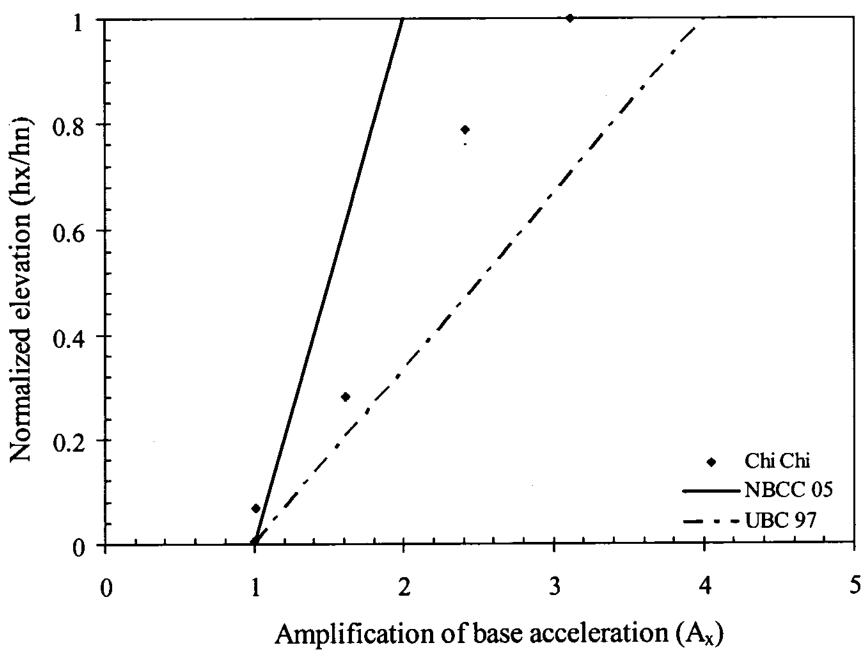

(b) Y-direction

Figure 3-14 Amplification of horizontal accelerations in CHYBA7

(a) X-direction (b) Y-direction

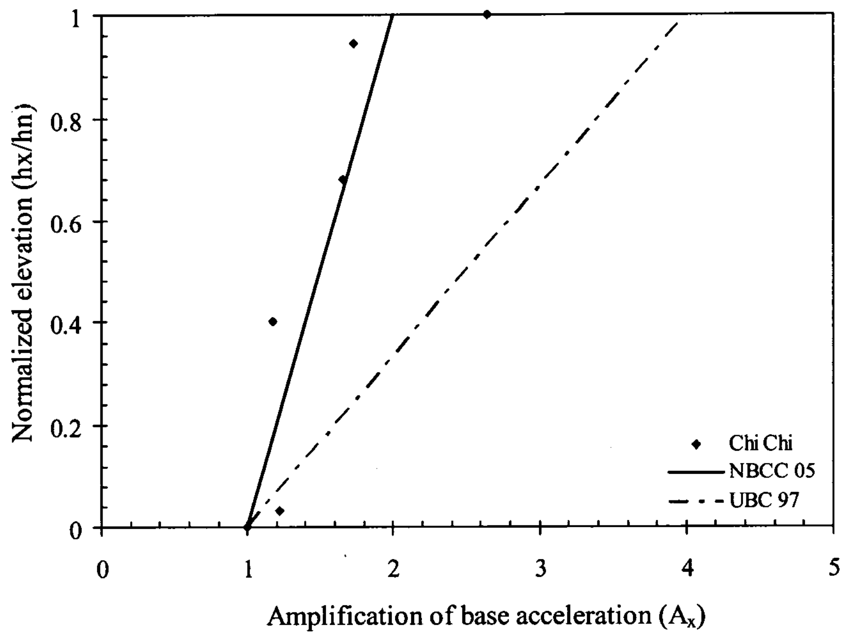

(a) X-direction

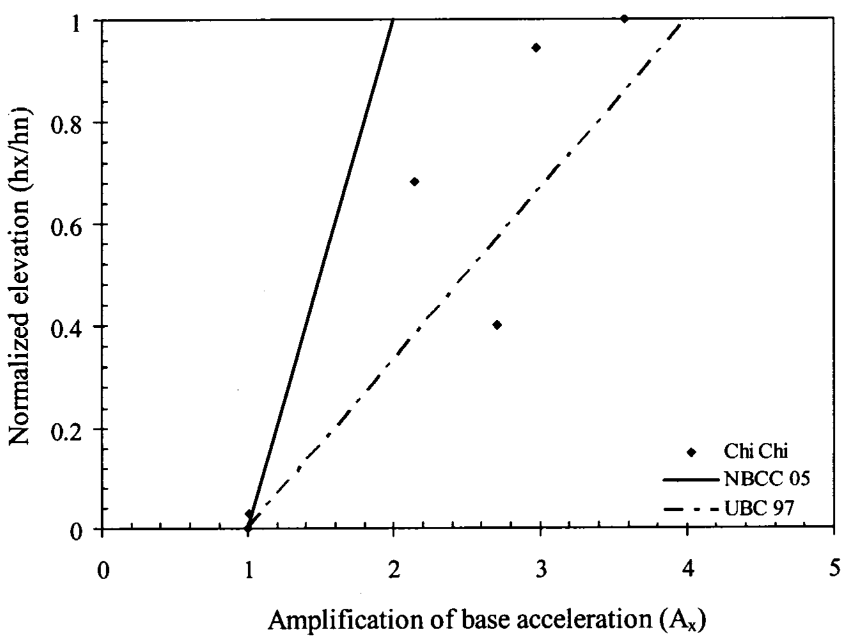

(b) Y-direction

Figure 3-15 Amplification of horizontal accelerations in TAPBA7
(a) X-direction (b) Y-direction

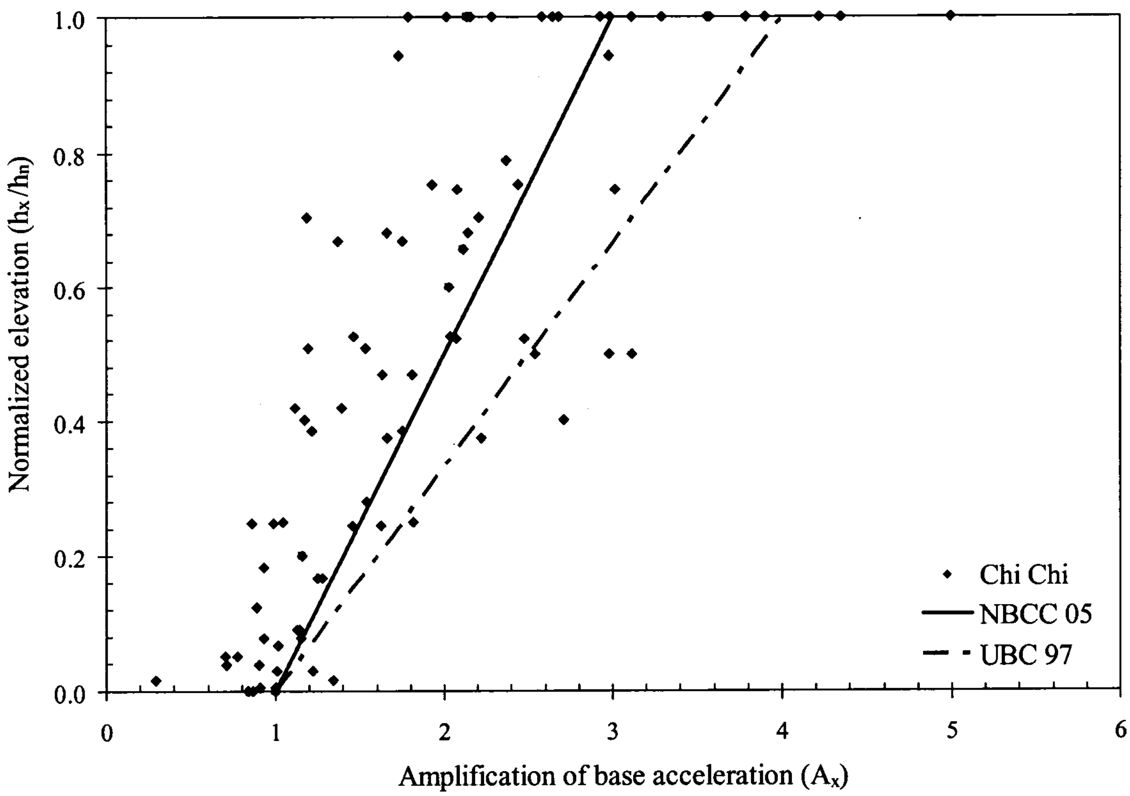

Figure 3-16 Peak floor acceleration amplification profiles for the 11 buildings studied in principal horizontal directions X and Y

3.5.2 Remarks on the acceleration amplification factor

Based on the plots of Figures 3-5 to 3-15, we observe that in case of flexible buildings, such as the buildings labeled TCUBA4, CHYBA7 and TAPBA7 (Figures 3-13, 3-14, and 3-15), the amplification of accelerations along the building height is more important at the upper part of the building. For low/medium-rise buildings having relatively regular geometry, such as the buildings labeled CHYBA9, CHYBA4, CHYBA5, TCUBA0, CHYBA0 and TCUBA6 (Figures 3-5, 3-6, 3-7, 3-8, 3-10, and 3-11), the rate of amplification of seismic accelerations is more uniform, indicating that the accelerations are mostly affected by the fundamental sway mode of the building. It should be noted that the buildings labeled TCUBAA and TCUBA2 (Figures 3-9 and 3-12) have a rather complex geometry. Also, for some buildings, the variation of the accelerations along the height may be different in orthogonal directions, depending on the corresponding structural properties. Overall, the maximum amplification of 4 at the rooftop level seems conservative, except for the building CHYBA9 (Figure 3-5), where the maximum acceleration amplification reaches a value of 5.

3.5.3 Rooftop accelerations and rooftop acceleration amplification factor

Peak rooftop accelerations are obtained from the processed accelerograms. The corresponding amplification ratios in the orthogonal horizontal directions X and Y are summarized in Table 3-2. The peak rooftop acceleration amplification ratio is defined as the ratio of peak acceleration at the rooftop level in one direction, A_{roof}, to the corresponding peak ground acceleration in the same direction, A_g. These measured ratios can be compared to the height amplification factor A_x proposed in the NBCC 2005 and the IBC 2000, which reaches a maximum value of 3 at the rooftop. Note that this recommendation is based on recorded strong motion data at sites with peak ground accelerations in excess of 0.1g (BSSC 2001), whereas all the recorded accelerations presented in Table 3-2 are much lower.

Table 3-2 Rooftop acceleration amplification

Building ID	Location	Peak accelerations (cm/s^2)					
		X - direction			Y - direction		
		A_g	A_{roof}	A_{roof}/A_g	A_g	A_{roof}	A_{roof}/A_g
CHYBA9	Tainan	36.47	182	5.00	37.1	177.0	4.76
CHYBA4	Jia-Yi	21.84	47.1	2.16	24.56	43.92	1.79
CHYBA5	Hsin-Yen	46.59	93.75	2.01	46.13	136.1	3.29
TCUBA0	Zhungli	43.57	118	2.71	45.00	130.0	2.90
TCUBAA	Hsinchu	28.68	121	4.21	35.71	135.2	3.79
CHYBA0	Tainan	22.46	51.27	2.28	35.71	135.2	3.56
TCUBA6	Hsinchu	54.05	161.5	2.99	52.4	135.4	2.58
TCUBA2	Miaoli	69.27	147	2.13	53.92	126.1	2.34
TCUBA4	Tao-Yuan	33.74	46.8	4.35	41.3	161.1	3.90
CHYBA7	Tainan	13.85	51.4	3.70	16.0	48.75	3.11
TAPBA7	Taipei	33.81	89.4	2.65	22.0	78.0	3.57

The mean value of the acceleration amplification ratios at the rooftop level for the 11 buildings presented in Table 3-2 is equal to 3.17 for the principal horizontal directions X and Y, with a standard deviation of 0.91. For the range of buildings studied, a maximum amplification ratio of 4 at the rooftop is suggested, as was proposed in the study of Bachman and Drake (1994, 1995) and the 1997 Uniform Building Code (ICBO 1997). In the 1995 edition of the NBCC (NRC/IRC 1995), A_x is defined as $1+h_x/h_n$, giving a maximum acceleration amplification of 2 at the rooftop, which is much less than the computed maximum acceleration amplification ratios for most of the buildings used in this study.

The mean percentage of difference in the acceleration amplification ratios in the orthogonal directions X and Y is 18%, which suggests that the codes assumption that the amplification is the same in both directions seems reasonable. As expected, this difference increases for buildings of complex geometry, and detailed analysis is usually necessary for these buildings. It is further observed that the maximum rooftop acceleration amplification ratio does not always occur in the direction of larger input ground acceleration, although the magnitude of acceleration is larger.

3.5.4 Correlation between rooftop acceleration amplification ratio and the number of stories

Since the acceleration amplification ratios were presented as a function of normalized elevation (h_x/h_n), the possible correlation between the number of stories and the maximum rooftop acceleration amplification ratio needs to be investigated. As indicated in Figure 3-17, there is no evidence of correlation between these two factors. These results support the fact that the number of stories is not a factor taken into account in the current code provisions.

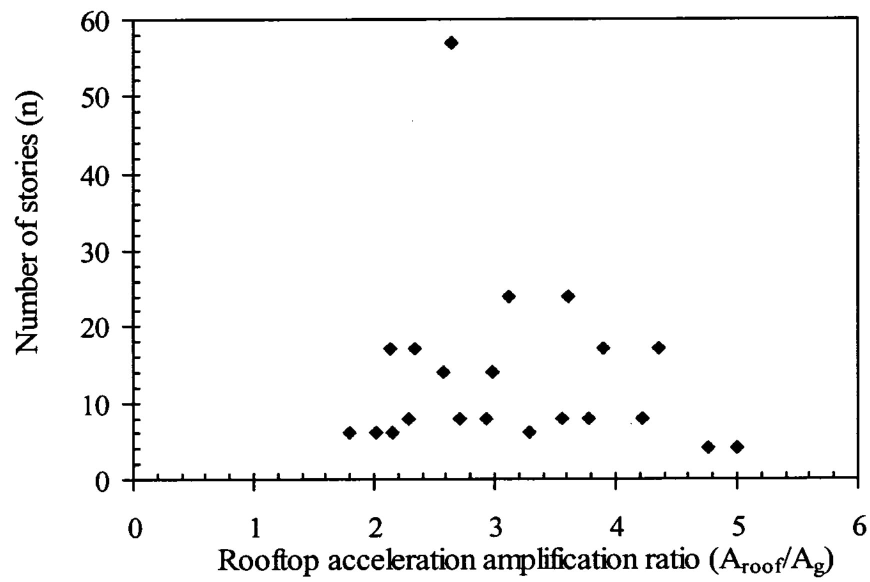

Figure 3-17 Number of stories versus the rooftop acceleration amplification ratio (A_{roof}/A_g)

3.6 Frequency-domain analysis

The first two fundamental periods of the buildings were extracted from the peaks of the transfer functions of the records; these transfer functions are presented in Appendix B. The fundamental periods extracted were then compared to values calculated from a previous study by Huang (1997), where the buildings were subjected to different earthquakes (labeled EQ in Table 3-3) of smaller amplitudes than those measured during the Chi Chi earthquake. Table 3-3 summarizes the results for the fundamental periods only, in the orthogonal directions X and Y.

In two cases, there was too much noise in the Chi Chi records; therefore, no clear peak could be identified. For the buildings labeled CHYBA9 and TCUBAA, ambient vibration tests were performed because no other earthquake records were available. The elongation of the fundamental periods of the buildings during the Chi Chi earthquake compared to previous events can be explained by the fact that concrete, in partition walls for example, may crack at relatively low levels of shaking; therefore, the response becomes slightly nonlinear, with softening behavior. As expected, the periods obtained from small amplitude ambient vibration tests are also shorter than those obtained during the Chi Chi earthquake.

Table 3-3 Comparison of building periods from the Chi Chi earthquake versus previous events

Building ID	Year of construction	Fundamental Period (s)			
		X - direction		Y - direction	
		Chi Chi	EQ	Chi Chi	EQ
CHYBA9*	1980	0.29	0.28	0.26	0.23
CHYBA4	1983	Too many peaks	0.52	0.31	0.32
CHYBA5	1984	0.42	0.38	0.38	0.30
TCUBA0	1994	0.59	0.54	0.55	0.49
TCUBAA*	1996	0.65	0.59	1.04	0.78
CHYBA0	1989	0.54	0.48	0.42	0.41
TCUBA6	1991	0.83	0.61	0.64	0.5
TCUBA2	1992	0.85	0.78	0.73	0.66
TCUBA4	1994	1.63	1.43	1.3	1.37
CHYBA7	1995	0.93	0.88	1.72	1.45
TAPBA7	1993	2.47	1.82	Too many peaks	1.52

* Periods obtained from ambient vibrations tests for these buildings, instead of previous earthquake.

3.6.1 Correlation between rooftop acceleration amplification ratios and the building periods

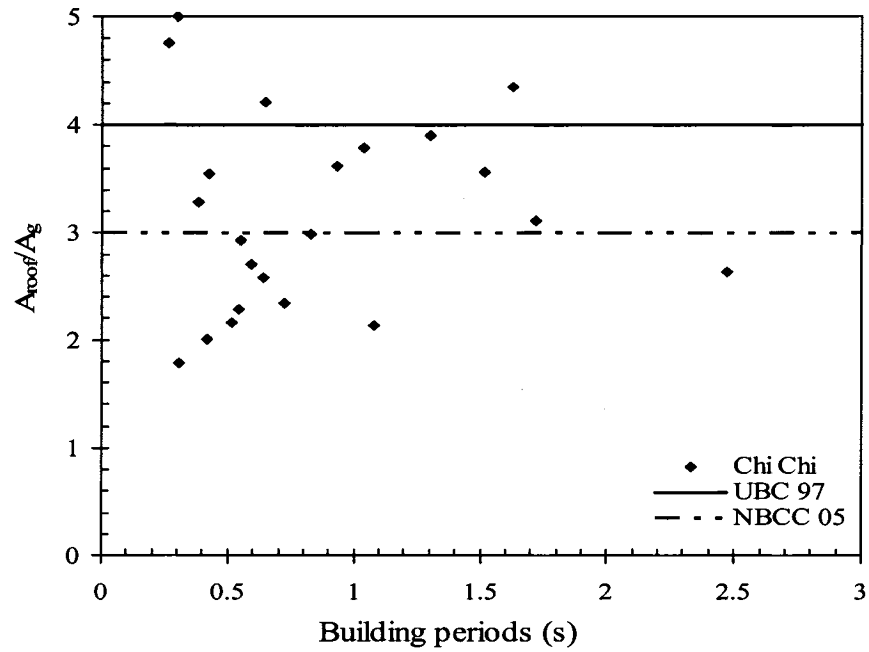

Figure 3-18 The rooftop acceleration amplification versus the building periods

Figure 3-18 shows the relationship between the acceleration amplification ratios at the rooftop of the buildings and their fundamental periods extracted from the Chi Chi records. Also shown are the maximum values of the suggested amplification ratios at the rooftop by the NBCC 2005 and the UBC 1997, for direct comparison. It is observed that for periods larger than 0.7s, the acceleration amplification factor at the rooftop does not always decrease with larger building periods; this is contrary to the trends in typical design spectra for buildings. Therefore, no strong correlation between the height factor and the building's period can be established.

3.7 Comparison of building periods extracted from the Chi Chi records with the values suggested in the NBCC 2005

The fundamental period of a building is an important design parameter, especially for the calculation of seismic design base shear forces and for the evaluation of spectral accelerations. Several empirical formulas are suggested in the 2005 edition of the NBCC to calculate the fundamental period of vibration of buildings, T_a, corresponding to different lateral load resisting systems; they are given in Equations 3-12 to 3-16:

For concrete moment frames:

$$T_a = 0.075(h_n)^{\frac{3}{4}} \tag{3-12}$$

For steel moment frames:

$$T_a = 0.085(h_n)^{\frac{3}{4}} \tag{3-13}$$

For all other moment frames:

$$T_a = 0.1N \tag{3-14}$$

For braced frames:

$$T_a = 0.025h_n \tag{3-15}$$

For shear walls and other structures:

$$T_a = 0.05(h_n)^{\frac{3}{4}} \tag{3-16}$$

Where N is the number of stories above grade level and h_n is the total height of the building above the base in m.

The fundamental periods of the 11 buildings calculated from Equations 3-12 to 3-16 and those extracted from the records of the Chi Chi earthquake are presented in Table 3-4, where the ratio of the NBCC 2005 prediction to the measured value is also given.

Table 3-4 Comparison of building periods extracted from the Chi Chi records and calculated with the NBCC 2005 formulas

Building ID	Year of construction	Fundamental Period (s)					
		X-direction			Y-direction		
		Chi Chi	NBCC 05	Ratio	Chi Chi	NBCC 05	Ratio
CHYBA9	1980	0.29	0.47	1.58	0.26	0.47	1.80
CHYBA4	1983	-	0.82	-	0.31	0.82	2.66
CHYBA5	1984	0.42	0.79	1.87	0.38	0.79	2.07
TCUBA0	1994	0.59	1.01	1.72	0.55	1.01	1.84
TCUBAA	1996	0.65	0.97	1.49	1.04	0.97	0.93
CHYBA0	1989	0.54	0.97	1.79	0.42	0.97	2.29
TCUBA6	1991	0.83	1.25	1.51	0.64	1.25	1.95
TCUBA2	1992	0.85	1.54	1.42	0.73	1.54	2.11
TCUBA4	1994	1.63	1.79	1.10	1.30	1.79	1.37
CHYBA7	1995	0.93	1.91	2.06	1.72	1.91	1.11
TAPBA7	1993	2.47	4.34	1.76	-	4.34	-

The results shown in Table 3-4 indicate that fundamental periods calculated from Equations 3-12 to 3-16 as proposed in the NBCC 2005 are larger (with only one exception) than the periods extracted from experimental measurements. The discrepancy in the results suggests that the equations in the NBCC 2005 provide only rough estimates of the actual building periods and need further calibration. In addition, the average of periods given by Equations 3-12 and 3-13 was used for computing the fundamental periods for the TAPBA7 and TCUBA4 buildings since no expression exists in the NBCC for this kind of lateral load resisting system (SRC). Also, Equation 3-14 yields an unrealistic estimate for the high-rise building TAPBA7.

3.8 Conclusions

In this chapter, the amplification of seismic accelerations along a building elevation has been discussed, based on the analysis of acceleration records of 11 instrumented buildings located in Taiwan. It was observed that the height amplification factor, $A_x = 1+3h_x/h_n$, is more conservative for the upper levels of the building near the rooftop, and for the lowest levels within 30% of the total height. For the range of buildings studied, the maximum rooftop acceleration amplification factor of 3 as proposed in the NBCC 2005 agrees fairly well with the experimental results, especially for the range of building periods below 0.7 s, with three exceptions. For more flexible structures or structures with discontinuities in the vertical direction, the acceleration amplification factors at the rooftop level lie in the range of 3 to 4; therefore, we propose an acceleration amplification factor of 4 in the range of periods below 1.7 s. For the most flexible structure, TAPBA7, the acceleration amplification factor is less than 3. We believe that more case studies of very flexible buildings are needed before final conclusions can be drawn. For the whole set of data, a rooftop acceleration amplification factor of 4 envelopes 82% of the cases and is then recommended for use in design. Besides, no strong correlation can be established between the height factor and either the building's period or its number of stories. Finally, since all the buildings studied were far from the epicenter (70 km and more), it is suggested to study buildings having near-source earthquake records with different frequency characteristics in order to verify whether these observations remain valid. Also, It was found that the equations suggested in the NBCC 2005 to compute the fundamental building periods provide only rough estimates of the actual values and need further calibration.

Chapter 4
Finite Element Models of Building/Tower Systems and Rooftop Accelerations

Detailed 3-D finite element models of four buildings having different lateral load resisting systems and four telecommunication towers were generated in the commercial software SAP 2000 v.8.2.3 (Wilson and Habibullah 2003). The self-supporting steel lattice telecommunication towers of different heights (10-30m) and geometric properties were assumed to be mounted on the rooftop of the four buildings. The detailed finite element model of each building-tower combination was subjected to two sets of earthquake records, applied to the buildings' longitudinal and transverse directions, U1 and U2, separately. First, details of the geometric properties of the buildings and towers, the modeling assumptions, and the earthquake records are presented. Secondly, the rooftop acceleration demands in the buildings resulting from numerical simulations are discussed. Results of the numerical simulations for the building-tower combinations are presented in Chapter 5.

4.1 Geometric properties of the buildings and towers

4.1.1 Buildings

The building labeled CHYBA9 (see Table 3-1) is a five-story building owned by China Telecom and located in a small town of Tainan County, which is about 120 km from the 1999 Chi Chi epicenter. This 20 m high reinforced concrete telecommunication building was built in 1980. The lateral load resisting system consists of a combination of concrete moment resisting frames and predominant structural walls. Of particular interest is that the building is extensively instrumented at several locations (18 sensors) and supports on its rooftop a 10 m self-supporting steel lattice telecommunication tower (labeled TC1) having a 4.7 m × 4.7 m square base. The tower is also equipped with 3 sensors in the x, y, and z directions at its mid-height. As shown in Table 3-2, the maximum absolute accelerations measured during the 1999 Chi Chi earthquake at the grade level are 36.47 cm/s^2 in the longitudinal direction and 37.1 cm/s^2 in the transverse direction, while at the rooftop level the maximum absolute accelerations are 182 cm/s^2 in the longitudinal direction and 177 cm/s^2 in the transverse direction. Therefore, the maximum rooftop acceleration amplification is 5.0 in the longitudinal direction and 4.76 in the transversal direction. Figure 4-1 shows a photograph and an elevation view of this building illustrating the instrumentation scheme.

The building labeled CHYBA4 (see Table 3-1) is a 7-story building located in Jia-Yi city, which is about 72 km from the 1999 Chi Chi epicenter. This 24 m high reinforced concrete hospital was built in 1983. The lateral load resisting system consists of a combination of concrete moment resisting frames and structural walls. Figure 4-2 shows a photograph and an elevation view of this building illustrating the instrumentation scheme.

The building is equipped with 26 sensors. As shown in Table 3-2, the maximum free-field accelerations measured during the 1999 Chi Chi earthquake are 21.84 cm/s^2 in the longitudinal direction and 24.56 cm/s^2 in the transverse direction, while at the rooftop level the maximum absolute accelerations are 47 cm/s^2 in the longitudinal direction and 44 cm/s^2 in the transverse direction. Therefore, the rooftop acceleration amplification is 2.16 in the longitudinal direction and 1.8 in the transverse direction. The maximum absolute accelerations at the grade level are 18.52 cm/s^2 in the longitudinal direction and 22.25 cm/s^2 in the transverse direction. For this building, free field records match very well with those at the basement, indicating that there was no soil-structure interaction (Figure 4-3).

The building labeled TCUBAA (see Table 3-1) is a 9-story building in Hsinchu city, which is about 113.6 km from the 1999 Chi Chi epicenter. This 30.5 m high reinforced concrete university library was built in 1996. The lateral load resisting system consists of a combination of predominant concrete moment resisting frames and structural walls. Special features of this building are that it is located on a slope, its geometry is relatively complex, and it suffered serious non-structural seismic damage in 1999. Figure 4-4 shows a photograph and an elevation view of this building illustrating the instrumentation scheme. The building is equipped with 28 sensors. As shown in Table 3-2, the maximum free-field accelerations measured during the 1999 Chi Chi earthquake are 28.7 cm/s^2 in the longitudinal direction and 35.7 cm/s^2 in the transverse direction, while at the rooftop level the maximum absolute accelerations are 121.04 cm/s^2 in the longitudinal direction and 135.22 cm/s^2 in the transverse direction. Therefore, the rooftop acceleration amplification is 4.2 in the longitudinal direction and 3.8 in the transverse direction. The maximum absolute accelerations at the grade level are 25.4 cm/s^2 in the longitudinal direction and 30.6 cm/s^2 in the transverse direction. For this building, free field records match very well with those at the grade level, indicating that there was no soil-structure interaction (Figure 4-5).

The building labeled 2020 University is a 27-story building located in downtown Montreal on University Street. This 115.2 m high reinforced concrete office building was built in 1973. The lateral load resisting system is composed of reinforced concrete moment frames and a shear wall elevator core. An isometric view of the building is shown in Figure 4-6. Although there is no seismic instrumentation in this building, we have retained it to provide a Montreal building example subjected to the NBCC 2005 seismic hazard levels.

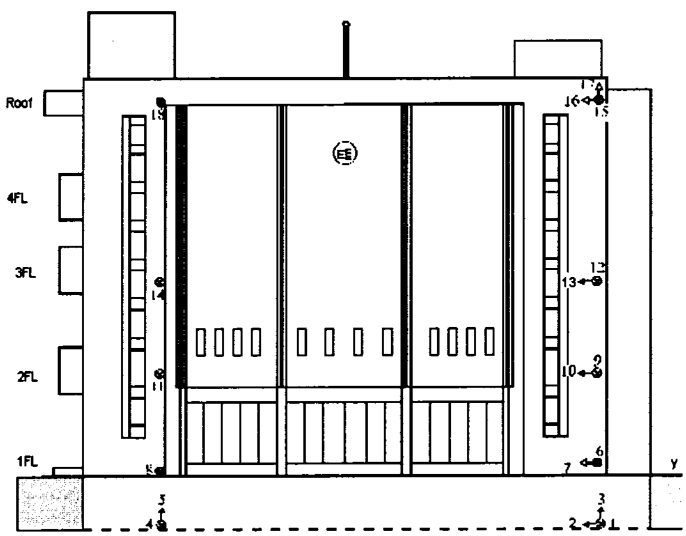

Figure 4-1 Isometric and facade elevation views of the CHYBA9 building

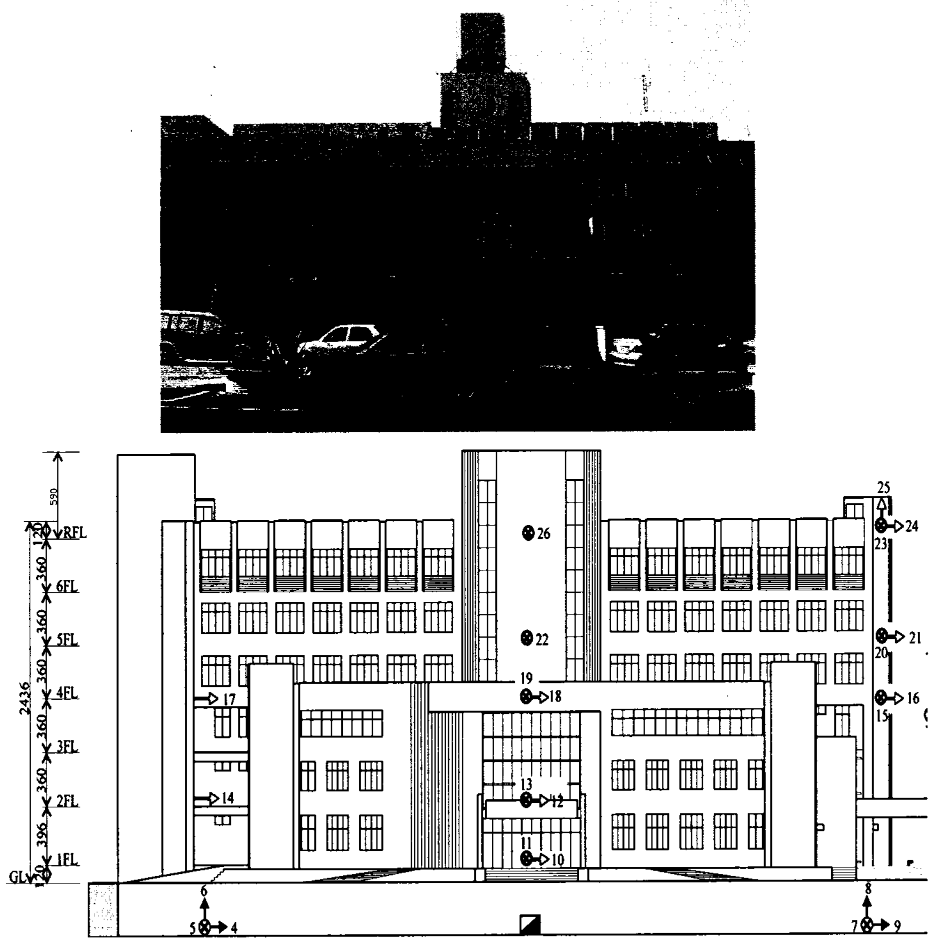

Figure 4-2 Isometric and facade elevation views of the CHYBA4 building

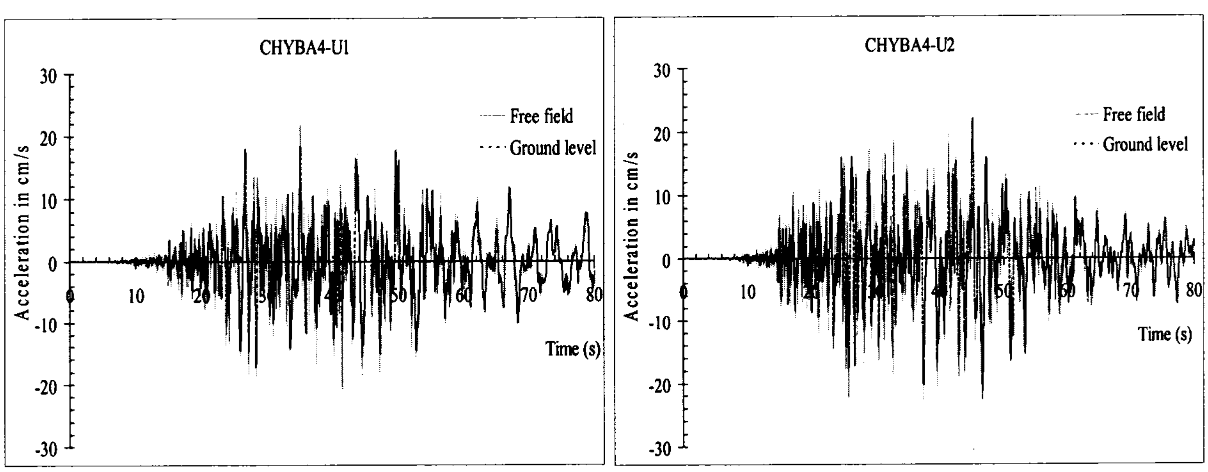

Figure 4-3 Free field and ground level accelerograms of CHYBA4 in the directions U1 and U2

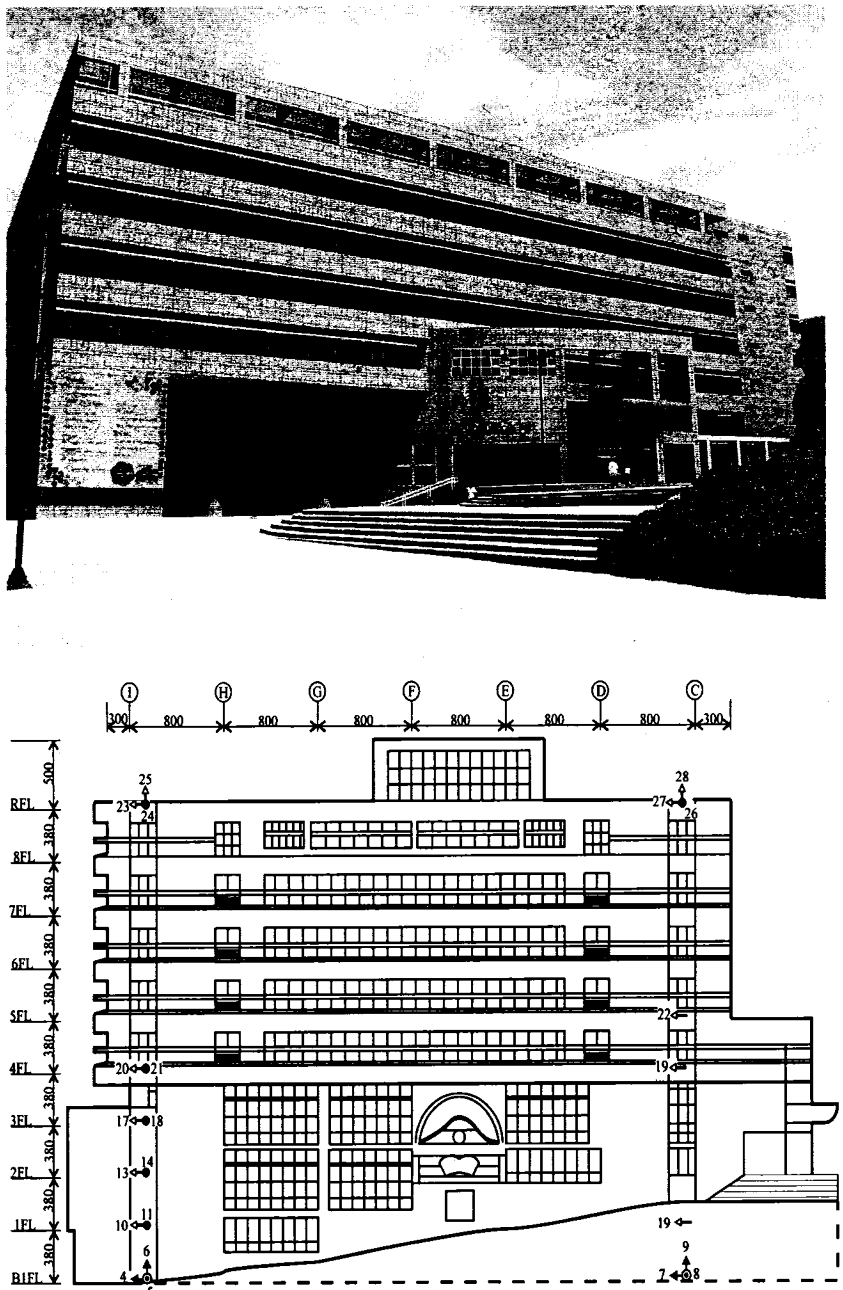

Figure 4-4 Isometric and facade elevation views of the TCUBAA building

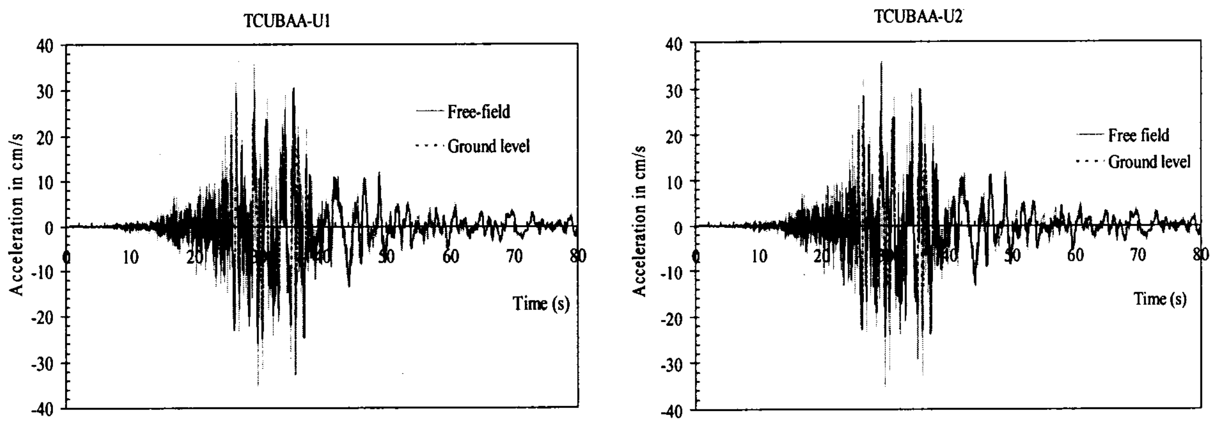

Figure 4-5 Free field and ground level accelerograms of TCUBAA in the directions U1 and U2

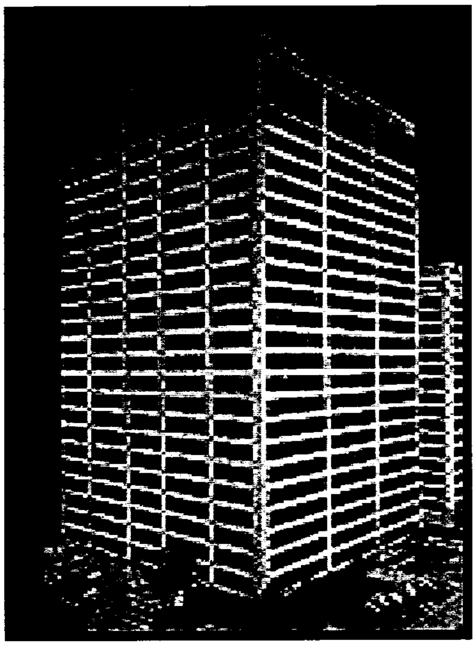

Figure 4-6 Isometric view of the 2020 University building in Montreal

4.1.2 Steel lattice towers

Three typical medium-height towers and one short rigid tower were studied. The tower labeled TC1 is a 4-legged lattice tower having a square base. This tower is the only one that is actually mounted on a building (CHYBA9). The towers labeled TC2, TC3, and TC4 are 3-legged lattice towers and their bases form equilateral triangles. Table 4-1 summarizes the geometric properties of the towers, including the type, height, base width, top width, and total mass of the bare framework, except for TC1 whose mass includes all antennas and appurtenances.

Table 4-1 Geometric properties of the telecommunication towers

Tower ID	Type	Height (m)	Base width (m)	Top width (m)	Mass (kg)
TC1	4-legged	10.73	4.7	0.7	9566
TC2	3-legged	30	2.5	1.5	2245
TC3	3-legged	20	2.5	1.5	1735
TC4	3-legged	20	5.5	1.3	2920

4.2 Modeling assumptions

4.2.1 Buildings

Three-dimensional elastic models of the four buildings were generated in SAP 2000 version 8.2.3 (Wilson and Habibullah 2003). Isometric views of the wire meshes of these building models are shown in Figures 4-7 to 4-10. The floors are assumed as rigid diaphragms in all models. Masses of slabs, external and inner walls were lumped in the three Cartesian directions at columns and walls according to their tributary area. The mass of floors was increased by 20% to account for non-structural components and finishing. The concrete material used in the models has a density of 23600 N/m^3 and a compressive strength of 27.6 MPa. Detailed structural drawings were available for the three Taiwanese buildings, while only structural sketches were available for the 2020 University model, which had been used as a case study in a structural dynamics course at McGill University. In the CHYBA9 and the 2020 University models, the shear walls were modeled as equivalent shear beam/column members, while in the TCUBAA and CHYBA4 models the shear walls were modeled as plane stress panel elements.

In all cases, the foundations are assumed to be rigid enough to provide a fixed base to the buildings; consequently, soil-structure interaction is neglected. The dynamic analysis is done by modal superposition using 20 modes of vibration and a viscous damping ratio of 3% critical for all modes, which is a common practice for elastic buildings and for bolted steel lattice structures. The Taiwanese models are calibrated using the recorded floor accelerograms from 1999 the Chi Chi earthquake, the fundamental periods extracted by system identification techniques as discussed in Chapter 3, and the results of ambient vibration tests whenever available (Tables 4-2 to 4-4). The dynamic properties for the first three modes of the building models are summarized in Table 4-5.

Table 4-2 Comparison of existing building and generated model for CHYBA9

	CHYBA9	Chi Chi records	Ambient vibration	Other EQ	SAP model
Maximum accelerations (cm/s^2)	Channel 6	35.73	N/A	N/A	32.67
	Channel 7	37.1	N/A	N/A	29.84
	Channel 9	55	N/A	N/A	52.27
	Channel 10	75.22	N/A	N/A	59.66
	Channel 12	93.6	N/A	N/A	86.00
	Channel 13	93.9	N/A	N/A	95.93
	Channel 15	144	N/A	N/A	141.19
	Channel 16	178	N/A	N/A	167.55
Periods (s)	T_1	0.29	0.28	0.28	0.30
	T_2	0.26	0.23	0.23	0.26

Table 4-3 Comparison of existing building and generated model for CHYBA4

	CHYBA4	Chi Chi records	Other EQ	SAP model
Maximum accelerations (cm/s^2)	Channel 10	17.25	N/A	19.11
	Channel 11	22.25	N/A	22.70
	Channel 12	20.11	N/A	23.27
	Channel 13	22.60	N/A	23.00
	Channel 18	25.45	N/A	44.90
	Channel 19	29.22	N/A	30.00
	Channel 22	33.60	N/A	35.00
	Channel 26	45.70	N/A	44.00
Periods (s)	T_1	N/A	0.51	0.41
	T_2	0.31	0.32	0.31

Table 4-4 Comparison of existing building and generated model for TCUBAA

	TCUBAA	Chi Chi records	Ambient vibration	SAP model
Maximum accelerations (cm/s^2)	Channel 5	29.87	N/A	35.63
	Channel 7	24.83	N/A	28.57
	Channel 11	31.74	N/A	36.04
	Channel 14	37.17	N/A	36.04
	Channel 18	59.34	N/A	69.04
	Channel 19	63.7	N/A	51.30
	Channel 21	90.58	N/A	82.06
	Channel 22	89.37	N/A	99.83
	Channel 24	135.2	N/A	150.68
	Channel 27	120.6	N/A	152.75
Periods (s)	T_1	1.04	0.77	0.75
	T_2	0.65	0.59	0.69

Tables 4-2 to 4-4 show that the natural periods of the generated elastic models and those extracted from the records match well, indicating that the response of the buildings was linear elastic or only slightly nonlinear. In addition, the floor acclerations of the existing buildings and their generated models are in good agreement. The small differences between recorded and computed accelerations can be attributed to the effects of initial defects, poor workmanship, the limitations of current analytical methods, and modeling assumptions.

Table 4-5 Natural periods of the buildings from FE models

Building ID	T_1 (s)	T_2 (s)	T_3 (s)
CHYBA9	0.30 (sway)	0.26 (sway)	0.18 (torsional)
CHYBA4	0.41 (sway)	0.31 (sway)	0.24 (torsional)
TCUBAA	0.75 (sway)	0.69 (sway)	0.62 (torsional)
2020 University	2.01 (sway)	1.90 (sway)	1.36 (torsional)

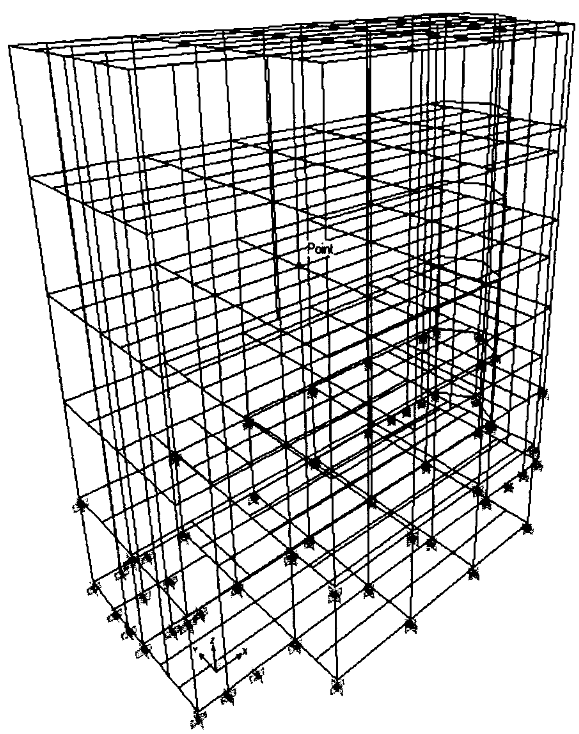

Figure 4-7 3-D finite element model of the CHYBA9 building

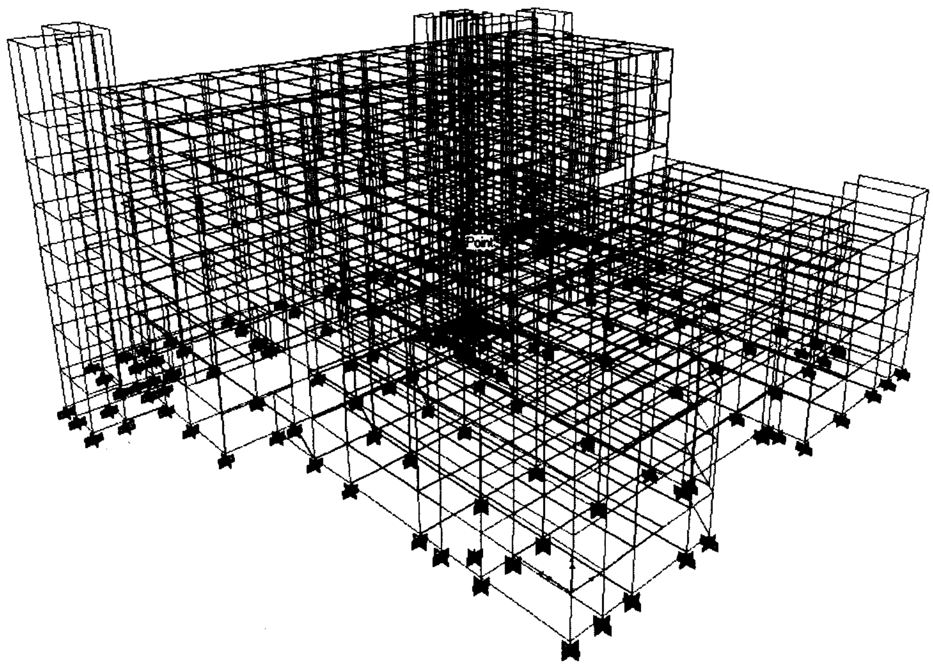

Figure 4-8 3-D finite element model of the CHYBA4 building

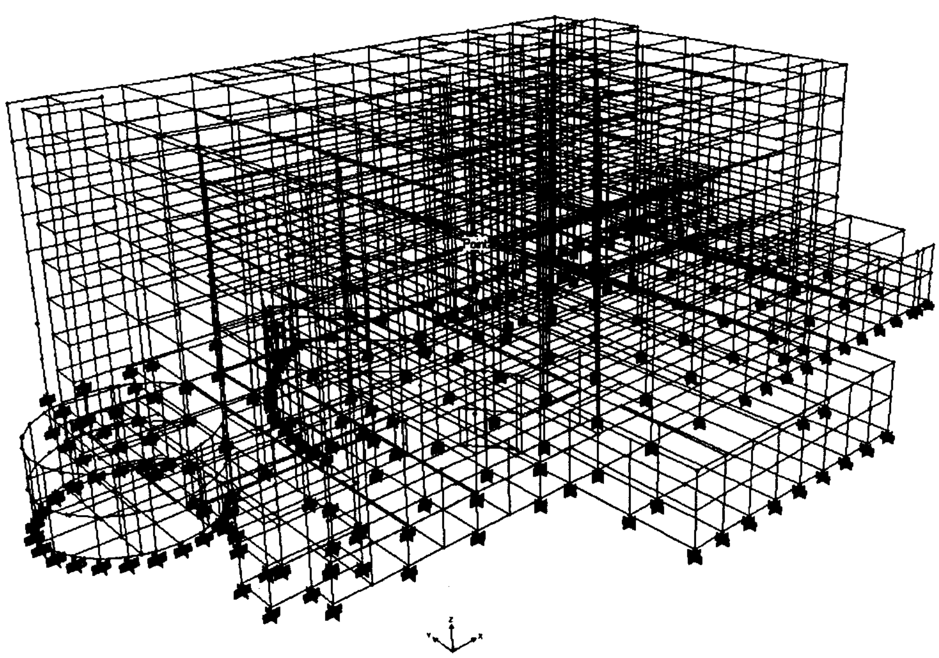

Figure 4-9 3-D finite element model of the TCUBAA building

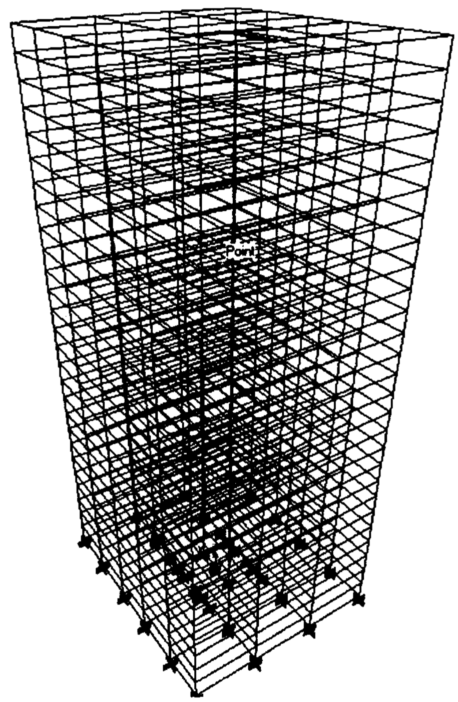

Figure 4-10 3-D finite element model of the 2020 University building

4.2.2 Steel lattice towers

The towers were modeled in SAP 2000 as three-dimensional frame-truss linear elastic structures. Frame elements were used for the main legs and truss elements for diagonal and horizontal members. All secondary and redundant members were removed from the numerical models because they did not contribute any stiffness, but their masses were lumped to stable leg joints. The mass of the main legs and their corresponding bracing members were lumped at the leg joints in order to avoid local spurious modes of vibration. The towers were attached to the buildings by rigid vertical frame elements protruding from the rooftop. Figures 4-11 and 4-12 show the actual attachment of the TC1 tower to the CHYBA9 building. In all cases, the towers were assumed to be rigidly connected to the building models at the building-tower interface. Figure 4-13 shows the wire meshes of the numerical models of the four towers studied, and Table 4-6 summarizes their dynamic properties as calculated on a rigid base. The towers were modeled without any attachment, except in the case of the TC1 tower where detailed architectural/equipment drawings are available. The appurtenances and antennas attached to a tower increase its mass and fundamental period of vibration and, consequently, its mode shapes.

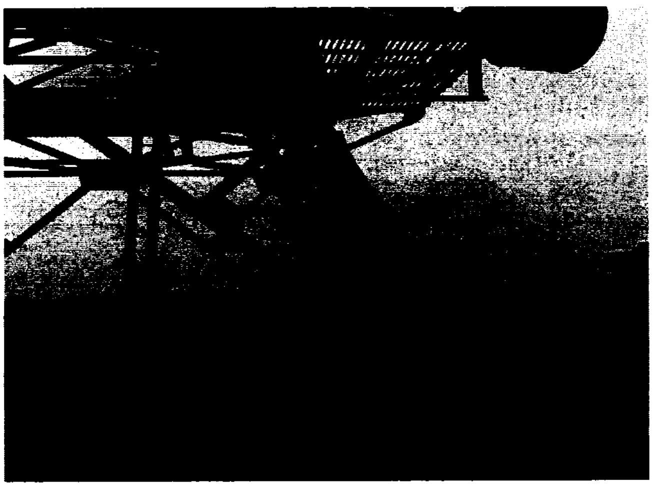

Figure 4-11 Tower base

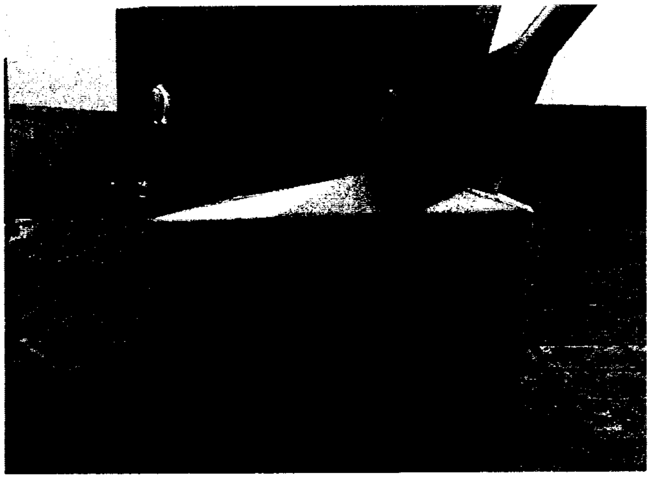

Figure 4-12 Close-up of the tower base

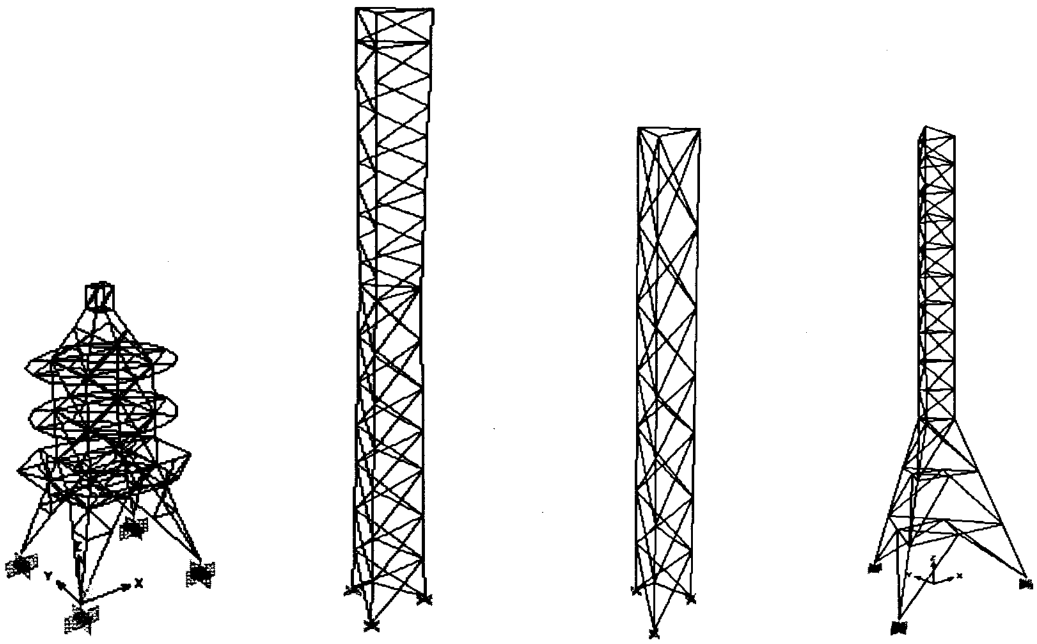

(a) TC1 (b) TC2 (c) TC3 (d) TC4

Figure 4-13 Finite element meshes of the generated tower models

Table 4-6 Dynamic properties of the towers

Tower ID	Type	T_1 (s)	T_2 (s)	T_3 (s)	T_4 (s)
TC1	4-legged	0.138 (flexural)	0.135 (flexural)	0.095 (torsional)	0.095 (flexural)
TC2	3-legged	0.372 (flexural)	0.372 (flexural)	0.109 (torsional)	0.099 (flexural)
TC3	3-legged	0.186 (flexural)	0.186 (flexural)	0.081 (torsional)	0.049 (flexural)
TC4	3-legged	0.254 (flexural)	0.254 (flexural)	0.084 (torsional)	0.048 (flexural)

4.3 Method of analysis

As mentioned earlier, the modal superposition method is used in this study. The mode shapes and frequencies for the 20 lowest modes of the building/tower combinations are evaluated and presented in Appendix C. The damping ratio is taken as 3% of the critical viscous damping and kept constant for all modes. An explanation of the modal analysis technique will be summarized next; more details can be found in Clough and Penzien (1993) and Chopra (2001).

4.3.1 Modal superposition analysis method

The basic concept of modal analysis depends upon the fact that the response in each natural mode of vibration can be computed independently of the others, and the modal responses of the system can be combined to determine its total response. This method provides the response as a function of time and is adequate when the response of the structure is basically linear elastic with classical damping. The modal analysis procedure permits avoiding the solution of simultaneous coupled equations by transforming the continuous or multi-degree-of-freedom system into a set of uncoupled algebraic equations representing SDOF systems through the separation of variables. Each mode responds with its own pattern of deformation known as the natural mode of vibration ϕ_n, its own circular frequency ω_n, its own critical viscous damping ratio ξ_n, and its own modal particpation factor. The procedure of modal response analysis is summarized next.

The equation of motion governing the dynamic response of a MDOF system subjected to earthquake induced ground motion is given in Equation 4-1 (Chopra 2001):

$$M\ddot{u}+C\dot{u}+Ku=P_{eff}(t)=-M\iota\ddot{u}_g(t) \tag{4-1}$$

Where:

M : mass matrix.

C : viscous damping matrix.

K : stiffness matrix.

ι : influence vector equal to 1 because all floor displacements are in the same direction.

$\ddot{u}_g$: base acceleration (uniform at all support points).

$\ddot{u},\dot{u},u$: vectors containing the relative accelerations, velocities, and displacements, respectively, with respect to the moving base and are functions of time t.

The response of a structure having N-DOF can be determined by solving N differential equations represented by the matrix equation given in Equation 4-1. The displacement vector u can be written in the modal basis using the expansion theorem with N generalized coordinates q_n:

$$u(t)=\sum_{n=1}^{N}u_n(t)=\sum_{n=1}^{N}\phi_n q_n(t) \tag{4-2}$$

Equation 4-2 superposes the separate modal displacements; therefore, it is referred to as the modal superposition method. For buildings subjected to earthquakes, the modes with the lowest natural frequencies contribute significantly to the response.

Substituting Equation 4-2 into Equation 4-1:

$$\sum_{n=1}^{N}M\phi_n\ddot{q}_n(t)+\sum_{n=1}^{N}C\phi_n\dot{q}(t)+\sum_{n=1}^{N}K\phi_n q_n(t)=P_{eff}(t)=-M\iota\ddot{u}_g(t) \tag{4-3}$$

Pre-multiplying each term in Equation 4-3 by ϕ_n^T:

$$\sum_{n=1}^{N}\phi_n^T M\phi_n \ddot{q}_n(t)+\sum_{n=1}^{N}\phi_n^T C\phi_n \dot{q}(t)+\sum_{n=1}^{N}\phi_n^T K\phi_n q_n(t)=\phi_n^T P_{eff}(t)=base\ motion \qquad 4\text{-}4$$

Equation 4-4 can be rewritten as:

$$M_n \ddot{q}_n(t)+\sum_{n=1}^{N} C_{nr}\dot{q}_n(t)+K_n q_n(t)=P_n(t) \qquad 4\text{-}5$$

M_n and K_n are diagonal matrices, while C_{nr} is a nondiagonal matrix. The N equations are coupled through the damping terms of Equation 4-5. For systems having classical damping, it is possible to formulate a damping matrix C such that $\phi^T C\phi$ is diagonal, so that Equation 4-5 becomes:

$$M_n \ddot{q}_n(t)+C_n \dot{q}_n(t)+K_n q_n(t)=P_n(t) \qquad 4\text{-}6$$

Equation 4-6 represents a series of n uncoupled equations identical to the equation of motion of a linear SDOF system. Dividing Equation 4-6 by the generalized mass, $\phi_n^T M\phi_n$, yields the classical form:

$$\ddot{q}_n+2\xi_n\omega_n \dot{q}_n+\omega_n^2 q_n=\frac{P_n(t)}{M_n} \qquad 4\text{-}7$$

With:

$$M_n=\phi_n^T M\phi=1 \qquad 4\text{-}8$$

$$C_n=\phi_n^T C\phi_n=2\xi\omega_n \qquad 4\text{-}9$$

$$K_n=\phi_n^T K\phi=\omega_n^2 \qquad 4\text{-}10$$

$$P_n(t)=\phi_n^T P_{eff}(t)=base\ \ motion \qquad 4\text{-}11$$

Equations 4-7 to 4-11 are valid if mode shapes are orthonormal with respect to [M]. The method is called the classical modal superposition method because individual uncoupled modal equations are solved to determine the modal coordinates $q_n(t)$ and the modal responses $u_n(t)$, which are combined to obtained the total response u(t).

4.4 Earthquake records

Currently, information about seismicity in Canada can be found in published uniform seismic hazard maps, and corresponding earthquake data are prescribed by the National Building Code of Canada (NRC/IRC 2005). The hazard levels on these maps were particularly selected for buildings to ensure life safety by resisting moderate earthquakes without significant damage and major earthquakes without collapse or catastrophic failure. The Uniform Hazard Spectra (UHS) are provided for a probability of exceedance of 2% in 50 years, corresponding to a return period of 2500 years. Other data for higher probability levels such as 10% and 50% in 50 years are also available.

In Canada, design of telecommunication structures is currently addressed by the Canadian Standards Association CSA S37-01 document (CSA 2001 a). Appendix M, not a mandatory part of the standard, is devoted to earthquake-resistant design. To define the seismicity level, this document uses a simple classification based on the peak horizontal ground acceleration, with three categories of high (> 30 % g), moderate (15 to 30 % g), and low (< 15 % g). Although this classification may need revision to comply with recent changes in the Canadian seismic hazard maps, it is still useful since self-supporting lattice towers founded on the ground are mostly acceleration-sensitive.

4.4.1 Earthquake records used in this project

In this study, the generated models are subjected to two sets of horizontal inputs. The first set comprises 44 historical records resulting from 23 events given in Table 4-7. The records are classified into three categories according to the ratio of the peak ground horizontal acceleration to the peak ground horizontal velocity (a/v), including 14 records with high a/v ratio, 15 records with medium a/v ratio, and 15 records with low a/v ratio. More details about these earthquake records can be found in Tso et al. (1992). The second set comprises three series, each including 10 generated time-histories compatible with the target Uniform Hazard Spectra for Montreal (Adams and Halchuk 1999), corresponding to probabilities of exceedance of 2%, 10% and 50% in 50 years, respectively. These synthetic time-histories were generated based on a stochastic approach presented by Atkinson and Beresnev (1998). A total of 15 magnitude-distance (M-R) scenarios were applied to cover the entire frequency range of interest. Due to the randomness of the generated records, two acceleration time-histories were used for each M-R scenario; details are listed in Table 4-8. The reference ground condition for the NBCC seismic hazard maps is site Class C: this represents very dense soil or soft rock, with average shear wave velocity in the upper 30 m between 360 and 760 m/s.

Different sets of records were used in order to investigate the effects of frequency content of ground motion on the elastic response of the towers and their supporting buildings.

Table 4-7 Earthquake records classified according to their a/v ratio

Earthquake & Location	Date	Magnitude
Long Beach, California	10/03/1933	$M_L^* = 6.3$
Lower California	10/12/1934	$M_L = 6.5$
Helena, Montana	31/10/1935	$M_L = 6.0$
Imperial Valley, California	18/05/1940	$M_L = 6.6$
Kern County	21/07/1952	$M_L = 7.6$
San Francisco, California	22/03/1957	$M_L = 5.3$
Honshu, Japan	5/04/1966	$M_{JMA}^* = 5.4$
Parkfield, California	27/06/1966	$M_L = 5.6$
Borrego Mtn., California	8/04/1968	$M_L = 6.5$
Near E. Cost of Honshu, Japan	16/05/1968	$M_{JMA} = 7.9$
Lytle Creek	12/09/1970	$M_L = 5.4$
San Fernando, California	9/02/1971	$M_L = 6.6$
Central Honshu, Japan	26/02/1971	$M_{JMA} = 5.5$
Near S. Coast of Honshu, Japan	02/08/1971	$M_{JMA} = 7.0$
Near E. Coast of Honshu, Japan	11/05/1972	$M_{JMA} = 5.8$
Near E. Coast of Honshu, Japan	17/06/1973	$M_{JMA} = 7.4$
Near E. Coast of Honshu, Japan	16/11/1974	$M_{JMA} = 6.1$
Oroville, California	1/08/1975	$M_L = 5.7$
Monte Negro, Yugoslavia	9/04/1979	$M_L = 5.4$
Monte Negro, Yugoslavia	15/04/1979	$M_L = 7.0$
Banja Luka, Yugoslavia	13/08/1981	$M_L = 6.1$
Michoacan, Mexico	19/09/1985	$M_S^* = 8.1$
Nahanni, N.W.T, Canada	23/12/1985	$M_S = 6.9$

* M_L = Local Magnitude
M_{JMA} = Japan Meteorological Agency Scale
M_S = Surface Wave Magnitude

Table 4-8 Characteristics of M-R scenarios considered for Montreal

Magnitude M	Epicentral distance (km)	Record 1		Record 2		Δt (s)	Length [s]	Return Period (years)
		PGA (g)	PGV (m/s)	PGA (g)	PGV (m/s)			
6.0	30	0.430	0.170	0.520	0.150	0.01	8.89	2500
6.0	50	0.240	0.072	0.190	0.084	0.01	8.89	2500
7.0	50	0.510	0.190	0.630	0.290	0.01	12.39	2500
7.0	70	0.300	0.140	0.290	0.160	0.01	12.39	2500
7.0	100	0.240	0.150	0.260	0.210	0.01	20.56	2500
5.5	30	0.180	0.047	0.190	0.045	0.01	20.56	475
6.0	50	0.240	0.072	0.190	0.084	0.01	20.56	475
7.0	150	0.130	0.079	0.130	0.086	0.01	20.56	475
7.0	200	0.084	0.072	0.087	0.067	0.01	24.08	475
7.0	300	0.042	0.042	0.040	0.040	0.01	24.08	475
5.5	50	0.069	0.022	0.083	0.028	0.01	23.08	75
6.0	70	0.045	0.015	0.045	0.018	0.01	23.08	75
7.0	100	0.039	0.015	0.035	0.015	0.01	5.83	75
7.0	200	0.084	0.072	0.087	0.067	0.01	5.83	75
7.0	300	0.042	0.042	0.040	0.040	0.01	12.39	75

4.5 Amplification of rooftop accelerations

An accurate prediction of rooftop seismic accelerations is key in determining the shear forces and overturning moments at the base of a telecommunication tower mounted on a building rooftop. In order to study the rooftop seismic accelerations, both time-history and response spectrum dynamic analyses were carried out with the numerical models.

4.5.1 Time-history analyses

The earthquake sets of records were applied to both main orthogonal horizontal directions of each building independently, as prescribed in the 2005 edition of NBCC (Section 4.1.8.8); U1 and U2 are the longitudinal and transverse directions of the building models, respectively. For each input earthquake, the maximum absolute horizontal acceleration was computed at the rooftop, in a location corresponding to the center of mass in order to avoid torsional effects. The acceleration amplification ratio in a direction is calculated as the ratio of the maximum absolute acceleration at the location considered and the maximum input acceleration at the ground level. For each set of earthquake records, the average (μ) and standard deviations (σ) of the acceleration amplification ratios at the rooftop are summarized in Tables 4-9 to 4-12, including 14 records for the a/v ratio group *H*, 15 records for each of the a/v ratio groups *M* and *L*, and 10 records for each of 2%, 10%, and 50% probabilities of exceedance in 50 years. In this chapter, rooftop acceleration amplification is discussed, while the acceleration amplification along the towers will be discussed in Chapter 5.

Table 4-9 Rooftop acceleration amplification for CHYBA9

CHYBA9	Rooftop acceleration amplification			
Direction	U1		U2	
Load case	μ	σ	μ	σ
H	3.56	1.03	2.90	0.98
M	4.02	1.25	3.58	0.89
L	4.19	1.79	3.37	1.30
2%	3.42	0.43	2.50	0.49
10%	4.21	0.95	3.11	0.61
50%	4.19	0.98	2.59	0.52
All records	3.92	1.19	3.05	0.95

Table 4-10 Rooftop acceleration amplification for CHYBA4

CHYBA4	Rooftop acceleration amplification			
Direction	U1		U2	
Load case	μ	σ	μ	σ
H	3.49	0.68	4.26	1.19
M	3.92	1.00	4.93	1.06
L	4.02	0.88	4.40	1.57
2%	3.15	0.48	4.20	0.98
10%	3.60	1.21	4.85	1.25
50%	3.38	1.18	3.92	1.13
All records	3.63	0.94	4.44	1.23

Table 4-11 Rooftop acceleration amplification for TCUBAA

TCUBAA	Rooftop acceleration amplification			
Direction	U1		U2	
Load case	μ	σ	μ	σ
H	1.83	0.50	3.22	0.62
M	2.85	0.84	4.21	0.88
L	3.09	0.90	3.71	0.54
2%	1.84	0.49	3.10	0.64
10%	2.09	0.69	3.67	1.00
50%	2.03	0.67	3.61	1.05
All records	2.34	0.86	3.60	0.85

Table 4-12 Rooftop acceleration amplification for 2020 University

2020 University	Rooftop acceleration amplification			
Direction	U1		U2	
Load case	μ	σ	μ	σ
H	2.36	0.35	2.54	0.56
M	2.87	0.64	3.28	0.58
L	3.08	0.70	3.52	0.44
2%	2.29	0.50	2.29	0.50
10%	2.67	0.61	2.95	0.75
50%	2.46	0.60	2.69	0.85
All records	2.65	0.63	2.91	0.73

The results presented in Tables 4-9 to 4-12 indicate that the maximum amplification of rooftop accelerations occurs for the sets of records of medium and low a/v ratios as well as for the records compatible with the Uniform Hazard Spectra having probabilities of exceedance of 10% and 50% in 50 years. It is noticed that less amplification is obtained for the records compatible with the UHS having a probability of exceedance of 2% in 50 years and those having high a/v ratios; this may explain why the height amplification ratio was decreased from 4 to 3 in the NEHRP 2000 (BSSC 2001), as provisions for acceleration amplification are for ground accelerations larger than 0.1g. For medium and low a/v ratio records, it is proposed that a maximum acceleration amplification of 4 be considered, while for high a/v ratio records a factor of 3 is sufficient. In general, since an amplification factor of 4 is conservative, it is recommended for all cases. The results of numerical simulations correlate well with the findings in Chapter 3, since the records of the Chi Chi earthquake can be associated with the sets of medium and low a/v ratios. Therefore, the recommended maximum rooftop acceleration of 4 based on the study of recorded accelerations undertaken in Chapter 3 agrees with related recommendations resulting from the numerical simulations of the generated models presented in this chapter.

The results further indicate a close correlation between the amplification obtained with the records classified according to the a/v ratio and the records compatible with the UHS classified according to the M-R scenarios, although the different records have different frequency content characteristics. This observation is proved by computing the mean acceleration response spectra of records normalized to 1g, as shown in Figures 4-14 to 4-16. The mean spectral accelerations of 2%/50 years and high a/v ratios at 5%

damping (Figure 4-14) are very similar in all period ranges and decrease rapidly beyond 0.2 s. In the case of 10%/50 years and medium a/v ratios (Figure 4-15), the mean spectral accelerations are very similar in the 0.2-0.5 s period range; however, the average spectrum of the data corresponding to medium a/v ratios decreases less rapidly than that of UHS at periods longer than 0.5 s. In the case of 50%/50 years and low a/v ratios (Figure 4-16), the two curves of mean spectral accelerations follow the same trend in the range of periods larger than 0.3 s, with larger values for the set of low a/v ratios.

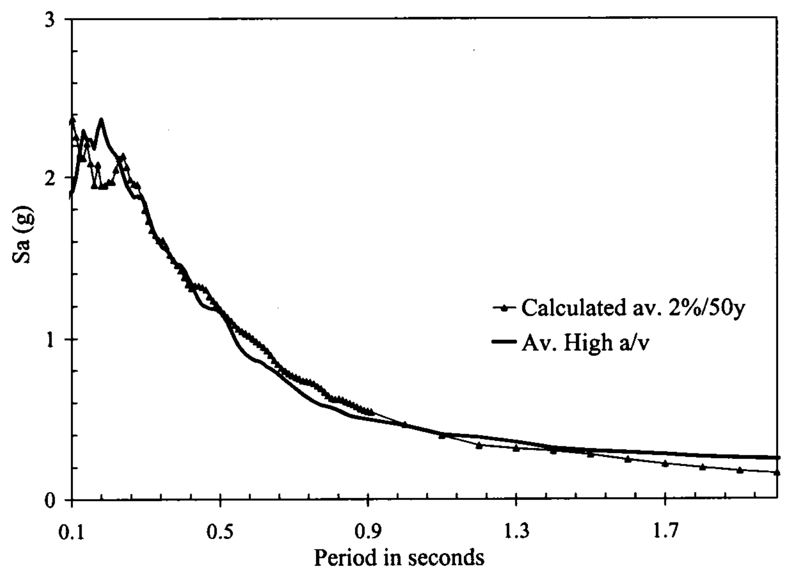

Figure 4-14 Mean 5% damped elastic acceleration response spectra for the sets of High a/v and 2%/50 years normalized to 1g

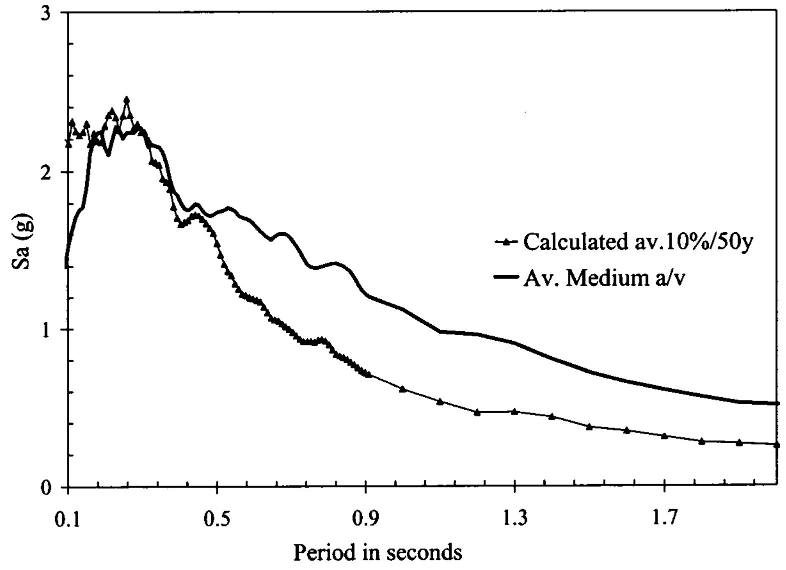

Figure 4-15 Mean 5% damped elastic acceleration response spectra for the sets of Medium a/v and 10%/50 years normalized to 1g

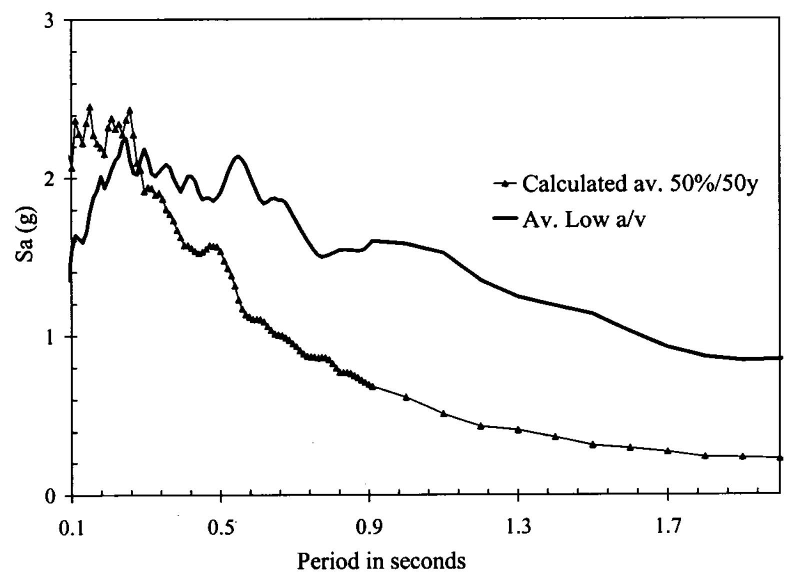

Figure 4-16 Mean 5% damped elastic acceleration response spectra for the sets of Low a/v and 50%/50 years normalized to 1g

4.5.2 Rooftop seismic spectral accelerations

For each seismic input record, the response spectrum at 5% damping was computed. Spectral accelerations were evaluated at 0.2 s, as suggested in the NBCC 2005 (NRC/IRC 2005), and at the sway fundamental periods of vibration of the building models, T_1 and T_2. The Uniform Hazard Spectra proposed in the NBCC 2005 and the computed 5% damped absolute acceleration response spectra for exceedance levels of 2%, 10% and 50% in 50 years earthquake records are presented in Figures 4-17 to 4-19. The spectral accelerations of the earthquakes classified according to a/v ratios are presented in Figures 4-20 to 4-22. All generated spectra are plotted on the figures and the average curve is also shown. The peak rooftop acceleration (PRA) was computed in the direction of the applied motion. For each record, the ratio $PRA/(0.3*S_a(T)*S_p)$ was computed, taking S_p as being equal to 4: referring again to Equation 2-11, this ratio is equal to the importance factor I_E. Tables 4-13 to 4-16 summarize the average and standard deviations of the ratios corresponding to each set of records and each of the four buildings.

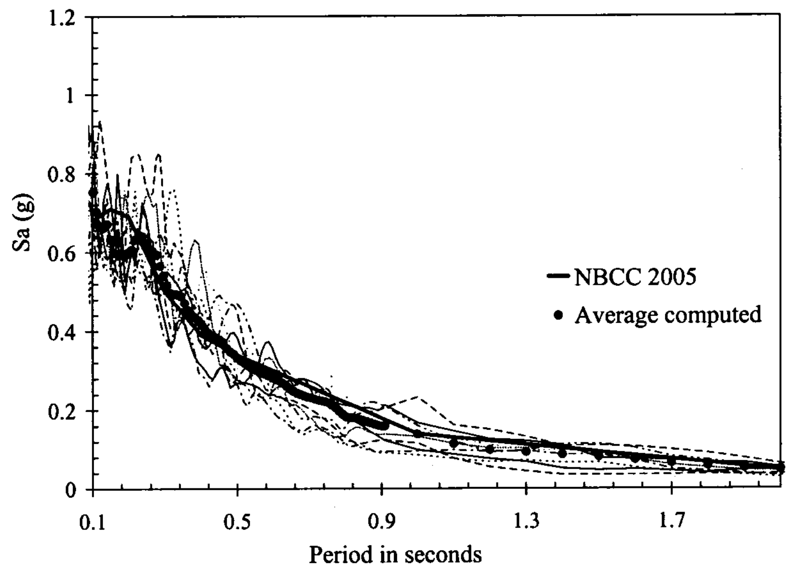

Figure 4-17 UHS proposed in NBCC 2005 and computed 5% damped average absolute acceleration response spectra for 2%/50 years

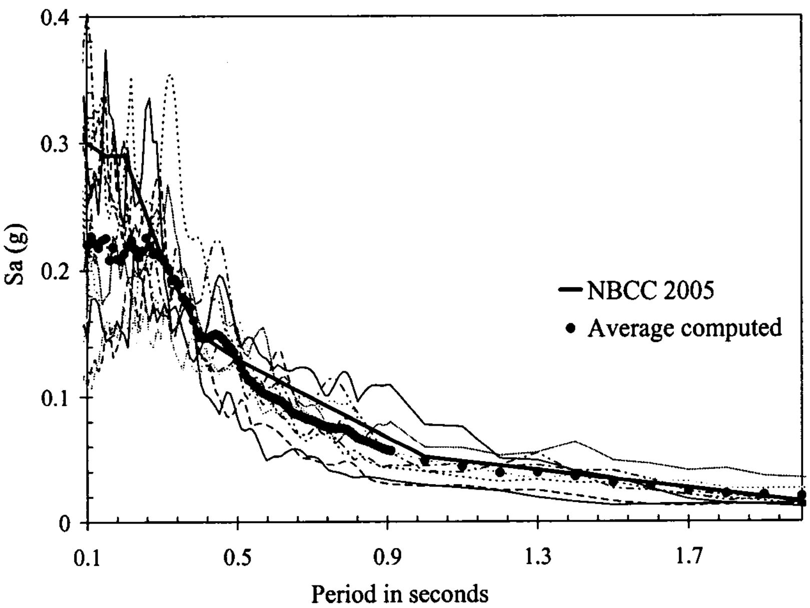

Figure 4-18 UHS proposed in NBCC 2005 and computed 5% damped elastic average acceleration response spectra for 10%/50 years

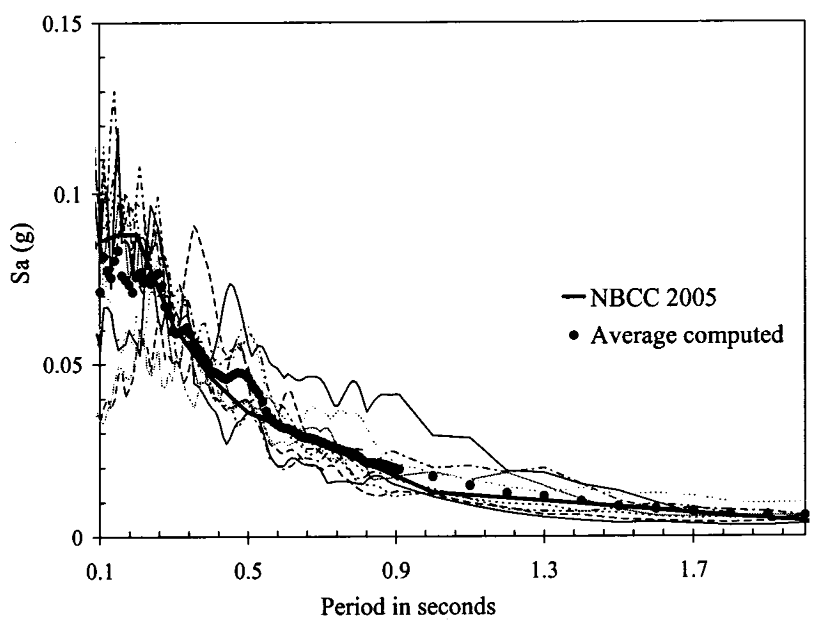

Figure 4-19 UHS proposed in NBCC 2005 and computed 5% damped elastic average acceleration response spectra for 50%/50 years

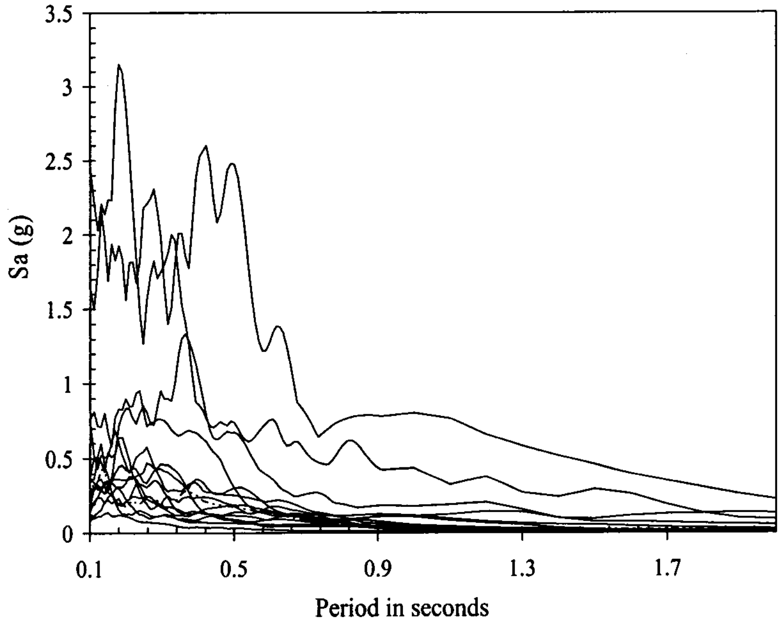

(a)

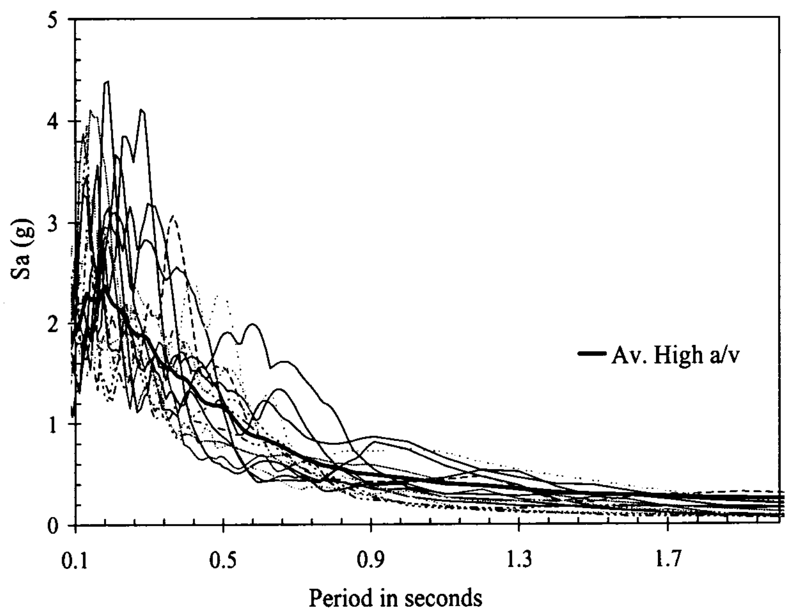

(b)

Figure 4-20 Computed 5% damped elastic acceleration response spectra for the set High a/v. (a) Without normalization (b) Normalized to 1g

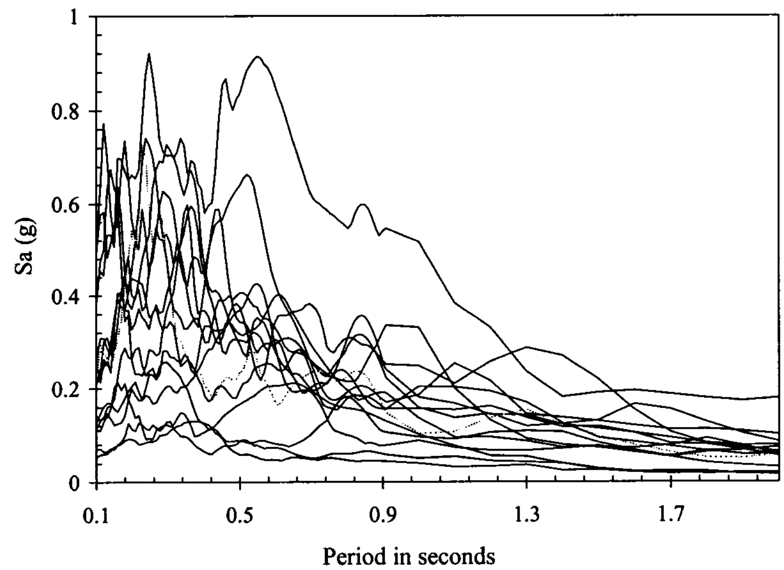

(a)

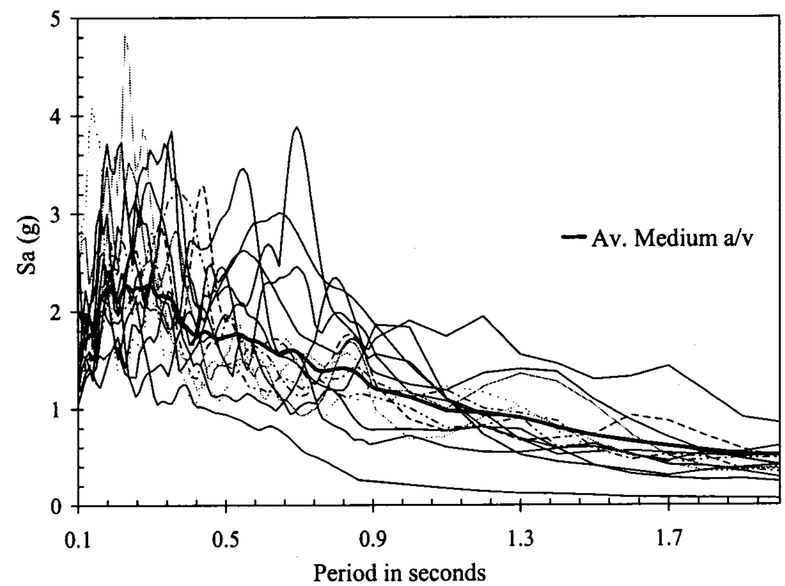

(b)

Figure 4-21 Computed 5% damped elastic acceleration response spectra for the set Medium a/v. (a) Without normalization (b) Normalized to 1g

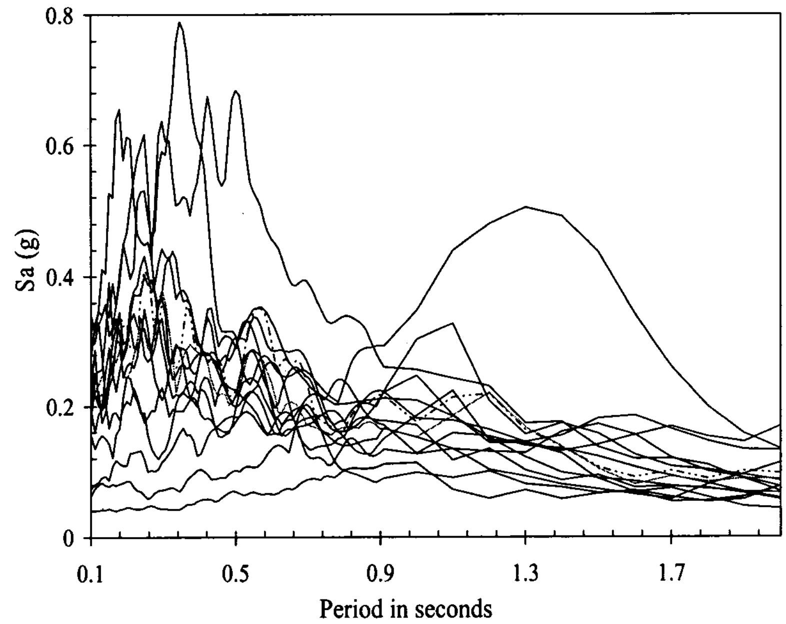

(a)

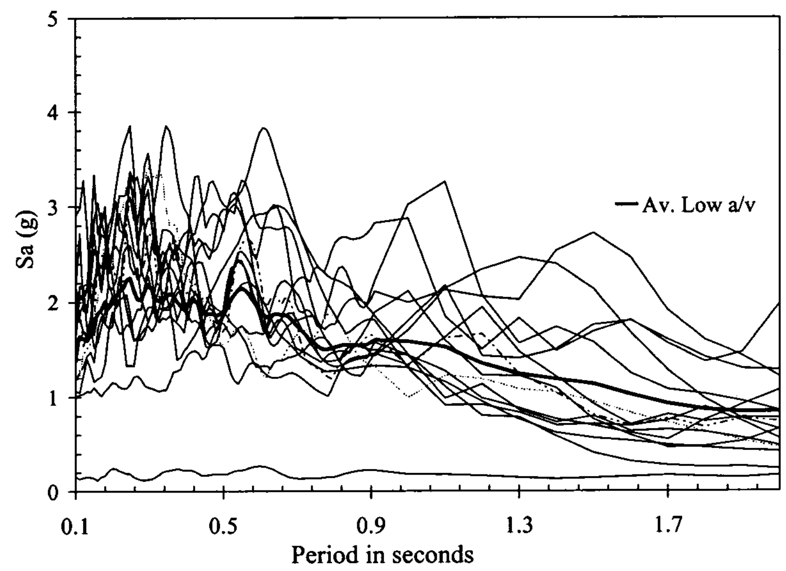

(b)

Figure 4-22 Computed 5% damped elastic acceleration response spectra for the set Low a/v. (a) Without normalization (b) Normalized to 1g

Table 4-13 Comparison of rooftop peak and spectral accelerations for the CHYBA9 building

CHYBA9	PRA/1.2*S_a(0.2)				PRA/1.2*$S_a(T_1)$				PRA/1.2*$S_a(T_2)$			
Direction	U1		U2		U1		U2		U1		U2	
Load case	μ	σ	μ	σ	μ	σ	μ	σ	μ	σ	μ	σ
H	1.19	0.41	1.24	0.49	1.36	0.32	1.37	0.08	1.24	0.08	1.30	0.29
M	1.37	0.26	1.46	0.37	1.25	0.24	1.31	0.14	1.32	0.11	1.42	0.24
L	1.45	0.39	1.42	0.42	1.38	0.47	1.28	0.13	1.38	0.20	1.36	0.35
2%	1.38	0.31	1.13	0.17	1.55	0.46	1.25	0.14	1.33	0.19	1.11	0.19
10%	1.48	0.31	1.25	0.18	1.49	0.35	1.25	0.17	1.35	0.14	1.19	0.33
50%	1.48	0.29	1.04	0.09	1.79	0.42	1.27	0.18	1.38	0.14	1.00	0.19
All records	1.39	0.33	1.26	0.28	1.47	0.38	1.29	0.14	1.33	0.14	1.23	0.27

Table 4-14 Comparison of rooftop peak and spectral accelerations for the CHYBA4 building

CHYBA4	PRA/1.2*S_a(0.2)				PRA/1.2*$S_a(T_1)$				PRA/1.2*$S_a(T_2)$			
Direction	U1		U2		U1		U2		U1		U2	
Load case	μ	σ	μ	σ	μ	σ	μ	σ	μ	σ	μ	σ
H	2.49	1.22	2.38	0.85	3.66	1.54	3.70	1.50	3.09	1.30	2.90	0.81
M	2.13	0.71	2.19	0.63	2.48	0.75	2.77	1.41	1.93	0.46	1.99	0.40
L	2.10	0.34	2.17	0.58	2.07	0.22	2.18	0.68	2.09	0.46	2.02	0.27
2%	2.23	0.30	2.63	0.59	3.28	0.72	3.85	0.98	2.62	0.53	3.01	0.35
10%	2.15	0.39	2.39	0.26	3.06	0.62	3.44	0.78	2.17	0.37	2.43	0.32
50%	2.05	0.29	2.22	0.22	3.19	0.90	3.42	0.77	2.52	0.54	2.73	0.51
All records	2.19	0.54	2.33	0.52	2.96	0.79	3.23	1.02	2.40	0.61	2.51	0.44

Table 4-15 Comparison of rooftop peak and spectral accelerations for the TCUBAA building

TCUBAA	PRA/1.2*S_a(0.2)				PRA/1.2*$S_a(T_1)$				PRA/1.2*$S_a(T_2)$			
Direction	U1		U2		U1		U2		U1		U2	
Load case	μ	σ	μ	σ	μ	σ	μ	σ	μ	σ	μ	σ
H	1.29	0.54	0.72	0.30	4.68	1.52	2.58	0.63	4.10	1.60	2.24	0.63
M	1.56	0.51	1.07	0.45	2.53	0.60	1.67	0.35	2.23	0.55	1.46	0.19
L	1.45	0.40	1.24	0.62	1.93	0.47	1.55	0.29	1.67	0.36	1.33	0.14
2%	1.25	0.20	0.73	0.18	3.68	1.00	2.09	0.50	3.44	0.91	1.98	0.54
10%	1.28	0.16	0.73	0.19	4.16	2.31	2.17	0.76	3.77	1.90	1.97	0.61
50%	1.26	0.19	0.71	0.19	3.99	1.53	2.14	0.55	3.66	1.36	1.96	0.51
All records	1.35	0.34	0.87	0.32	3.49	1.24	2.03	0.51	3.15	1.11	1.82	0.44

Table 4-16 Comparison of rooftop peak and spectral accelerations for the 2020 University building

2020 University	PRA/1.2*S_a(0.2)				PRA/1.2*$S_a(T_1)$				PRA/1.2*$S_a(T_2)$			
Direction	U1		U2		U1		U2		U1		U2	
Load case	μ	σ	μ	σ	μ	σ	μ	σ	μ	σ	μ	σ
H	0.93	0.33	0.97	0.27	18.0	8.57	19.2	8.71	16.1	7.38	17.2	7.44
M	1.08	0.42	1.20	0.36	5.8	1.45	6.81	2.32	5.48	1.39	6.42	2.18
L	1.24	0.61	1.37	0.34	3.42	1.55	4.15	2.04	3.27	1.19	3.92	1.60
2%	0.96	0.24	1.14	0.23	12.5	5.51	14.5	5.05	11.5	4.64	13.4	4.75
10%	0.97	0.20	1.07	0.17	12.0	6.06	13.3	6.48	11.0	5.03	12.2	5.71
50%	0.90	0.13	0.98	0.19	12.4	5.49	13.3	5.67	11.9	5.88	12.8	6.35
All records	1.02	0.32	1.12	0.26	10.7	4.77	11.9	5.04	9.87	4.25	11.0	4.67

Tables 4-13 to 4-16 indicate that for the sets of UHS records, the amplified uniform hazard spectral acceleration at 0.2 s, $S_a(0.2)$, gives the best estimate of peak rooftop acceleration demand of the structure, which complies with the NBCC recommendations. For short period structures (CHYBA9 and CHYBA4), considering either 0.2 s, T_1, or T_2 did not result in considerable variability in the results. On the other hand, only the spectral acceleration at 0.2 s is adequate for flexible structures such as the TCUBAA and the 2020 University buildings.

4.6 Conclusions

The modeling details and assumptions used for the buildings and the towers of the study undertaken are presented in this chapter. The dynamic analysis procedure and the earthquake records used are described. Many records of different characteristics were used as input at the base of the buildings to investigate the effect of the frequency content of the ground motion on the acceleration amplification at the rooftop, irrespective of the building's period. It was found that the frequency content does have some effect in terms of individual time-history, but this is smoothed out when the responses are averaged. It is observed that less amplification occurs for the records having high a/v ratios and those having a low probability of occurrence (2%/50 years). As a result of the study, a maximum rooftop acceleration amplification of 4 is proposed for low/medium rise buildings and 3 for high-rise flexible buildings (T > 1.7 s). These recommendations are in good agreement with those resulting from the experimental study of real recorded accelerations in existing instrumented buildings in Taiwan (Chapter 3). Finally, the estimation of rooftop accelerations from input acceleration response spectra was discussed. It was found that evaluating the spectral acceleration at 0.2 s is adequate for all building cases.

Chapter 5
Proposed Simplified Method of Seismic Analysis of Rooftop Towers

The present chapter describes the procedure followed to develop an equivalent static method intended to provide a useful tool for the quick estimation of the seismic efforts, namely the base shear and overturning moment, at the base of acceleration-sensitive, self-supporting steel lattice telecommunication towers mounted on building rooftops. The method is based on the prediction of input seismic rooftop acceleration at the building-tower interface, which was discussed in Chapters 3 and 4; the definition of an acceleration profile along the height of the building-mounted tower and the prediction of fundamental mode shapes of the tower on a rigid base, both of which will be discussed in this chapter; and finally, the computation of the mass distribution of the tower from its structural plans. In addition, the component force amplification factor A_r for telecommunication towers is discussed.

5.1 Component force amplification factor A_r for telecommunication towers of the building-tower combinations

The equation proposed in NBCC 2005 (NRC/IRC 2005) for calculating the input seismic base shear forces for design of operational and functional components (OFCs) in buildings was presented in Chapter 2 (Equation 2-11). This equation comprises an empirical component force amplification factor A_r that needs further study. In case of the unavailability of the building's and/or tower's dynamic properties, the NBCC 2005

(Table 4.1.8.17) proposes a component force amplification factor A_r equal to 2.5 for telecommunication towers. When the ratio of the tower's fundamental period over the building's fundamental period $T_{tower}/T_{builing}$ is known, A_r can be obtained from the graph shown in Figure 2-4. In order to investigate the adequacy of the factor A_r as proposed in NBCC 2005, the maximum absolute seismic accelerations were estimated along the tower height for each building-tower combination in both principal horizontal directions U1 and U2 of the generated models separately. A_r is computed as the average value of the maximum acceleration amplification at different levels of the tower, from the building-tower interface to the tower top. The graphs shown in Figures 5-1 to 5-8 illustrate the average values and standard deviations of the A_r factors resulting from the numerical simulations for each building-tower combination subjected to the earthquake sets depicted in Chapter 4. Also shown on each graph is the component force amplification factor as suggested in NBCC 2005. In this study, the ratio $T_{tower}/T_{builing}$ is known; therefore, the A_r values were calculated as suggested in NBCC 2005 and compared to the average amplification of accelerations. Results are presented in Tables 5-1 to 5-15.

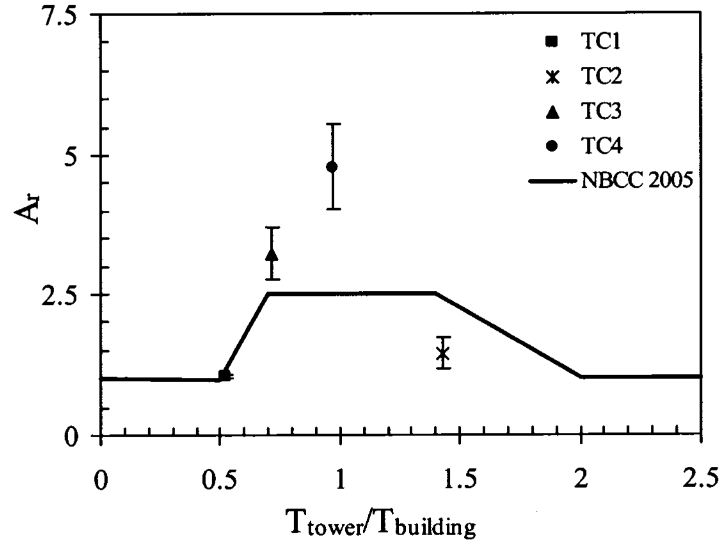

Figure 5-1 A_r for CHYBA9 in the U1 direction

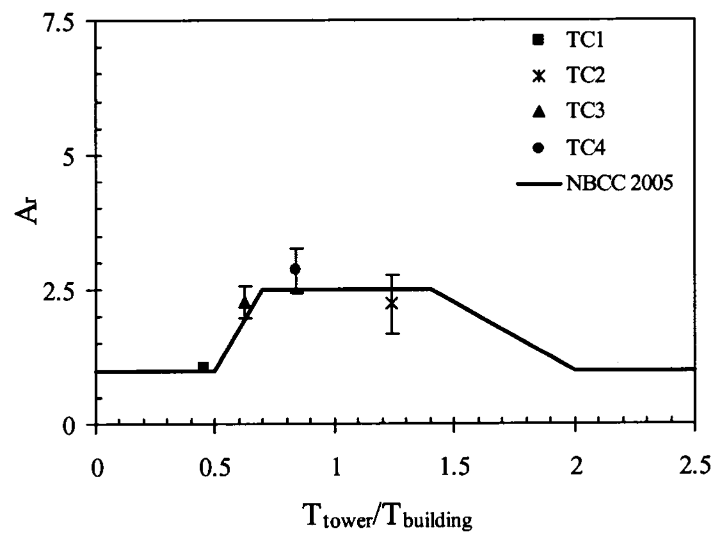

Figure 5-2 A_r for CHYBA9 in the U2 direction

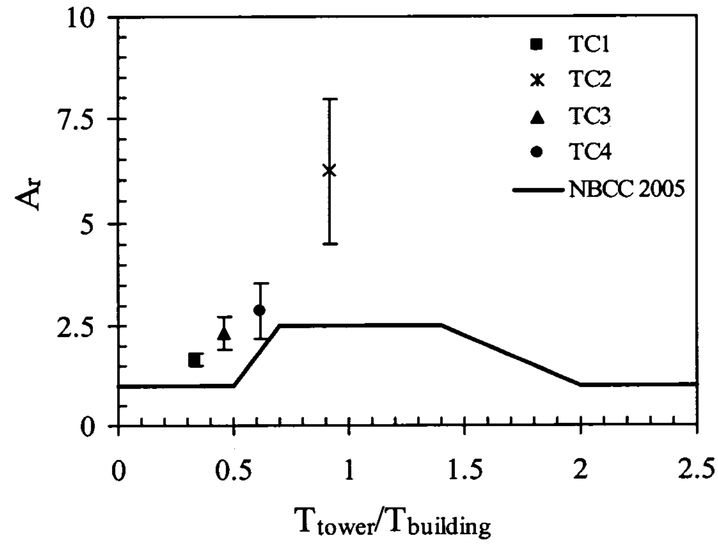

Figure 5-3 A_r for CHYBA4 in the U1 direction

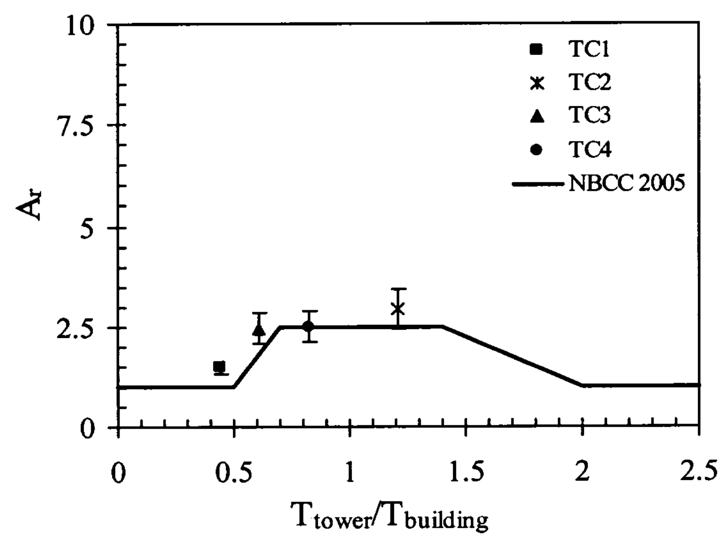

Figure 5-4 A_r for CHYBA4 in the U2 direction

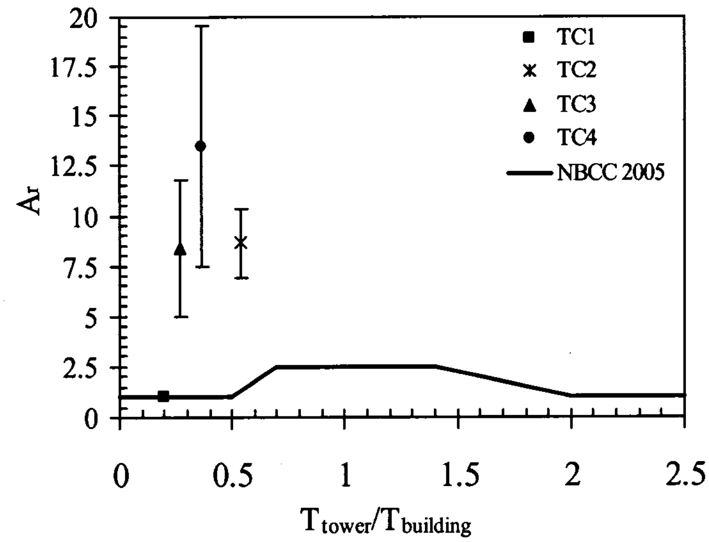

Figure 5-5 A_r for TCUBAA in the U1 direction

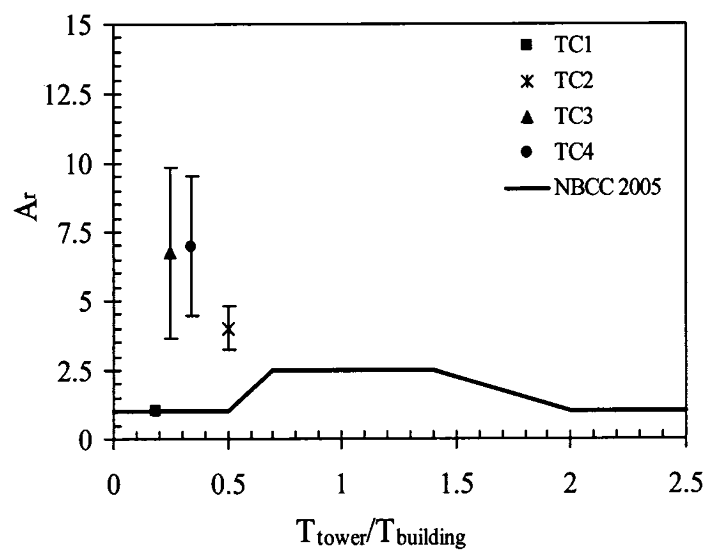

Figure 5-6 A_r for TCUBAA in the U2 direction

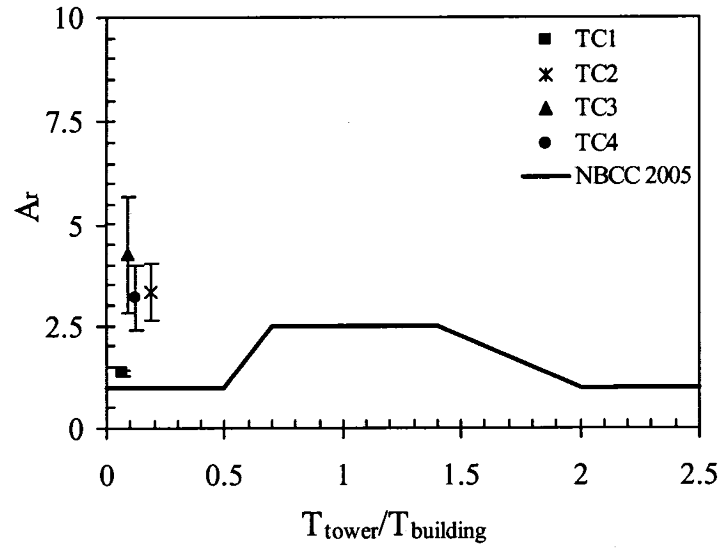

Figure 5-7 A_r for 2020 University in the U1 direction

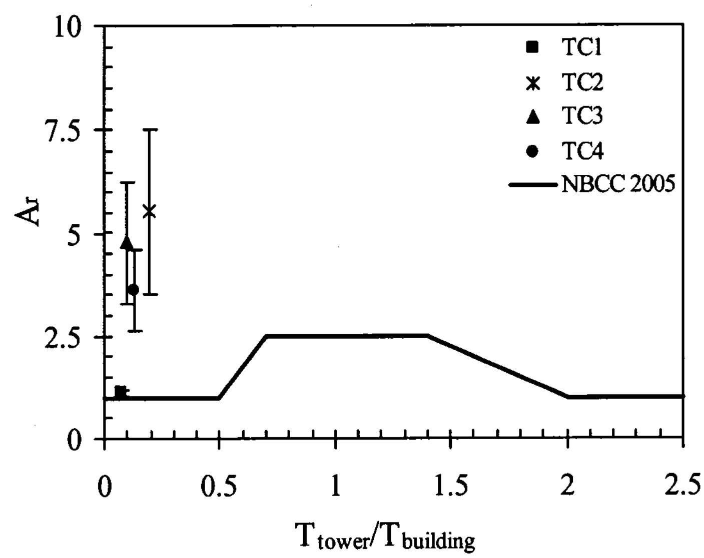

Figure 5-8 A_r for 2020 University in the U2 direction

5.1.1 Results for the building labeled CHYBA9

The three largest natural periods of the CHYBA9 building are:

$T_1 = 0.30$ s (U2-direction) $T_2 = 0.26$ s (U1-direction) $T_3 = 0.17$ s (torsion).

Table 5-1 A_r factors for the TC1, TC2, TC3, and TC4 towers mounted on the CHYBA9 building calculated according to NBCC 2005

CHYBA9	U1		U2	
	$T_{tower}/T_{building}$	A_r	$T_{tower}/T_{building}$	A_r
TC1	0.52	1.15	0.45	1
TC2	1.43	2.5	1.24	2.5
TC3	0.72	2.5	0.62	1.9
TC4	0.97	2.5	0.84	2.5

Table 5-2 A_r factors for CHYBA9-TC1

CHYBA9 - TC1	TC1 ($T_1 = T_2 = 0.14$ s) Average tower acceleration amplification			
Load case	U1		U2	
	μ	σ	μ	σ
H	1.02	0.02	1.05	0.03
M	1.03	0.01	1.02	0.01
L	1.02	0.01	1.03	0.01
2%	1.08	0.03	1.07	0.06
10%	1.08	0.05	1.05	0.05
50%	1.07	0.04	1.05	0.04
All records	1.04	0.04	1.05	0.04

Table 5-3 A_r factors for CHYBA9-TC2

CHYBA9 - TC2	TC2 ($T_1 = T_2 = 0.37$ s)			
	Average tower acceleration amplification			
Load case	U1		U2	
	μ	σ	μ	σ
H	1.51	0.30	2.41	0.34
M	1.56	0.38	2.17	0.33
L	1.51	0.30	2.12	0.26
2%	1.34	0.15	2.38	0.23
10%	1.38	0.19	2.21	0.24
50%	1.33	0.22	2.39	0.25
All records	1.45	0.29	2.27	0.30

Table 5-4 A_r factors for CHYBA9-TC3

CHYBA9 - TC3	TC3 ($T_1 = T_2 = 0.19$ s)			
	Average tower acceleration amplification			
Load case	U1		U2	
	μ	σ	μ	σ
H	3.40	0.65	2.12	0.55
M	3.18	0.57	2.18	0.45
L	3.18	0.45	2.27	0.71
2%	3.59	0.38	2.25	0.48
10%	3.20	0.41	2.02	0.37
50%	3.20	0.28	2.58	0.51
All records	3.28	0.50	2.23	0.54

Table 5-5 A_r factors for CHYBA9-TC4

CHYBA9 - TC4	TC4 ($T_1 = T_2 = 0.25$ s) Average tower acceleration amplification			
Load case	U1		U2	
	μ	σ	μ	σ
H	4.19	0.87	2.83	0.39
M	4.61	0.90	2.63	0.24
L	4.83	0.92	2.77	0.49
2%	5.30	0.48	3.11	0.34
10%	4.92	0.44	2.84	0.29
50%	4.95	0.57	3.06	0.45
All records	4.76	0.81	2.85	0.40

5.1.2 Results for the building labeled CHYBA4

The largest natural periods of the CHYBA4 building are:

$T_1 = 0.41$ s (U1-direction) $T_2 = 0.31$ s (U2-direction) $T_3 = 0.24$ s (torsion).

Table 5-6 A_r factors for the TC1, TC2, TC3, and TC4 towers mounted on the CHYBA4 building calculated according to NBCC 2005

CHYBA4	U1		U2	
	$T_{tower}/T_{building}$	A_r	$T_{tower}/T_{building}$	A_r
TC1	0.33	1	0.44	1
TC2	0.92	2.5	1.21	2.5
TC3	0.46	1	0.61	1.83
TC4	0.62	1.9	0.82	2.5

Table 5-7 A_r factors for CHYBA4-TC1

CHYBA4 - TC1	TC1 ($T_1 = T_2 = 0.14$ s)			
	Average tower acceleration amplification			
Load case	U1		U2	
	μ	σ	μ	σ
H	1.70	0.19	1.55	0.15
M	1.53	0.18	1.31	0.18
L	1.49	0.17	1.37	0.22
2%	1.73	0.12	1.57	0.10
10%	1.69	0.16	1.51	0.11
50%	1.70	0.15	1.56	0.15
All records	1.63	0.19	1.47	0.19

Table 5-8 A_r factors for CHYBA4-TC2

CHYBA4 - TC2	TC2 ($T_1 = T_2 = 0.37$ s)			
	Average tower acceleration amplification			
Load case	U1		U2	
	μ	σ	μ	σ
H	5.06	1.82	2.79	0.60
M	6.58	1.64	2.94	0.48
L	7.31	1.20	3.17	0.78
2%	5.76	1.26	2.83	0.17
10%	6.07	1.61	2.93	0.14
50%	6.39	2.10	3.00	0.27
All records	6.24	1.73	2.95	0.51

Table 5-9 A_r factors for CHYBA4-TC3

CHYBA4 - TC3	TC3 ($T_1 = T_2 = 0.19$ s) Average tower acceleration amplification			
Load case	U1		U2	
	μ	σ	μ	σ
H	2.26	0.59	2.43	0.64
M	2.23	0.54	2.59	0.29
L	2.25	0.35	2.46	0.35
2%	2.51	0.28	2.33	0.31
10%	2.30	0.31	2.38	0.20
50%	2.34	0.29	2.48	0.26
All records	2.30	0.42	2.46	0.38

Table 5-10 A_r factors for CHYBA4-TC4

CHYBA4 - TC4	TC4 ($T_1 = T_2 = 0.25$ s) Average tower acceleration amplification			
Load case	U1		U2	
	μ	σ	μ	σ
H	2.91	0.72	2.33	0.43
M	3.09	0.98	2.75	0.40
L	2.49	0.49	2.56	0.40
2%	2.83	0.47	2.35	0.29
10%	2.92	0.64	2.42	0.20
50%	3.02	0.45	2.50	0.27
All records	2.87	0.68	2.50	0.38

5.1.3 Results for the TCUBAA building

The largest natural periods of the TCUBAA building are:

$T_1 = 0.75$ s (U2-direction) $T_2 = 0.69$ s (U1-direction) $T_3 = 0.62$ s (torsion).

Table 5-11 A_r factors for the TC1, TC2, TC3, and TC4 towers mounted on the TCUBAA building calculated according to NBCC 2005

TCUBAA	U1		U2	
	$T_{tower}/T_{building}$	A_r	$T_{tower}/T_{building}$	A_r
TC1	0.2	1	0.18	1
TC2	0.54	1.3	0.5	1
TC3	0.27	1	0.25	1
TC4	0.37	1	0.34	1

Table 5-12 A_r factors for TCUBAA-TC1

TCUBAA - TC1	TC1 ($T_1 = T_2 = 0.14$s)			
	Average tower acceleration amplification			
Load case	U1		U2	
	μ	σ	μ	σ
H	1.01	0.03	1.01	0.03
M	0.99	0.02	0.99	0.02
L	0.98	0.01	0.98	0.01
2%	0.99	0.02	0.99	0.02
10%	1.00	0.02	1.00	0.02
50%	1.00	0.02	1.00	0.02
All records	1.00	0.02	1.00	0.02

Table 5-13 A_r factors for TCUBAA-TC2

TCUBAA - TC2	TC2 ($T_1 = T_2 = 0.37$ s)			
	Average tower acceleration amplification			
Load case	U1		U2	
	μ	σ	μ	σ
H	6.76	0.96	4.24	0.80
M	8.67	1.66	3.86	0.96
L	8.65	1.56	3.93	0.59
2%	9.87	1.29	3.92	0.78
10%	9.25	1.55	4.11	0.92
50%	9.21	1.09	4.11	0.74
All records	8.62	1.67	4.02	0.79

Table 5-14 A_r factors for TCUBAA-TC3

TCUBAA - TC3	TC3 ($T_1 = T_2 = 0.19$ s)			
	Average tower acceleration amplification			
Load case	U1		U2	
	μ	σ	μ	σ
H	10.68	5.66	7.73	3.65
M	7.76	2.70	5.06	2.30
L	6.06	2.20	4.08	1.46
2%	8.87	1.53	5.38	0.96
10%	8.77	1.95	6.50	3.13
50%	8.43	2.18	6.17	2.63
All records	8.35	3.41	5.75	2.74

Table 5-15 A_r factors for TCUBAA-TC4

TCUBAA - TC4	TC4 ($T_1 = T_2 = 0.25$ s)			
	Average tower acceleration amplification			
Load case	U1		U2	
	μ	σ	μ	σ
H	15.68	7.09	9.05	3.13
M	9.12	3.84	3.88	1.26
L	8.79	4.60	3.62	1.42
2%	17.41	4.43	9.47	1.61
10%	17.21	4.61	8.34	1.66
50%	16.26	3.07	8.12	1.21
All records	13.47	6.04	6.74	3.10

5.1.4 Results for the 2020 University building

The largest natural periods of the 2020 University building are:

$T_1 = 2.01$ s (U1-direction) $T_2 = 1.88$ s (U2-direction) $T_3 = 1.36$ s (torsion).

Table 5-16 A_r factors for the TC1, TC2, TC3, and TC4 towers mounted on the 2020 University building calculated according to NBCC 2005

2020 University	U1		U2	
	$T_{tower}/T_{building}$	A_r	$T_{tower}/T_{building}$	A_r
TC1	0.07	1	0.07	1
TC2	0.19	1	0.20	1
TC3	0.09	1	0.10	1
TC4	0.13	1	0.13	1

Table 5-17 A_r factors for 2020 University-TC1

2020 University – TC1	TC1 ($T_1 = T_2 = 0.14$ s)			
	Average tower acceleration amplification			
Load case	U1		U2	
	μ	σ	μ	σ
H	1.38	0.06	1.13	0.07
M	1.29	0.07	1.06	0.04
L	1.23	0.08	1.04	0.04
2%	1.41	0.05	1.17	0.06
10%	1.37	0.10	1.14	0.08
50%	1.40	0.11	1.15	0.07
All records	1.34	0.10	1.11	0.08

Table 5-18 A_r factors for 2020 University-TC2

2020 University - TC2	TC2 ($T_1 = T_2 = 0.37$ s)			
	Average tower acceleration amplification			
Load case	U1		U2	
	μ	σ	μ	σ
H	3.30	0.86	6.15	1.59
M	3.55	0.77	3.98	0.79
L	3.29	0.77	3.79	0.81
2%	3.16	0.53	7.23	1.72
10%	3.31	0.61	6.58	2.07
50%	3.24	0.60	6.80	1.80
All records	3.32	0.71	5.52	1.99

Table 5-19 A_r factors for 2020 University-TC3

2020 University - TC3	TC3 ($T_1 = T_2 = 0.19$ s)			
	Average tower acceleration amplification			
Load case	U1		U2	
	μ	σ	μ	σ
H	4.77	1.68	5.47	1.56
M	4.44	1.45	5.04	1.39
L	3.42	1.08	3.80	1.04
2%	5.06	1.87	5.40	1.27
10%	4.51	0.74	5.40	1.16
50%	5.09	0.98	6.32	1.38
All records	4.25	1.45	4.77	1.47

Table 5-20 A_r factors for 2020 University-TC4

2020 University - TC4	TC4 ($T_1 = T_2 = 0.25$ s)			
	Average tower acceleration amplification			
Load case	U1		U2	
	μ	σ	μ	σ
H	3.55	0.90	4.16	0.97
M	3.13	0.76	3.52	0.80
L	2.54	0.73	2.54	0.73
2%	3.44	0.64	4.03	0.85
10%	3.28	0.70	3.81	0.52
50%	3.33	0.51	4.03	0.94
All records	3.18	0.79	3.62	0.99

5.1.5 Discussion of the component force amplification factor A_r for telecommunication towers

Operational and functional components attached to a building framework receive filtered and amplified input ground acceleration. The elastic base shear at the component-building interface can be taken as the product of the input acceleration at the base of the component, the weight of the component, and a force modification factor equivalent to the component force amplification factor A_r. If the component is rigid or rigidly attached to the building, the component is assumed to follow the motion of the building; therefore, the proposed component force amplification factor proposed in the NBCC 2005 and other codes is equal to 1. On the other hand, when the component is flexible or flexibly attached to the building, this amplification factor increases as the fundamental frequencies of the building and component come close: a maximum value of 2.5 is suggested in the NBCC 2005 and other codes. Most telecommunication towers can be classified as flexible components, and it is expected that their A_r factor be greater than 1. This is reflected in the results shown in the Tables 5-1 to 5-15, where the A_r values are greater than 1 in most cases.

For low-rise buildings, such as CHYBA9 (Figures 5-1 and 5-2) and CHYBA4 (Figures 5-3 and 5-4), the component force amplification factor proposed in the NBCC 2005 gives reasonable results, especially for the TC1 tower, which is relatively rigid. However, when the tower's period approaches the building's period, an amplification factor of 6 seems more adequate. In case the period of the tower exceeds the period of the building, such as the TC2 tower mounted on the CHYBA9 building, the factor 2.5 proposed by the NBCC seems reasonable.

In case of medium and high-rise buildings, such as TCUBAA (Figures 5-5 and 5-6) and 2020 University (Figures 5-7 and 5-8), the amplification factor of 1 seems reasonable for the TC1 tower, which is very rigid; however, for more flexible towers, it is suggested to increase the value of A_r from 2.5, as proposed in the NBCC 2005, to a value of 8. Besides, the somewhat arbitrary distinction of flexible and rigid component does not apply for medium and tall buildings because there is significant amplification of accelerations in the towers regardless of the fact that the ratio T_p/T becomes very small in most of the cases. Moreover, it is noted that the amplification of accelerations for the TC1 tower is negligible for all building models, except for the CHYBA4 building, indicating that the NBCC limit of 0.06 s set for the fundamental period of rigid components is conservative.

5.2 Prediction of forces at the building-tower interface

5.2.1 Evaluation of shear force demands

In order to evaluate the adequacy of the NBCC provisions in predicting the input seismic shear forces at the base of steel lattice telecommunication towers mounted on building rooftops, the shear forces resulting from the dynamic modal analysis of all building-tower combinations modeled in SAP 2000 and subjected to the earthquake ground motions depicted in Chapter 4 were calculated and compared to the shear forces computed using Equation 2-11. The shear force demand evaluated from the numerical simulations at the building-tower interface is calculated as the sum of the maximum absolute shear forces at the tower's legs corresponding to the direction of the applied earthquake records. This method of calculation results in upper bound values of V.

Detailed calculations for shear force demands for the combination CHYBA9-TC2 are presented in Appendix D. Similar calculations were done for the other building-tower combinations. The acceleration in Equation 2-11 is estimated from the maximum time-history rooftop acceleration and from the spectral acceleration. The latter was evaluated in order to make direct comparison with the NBCC 2005 provisions that use the amplified spectral acceleration at the ground level of the building as input acceleration to operational and functional components in buildings. The response spectra were calculated from the rooftop acceleration time-history, considering 5% damping ratio as suggested in the NBCC 2005. The mass of the towers studied is negligible in comparison to the mass of the buildings; therefore, it was assumed that dynamic interaction between the buildings and towers is negligible and their responses are uncoupled. Towers having different dynamic and geometric properties were chosen since the base shear forces are directly related to the component's period of vibration. It should be noted that the R_p factor in Equation 2-11 is taken as being equal to 1.0 because it is assumed that neither the tower nor its attachment to the building is experiencing ductile nonlinear deformation, while the C_p factor in Equation 2-11 is taken as equal 1.0, as suggested in Table 4.1.8.17 of the NBCC 2005. The prediction of maximum rooftop accelerations from time-history input records at a building's base was discussed in Chapter 4, but a methodology for generating the building rooftop response spectra is outside the scope of this study. Such methods can be found in Singh (1975) and Gupta (1990). The ratio of shear force demand, V, calculated from the numerical models generated in SAP 2000 and the shear force determined from Equation 2-11 using either the time-history accelerations ($ma_{rooftop}$) or spectral accelerations ($W*S_a(T)$) was calculated. This ratio represents the component force amplification factor A_r of the tower when time-history acceleration is used. Results of numerical simulations for each building-tower combination and corresponding component force amplification factors calculated according to the NBCC 2005 are summarized in Tables 5-21 to 5-32. Only the results of the buildings labeled CHYBA9, CHYBA4, and 2020 University are presented. It is recommended to perform detailed dynamic analysis and modeling for buildings of complex geometry like the TCUBAA building, which is not a representative case and thus it will not be considered in subsequent sections. All calculations were done separately in both the U1 and U2 directions.

5.2.1.1 Shear forces for the towers mounted on the CHYBA9 building

The results of shear forces for the CHYBA9 building combined with each of the TC1, TC2, TC3, and TC4 towers are presented in Tables 5-21 to 5-24.

Table 5-21 Shear forces for the combination CHYBA9-TC1

CHYBA9	TC1 ($T_1 = T_2 = 0.14$ s)									
Ratio / Load case	$V_{demand}/W*S_a(T)$				$V_{demand}/ma_{rooftop}$				A_r	
	U1		U2		U1		U2		U1	U2
	μ	σ	μ	σ	μ	σ	μ	σ		
H	0.71	0.11	0.73	0.13	1.30	0.03	1.17	0.02	1.15	1
M	0.84	0.08	0.86	0.11	1.19	0.02	1.19	0.03	1.15	1
L	0.86	0.14	0.92	0.08	1.21	0.05	1.29	0.44	1.15	1
2%	0.68	0.11	0.74	0.11	1.11	0.14	1.18	0.05	1.15	1
10%	0.72	0.07	0.77	0.08	1.18	0.04	1.18	0.04	1.15	1
50%	0.74	0.06	0.71	0.05	1.18	0.03	1.17	0.03	1.15	1
All records	0.77	0.12	0.80	0.13	1.20	0.09	1.20	0.32	1.15	1

Table 5-22 Shear forces for the combination CHYBA9-TC2

CHYBA9	TC2 ($T_1 = T_2 = 0.37$ s)									
Ratio / Load case	$V_{demand}/W*S_a(T)$				$V_{demand}/ma_{rooftop}$				A_r	
	U1		U2		U1		U2		U1	U2
	μ	σ	μ	σ	μ	σ	μ	σ		
H	0.43	0.16	0.45	0.13	0.66	0.22	1.03	0.36	2.5	2.5
M	0.41	0.15	0.38	0.11	0.77	0.34	0.98	0.32	2.5	2.5
L	0.53	0.12	0.50	0.09	0.84	0.30	1.21	0.50	2.5	2.5
2%	0.43	0.10	0.48	0.11	0.58	0.16	1.01	0.28	2.5	2.5
10%	0.43	0.08	0.41	0.06	0.60	0.15	0.89	0.22	2.5	2.5
50%	0.38	0.08	0.42	0.07	0.55	0.12	1.07	0.31	2.5	2.5
All records	0.44	0.13	0.44	0.11	0.68	0.26	1.04	0.27	2.5	2.5

Table 5-23 Shear forces for the combination CHYBA9-TC3

CHYBA9	TC3 ($T_1 = T_2 = 0.19$ s)									
Ratio / Load case	$V_{demand}/W*S_a(T)$				$V_{demand}/ma_{rooftop}$				A_r	
	U1		U2		U1		U2		U1	U2
	μ	σ	μ	σ	μ	σ	μ	σ		
H	1.07	0.17	1.05	0.10	3.07	0.52	2.18	0.27	2.5	1.9
M	1.17	0.17	1.11	0.14	2.84	0.50	2.03	0.19	2.5	1.9
L	1.24	0.13	1.08	0.06	2.81	0.49	1.90	0.24	2.5	1.9
2%	1.26	0.17	1.13	0.11	3.22	0.36	2.14	0.19	2.5	1.9
10%	1.20	0.16	1.05	0.12	3.03	0.38	1.94	0.22	2.5	1.9
50%	1.19	0.15	1.11	0.12	2.83	0.26	2.12	0.23	2.5	1.9
All records	1.19	0.17	1.09	0.11	2.96	0.45	2.05	0.81	2.5	1.9

Table 5-24 Shear forces for the combination CHYBA9-TC4

CHYBA9	TC4 ($T_1 = T_2 = 0.25$ s)									
Ratio / Load case	$V_{demand}/W*S_a(T)$				$V_{demand}/ma_{rooftop}$				A_r	
	U1		U2		U1		U2		U1	U2
	μ	σ	μ	σ	μ	σ	μ	σ		
H	0.60	0.07	0.49	0.04	3.13	0.74	2.10	0.33	2.5	2.5
M	0.60	0.04	0.56	0.03	3.51	0.76	2.03	0.19	2.5	2.5
L	0.62	0.02	0.66	0.24	3.68	0.68	2.62	1.15	2.5	2.5
2%	0.64	0.07	0.49	0.04	3.98	0.49	2.36	0.30	2.5	2.5
10%	0.57	0.04	0.52	0.03	3.69	0.32	2.11	0.30	2.5	2.5
50%	0.58	0.04	0.57	0.03	3.71	0.48	2.32	0.34	2.5	2.5
All records	0.60	0.05	0.55	0.12	3.60	0.66	2.26	1.03	2.5	2.5

Discussion of the shear forces for the towers mounted on the CHYBA9 building

A close look at the values presented in Tables 5-21 to 5-24 indicates that in the case of very flexible towers such as the TC2 tower, the actual shear force demand at the tower's base is much lower than the shear force demand calculated according to the equation suggested in the NBCC 2005. When the ratio $T_{tower}/T_{building}$ approaches unity, the floor response spectra reach their peak values at the building's period which is close to the tower's period; this explains why the acceleration amplification factor to obtain the shear force demand becomes smaller. Therefore, the shear force calculated as a product of the tower's weight and the spectral acceleration $S_a(T)$ in g corresponding to the tower's period gives a conservative estimate of the shear force demand at the base of flexible towers mounted on buildings similar to CHYBA9. For less flexible towers, such as the TC3 and TC4 towers, the shear force demand is in general larger than values calculated according to the method suggested in the NBCC 2005. In the case of the rigid tower TC1, the time-history approach appears to be more adequate than the spectral acceleration approach. Finally, when the ratio $T_{tower}/T_{building}$ is greater than 1, it is suggested that the shear force be calculated as the product of input acceleration and tower mass with a component force amplification factor of 1, since the tower response is not greatly affected by the building's response.

It should be noted that using the spectral accelerations results in less variability in the results.

5.2.1.2 Shear forces for the towers mounted on the CHYBA4 building

Table 5-25 Shear forces for the combination CHYBA4-TC1

CHYBA4	TC1 ($T_1 = T_2 = 0.14$ s)									
Ratio / Load case	$V_{demand}/W*S_a(T)$				$V_{demand}/ma_{rooftop}$				A_r	
	U1		U2		U1		U2		U1	U2
	μ	σ	μ	σ	μ	σ	μ	σ		
H	0.57	0.17	0.76	0.82	1.77	0.16	1.69	0.22	1	1
M	0.67	0.17	0.77	0.74	2.88	0.45	2.86	0.31	1	1
L	0.62	0.15	0.37	0.10	1.60	0.17	1.61	0.26	1	1
2%	0.47	0.05	1.13	0.45	1.74	0.11	1.80	0.14	1	1
10%	0.49	0.04	0.68	0.34	1.75	0.15	1.73	0.15	1	1
50%	0.46	0.05	0.50	0.39	1.80	0.15	1.78	0.17	1	1
All records	0.56	0.14	0.71	0.58	1.95	0.52	1.96	0.70	1	1

Table 5-26 Shear forces for the combination CHYBA4-TC2

CHYBA4	TC2 ($T_1 = T_2 = 0.37$ s)									
Ratio / Load case	$V_{demand}/W*S_a(T)$				$V_{demand}/ma_{rooftop}$				A_r	
	U1		U2		U1		U2		U1	U2
	μ	σ	μ	σ	μ	σ	μ	σ		
H	1.35	0.24	1.12	0.24	4.06	1.63	1.79	0.57	2.5	2.5
M	1.28	0.07	0.88	0.14	5.36	1.41	1.92	0.46	2.5	2.5
L	1.45	0.16	0.84	0.14	6.01	0.99	2.17	0.74	2.5	2.5
2%	1.33	0.09	1.12	0.27	4.68	1.21	1.68	0.30	2.5	2.5
10%	1.31	0.15	0.99	0.19	4.85	1.49	1.86	0.25	2.5	2.5
50%	1.43	0.21	1.13	0.21	5.31	1.71	2.01	0.20	2.5	2.5
All records	1.36	0.17	1.00	0.23	5.07	1.51	1.91	0.48	2.5	2.5

Table 5-27 Shear forces for the combination CHYBA4-TC3

CHYBA4	TC3 ($T_1 = T_2 = 0.19$ s)									
Ratio / Load case	$V_{demand}/W*S_a(T)$				$V_{demand}/ma_{rooftop}$				A_r	
	U1		U2		U1		U2		U1	U2
	μ	σ	μ	σ	μ	σ	μ	σ		
H	1.15	0.11	1.31	0.14	2.03	0.69	2.34	0.74	1	1.83
M	1.19	0.17	1.32	0.07	2.16	0.59	2.61	0.35	1	1.83
L	1.30	0.16	1.34	0.09	2.20	0.34	2.46	0.38	1	1.83
2%	1.25	0.12	1.34	0.06	2.10	0.32	2.20	0.28	1	1.83
10%	1.24	0.17	1.31	0.04	2.09	0.42	2.31	0.18	1	1.83
50%	1.28	0.17	1.30	0.06	2.15	0.40	2.37	0.27	1	1.83
All records	1.23	0.16	1.32	0.08	2.12	0.48	2.40	0.64	1	1.83

Table 5-28 Shear forces for the combination CHYBA4-TC4

CHYBA4	TC4 ($T_1 = T_2 = 0.25$ s)									
Ratio / Load case	$V_{demand}/W*S_a(T)$				$V_{demand}/ma_{rooftop}$				A_r	
	U1		U2		U1		U2		U1	U2
	μ	σ	μ	σ	μ	σ	μ	σ		
H	1.33	0.48	0.67	0.20	1.94	0.54	1.98	0.49	1.9	2.5
M	1.19	0.43	0.70	0.10	2.12	0.62	2.33	0.37	1.9	2.5
L	1.09	0.20	0.71	0.15	1.88	0.39	2.28	0.38	1.9	2.5
2%	1.28	0.20	0.69	0.10	1.88	0.36	1.92	0.20	1.9	2.5
10%	1.23	0.27	0.67	0.06	2.00	0.41	2.03	0.25	1.9	2.5
50%	1.28	0.36	0.74	0.10	2.05	0.38	2.11	0.23	1.9	2.5
All records	1.23	0.34	0.70	0.13	1.98	0.46	2.12	0.59	1.9	2.5

Discussion of the shear forces for the towers mounted on the CHYBA4 building

The results presented in Tables 5-25 to 5-28 indicate that a component force amplification factor of 2.5 is adequate for flexible towers mounted on this type of building, except for the TC2 tower where the ratio $T_{tower}/T_{building}$ approaches unity from the lower side, resulting in larger acceleration amplification; therefore, a factor equal to 6 is suggested. It is noted that using the spectral accelerations as input produces less variability in the results. For this building, the values of input seismic shear forces as proposed in the NBCC 2005 are inadequate and unconservative, especially for the flexible tower TC2.

5.2.1.3 Shear forces for the towers mounted on the 2020 University building

Table 5-29 Shear forces for the combination 2020 University-TC1

2020 University	TC1 ($T_1 = T_2 = 0.14$ s)									
Ratio / Load case	$V_{demand}/W*S_a(T)$				$V_{demand}/ma_{rooftop}$				A_r	
	U1		U2		U1		U2		U1	U2
	μ	σ	μ	σ	μ	σ	μ	σ		
H	0.34	0.09	0.32	0.07	0.83	0.10	0.83	0.52	1	1
M	0.66	0.18	0.47	0.10	1.14	0.16	0.76	0.06	1	1
L	1.20	0.66	0.60	0.16	1.60	0.52	0.82	0.09	1	1
2%	0.45	0.07	0.37	0.05	0.90	0.09	0.70	0.04	1	1
10%	0.49	0.13	0.37	0.08	1.03	0.25	0.73	0.06	1	1
50%	0.45	0.14	0.36	0.09	0.89	0.09	0.73	0.06	1	1
All records	0.62	0.43	0.42	0.14	1.09	0.38	0.77	0.40	1	1

Table 5-30 Shear forces for the combination 2020 University-TC2

2020 University	TC2 ($T_1 = T_2 = 0.37$ s)									
Ratio / Load case	$V_{demand}/W*S_a(T)$				$V_{demand}/ma_{rooftop}$				A_r	
	U1		U2		U1		U2		U1	U2
	μ	σ	μ	σ	μ	σ	μ	σ		
H	1.28	0.10	2.10	0.58	2.11	0.68	3.28	0.71	1	1
M	1.20	0.16	1.58	0.30	2.52	0.57	2.64	0.44	1	1
L	1.19	0.10	1.56	0.34	2.35	0.53	2.47	0.49	1	1
2%	1.28	0.10	2.79	0.91	2.15	0.36	3.90	1.07	1	1
10%	1.32	0.13	2.41	1.05	2.23	0.44	3.77	1.37	1	1
50%	1.31	0.08	2.60	0.78	2.22	0.46	3.76	0.85	1	1
All records	1.26	0.12	2.10	0.81	2.28	0.53	3.22	0.68	1	1

Table 5-31 Shear forces for the combination 2020 University-TC3

2020 University	TC3 ($T_1 = T_2 = 0.19$ s)									
Ratio / Load case	$V_{demand}/W*S_a(T)$				$V_{demand}/ma_{rooftop}$				A_r	
	U1		U2		U1		U2		U1	U2
	μ	σ	μ	σ	μ	σ	μ	σ		
H	1.37	0.11	1.52	0.30	4.16	1.55	4.84	1.37	1	1
M	1.32	0.20	1.53	0.29	3.87	1.36	4.45	1.32	1	1
L	1.31	0.16	1.55	0.26	2.94	0.98	3.36	0.96	1	1
2%	1.33	0.18	1.65	0.14	4.37	1.49	5.20	1.30	1	1
10%	1.33	0.12	1.53	0.19	3.87	0.68	4.84	1.21	1	1
50%	1.37	0.10	1.62	0.16	4.39	0.89	5.63	1.27	1	1
All records	1.34	0.15	1.56	0.24	3.89	1.30	4.63	1.44	1	1

Table 5-32 Shear forces for the combination 2020 University-TC4

2020 University	TC4 ($T_1 = T_2 = 0.25$ s)									
Ratio / Load case	$V_{demand}/W^*S_a(T)$				$V_{demand}/ma_{rooftop}$				A_r	
	U1		U2		U1		U2		U1	U2
	μ	σ	μ	σ	μ	σ	μ	σ		
H	1.39	0.58	1.16	0.67	2.71	0.70	2.72	0.67	1	1
M	1.28	0.44	1.00	0.28	2.46	0.63	2.41	0.54	1	1
L	1.16	0.27	1.19	1.18	2.00	0.55	2.40	1.69	1	1
2%	1.25	0.32	1.09	0.25	3.23	0.64	3.35	0.73	1	1
10%	1.25	0.28	0.99	0.13	3.61	0.75	3.52	0.65	1	1
50%	1.18	0.26	1.07	0.18	2.55	0.37	2.54	0.52	1	1
All records	1.26	0.38	1.09	0.61	2.70	0.79	2.78	0.89	1	1

Discussion of the shear forces for the towers mounted on the 2020 University building

For this high-rise and very flexible building, the results presented in Tables 5-29 to 5-32 indicate that the response of the towers is much influenced by the building's response. The input acceleration at the tower base is much amplified and the formula suggested in the NBCC is not suitable; therefore, a higher component amplification factor should be used, even if the ratio of the fundamental periods is very small; a factor of 5 is suggested for towers mounted on this type of building. The method proposed in the NBCC 2005 can be considered adequate and conservative only for the very rigid tower TC1.

5.2.2 General remarks

Based on the aforementioned results, it can be concluded that the equation proposed in the NBCC 2005 for the estimation of seismic shear forces at the base of rooftop OFCs is inadequate, especially in case of flexible towers mounted on flexible buildings. Moreover, provisions do not exist for the estimation of seismic overturning moments at the building-tower interface. This has motivated our development of a simplified method to estimate these forces while avoiding time-consuming detailed analyses, as a preliminary check.

5.2.3 Prediction of overturning moment demands for telecommunication towers mounted on building rooftops

Code provisions for the calculation of seismic overturning moments at the base of a telecommunication tower mounted on a building rooftop do not yet exist, to our best knowledge. The seismic base shear forces, V, and overturning moments, M, at the base of telecommunication towers mounted on building rooftops were calculated from the numerical models of all building-tower combinations subjected to the earthquake records depicted in Chapter 4. Detailed calculations of V and M for the combination CHYBA9-TC2 are presented in Appendix D. The computation of base shear forces was discussed in a previous section. The overturning moments are calculated as the sum of the product of maximum absolute vertical component of axial forces in the legs of the tower by the lever arm for each leg, which is the perpendicular distance between the leg and the geometrical center of the tower base. In order to gain insight into the relationship between the overturning moment, M, and base shear force, V, at the building-tower interface, the ratio

M/V was calculated. Tables 5-33 to 5-45 summarize the results of numerical simulations for all generated building-tower combinations. First, the average values and standard deviations for each set of data records are presented, followed by the results of all sets.

Table 5-33 Ratio M/V for CHYBA9-TC1

CHYBA9-TC1	M/V (m)			
Ratio / Load case	U1		U2	
	μ	σ	μ	σ
H	3.69	0.06	3.80	0.09
M	3.66	0.05	3.72	0.06
L	3.61	0.09	3.68	0.07
2%	3.94	0.51	3.85	0.10
10%	3.80	0.11	3.79	0.09
50%	3.77	0.09	3.82	0.09
All records	3.74	0.12	3.78	0.07

Table 5-34 Ratio M/V for CHYBA9-TC2

CHYBA9-TC2	M/V (m)			
Ratio / Load case	U1		U2	
	μ	σ	μ	σ
H	20.00	4.43	21.75	3.61
M	19.90	1.79	24.27	2.61
L	18.91	1.72	24.27	2.61
2%	20.09	2.03	20.09	2.03
10%	19.44	1.75	22.66	2.24
50%	19.90	1.50	20.88	1.54
All records	19.71	0.45	22.32	1.74

Table 5-35 Ratio M/V for CHYBA9-TC3

CHYBA9-TC3	M/V (m)			
Ratio / Load case	U1		U2	
	μ	σ	μ	σ
H	12.56	0.32	12.29	0.37
M	12.41	0.28	12.11	0.24
L	12.20	0.26	12.17	0.33
2%	12.50	0.31	12.32	0.25
10%	12.40	0.15	12.57	1.00
50%	12.32	0.17	12.47	0.38
All records	12.40	0.13	12.32	0.17

Table 5-36 Ratio M/V for CHYBA9-TC4

CHYBA9-TC4	M/V (m)			
Ratio / Load case	U1		U2	
	μ	σ	μ	σ
H	12.65	0.27	12.49	0.63
M	12.56	0.22	12.20	0.31
L	12.47	0.40	11.97	0.46
2%	12.57	0.37	12.49	0.46
10%	12.70	0.46	12.53	0.91
50%	12.63	0.18	12.37	0.59
All records	12.60	0.08	12.34	0.22

Table 5-37 Ratio M/V for CHYBA4-TC1

CHYBA4-TC1	M/V (m)			
Ratio / Load case	U1		U2	
	μ	σ	μ	σ
H	4.79	0.18	5.19	0.20
M	4.66	0.26	4.92	0.18
L	4.60	0.23	4.98	0.22
2%	4.88	0.12	5.20	0.10
10%	4.84	0.15	5.13	0.14
50%	4.86	0.14	5.19	0.16
All records	4.77	0.12	5.10	0.12

Table 5-38 Ratio M/V for CHYBA4-TC2

CHYBA4-TC2	M/V (m)			
Ratio / Load case	U1		U2	
	μ	σ	μ	σ
H	18.92	2.07	18.82	3.70
M	19.70	0.42	22.11	1.81
L	19.84	0.29	21.02	1.50
2%	19.27	0.70	18.54	2.47
10%	19.26	0.98	19.49	2.21
50%	18.14	2.10	17.83	2.45
All records	19.19	0.61	19.64	1.62

Table 5-39 Ratio M/V for CHYBA4-TC3

CHYBA4-TC3	M/V (m)			
Ratio / Load case	U1		U2	
	μ	σ	μ	σ
H	14.54	1.52	13.41	0.72
M	13.50	1.12	13.18	0.45
L	13.07	0.75	13.21	0.47
2%	14.11	0.77	13.46	0.43
10%	14.48	1.57	13.36	0.55
50%	14.40	1.26	13.58	0.64
All records	14.02	0.60	13.37	0.15

Table 5-40 Ratio M/V for CHYBA4-TC4

CHYBA4-TC4	M/V (m)			
Ratio / Load case	U1		U2	
	μ	σ	μ	σ
H	12.97	1.67	9.85	0.56
M	11.91	1.09	9.81	0.23
L	11.62	0.92	9.88	0.45
2%	12.83	1.14	9.99	0.41
10%	12.59	0.83	10.41	1.34
50%	13.01	0.74	10.29	0.77
All records	12.49	0.58	10.04	0.25

Table 5-41 Ratio M/V for 2020 University-TC1

2020 University-TC1	M/V (m)			
Ratio / Load case	U1		U2	
	μ	σ	μ	σ
H	4.20	0.42	3.17	0.14
M	4.86	0.26	3.01	0.14
L	4.71	0.16	2.67	0.20
2%	4.26	0.26	3.24	0.13
10%	4.36	0.47	3.14	0.14
50%	4.33	0.39	3.16	0.12
All records	4.45	0.27	3.07	0.21

Table 5-42 Ratio M/V for 2020 University-TC2

2020 University-TC2	M/V (m)			
Ratio / Load case	U1		U2	
	μ	σ	μ	σ
H	18.79	1.76	14.47	2.71
M	19.59	0.86	17.81	1.84
L	19.43	0.61	16.76	2.25
2%	18.72	1.34	12.11	1.97
10%	18.91	1.53	14.19	2.70
50%	19.01	0.74	13.69	2.22
All records	19.07	0.36	14.84	2.09

Table 5-43 Ratio M/V for 2020 University-TC3

2020 University-TC3	M/V (m)			
Ratio / Load case	U1		U2	
	μ	σ	μ	σ
H	14.65	0.26	14.63	0.21
M	14.48	0.29	14.58	0.25
L	14.35	0.53	14.45	0.34
2%	14.64	0.24	14.72	0.17
10%	14.63	0.22	12.57	1.12
50%	14.72	0.22	12.55	0.96
All records	14.58	0.14	13.92	1.06

Table 5-44 Ratio M/V for 2020 University-TC4

2020 University-TC4	M/V (m)			
Ratio / Load case	U1		U2	
	μ	σ	μ	σ
H	11.97	0.59	14.20	0.62
M	11.61	0.57	13.57	1.18
L	11.10	0.92	13.29	1.41
2%	11.97	0.42	13.93	0.65
10%	11.86	0.60	14.77	2.12
50%	11.80	0.58	14.52	1.64
All records	11.72	0.33	14.04	0.56

Table 5-45 Summary of results for M/V ratio for all building-tower combinations

Tower ID	M/V (m)				Arm (m)
	U1		U2		
	μ	σ	μ	σ	
TC1	4.32	0.47	3.98	0.88	4
TC2	19.32	0.54	18.93	3.62	12
TC3	13.66	1.01	13.20	0.90	9
TC4	12.27	0.55	12.14	1.73	7

Discussion of the calculation of overturning moments for telecommunication towers mounted on building rooftops

The results presented in Tables 5-33 to 5-45 indicate that for very rigid towers, such as the TC1 tower, the seismic overturning moment at the base of a telecommunication tower can be evaluated by multiplying the shear force at the tower's base by the lever arm, which is the distance between the center of mass of the tower and its base. This conclusion is valid whether the tower is mounted on a rigid or flexible building. On the other hand, the ratio of M/V is larger than the lever arm for the flexible towers TC2, TC3, and TC4. Therefore, the overturning moment at the tower base cannot be directly obtained from the total base shear force and a more accurate calculation is necessary to predict overturning moments.

Based on the results presented in the previous sections, it can be concluded that a simplified method is needed for estimating the seismic base shear force and overturning moment of a telecommunication tower mounted on a building rooftop. Such a method will be presented in the following sections.

5.3 A simplified method for calculating seismic base shear force and overturning moment at a building-tower interface

The purpose of our proposed simplified method is to provide a quick tool to determine the seismic forces on telecommunication towers mounted on building rooftops and compare them to the effects of other loads like wind and ice, while avoiding the detailed modeling of the supporting buildings. The simplified method requires the determination of: the input acceleration at the tower base, which was discussed in Chapters 3 and 4; the mass profile m(x) that can be calculated from the tower's structural drawings and localized attachments (antenna drums, platforms, and others); and the evaluation of a horizontal acceleration profile a(x) along the tower's height, which will be discussed in this chapter. The concept of the method is illustrated in Figure 5-9.

The prediction of the tower acceleration profile a(x) is the key factor in this method. It was found that the acceleration amplification profile along a telecommunication tower mounted on a building rooftop matches its fundamental mode shape when mounted on a rigid base. Equations 5-1 and 5-2 provide the basis for the method.

$$V_{calculated} = V_{base} = \int_0^l V_x dx = \int_0^l m(x)a(x)dx \qquad 5\text{-}1$$

$$M_{calculated} = M_{base} = \int_0^l V_x x dx = \int_0^l m(x)a(x)x dx \qquad 5\text{-}2$$

Where:

m(x) : mass of the tower at position x measured from the tower base.

l : tower's height.

V_x : shear force distribution along x.

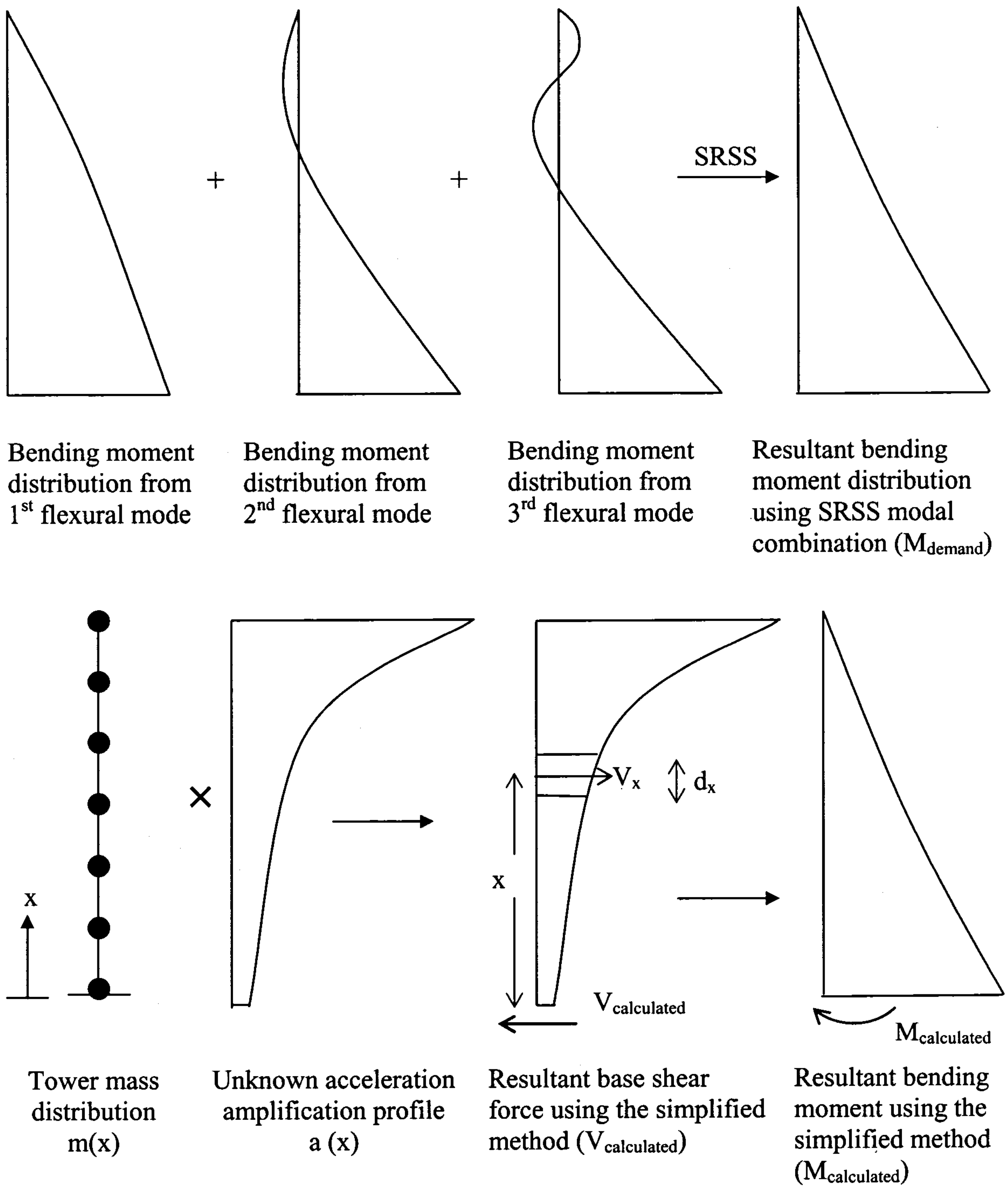

Figure 5-9 Concept of the proposed simplified method

5.3.1 Prediction of tower acceleration profiles a(x)

5.3.1.1 Tower mode shapes on rigid base

In order to gain insight into the dynamic behavior of the towers and to study the correlation between the towers' acceleration profiles and their lateral modes of vibration, the mode shapes corresponding to the first four sway modes of the towers on a rigid base were calculated in both principal directions U1 and U2 of the buildings. The mode shapes of the three flexible towers TC2, TC3, and TC4 used in this study are presented in Figures 5-10 to 5-15; the mode shapes of the TC1 tower are not shown since its acceleration profiles are fairly linear in all cases, with a maximum amplification of 1.5 at the tower top. The fundamental modes of vibration of towers TC2 and TC3 are translational (Figures 5-10 to 5-13) in the principal horizontal directions U1 and U2, while the first two fundamental modes of tower TC4 are biaxial (Figures 5-14 and 5-15).

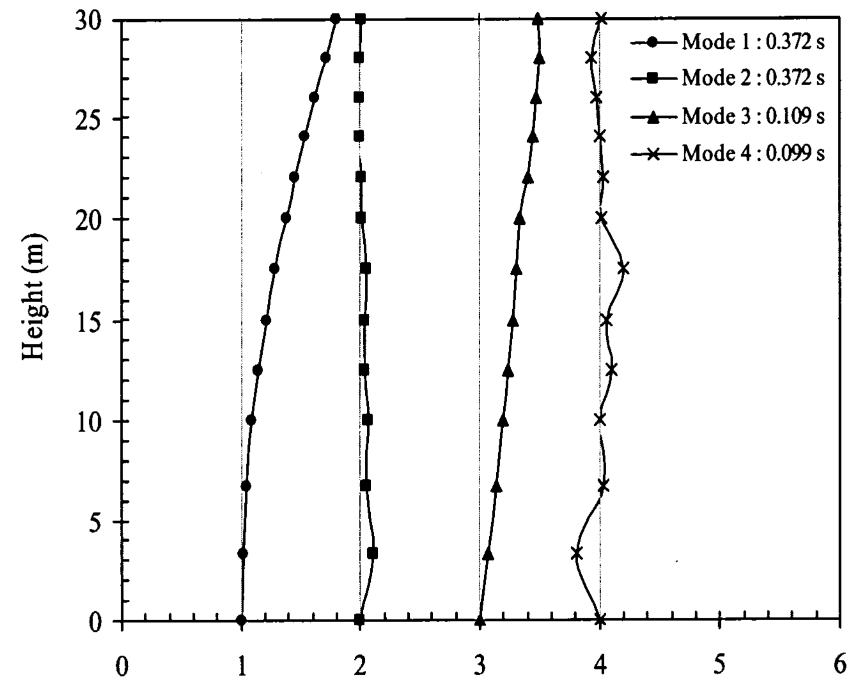

Figure 5-10 Mode shapes of TC2 tower projected on the U1 direction

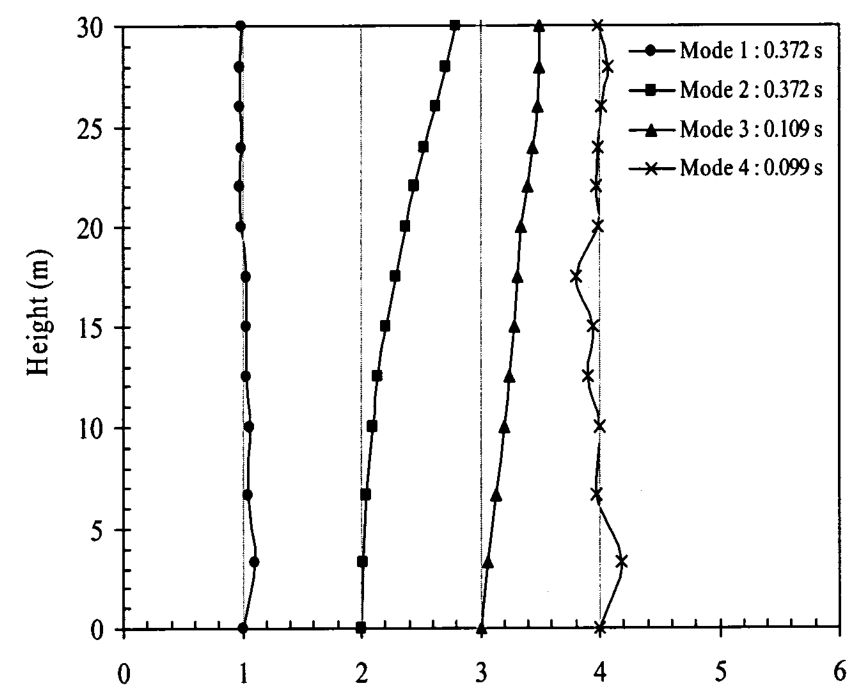

Figure 5-11 Mode shapes of TC2 tower projected on the U2 direction

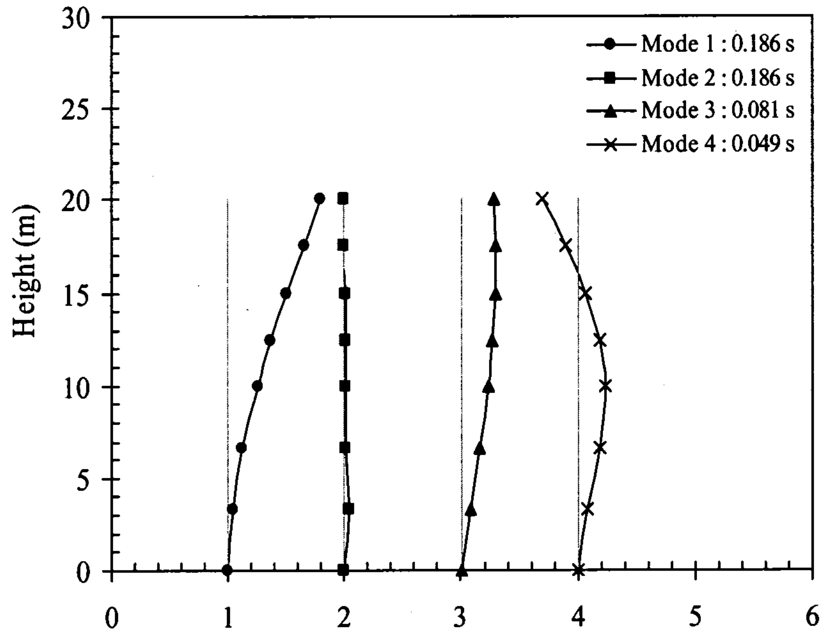

Figure 5-12 Mode shapes of TC3 tower projected on the U1 direction

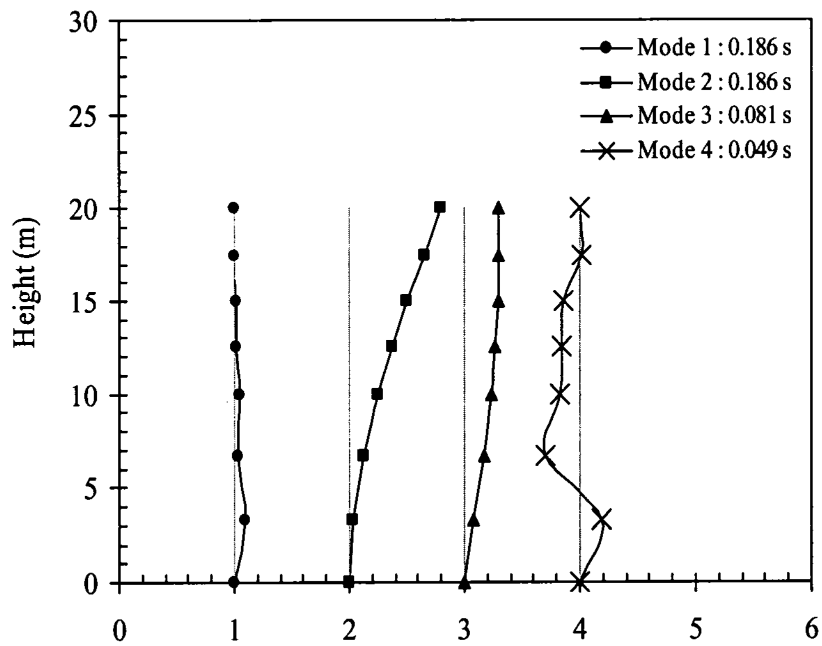

Figure 5-13 Mode shapes of TC3 tower projected on the U2 direction

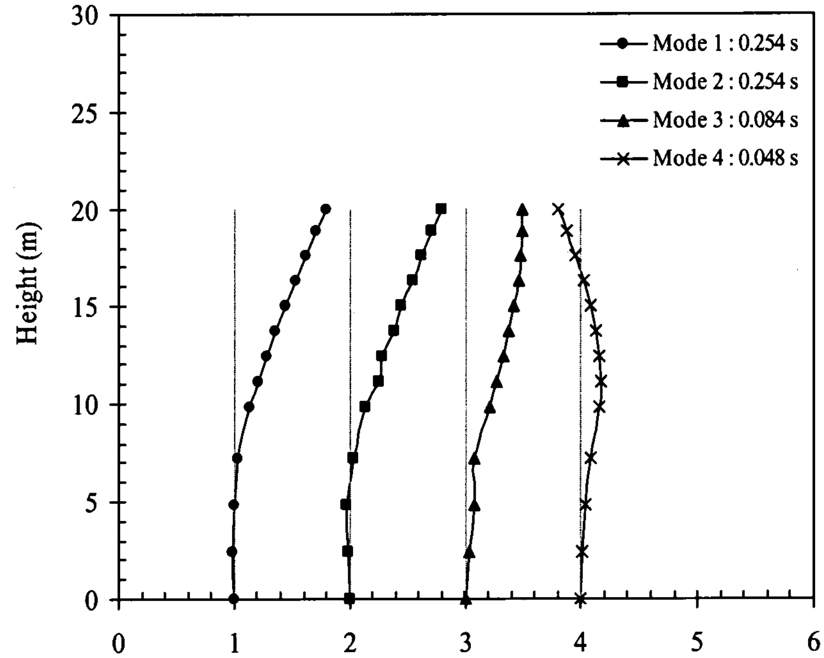

Figure 5-14 Mode shapes of TC4 tower projected on the U1 direction

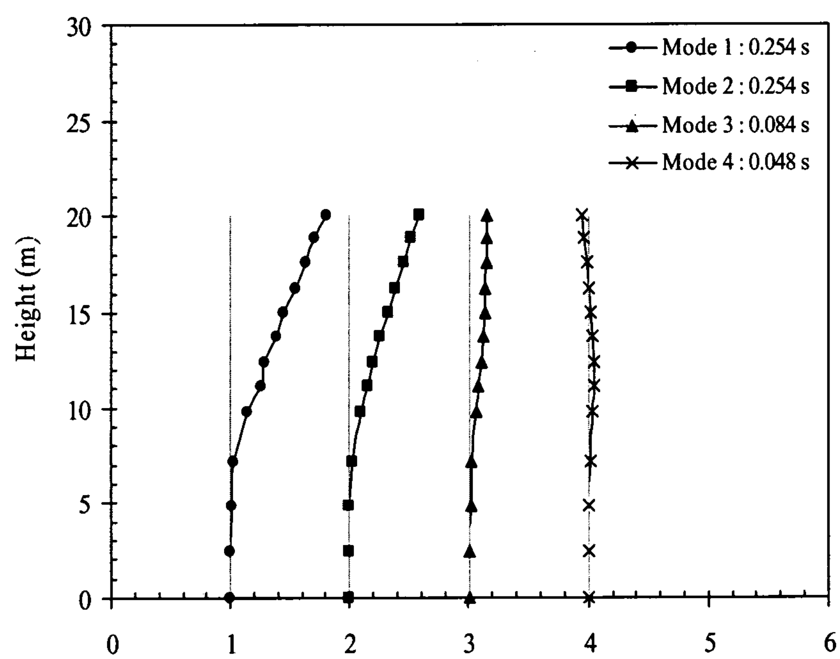

Figure 5-15 Mode shapes of TC4 tower projected on the U2 direction

5.3.2 Calculated and proposed acceleration profiles of the rooftop towers

A strong correspondence was found between the tower acceleration amplification profile and its fundamental sway mode shape. The graphs shown in Figures 5-17 to 5-34 represent the average acceleration amplification profiles along the heights of the towers mounted on each building. These profiles are calculated for each series of the earthquake records applied separately to both principal horizontal directions of the buildings, U1 and U2. Also added to the graphs is the proposed acceleration amplification profile corresponding to the fundamental mode shape of each tower mounted on a rigid base, adjusted to match the maximum acceleration amplification at the tower top. The detailed calculations of acceleration amplification at different stations along the tower height for the TC2, TC3, and TC4 towers mounted on the CHYBA9 building are presented in Appendix E, in addition to the average values and standard deviations of acceleration amplification at each station corresponding to each set of records. Calculations are also illustrated through the graphs presented in Appendix E.

The calculated tower acceleration amplification factors for each building-tower combination are presented in Tables 5-46 to 5-48 in the directions U1 and U2, separately. Following this study, factors were proposed to multiply the tower fundamental mode shape to obtain its acceleration amplification profile when mounted on a stiff building (T < 0.6 s), as illustrated in Table 5-49 and in the graph of Figure 5-16. When the tower is more flexible than the building, the former does not always experience amplification; however, a minimum factor of 1 is suggested to remain conservative. For a tower mounted on a flexible building, it is proposed to multiply its mode shape by a factor of 3 times the rooftop horizontal acceleration in order to obtain the tower acceleration profile.

Table 5-46 Calculated tower acceleration amplification factors for TC2 on 3 buildings

TC2	U1		U2	
	T_p/T	Factor	T_p/T	Factor
CHYBA9	1.43	0.40	1.24	0.80
CHYBA4	0.92	3.32	1.21	1.43
2020 University	0.19	1.25	0.20	3.21

Table 5-47 Calculated tower acceleration amplification factors for TC3 on 3 buildings

TC3	U1		U2	
	T_p/T	Factor	T_p/T	Factor
CHYBA9	0.72	1.09	0.62	0.60
CHYBA4	0.46	1.00	0.61	0.91
2020 University	0.09	2.12	0.10	2.75

Table 5-48 Calculated tower acceleration amplification factors for TC4 on 3 buildings

TC4	U1		U2	
	T_p/T	Factor	T_p/T	Factor
CHYBA9	0.97	2.70	0.84	1.31
CHYBA4	0.62	1.34	0.82	0.88
2020 University	0.13	1.59	0.13	1.96

Table 5-49 Proposed tower acceleration amplification factors for stiff buildings

T_p/T	Factor
0 to 0.6	1.0
0.9 to 1.1	4.0
≥1.2	1.0

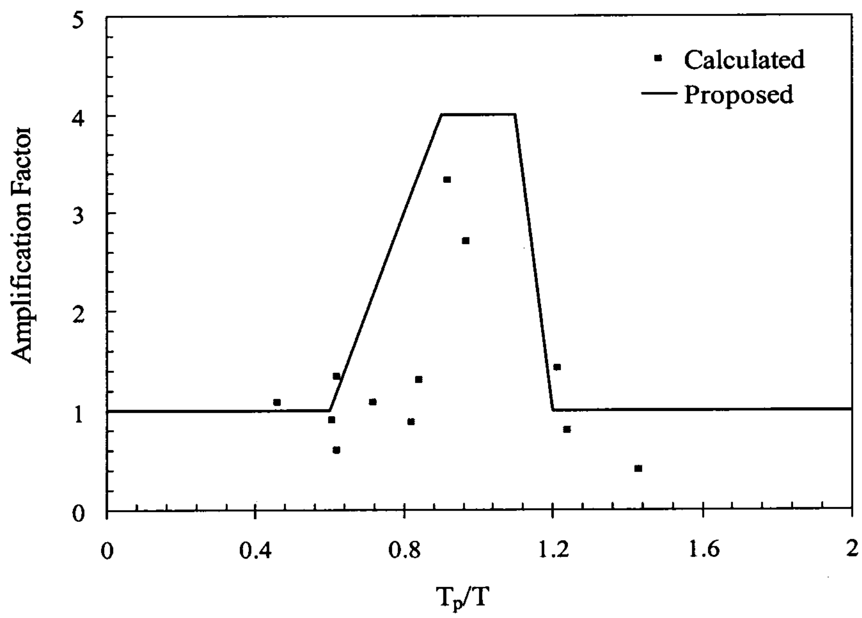

Figure 5-16 Proposed and calculated tower acceleration amplification factors versus T_p/T for stiff buildings ($T < 0.6$ s)

5.3.2.1 Acceleration amplification profiles for towers mounted on the CHYBA9 building

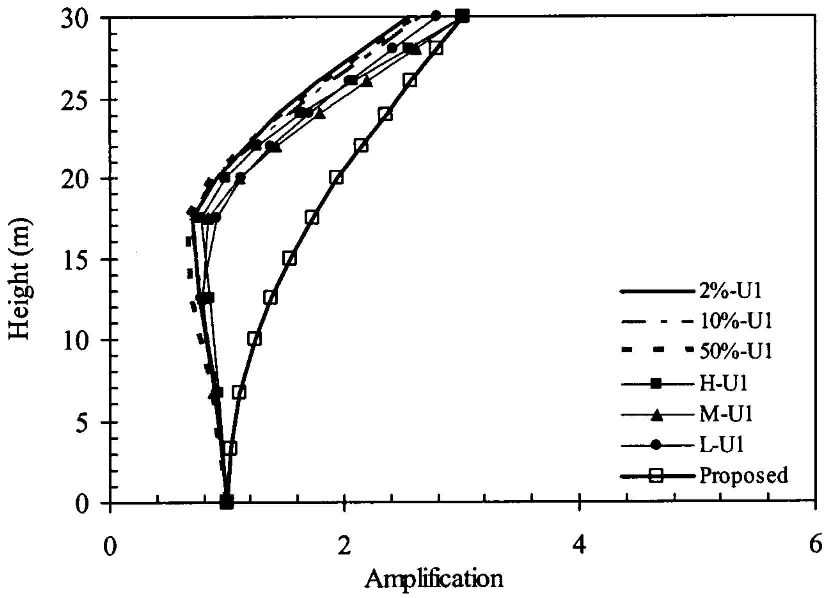

Figure 5-17 Acceleration amplification profiles of TC2 mounted on CHYBA9 - U1 direction

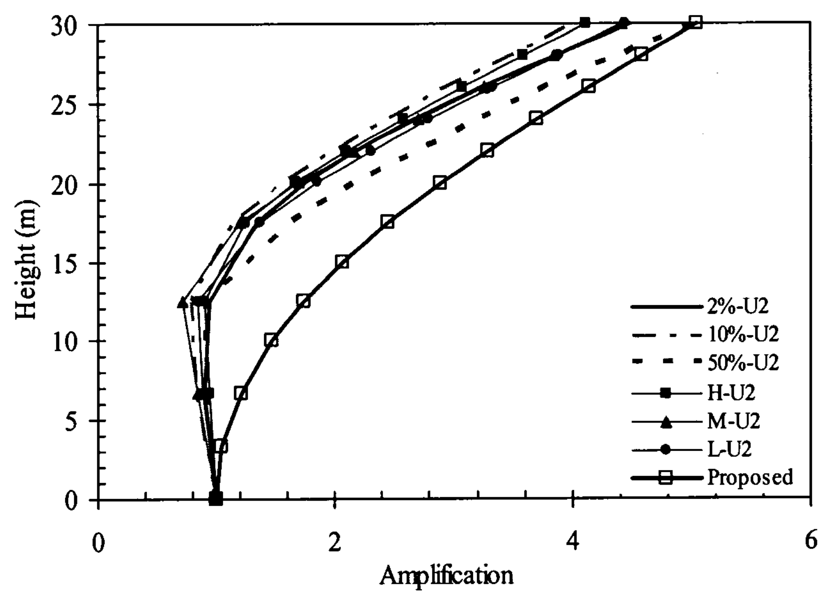

Figure 5-18 Acceleration amplification profiles of TC2 mounted on CHYBA9 - U2 direction

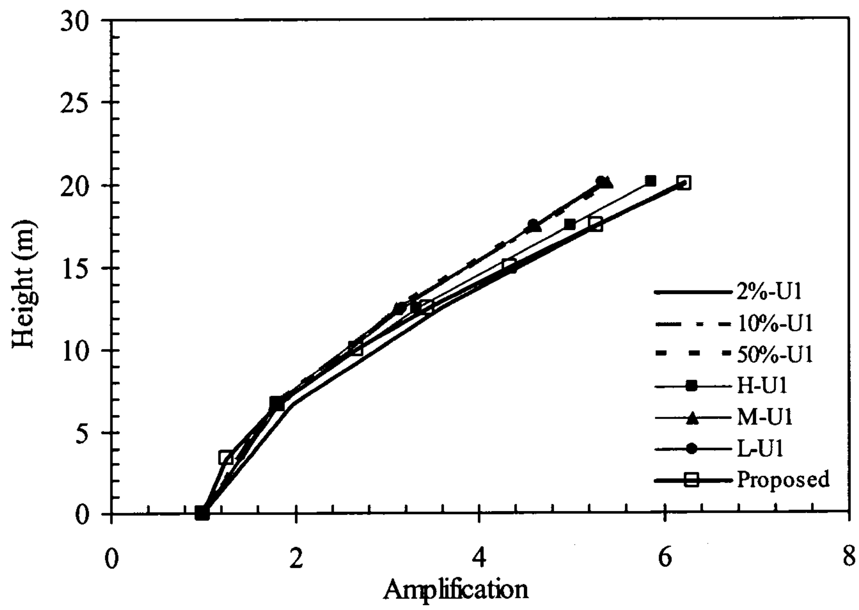

Figure 5-19 Acceleration amplification profiles of TC3 mounted on CHYBA9 - U1 direction

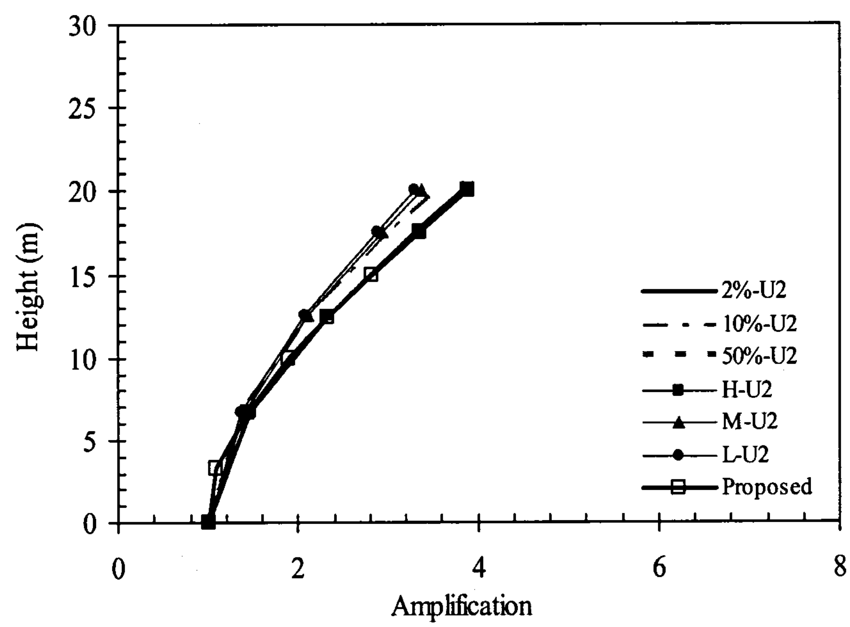

Figure 5-20 Acceleration amplification profiles of TC3 mounted on CHYBA9 - U2 direction

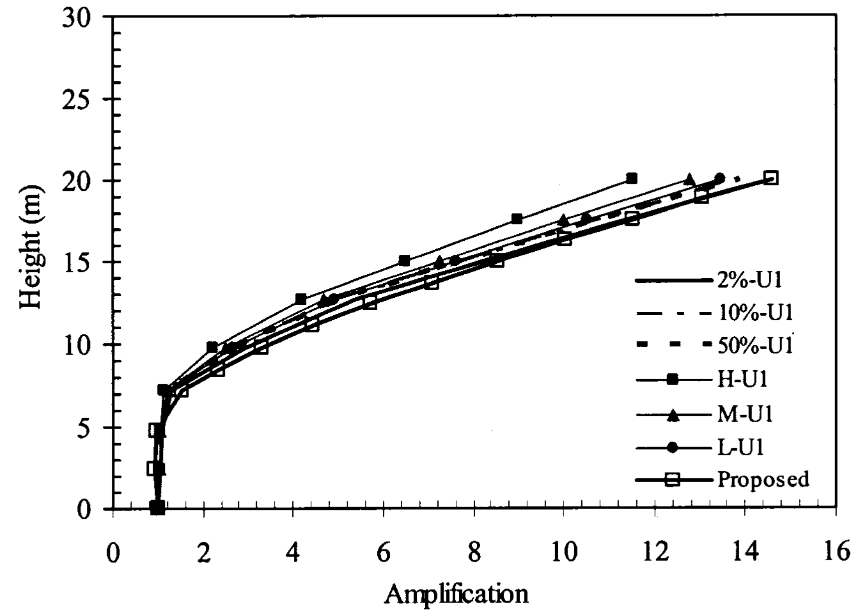

Figure 5-21 Acceleration amplification profiles of TC4 mounted on CHYBA9 - U1 direction

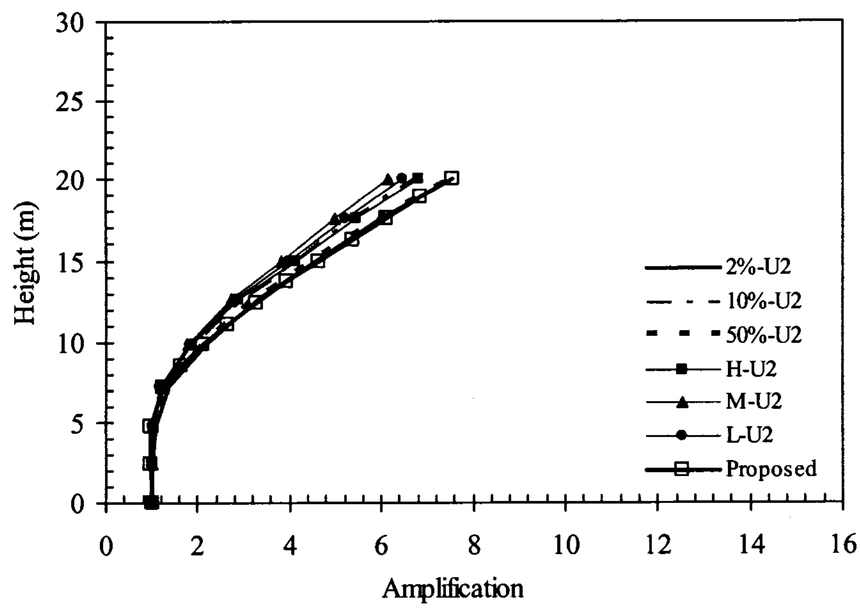

Figure 5-22 Acceleration amplification profiles of TC4 mounted on CHYBA9 - U2 direction

5.3.2.2 Acceleration amplification profiles of towers mounted on the CHYBA4 building

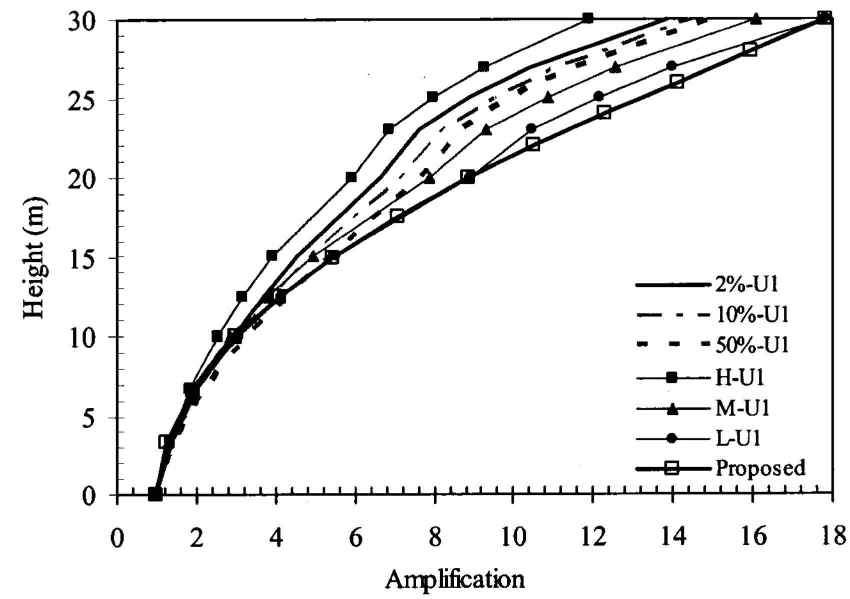

Figure 5-23 Acceleration amplification profiles of TC2 mounted on CHYBA4 - U1 direction

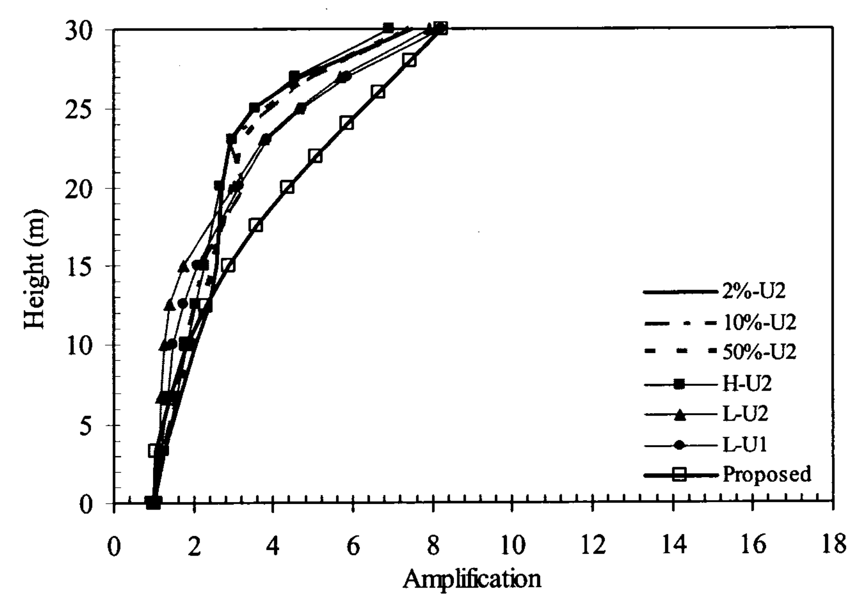

Figure 5-24 Acceleration amplification profiles of TC2 mounted on CHYBA4 - U2 direction

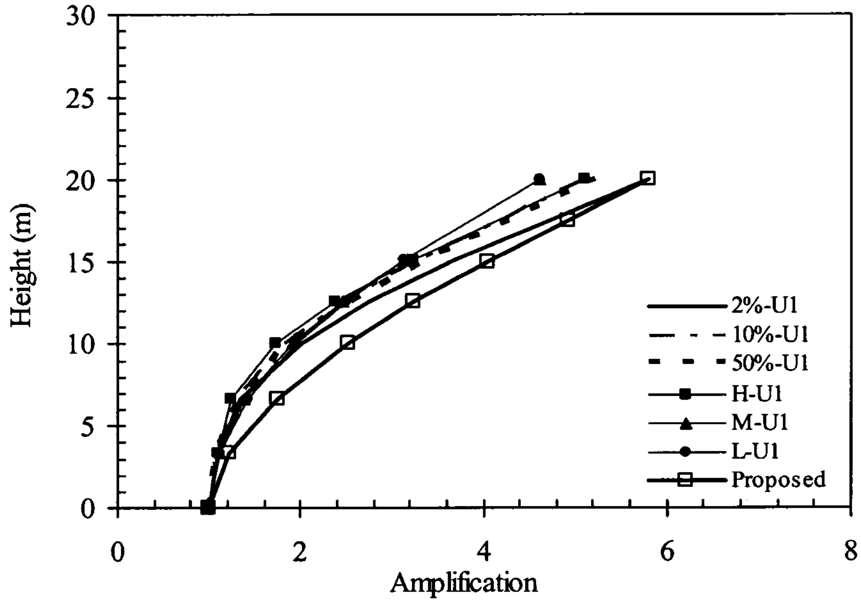

Figure 5-25 Acceleration amplification profiles of TC3 mounted on CHYBA4 - U1 direction

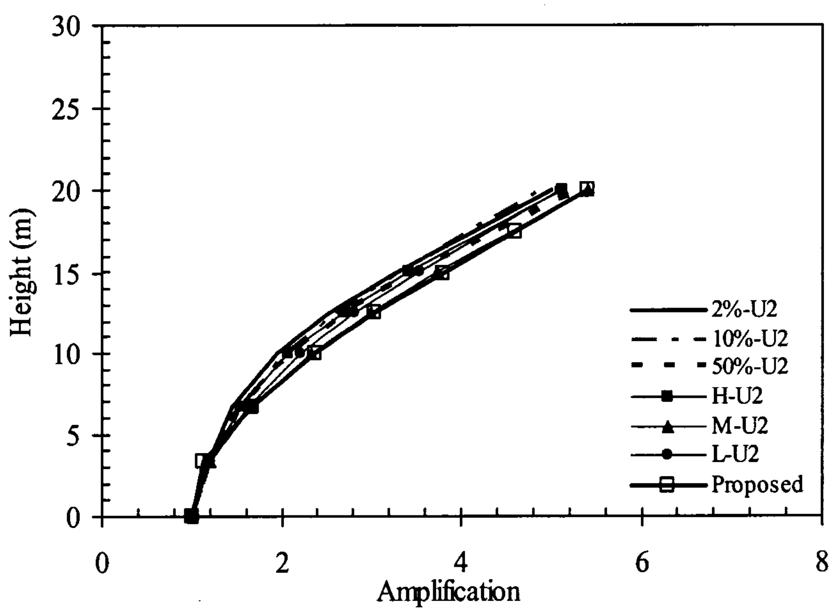

Figure 5-26 Acceleration amplification profiles of TC3 mounted CHYBA4 - U2 direction

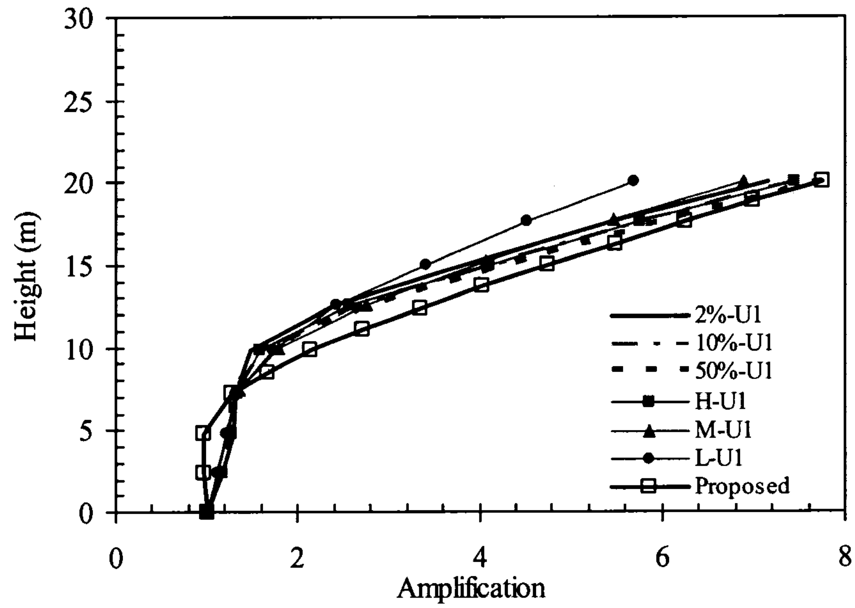

Figure 5-27 Acceleration amplification profiles of TC4 mounted on CHYBA4 - U1 direction

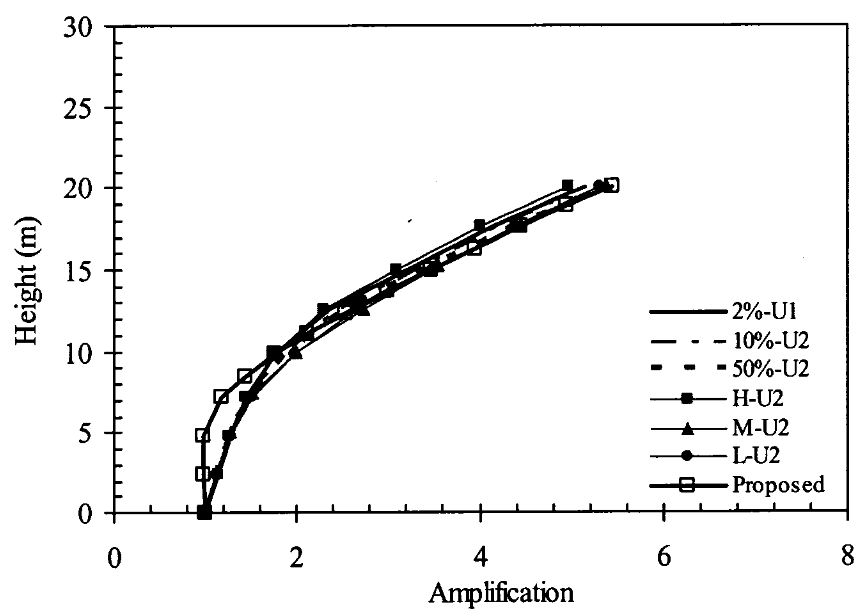

Figure 5-28 Acceleration amplification profiles of TC4 mounted on CHYBA4 - U2 direction

5.3.2.3 Acceleration amplification profiles of towers mounted on the 2020 University building

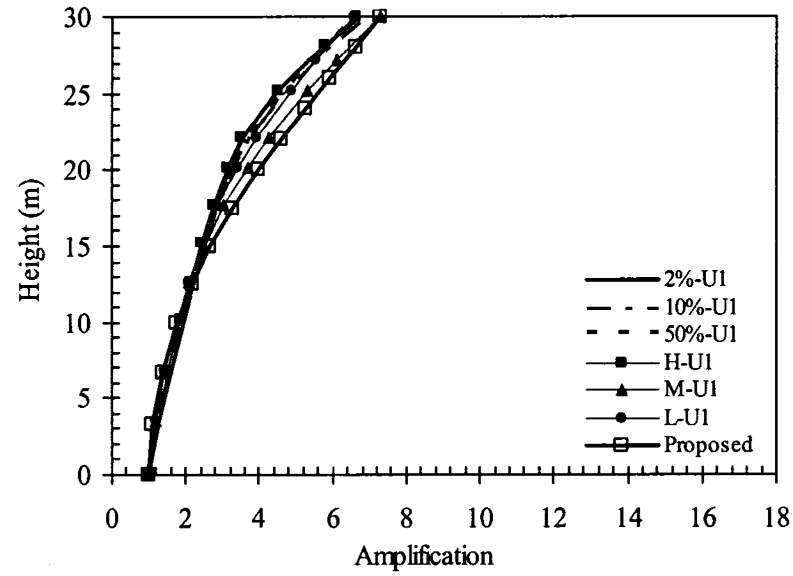

Figure 5-29 Acceleration amplification profiles of TC2 mounted on 2020 University - U1 direction

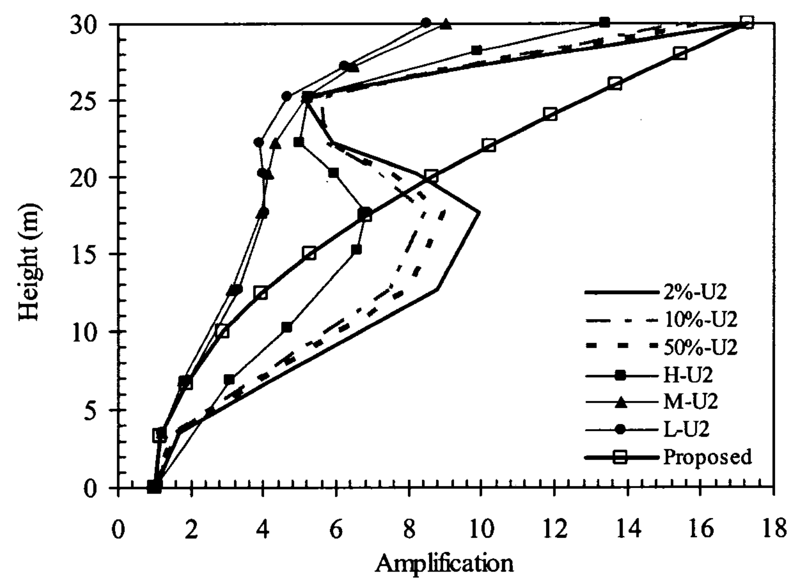

Figure 5-30 Acceleration amplification profiles of TC2 mounted on 2020 University - U2 direction

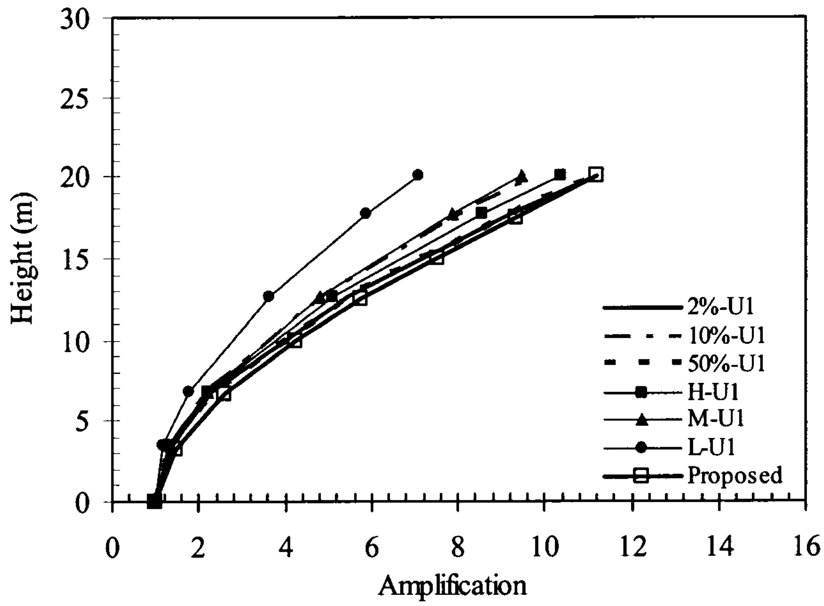

Figure 5-31 Acceleration amplification profiles of TC3 mounted on 2020 University - U1 direction

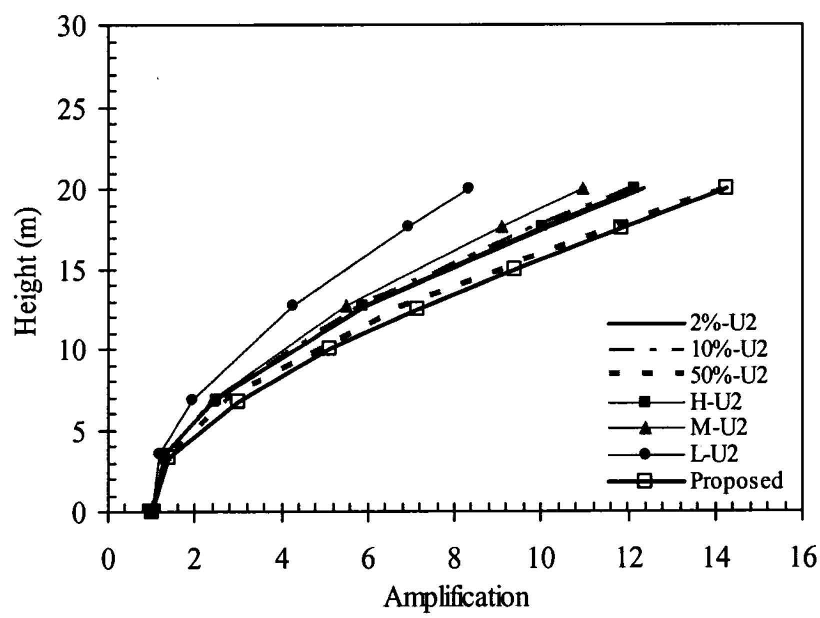

Figure 5-32 Acceleration amplification profiles of TC3 mounted on 2020 University - U2 direction

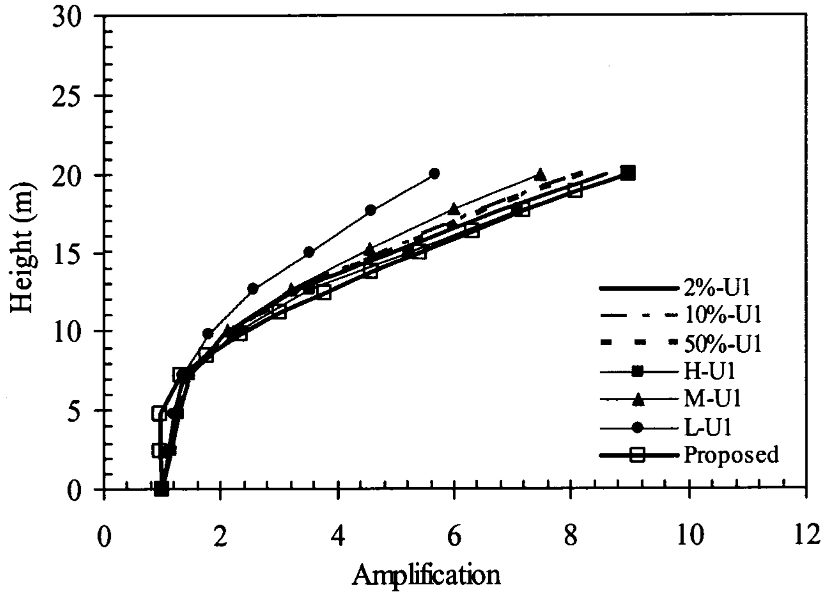

Figure 5-33 Acceleration amplification profiles of TC4 mounted on 2020 University - U1 direction

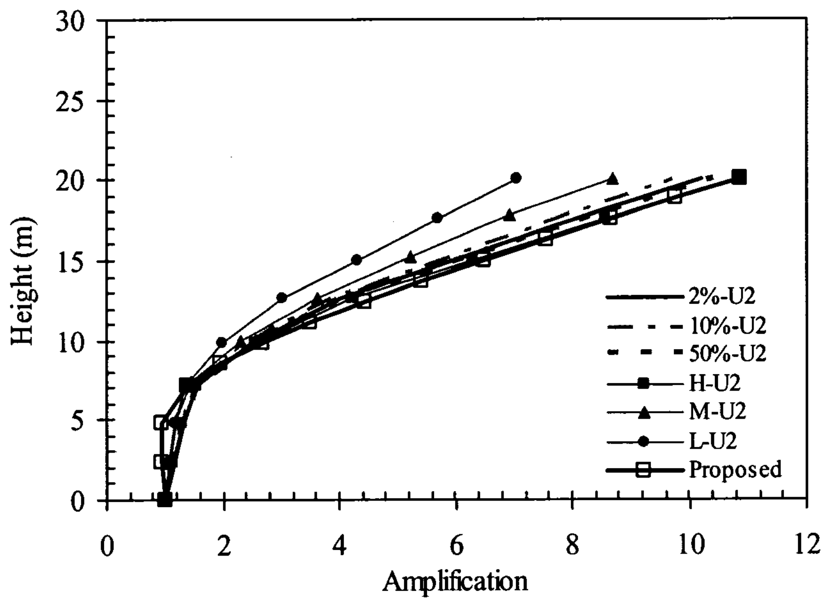

Figure 5-34 Acceleration amplification profiles of TC4 mounted on 2020 University - U2 direction

5.3.2.4 Discussion of the tower acceleration amplification profiles

5.3.2.4.1 CHYBA9 building with TC2 tower

The acceleration profile of the TC2 tower (Figures 5-17 and 5-18) is constant over about two-thirds of its height, and acceleration amplification occurs only at the upper one-third. In contrast to what is expected, this flexible tower supported on this rigid building does not experience significant amplification. This behavior is not reflected in current code provisions that tend to propose a larger component force amplification factor for flexible components without any reference to the supporting structure. In addition, the proposed acceleration amplification profile corresponding to the first mode shape in both principal directions does not follow the calculated amplification profiles. This can be explained by the influence of higher modes of vibration of the building CHYBA9 on the tower's response. It is noted that the first two sway modes of the tower in each principal direction are very close to those of the building, so that the building-tower interaction could explain why the shape of acceleration amplification profiles does not follow its mode shapes, especially in the U1 direction. It is further observed that this 30 m tower is very flexible and represents a limit case of towers mounted on buildings rooftops.

5.3.2.4.2 CHYBA9 building with TC3 tower

For this building-tower combination, the acceleration amplification profiles of the TC3 tower match very well the proposed profiles (Figures 5-19 and 5-20).

5.3.2.4.3 CHYBA9 building with TC4 tower

For this building-tower combination, both the calculated and proposed acceleration amplification profiles (Figures 5-21 and 5-22) remain constant in the tapered part of the tower and match very well.

5.3.2.4.4 CHYBA4 building with TC2, TC3, and TC4 towers

In all building-tower combinations, the calculated and proposed acceleration amplification profiles of the towers mounted on the building's rooftop match fairly well (Figures 5-23 to 5-28). The building's first fundamental period exceeds the periods of all towers, resulting in no significant dynamic interaction between the building and towers. For these building-tower combinations, the tower acceleration amplification increases with the tower flexibility, which is reflected in the codes.

5.3.2.4.5 2020 University building with TC2 tower

For this building-tower combination, the calculated acceleration amplification profiles match the proposed acceleration amplification profile in the U1 direction (Figure 5-29). However, the calculated acceleration amplification profiles do not match the proposed acceleration amplification profile in the U2 direction (Figure 5-30). This unusual behavior of the tower can be attributed to the influence of higher modes of the supporting building. It is recommended to perform detailed dynamic analysis for similar building-tower combinations.

5.3.2.4.6 2020 University building with TC3 and TC4 towers

In both cases, the calculated and proposed acceleration amplification profiles match very well (Figures 5-31 to 5-34).

5.3.3 Parametric study to validate the proposed simplified method

Using Equations 5-1 and 5-2 for each building-tower combination, the values of equivalent base shear forces and overturning moments at the building-tower interfaces were calculated as shown schematically in Figure 5-9. The shear force diagram was obtained by multiplying the mass profile and the acceleration profile; the base overturning moment was obtained by multiplying the mass profile, the acceleration profile, and the moment arm. Detailed calculations using the proposed simplified method for the TC2, TC3, and TC4 towers combined with the CHYBA9 building are presented in Appendix D. Results were compared to the values obtained from the detailed SAP models using the SRSS modal combination method. The average results and their standard deviations for all sets of records are presented in Tables 5-50 to 5-58. In these tables, V_{demand} and M_{demand} are the base reactions calculated in SAP 2000 from the numerical simulations, while $V_{calculated}$ and $M_{calculated}$ are the base reactions calculated according to the proposed simplified method.

Table 5-50 Validation of the simplified method for CHYBA9-TC2

Effort / Load case	CHYBA9-TC2							
	$M_{calculated}/M_{demand}$				$V_{calculated}/V_{demand}$			
	U1		U2		U1		U2	
	μ	σ	μ	σ	μ	σ	μ	σ
H	1.46	0.23	1.20	0.22	1.86	0.56	1.51	0.40
M	1.32	0.38	1.15	0.15	1.71	0.46	1.53	0.31
L	1.20	0.21	1.08	0.23	1.44	0.34	1.33	0.28
2%	1.45	0.25	1.27	0.15	1.87	0.37	1.55	0.21
10%	1.45	0.25	1.19	0.07	1.82	0.38	1.55	0.21
50%	1.45	0.18	1.41	0.18	1.87	0.28	1.62	0.22
All records	1.38	0.27	1.20	0.20	1.75	0.43	1.50	0.30

Table 5-51 Validation of the simplified method for CHYBA9-TC3

Effort / Load case	CHYBA9-TC3							
	$M_{calculated}/M_{demand}$				$V_{calculated}/V_{demand}$			
	U1		U2		U1		U2	
	μ	σ	μ	σ	μ	σ	μ	σ
H	0.97	0.17	0.96	0.04	0.96	0.16	0.98	0.05
M	0.98	0.10	0.97	0.14	0.98	0.09	0.98	0.13
L	1.03	0.05	0.99	0.07	1.01	0.05	1.00	0.07
2%	0.98	0.01	0.97	0.02	0.97	0.02	0.99	0.02
10%	0.94	0.13	0.97	0.02	0.93	0.12	1.02	0.09
50%	1.00	0.02	0.97	0.02	0.98	0.02	1.00	0.04
All records	0.99	0.13	0.97	0.07	0.97	0.10	0.99	0.08

Table 5-52 Validation of the simplified method for CHYBA9-TC4

Effort / Load case	CHYBA9-TC4							
	$M_{calculated}/M_{demand}$				$V_{calculated}/V_{demand}$			
	U1		U2		U1		U2	
	μ	σ	μ	σ	μ	σ	μ	σ
H	1.04	0.02	1.01	0.03	1.00	0.06	1.05	0.08
M	1.03	0.02	1.00	0.01	0.96	0.05	1.02	0.03
L	1.03	0.01	0.92	0.20	0.94	0.04	0.91	0.22
2%	1.03	0.02	1.00	0.03	0.97	0.07	1.01	0.04
10%	1.04	0.01	1.01	0.03	0.96	0.04	1.05	0.11
50%	1.04	0.01	1.01	0.03	0.96	0.03	1.01	0.05
All records	1.03	0.01	0.99	0.11	0.96	0.05	1.00	0.13

Table 5-53 Validation of the simplified method for CHYBA4-TC2

Effort / Load case	CHYBA4 - TC2							
	$M_{calculated}/M_{demand}$				$V_{calculated}/V_{demand}$			
	U1		U2		U1		U2	
	μ	σ	μ	σ	μ	σ	μ	σ
H	1.00	0.18	1.19	0.29	1.03	0.11	1.34	0.19
M	0.93	0.03	0.99	0.10	0.97	0.04	0.01	0.00
L	0.92	0.01	1.00	0.11	0.92	0.01	1.18	0.15
2%	0.98	0.05	1.27	0.14	1.02	0.08	1.38	0.09
10%	1.07	0.06	1.25	0.16	1.19	0.06	1.47	0.17
50%	1.08	0.05	1.29	0.20	1.13	0.09	1.39	0.11
All records	0.99	0.11	1.14	0.21	1.04	0.11	1.30	0.18

Table 5-54 Validation of the simplified method for CHYBA4-TC3

Load case \ Effort	CHYBA4 - TC3							
	$M_{calculated}/M_{demand}$				$V_{calculated}/V_{demand}$			
	U1		U2		U1		U2	
	μ	σ	μ	σ	μ	σ	μ	σ
H	1.02	0.04	1.00	0.04	1.15	0.16	1.07	0.09
M	0.98	0.03	0.98	0.01	1.05	0.10	1.01	0.04
L	0.99	0.02	0.97	0.02	1.03	0.04	1.01	0.03
2%	1.17	0.12	1.01	0.07	1.23	0.19	1.08	0.06
10%	0.90	0.02	0.87	0.03	1.13	0.12	1.04	0.03
50%	0.90	0.02	0.89	0.03	1.12	0.10	1.07	0.05
All records	0.99	0.09	0.96	0.06	1.11	0.14	1.04	0.06

Table 5-55 Validation of the simplified method for CHYBA4-TC4

Load case \ Effort	CHYBA4 - TC4							
	$M_{calculated}/M_{demand}$				$V_{calculated}/V_{demand}$			
	U1		U2		U1		U2	
	σ	μ	σ	μ	σ	μ	σ	μ
H	1.10	0.08	1.08	0.07	1.20	0.21	0.99	0.13
M	1.12	0.41	1.03	0.03	1.10	0.28	0.89	0.05
L	1.09	0.30	1.05	0.03	1.10	0.28	0.92	0.05
2%	1.11	0.04	1.09	0.04	1.18	0.10	0.99	0.06
10%	1.08	0.04	1.05	0.03	1.14	0.07	0.98	0.11
50%	1.07	0.04	1.05	0.02	1.15	0.09	0.96	0.06
All records	1.10	0.23	1.06	0.06	1.14	0.20	0.95	0.09

Table 5-56 Validation of the simplified method for 2020 University-TC2

Effort / Load case	2020 University - TC2							
	$M_{calculated}/M_{demand}$				$V_{calculated}/V_{demand}$			
	U1		U2		U1		U2	
	μ	σ	μ	σ	μ	σ	μ	σ
H	1.14	0.20	1.83	0.47	1.23	0.16	1.49	0.17
M	1.00	0.05	1.19	0.23	1.09	0.06	1.19	0.15
L	1.00	0.03	1.27	0.33	1.00	0.03	1.21	0.12
2%	1.10	0.10	2.31	0.37	1.20	0.08	1.62	0.09
10%	1.08	0.11	1.85	0.36	1.17	0.09	1.55	0.29
50%	1.05	0.06	1.95	0.42	1.16	0.08	1.57	0.19
All records	1.05	0.12	1.67	0.53	1.16	0.11	1.41	0.24

Table 5-57 Validation of the simplified method for 2020 University-TC3

Effort / Load case	2020 University - TC3							
	$M_{calculated}/M_{demand}$				$V_{calculated}/V_{demand}$			
	U1		U2		U1		U2	
	μ	σ	μ	σ	μ	σ	μ	σ
H	0.99	0.02	0.96	0.02	1.08	0.04	1.04	0.03
M	0.99	0.02	0.97	0.01	1.09	0.03	1.05	0.03
L	1.00	0.01	0.96	0.01	1.11	0.04	1.05	0.03
2%	1.00	0.02	0.97	0.02	1.09	0.03	1.05	0.05
10%	1.00	0.01	1.16	0.02	1.09	0.02	1.08	0.10
50%	0.99	0.01	1.16	0.02	1.08	0.02	1.06	0.07
All records	0.99	0.02	1.02	0.09	1.09	0.03	1.05	0.05

Table 5-58 Validation of the simplified method for 2020 University-TC4

Effort / Load case	2020 University - TC4							
	$M_{calculated}/M_{demand}$				$V_{calculated}/V_{demand}$			
	U1		U2		U1		U2	
	μ	σ	μ	σ	μ	σ	μ	σ
H	1.04	0.04	1.04	0.03	1.01	0.08	1.15	0.10
M	1.09	0.30	1.03	0.03	1.03	0.25	1.12	0.08
L	1.03	0.03	1.36	1.19	1.02	0.06	1.37	0.92
2%	1.07	0.04	1.04	0.04	1.03	0.08	1.15	0.07
10%	1.04	0.04	1.03	0.01	1.02	0.07	1.20	0.17
50%	1.05	0.02	1.04	0.03	1.00	0.04	1.18	0.09
All records	1.05	0.13	1.10	0.53	1.01	0.13	1.20	0.43

Discussion of the proposed simplified method

For the TC2 tower, the global average ratios for overturning moments and shear forces corresponding to 444 load cases are equal to 1.24 and 1.36 respectively, with standard deviations of 0.36 and 0.34 respectively; for the TC3 tower, the average ratios are 0.99 and 1.04, with standard deviations of 0.09 and 0.1; while for the TC4 tower, the average ratios and standard deviations are equal to 1.05 and 0.25 for both M and V. This indicates that the proposed simplified method gives higher values than the detailed calculation in most cases, so it is conservative in the base force/moment predictions. Moreover, the proposed method becomes more accurate as the fundamental period of the tower decreases.

The small standard deviations between the loading cases for individual building-tower combinations suggest that the method is suitable regardless of the frequency content of the input seismic excitations. It is also noted that the method is more accurate for the calculation of overturning moments than for the calculation of base shear forces. This was also observed by McClure et al. (2000) in relation to the predicted response of towers founded on the ground.

5.4 Summary

From the 16 building-tower combinations studied, it can be concluded that the component force amplification factor as proposed in the NBCC 2005 is not adequate for most of the cases and therefore needs revision, particularly in the case of flexible towers mounted on flexible buildings. A simplified method for telecommunications towers mounted on rooftops was proposed. The method is intended to help tower designers to assess whether seismic effects at the tower base are important enough to be taken into account and their importance relative to those generated by ice and wind loads, and consequently, to decide whether a detailed dynamic analysis is necessary. The proposed method was validated by comparing its predictions to the results of detailed numerical simulations of 9 building-tower combinations generated in SAP 2000 and subjected to 74 input accelerograms applied separately in the two main building directions, U1 and U2. It was found that the method yields conservative results for the base shear forces and overturning moments. It is suggested, however, that a detailed dynamic analysis be performed for towers mounted on high-rise buildings and for towers supporting heavy attachments, especially in high seismicity zones.

Chapter 6
Summary and Conclusions

The research conducted in this thesis has met its main objectives:

- To gain further insight into the prediction of seismic floor acceleration demands in buildings, especially at the rooftop level, based on rational analysis of both experimental data and numerical results.
- To formulate a simplified method for the seismic analysis of steel lattice telecommunication towers mounted on building rooftops. Such a method is particularly needed for flexible towers.

This research program has lead to important findings and conclusions in the field of seismic analysis of operational and functional components in buildings (OFCs), specifically for steel lattice telecommunication towers mounted on building rooftops.

6.1 Seismic floor acceleration demands

Seismic acceleration records from 11 instrumented buildings in Taiwan during the 1999 Chi Chi earthquake were processed and studied, followed by a parametric study of the different factors that can affect the floor acceleration amplification in buildings. These factors include the frequency content of the input motion, the number of stories of the building, and its fundamental period. Numerical finite element models of four existing buildings were generated in the software SAP 2000. Three of the building models were calibrated using records from the 1999 Chi Chi earthquake. Each of these models was subjected to 74 earthquake records of two large sets applied to both horizontal principal directions of the building, separately. The first set comprises 44 records classified into three categories according to the ratio of maximum horizontal acceleration a to the maximum horizontal velocity v (low, medium, high a/v), the second set comprises 30 records compatible with the target Uniform Hazard Spectra for the City of Montreal. The rooftop acceleration amplification resulting from each of the different simulations was computed. A good agreemeent between the results from instrumented buildings and generated models was observed. As a result, it was recommended to consider a maximum rooftop acceleration amplification of 4 for low and medium-rise buildings (T < 1.7 s) and 3 for flexible high-rise buildings.

The input seismic acceleration to OFCs using the spectral anlaysis as a substitute to time-history acceleration was also investigated. It was found that considering the spectral acceleration at 0.2 s as recommended in the NBCC 2005 is adequate, especially for flexible buildings; in case of rigid buildings, however, computing the spectral acceleration at either the building fundamental periods or 0.2 s resulted in negligible differences.

6.2 Simplified method for seismic analysis of telecommunication towers mounted on building rooftops

Four self-supporting steel lattice telecommunication towers of heights ranging from 10 m to 30 m were modeled as frame-truss finite element models and assumed to be mounted on four existing buildings studied in the first part of the thesis. The 10 m tower (TC1) actually exists on one of the buildings (CHYBA9). Each building-tower combination was subjected to the earthquake records of the two sets described earlier.

Acceleration amplification envelopes along the towers' height were then evaluated. The tower component force amplification factors, computed as the average of values at a number of stations along the envelopes of acceleration amplification, were evaluated for each building-tower combination and compared to the NBCC 2005 recommendations; then, new component force amplification factors for telecommunication towers were suggested. The tower base reactions, namely base shear force and overturning moment, resulting from numerical simulations were evaluated and compared to values computed from the proposed simplified method. This simplified method requires the determination of the input rooftop acceleration at the tower base, the maximum acceleration at the tower top, the fundamental sway mode shape of the tower on a rigid base, and the mass distribution of the tower along its height. It was found that the method yields conservative results.

6.3 Research limitations

First, the records of 11 instrumented buildings were processed and studied. All these buildings are far from the epicenter; therefore, near-fault acceleration records were not studied. In addition, most of the buildings are low to medium-rise, even though one of them (TAPBA7) is the second tallest building in Taiwan. Also, only buildings that behave in the linear elastic range were studied, as this research is intended for the design of components with continuous serviceability, which implies that the component does not experience any damage or only minor damage during an earthquake. This requires that the behavior of both the component and its supporting structure remain in the elastic or nearly elastic range.

Second, four buildings and four towers were modeled in detail. It is assumed that these models represent a wide range of existing constructions. The buildings were assumed to be founded on firm ground and soil-structure interaction was ignored. Furthermore, the effect of only the horizontal accelerations on the design of components was studied since it was assumed the effects of vertical accelerations are not critical at building rooftops. Moreover, the effect of attachments on a tower's response was ignored.

6.4 Recommendations for future work

The work presented in this thesis covers many aspects related to the seismic analysis of acceleration-sensitive components located in buildings and to steel lattice telecommunication towers mounted on building rooftops. However, a few topics need to be further investigated in future research.

On the topic of prediction of seismic accelerations in buildings, suggestions for future work are given below:

- Study more instrumented medium and high-rise buildings having records from events of different characteristics.
- Study the effect of soil type, foundation and floor flexibility on the floor acceleration amplification in buildings.
- Study the effect of nonlinear and post-elastic deformations of a building on the acceleration amplification. It is expected that nonlinear response of the building will decrease the acceleration amplification.

On the topic of seismic analysis of telecommunications towers mounted on buildings rooftops, suggestions for future work are given below:

- Study other existing towers of different heights and geometric properties, preferably equipped with sensors.
- Study the effect of attachments, like heavy antennas and accessories, on the prediction of tower mode shapes and frequencies, and eventually their acceleration amplification profiles.
- Study the component force amplification factor for building-tower combinations undergoing nonlinear deformations. It is believed that friction at supports, yielding of equipment, or yielding of anchorage would tend to reduce the component force amplification factor and flatten the plots of amplification vs T_p/T. This needs to be verified in detail.
- Study the applicability of the proposed simplified method in case of buildings and/or towers undergoing nonlinear deformations.
- Explore whether the proposed simplified method is applicable to seismic analysis of guyed towers mounted on building rooftops.

References

Adams, J., and Halchuck, S. (2003). *Fourth generation seismic hazard maps of Canada: values for over 650 canadian localities intended for the 2005 National Building Code of Canada*, Geological Survey of Canada Open File 4459, 30 pages, Ottawa, Canada.

Adams, J., and Atkinson, G. (2003). 'Developments in seismic hazard maps for building code applications in Canada', *Canadian Journal of Civil Engineering*, 30(2), 255-271.

Assi, R. (2003). *Seismic design of operational and functional components (OFCs) of buildings*. Structural Engineering Series No. 2003-03, Department of Civil Engineering and Applied Mechanics, McGill University, Montreal, Canada, 40 pages.

Atkinson, G., and Beresnev, I. (1998). 'Compatible ground motion time histories for new national seismic hazard maps', *Canadian Journal of Civil Engineering*, 25(2), 305-318.

Bachman, R.E., and Drake, R.M. (1994). '1994 provisions for architectural, mechanical and electrical components', *5th US National Conference on Earthquake Engineering*, July 10-14, Chicago, Illinois, 795-774.

Bachman, R.E., and Drake, R.M. (1995). *A study to empirically validate the in-structure response accelerations in the 1994 NEHRP provisions design force equations for architectural, mechanical, and electrical components*, letter report to the National Center for Earthquake Engineering Research, 52 pages.

Beck, J.L. (1978). *Determining models of structures from earthquake records*, Report EERL 78-01, Californina Institute of Technology, Pasadema, California, USA.

Bendat, J.S., and Piersol, A.G. (2000). *Random data: Analysis and measurement procedures,* Wiley and Sons.

Bloomfield, P. (2000). *Fourier analysis of time series: An introduction*, John Wiley and Sons.

Building Seismic Safety Council (1997). *NEHRP recommended provisions for seismic regulations for new buildings and other structures*, Reports FEMA 302 (guideline) and FEMA 303 (commentary), prepared by the BSSC for the Federal Emergency Management Agency, Washington, DC.

Building Seismic Safety Council (2001). *NEHRP recommended provisions for seismic regulations for new buildings and other structures*, Reports FEMA 368 (guideline) and FEMA 369 (commentary), prepared by the BSSC for the Federal Emergency Management Agency, Washington, DC.

Chen, Y., and Soong, T. T. (1988). 'Seismic response of secondary systems', *Engineering Structures*, 10(4), 218-228.

Chopra, A. (2001). *Dynamics of structures: Theory and applications to Earthquake Engineering*, Prentice Hall Inc., NJ.

Clough, R.W., and Penzien, J. (1993). *Dynamics of structures*, McGraw Hill, New York.

Cooley, J.W., and Tukey, J.W. (1965). 'An algorithm for the machine computation of Complex Fourier Series', *Mathematics of Computation*, American Mathematical Society, 19(90), 297-301.

CSA (2001 a). *S37-M01, Antennas, towers and antenna-supporting structures*, Canadian Standards Association, Rexdale, Ontario, 118 pages.

CSA (2001 b). *S832-01: Guideline for seimic risk reduction of operational and functional components (OFCs) of buildings*, Canadian Standards Association, Rexdale, Ontario, 105 pages.

Drake, R.M., and Bachman, R.E. (1995). 'Interpretation of instrumented building seismic data and implications for building codes components', *Proceedings of the 64th Annual Conference of the SEAOC*, October , Indian Wells, CA.

Drake, R.M., and Bachman, R.E. (1996). 'NEHRP provisions for 1994 for nonstructural components', *ASCE Journal of Architectural Engineering*, 2(1), 26-31.

Ewins E. (2000). *Modal testing: Theory, practice and application*, Research Studies Press LTD. Baldock, Hertfordshire, England.

Filiatrault, A., Christopoulos, C., and Stearns, C. (2001 a). *Guidelines, specifications, and seismic performance characterization of non-structural building components and equipment*, PEER 2002/05, Pacific Earthquake Engineering Research Institute, California, USA.

Filiatrault, A., Uang, C.-M., Folz, B., Christopoulos, C., and Gatto, K. (2001 b). *Reconnaissance report of the February 28, 2001 Nisqually earthquake*, Report No. SSRP-2001/02, Report of a field reconnaissance sponsored by the PEER and the CUREE center, Department of Structural Engineering, University of California, San Diego, La Jolla, California 92093-0085.

Gupta, A.K. (1990). *Response spectrum method: in seismic analysis and design of structures*, CRC Press Inc., Florida.

Heidebrecht, A.C. (2003). 'Overview of seismic provisions of the proposed 2005 edition of the National Building Code of Canada', *Canadian Journal of Civil Engineering*, 30(2), 241-254.

Hiramatsu, K., Sato, Y., Akagi, H., Tomita, S. (1988). 'Seismic response observation of building appendage', *Proceedings of the 9th World Conference on Earthquake Engineering,* Tokyo, Japan, August 2-9, VI 237 - VI 242.

Huang, W. (1997). *Regression analysis to fundamental period and size of buildings*, Master thesis, Department of Civil Engineering, National Cheng Kung University, Tainan, Taiwan.

IBC (2000). *International Building Code*, International Code Council, Fall Church, Virginia, USA.

ICBO (1997). *Uniform Building Code*, International Conference of Building Officials, Whittier, California, USA.

Integrated Measurement and Control (IMC) (2000). *Famos v.3.2*, Mess-System, a part of MSC Software Solution, Berlin, Germany.

Kanazawa, K., and Hirata K. (2000). 'Seismic analysis for telecommunication towers built on the building', *Proceedings of the 12th World Conference on Earthquake Engineering*, Auckland, New Zealand, on CD-ROM, paper 0534.

Kao, A.S., Soong, T.T., and Amanda, V. (1999). *Nonstructural damage database*, Report MCEER-99-0014, Multidisciplinary Center for Earthquake Engineering Research, Buffalo, New York, USA.

Kehoe, B.E., and Freeman, S.A. (1998). 'A critique of procedures for calculating seismic design forces for nonstructural elements', *ATC-29-1: Proceedings of seminar on* *seismic design, retrofit, amd performance of nonstructural components*, Applied Technology Council, January 22-23, San Francisco, California, 57-70.

Khedr, M. (1998). *Seismic analysis of lattice towers*, Ph.D thesis, Department of Civil Engineering and Applied Mechanics, McGill University, Montreal, Canada.

Khedr, M., and McClure, G. (2000). A simplified method for seismic analysis of lattice telecommunication towers', *Canadian Journal of Civil Engineering*, 27(3), 533-542.

Konno, T., and Kimura, E. (1973). 'Earthquake effects on steel tower structures atop buildings', *Proceedings of the 5th World Conference on Earthquake Engineering*, Rome, Italy, June 25-29, Vol. 1, 184-193.

Lam, N., Wilson J., Doherty K., Griffiths, M. (1998). 'Horizontal seismic forces on rigid components within multistory buildings', *Proceedings of the Australian Structural Engineering Conference*, Auckland, New Zealand, September 28 - October 2, 721-726.

Madugula, M. (editor) (2002). *Dynamic response of lattice towers and gyued masts*, ASCE, Reston,Virgina, 266 pages.

Marsantyo, R., Shimazu, T., Akari, H., Kabayama, K., and Kobayashi, M. (1998). 'Experimental work on the seismic horizontal force for nonstructural systems mounted on the buildings', *Proceedings of the 10th Earthquake Engineering Symposium*, Yokohama, Japan, November 25-27, 2635-2640.

Marsantyo, R., Takayuski Shimazu, and Akira, H. (2000). 'Dynamic response of nonstructural systems mounted on floors of buildings', *Proceedings of the 12th*

World Conference on Earthquake Engineering, Auckland, New Zealand, January 29 - February 5, on CD-ROM, paper 1872.

McClure, G., Lapointe, M., and Khedr M. (2000). 'Seismic behavior of steel lattice telecommunication towers', *Proceedings of the Third International Conference STESSA 2000*, F.M. Mazzoanni and R. Tremblay Ed., Montreal, Canada, August 21-24, 335-337.

McClure, G., Georgi, L., and Assi, R. (2004). 'Seismic considerations for telecommunication towers mounted on building rooftops', *Proceedings of the 13th World Conference on Earthquake Engineering*, Vancouver, Canada, August 1-6, on CD- ROM, paper 1988.

McGavin, G.L., and Gates, B. (1998). 'Earthquake design considerations for nonstructural components...who is responsible?', *Proceedings of the 6th US National Conference on Earthquake Engineering*, EERI, Seattle, Washington, May 31-June 4, 6 pages.

McKevitt, W.E., Timler, P.A., and Lo, K.K. (1995). 'Nonstructural damage from the Northridge earthquake', *Canadian Journal of Civil Engineering*, 22(2), 428-437.

McKevitt, W. E. (2003). 'Proposed Canadian code provisions for seismic design of structures, non-structural components and equipment', *Canadian Journal of Civil Engineering*, 30(2), 366-377.

McVerry, G.H. (1979). *Frequency domain investigation of structural models from earthquake records*, Report EERL 79-02, California Institute of Technology, Pasadema, California.

Miranda, E., and Taghavi, S. (2005). 'Approximate floor acceleration demands in multi-story buildings I: Formulation', *ASCE Journal of Structural Engineering*, 131(2), 203-211.

Naeim, F. (1989). *Chapter 12: Design of non-structural systems and components, Seismic Design Handbook*, F. Naeim, ed., Kluwer Academic Publishers.

Naeim, F. (1999). 'Lessons learned from performance of non-structural components during the January 17, 1994 Northridge earthquake--Case studies of six instrumented multi-story buildings', *Journal of Seismology and Earthquake Engineering*, 2(1), 45-57.

Naeim, F. (2000). 'Learning from structural and non-structural seismic performance of 20 extensively instrumented buildings', *Proceedings of the 12th World Conference on Earthquake Engineering*, Auckland, New Zealand, January 29 - February 5, on CD-ROM, paper 0217.

Naeim, F. (2001). *Chapter 13: Design of nonstructural systems and components, The seismic design handbook*, F. Naeim, ed., Kluwer Academic Publishers.

NRC/IRC. (1941). *National Building Code of Canada*, National Research Council of Canada, Ottawa, Ontario.

NRC/IRC. (1953). *National Building Code of Canada*, National Research Council of Canada, Ottawa, Ontario.

NRC/IRC. (1960). *National Building Code of Canada*, National Research Council of Canada, Ottawa, Ontario.

NRC/IRC. (1965). *National Building Code of Canada*, National Research Council of Canada, Ottawa, Ontario.

NRC/IRC. (1970 a). *National Building Code of Canada*, National Research Council of Canada, Ottawa, Ontario.

NRC/IRC. (1970 b). *Part 4: Commentary on the National Building Code of Canada*, National Research Council of Canada, Ottawa, Ontario.

NRC/IRC. (1975 a). *National Building Code of Canada*, National Research Council of Canada, Ottawa, Ontario.

NRC/IRC. (1975 b). *Part 4: Commentary on the National Building Code of Canada*, National Research Council of Canada, Ottawa, Ontario.

NRC/IRC. (1980 a). *National Building Code of Canada*, National Research Council of Canada, Ottawa, Ontario.

NRC/IRC. (1980 b). *Part 4: Commentary on the National Building Code of Canada*, National Research Council of Canada, Ottawa, Ontario.

NRC/IRC. (1985 a). *National Building Code of Canada*, National Research Council of Canada, Ottawa, Ontario.

NRC/IRC. (1985 b). *Part 4: Commentary on the National Building Code of Canada*, National Research Council of Canada, Ottawa, Ontario.

NRC/IRC. (1990 a). *National Building Code of Canada*, National Research Council of Canada, Ottawa, Ontario.

NRC/IRC. (1990 b). *Part 4: Commentary on the National Building Code of Canada*, National Research Council of Canada, Ottawa, Ontario.

NRC/IRC. (1995 a). *National Building Code of Canada*, National Research Council of Canada, Ottawa, Ontario.

NRC/IRC. (1995 b). *Part 4: Commentary on the National Building Code of Canada*, National Research Council of Canada, Ottawa, Ontario.

NRC/IRC. (2005). *National Building Code of Canada*, National Research Council of Canada, Ottawa, Ontario.

Phan, L.T., and Taylor, A.W. (1996). *State of the art report on seismic design requirements for nonstructural components*, NISTIR 5857, National Institute of Standards and Technology, Gaithersburg, MD.

Phipps, M.T. (1997). 'The impact of non-structural damage on building performance: reflections of the 1994 Northridge earthquake', Report UCB/EERC-97-05, *The EERC-CUREe symposium in honour of Vitelmo V. Bertero,* Earthquake Engineering Research Center, University of California, Berkeley, California, 173-178.

Pierre, J.R. (1995). *Damage caused by the Hanshin-Awaji (Kobe-Japan) earthquake to electrical and telecommunication networks and its impact on the implementation of emergency measures*, Report No.RE-GEN-95-40, Hydro-Quebec, Montreal, Canada.

Reitherman, R. (1997). 'Contributions of earthquake reconnaissance reports to improved understanding of non-structural components', *Proceedings of the 1997 15th Structures Congress,* Richmond, CA, USA, 645-651.

Rodriguez, M., Restrepo, J. I., and Carr, A. J. (2000). *Earthquake resistant precast concrete buildings: floor accelerations*, Research report 2000-6, University of Canterbury, Christchurch, New Zealand.

Rodriguez, M., Restrepo, J. I., and Carr, A. J. (2002). 'Earthquake induced floor accelerations in buildings', *Journal of Earthquake Engineering and Structural Dynamics*, 31, 693-718.

Sato, Y., Fuse T., Akagi, H. (1984). 'Building appendage seismic design force based on observed floor response', *Proceedings of the 8th World Conference on Earthquake Engineering*, San Francisco, California, USA, July 21-28, 1167-1174.

Schiff, A.J. (1999). 'Case study of earthquake performance of communication towers', Private communication.

SEAOC (1999). *Recommended lateral force requirements and commentary*, 7th edition, Structural Engineering Association of California, Sacramento, California, USA.

Searer, G.R., and Freeman, S.A. (2002). 'Unintended consequences of code modification', *Proceedings of the 7th US National Conference on Earthquake Engineering*, EERI, Boston, Massachusetts, July 21-25, on CD-ROM, 10 pages.

Shin, T.C. (2000). 'Some geological aspects of the 1999 Chi Chi earthquake in Taiwan', *Journal of Terrestrial, Atmospheric and Oceanic Sciences (TAO)*, Geological Society and Geophysical Society of China, 11(3), 555-566.

Singh, M.P. (1975). 'Seismic design input for secondary systems', *ASCE Journal of Engineering Mechanics Division*, Vol. 101, No.EM5, 593-607.

Singh, M.P., and Suarez, L.E., Matheu E.E., Maldonado. G.O. (1993). *Simplified procedures for seismic design of non-structural components and assessment of current code provisions*, NCEER-93-0013, National Center for Earthquake Engineering Research, New York, NY.

Singh, M.P., Moreschi, L.M., and Suarez, L.E. (1998) 'Simplified method for calculating seismic forces for non-structural components', *ATC-29-1: Proceedings of seminar on seismic design, retrofit, and performance of non-structural components*, Applied Technology Council, January 22-23, San Francisco, California, 43-56.

Soong, T.T. (1990) 'Seismic performance of non-structural elements during the Loma Prieta earthquake', *Proceedings of the 22nd joint meeting US-Japan cooperative program in natural resources panel on wind and seismic effects*, National Institute of Standards and Technology, Gaithersburg, Maryland, May 15-18, 331-336.

Soong, T.T., Chen G., Wu Z., and Grigoriu M. (1993). *Assessment of the 1991 NEHRP provisions for nonstructural components and recommended provisions*, NCEER-93-0003, National Center for Earthquake Engineering Research, New York, NY.

Standards Association of Australia (1994). *AS 3995 (1994) - Design of steel lattice towers and masts*, Standards Association of Australia, 1 Crescent, Homebush, New South Wales 2140.

Taghavi, S., and Miranda E. (2005). 'Approximate floor acceleration demands in multi-story buildings II: Applications', *ASCE Journal of Structural Engineering*, 131(2), 212-220.

Tauby, J.R., Lloyd, R., Noce, T., and Tunnissen, J. (1999). *A practical guide to seismic restraint*, American Society for Heating, Refrigerating, and Air-conditioning Engineers (ASHRAE) , Atlanta, GA.

TIA/EIA (2005). *TIA EIA-222-G: Structural standard for antenna supporting structures and antennas*, Telecommunication Industry Association, Arlington, VA 22201, USA.

Tso, W.K., Zhu, T.J., and Heidebrecht, A.C. (1992). 'Engineering implication of ground motion A/V ratio', *Soil Dynamics and Earthquake Engineering*, 11(3), 133-144.

US Army (1986). *Seismic design guideline for essential buildings*, TM 5-809-10-1, joint Departments of the Army, Navy, and Air Forces, Washington, DC.

Villaverde, R. (1997). 'Seismic design of secondary structures: State of the art', *ASCE Journal of Structural Engineering*, 123(8), 1011-1019.

Wilson, E.L., and Habibullah, A. (2003). *SAP 2000 user's manual*, Computers and Structures Inc., Berkeley, California, USA.

Appendix A

Architectural Plans of the 11 Instrumented Buildings

Elevation

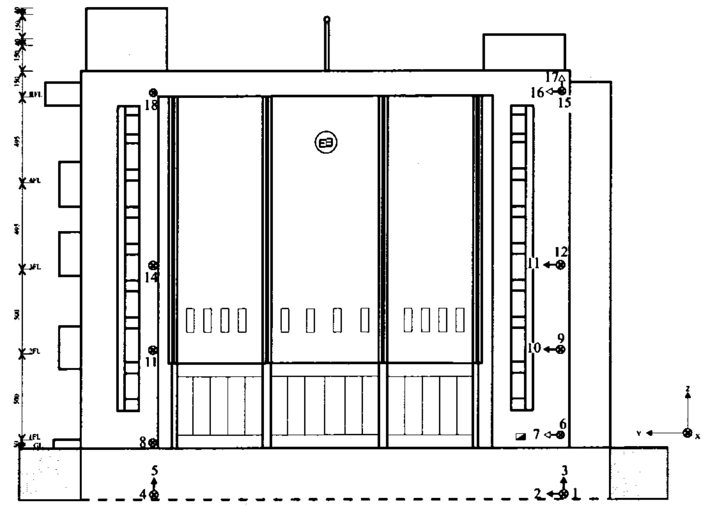

First floor

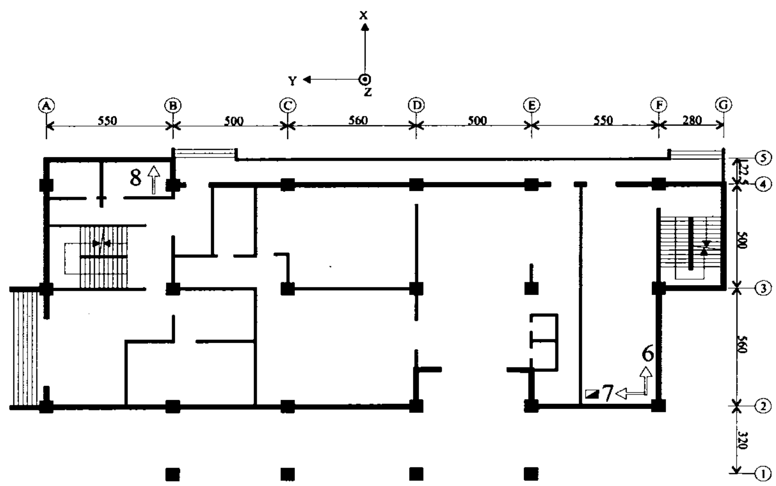

Tower on rooftop

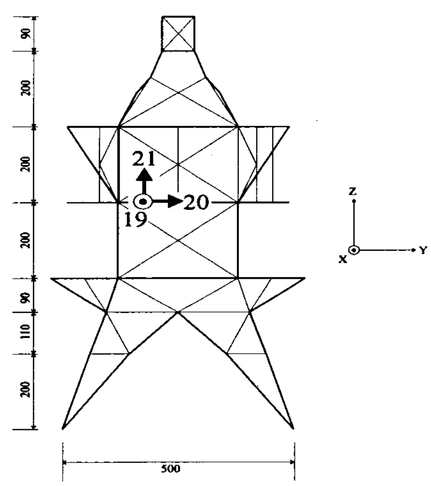

Figure A-1 CHYBA9 building - Elevation and plan views

Elevation

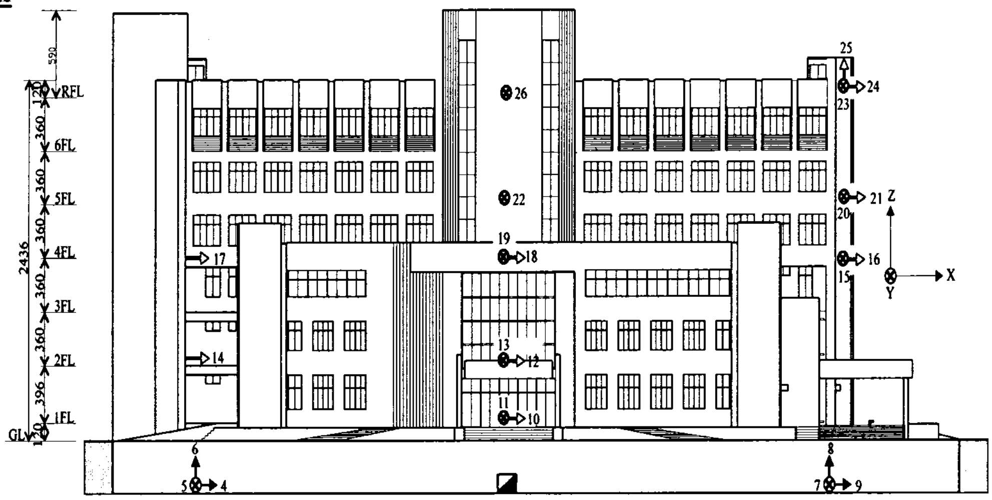

First floor

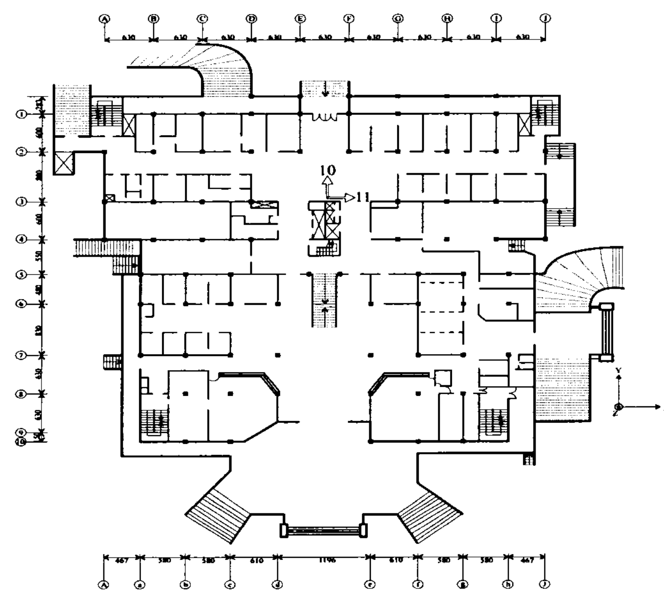

Rooftop

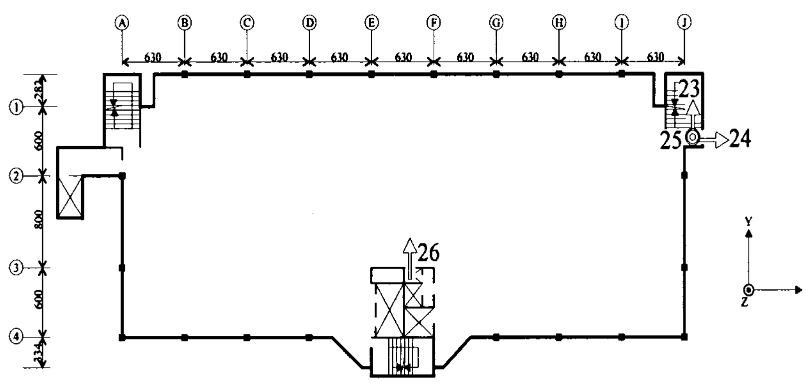

Figure A-2 CHYBA4 building - Elevation and plan views

Elevation

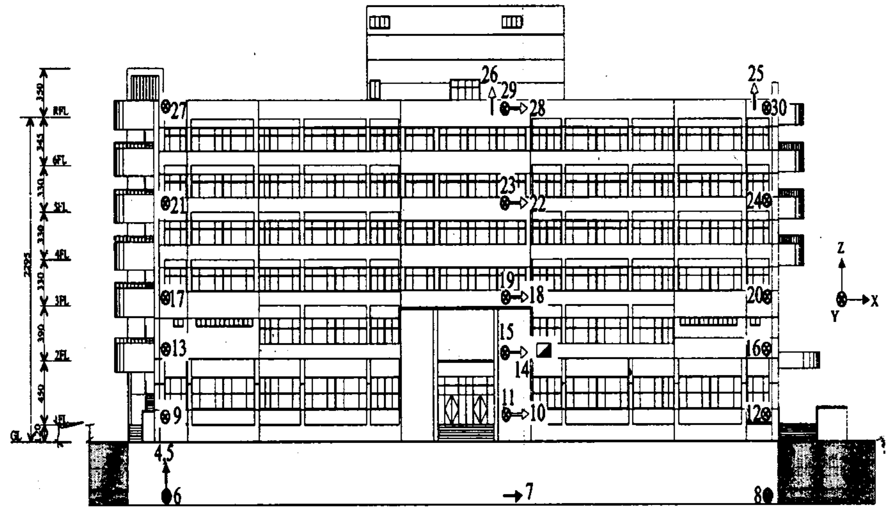

First floor

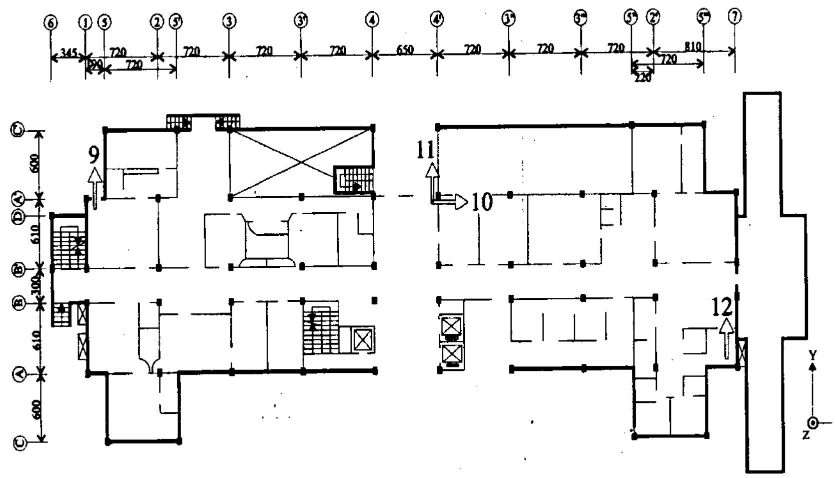

Rooftop

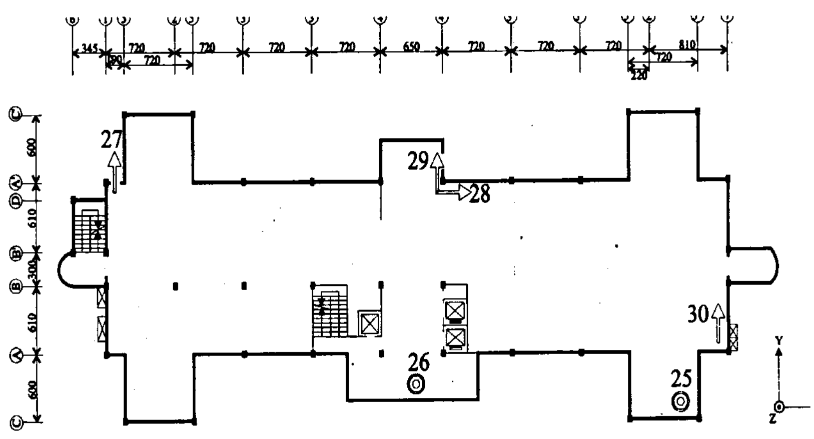

Figure A-3 CHYBA5 building - Elevation and plan views

Elevation

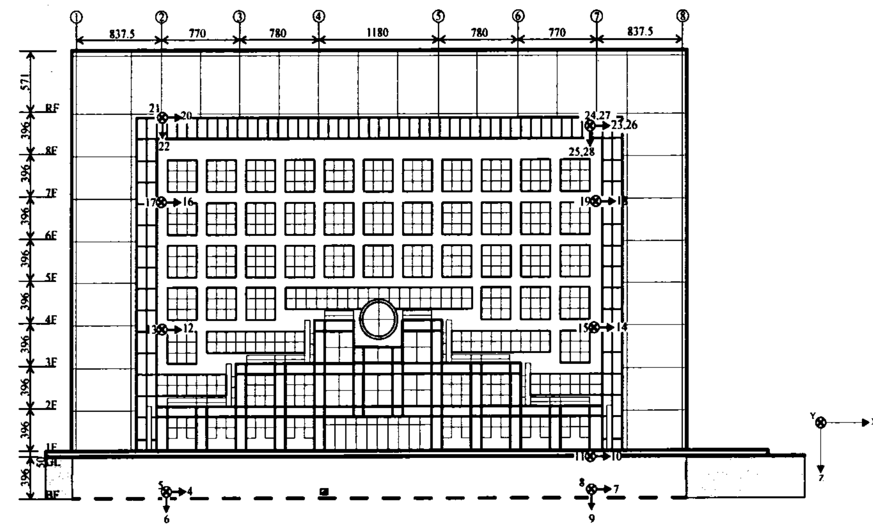

First floor

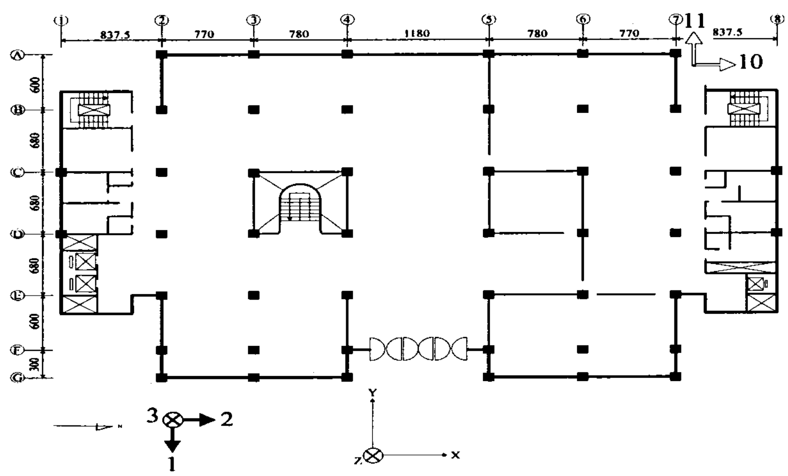

Rooftop

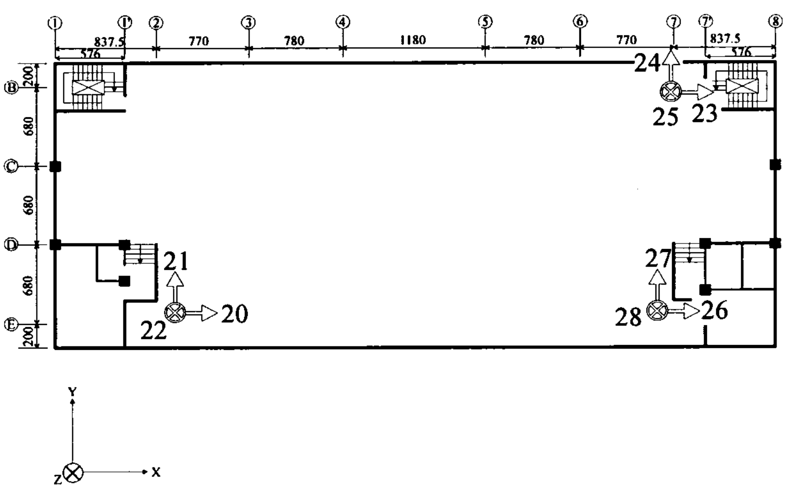

Figure A-4 TCUBA0 building - Elevation and plan views

Elevation

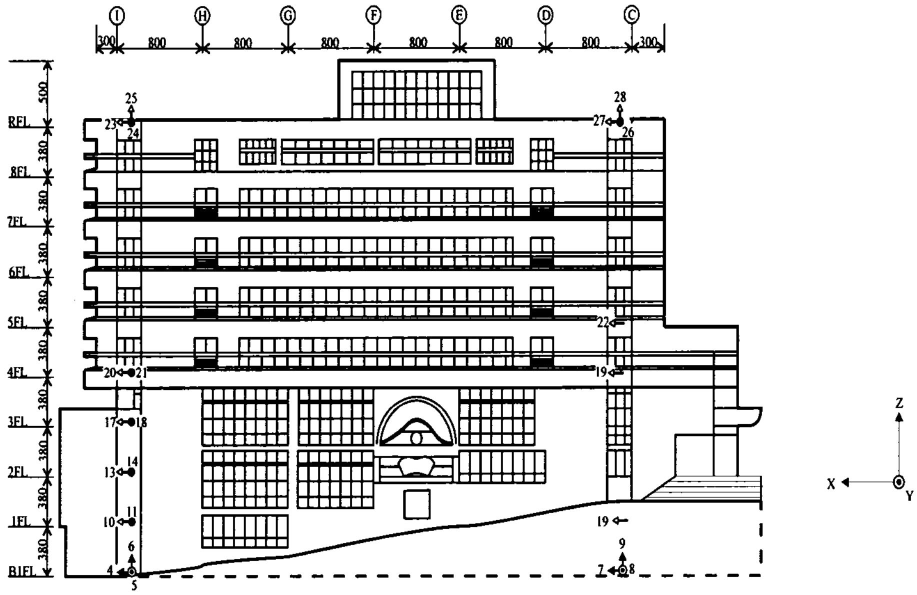

First floor

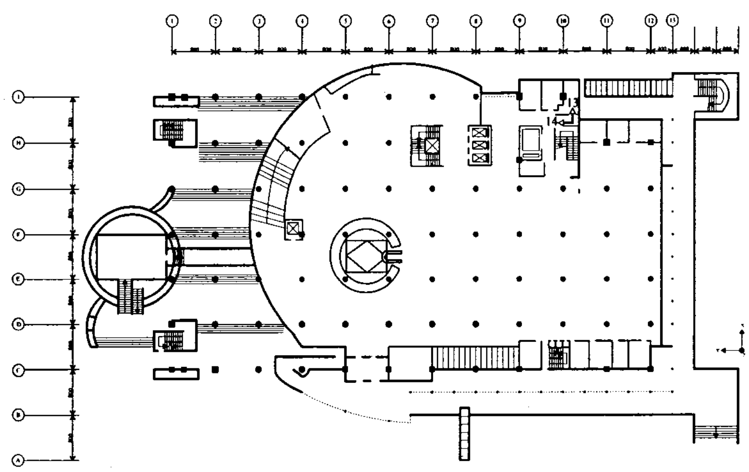

Rooftop

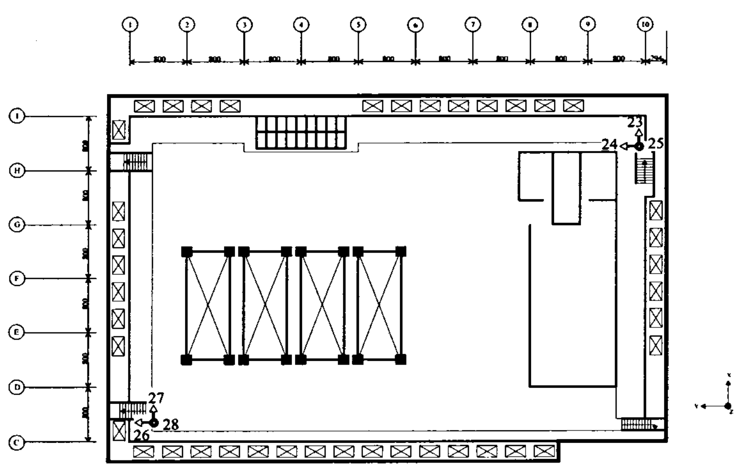

Figure A-5 TCUBAA building - Elevation and plan views

Elevation

First floor

Rooftop

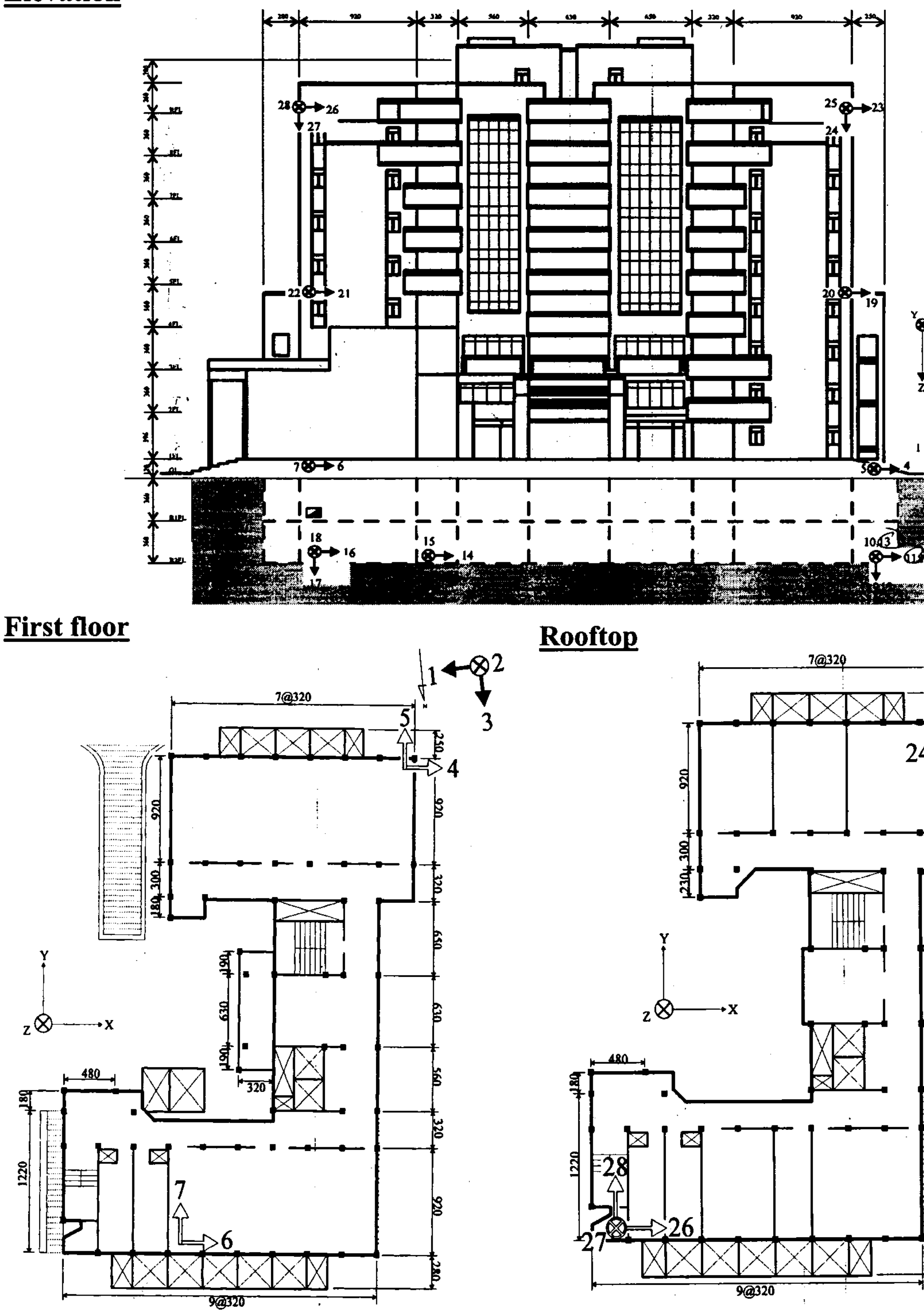

Figure A-6 CHYBA0 building - Elevation and plan views

Elevation

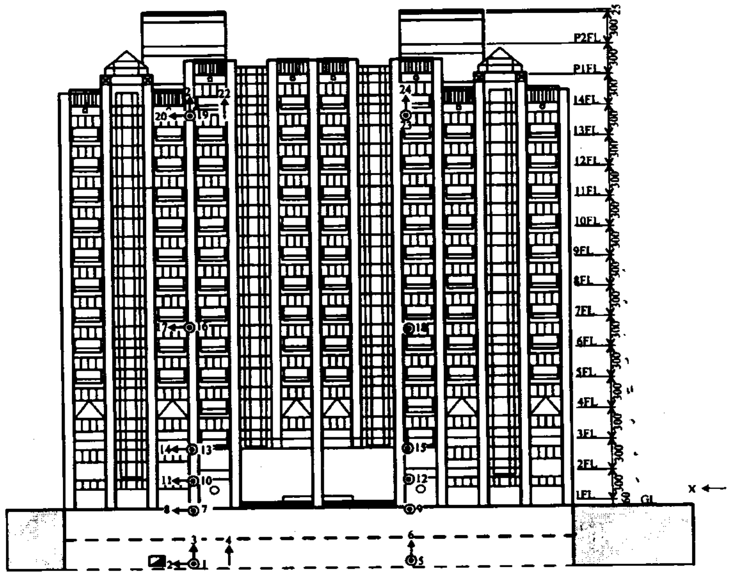

First floor

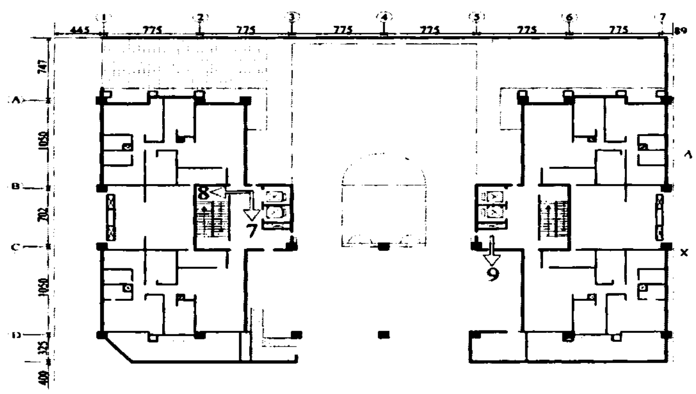

Rooftop

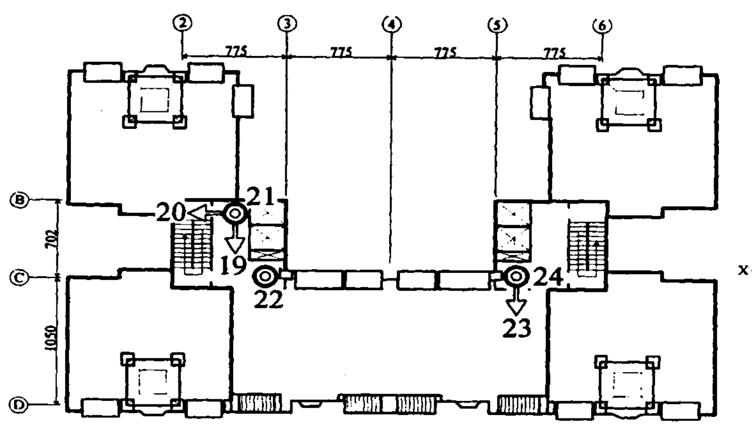

Figure A-7 TCUBA6 building - Elevation and plan views

Elevation

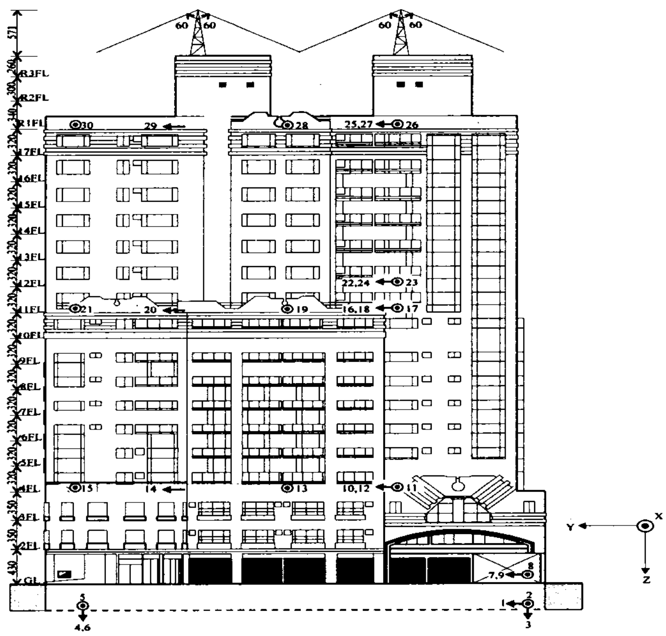

First floor

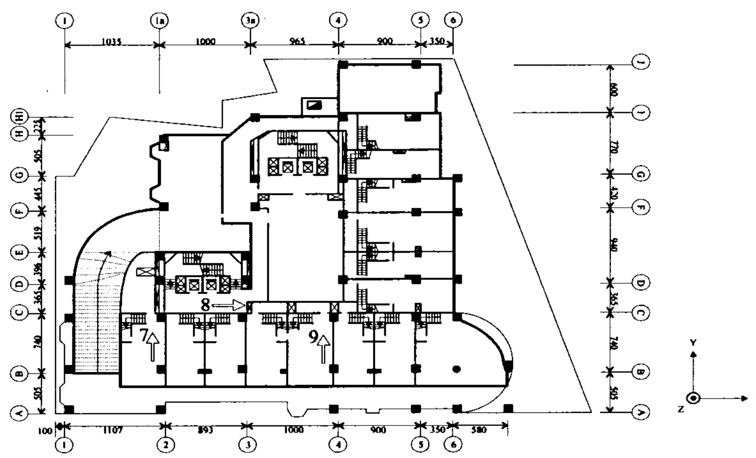

Rooftop

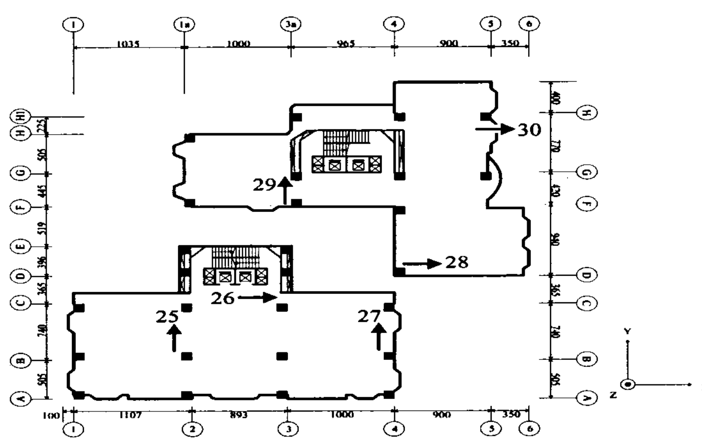

Figure A-8 TCUBA2 building - Elevation and plan views

Elevation

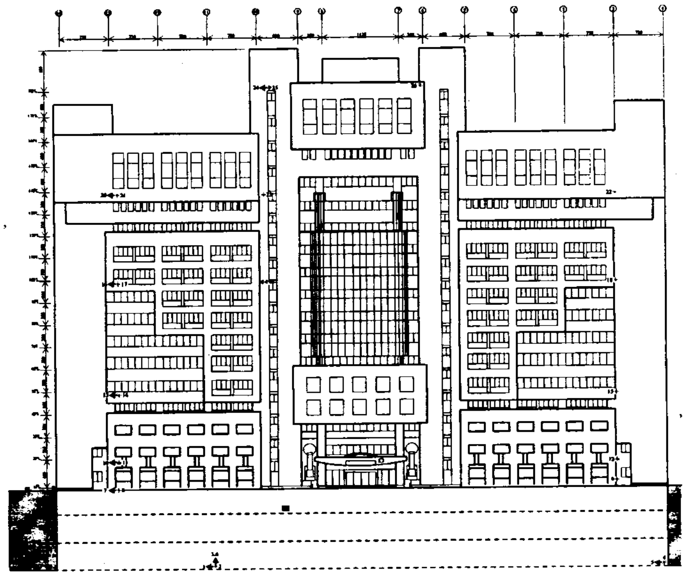

First floor

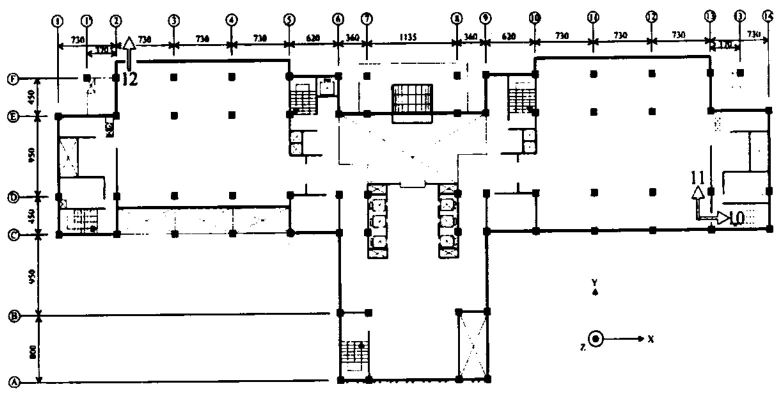

Rooftop

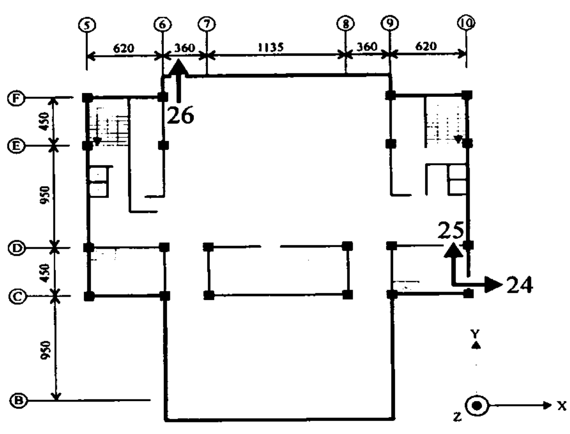

Figure A-9 TCUBA4 building - Elevation and plan views

Elevation

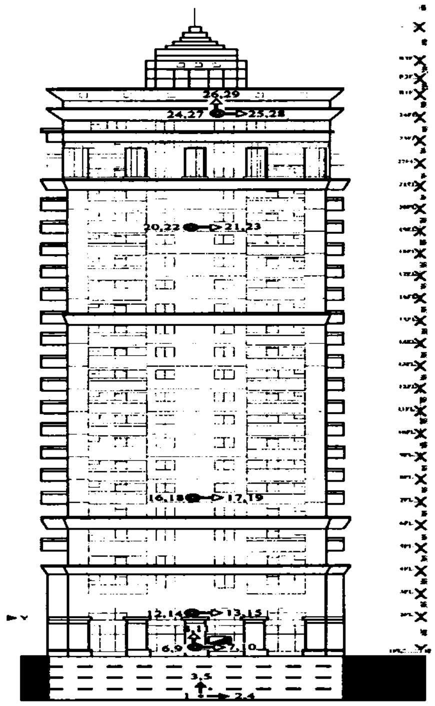

First floor

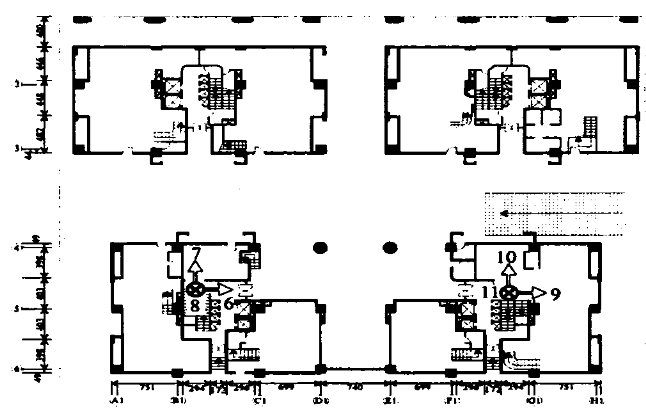

Rooftop

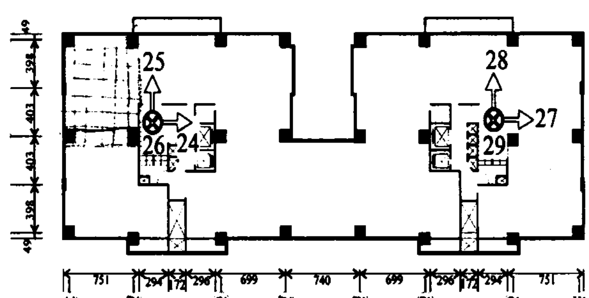

Figure A-10 CHYBA7 building - Elevation and plan views

Elevation

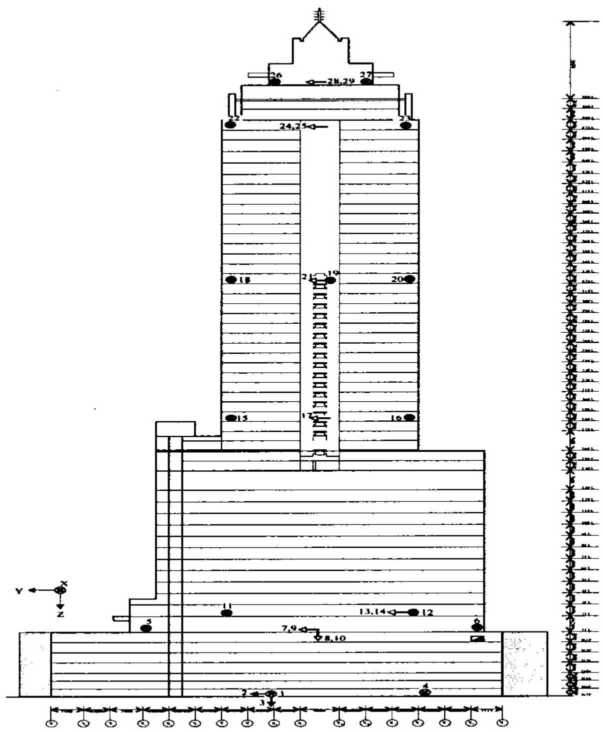

First floor

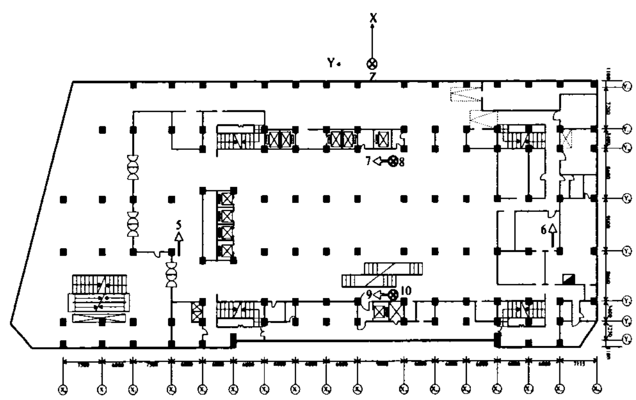

Rooftop

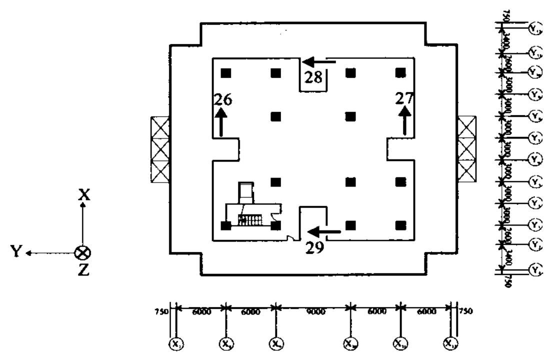

Figure A-11 TAPBA7 building - Elevation and plan views

Appendix B

Transfer Functions for the 11 Buildings Calculated Using the Software Famos

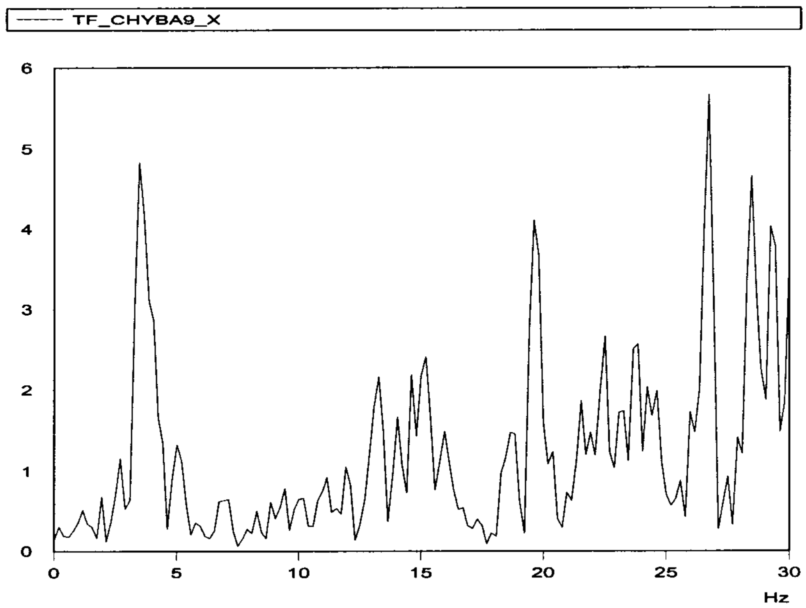

(a)

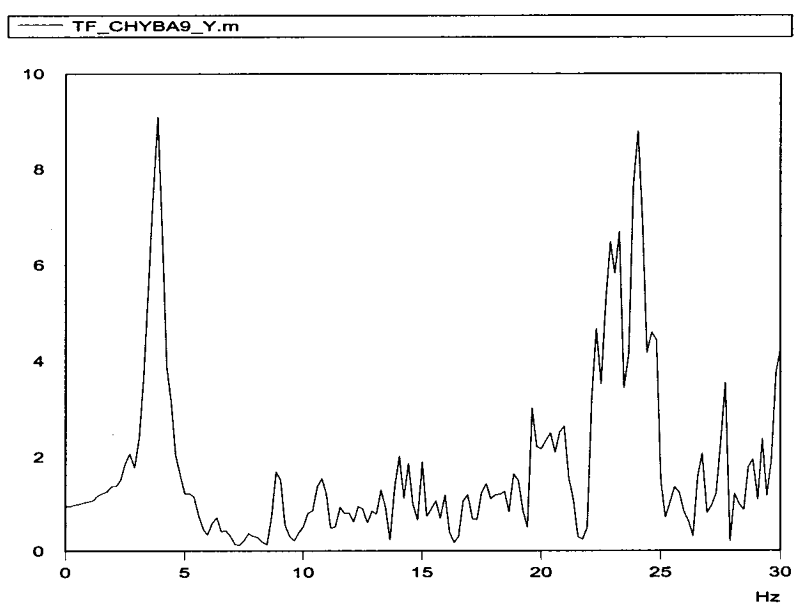

(b)

Figure B-1 Transfer functions for the CHYBA9 building

(a) X - direction (b) Y - direction

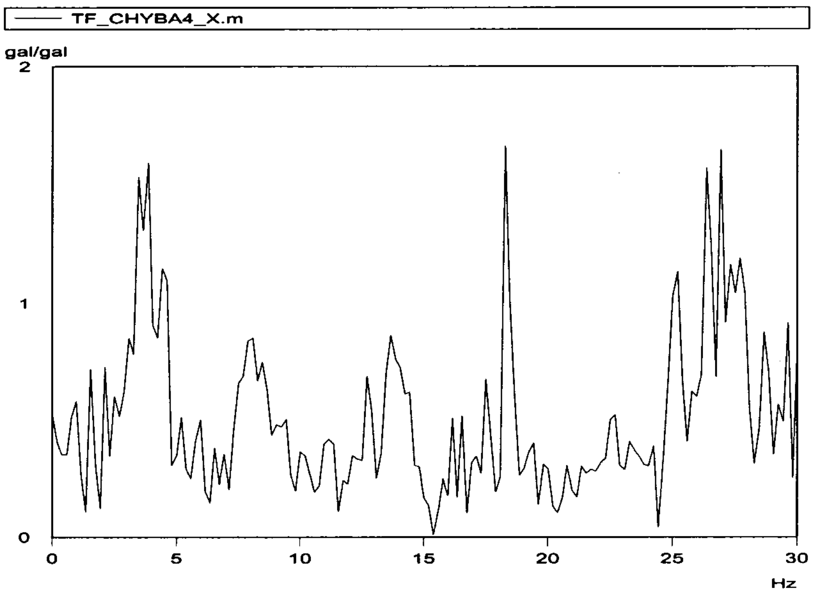

(a)

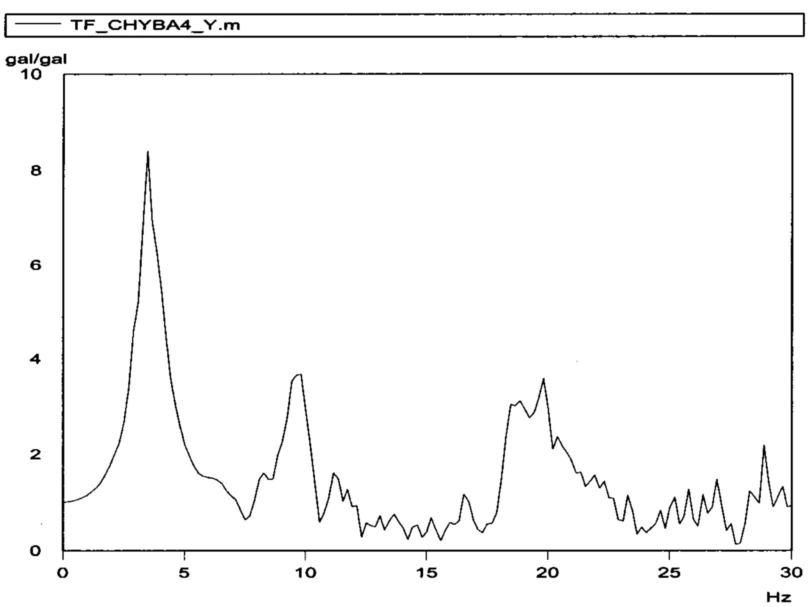

(b)

Figure B-2 Transfer functions for the CHYBA4 building
(a) X - direction (b) Y - direction

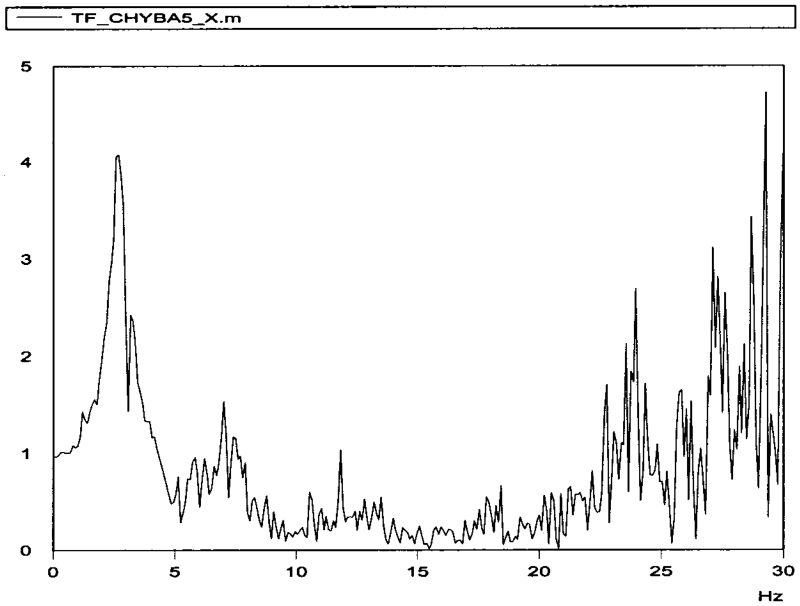

(a)

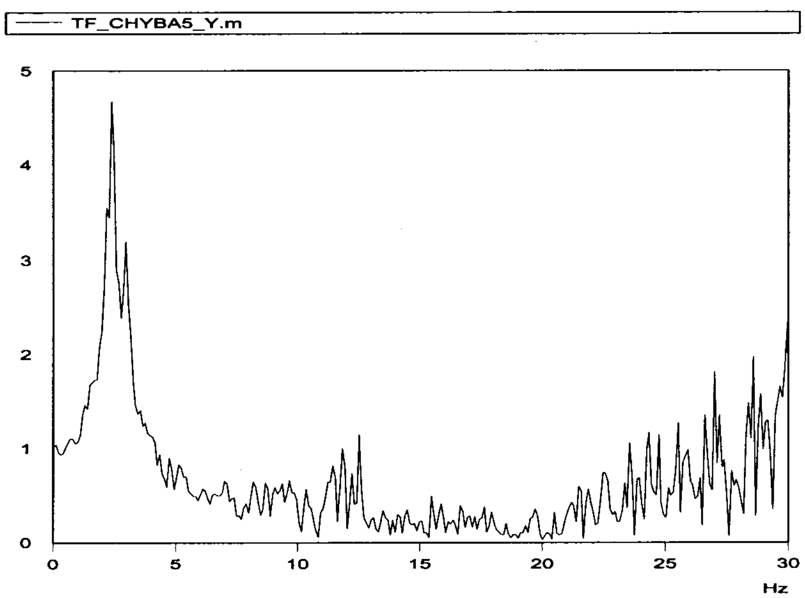

(b)

Figure B-3 Transfer functions for the CHYBA5 building

(a) X - direction (b) Y - direction

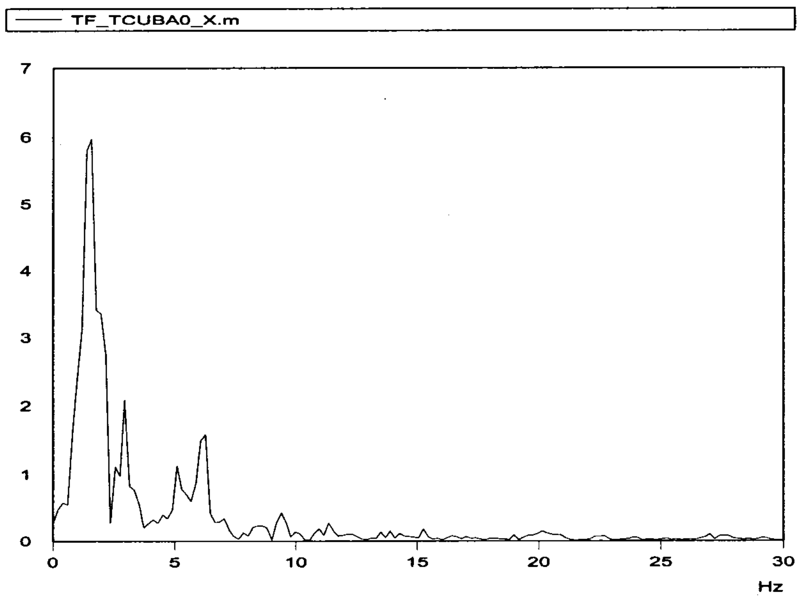

(a)

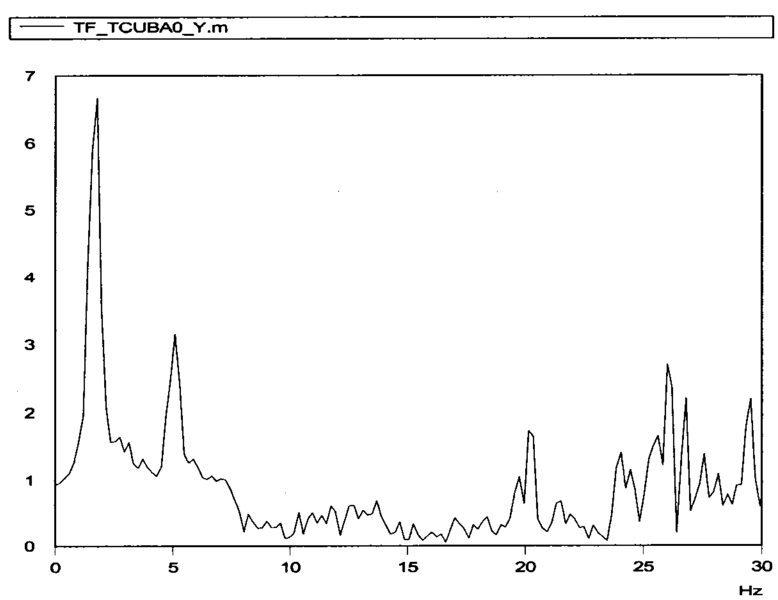

(b)

Figure B-4 Transfer functions for the TCUBA0 building

(a) X - direction (b) Y - direction

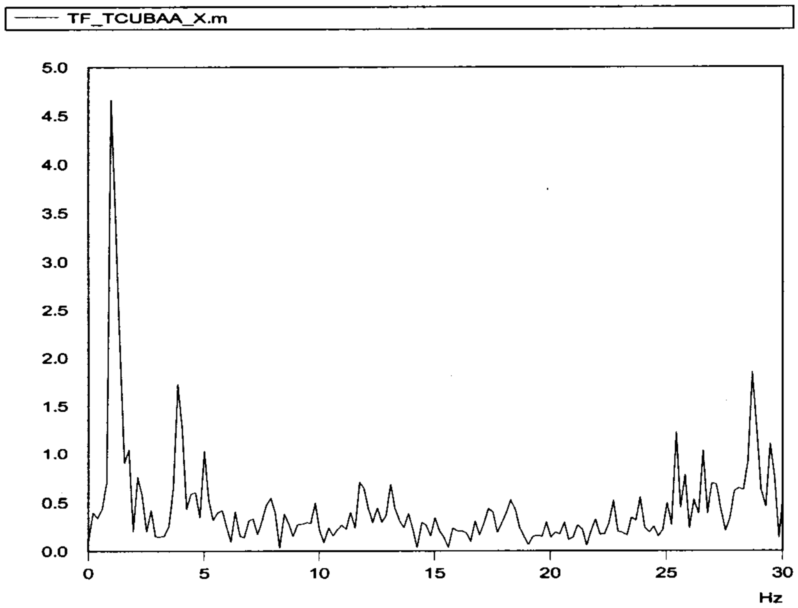

(a)

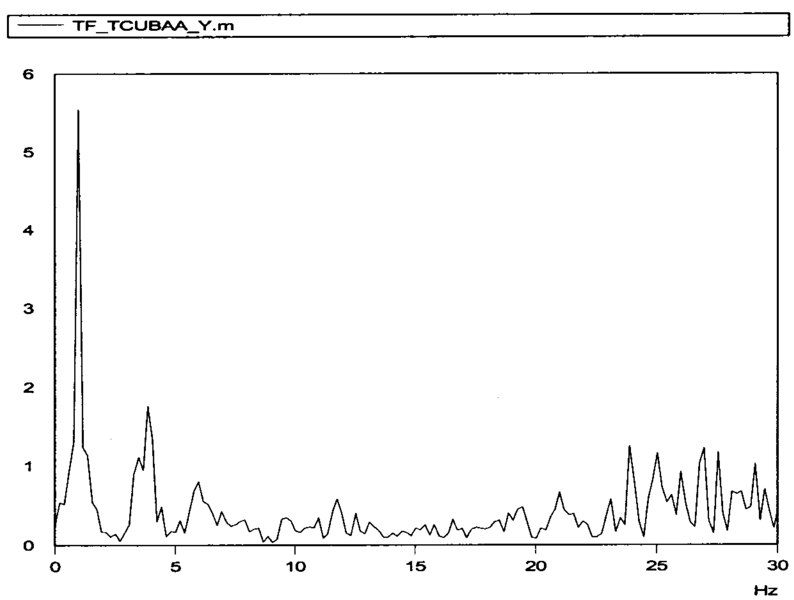

(b)

Figure B-5 Transfer functions for the TCUBAA building

(a) X - direction (b) Y - direction

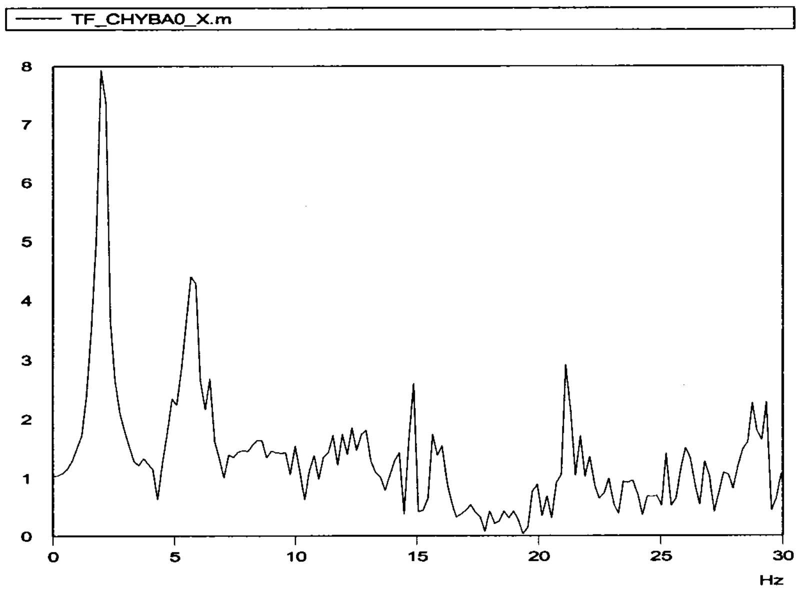

(a)

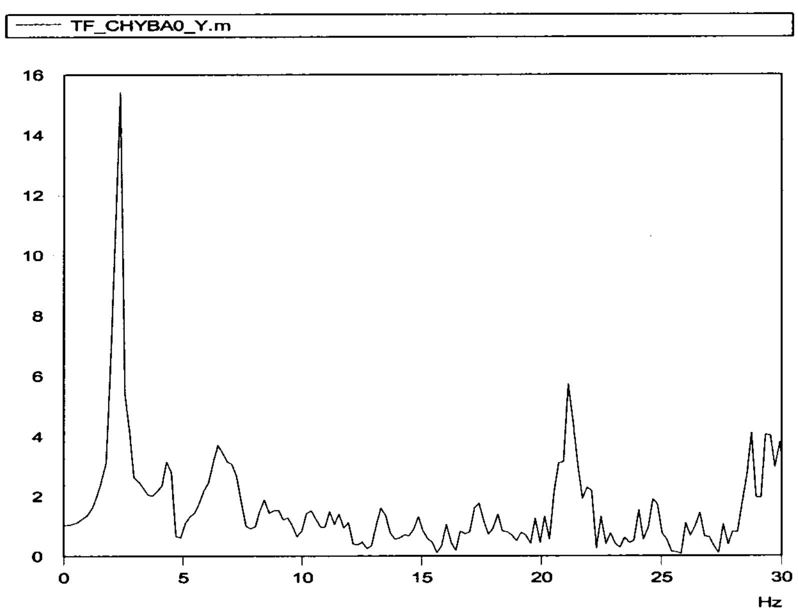

(b)

Figure B-6 Transfer functions for the CHYBA0 building

(a) X - direction (b)Y - direction

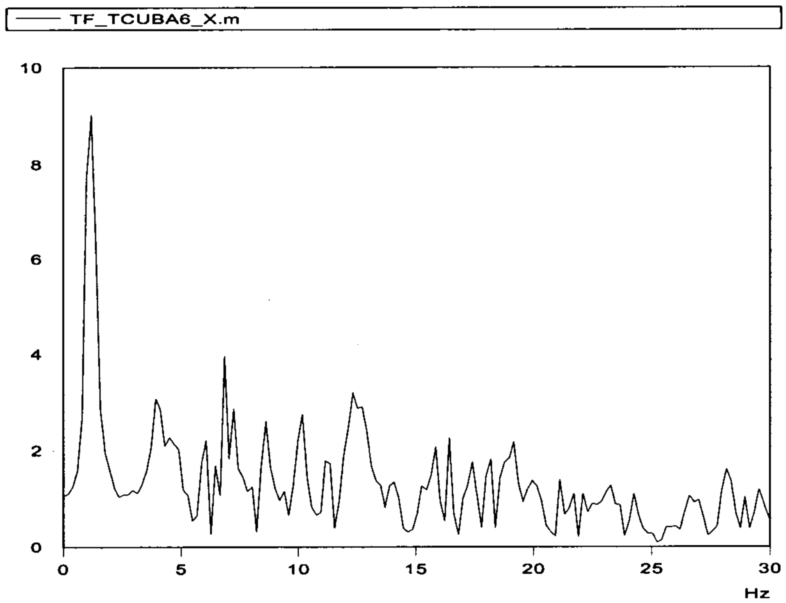

(a)

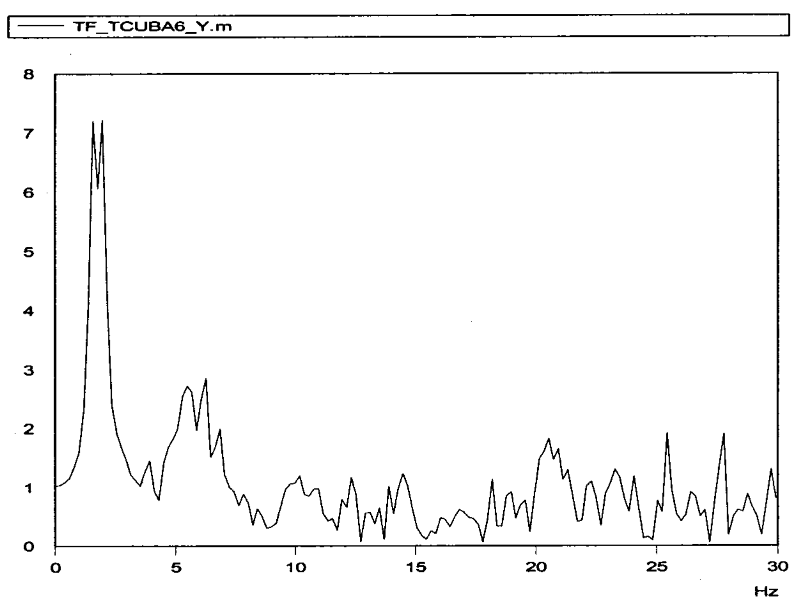

(b)

Figure B-7 Transfer functions for the TCUBA6 building

(a) X - direction (b) Y - direction

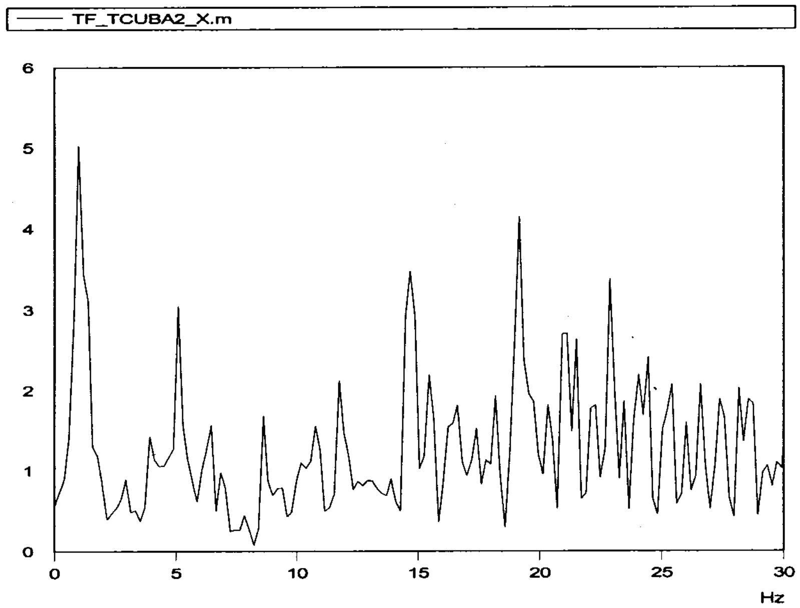

(a)

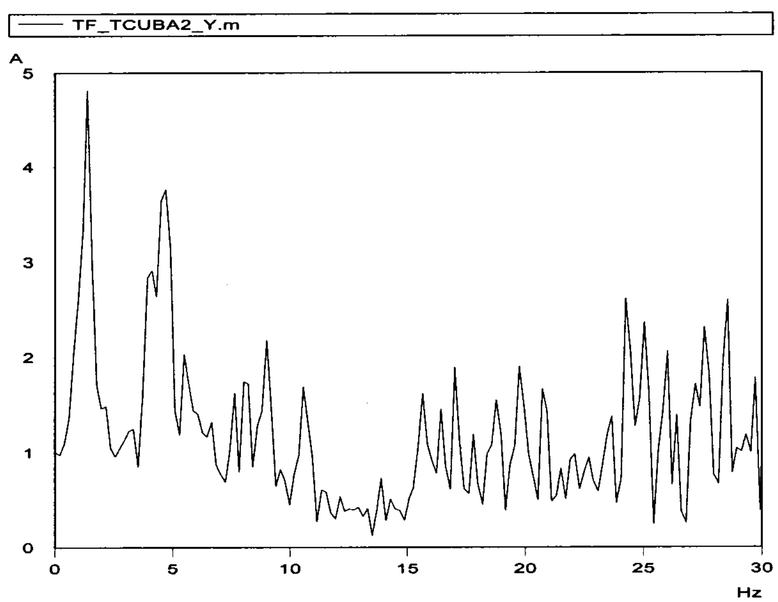

(b)

Figure B-8 Transfer functions for the TCUBA2 building

(a) X - direction (b) Y - direction

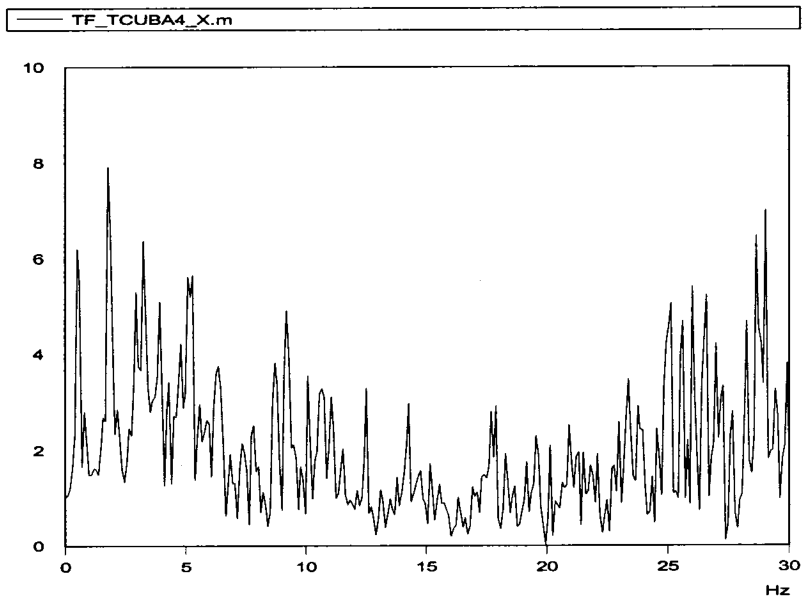

(a)

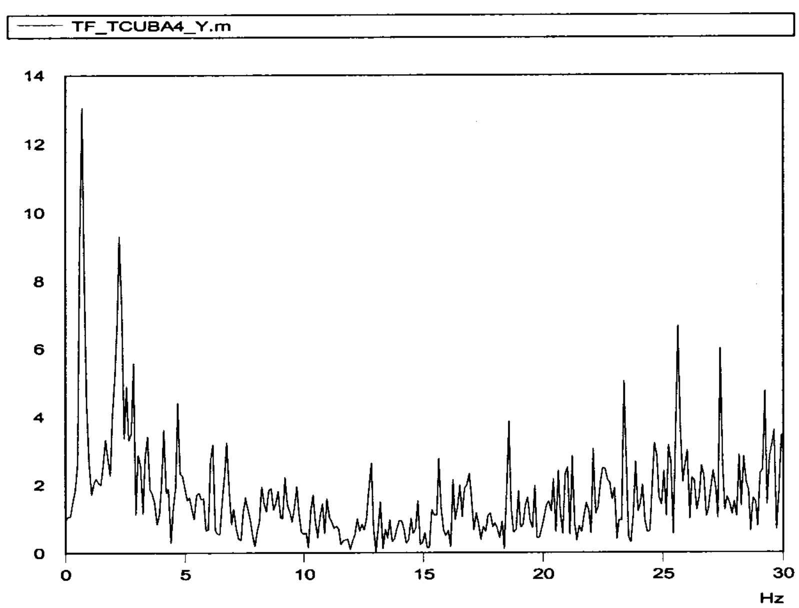

(b)

Figure B-9 Transfer functions for the TCUBA4 building

(a) X - direction (b) Y - direction

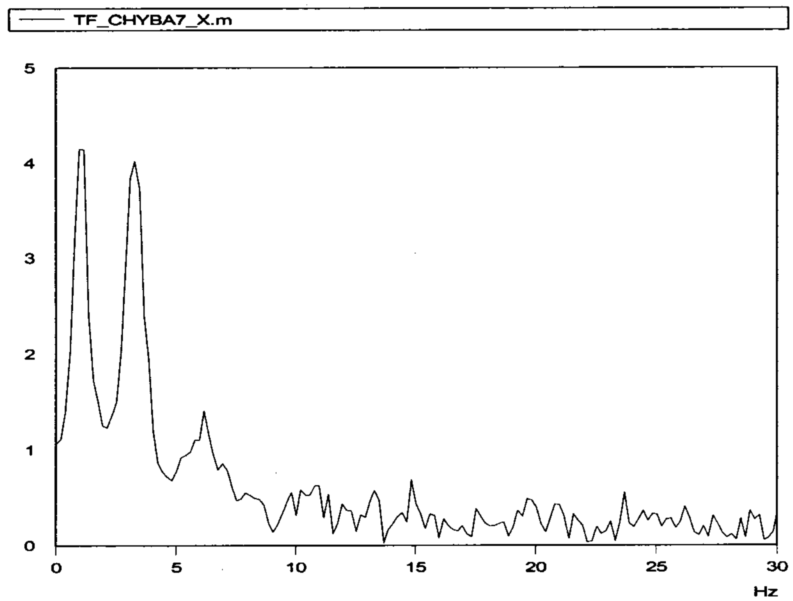

(a)

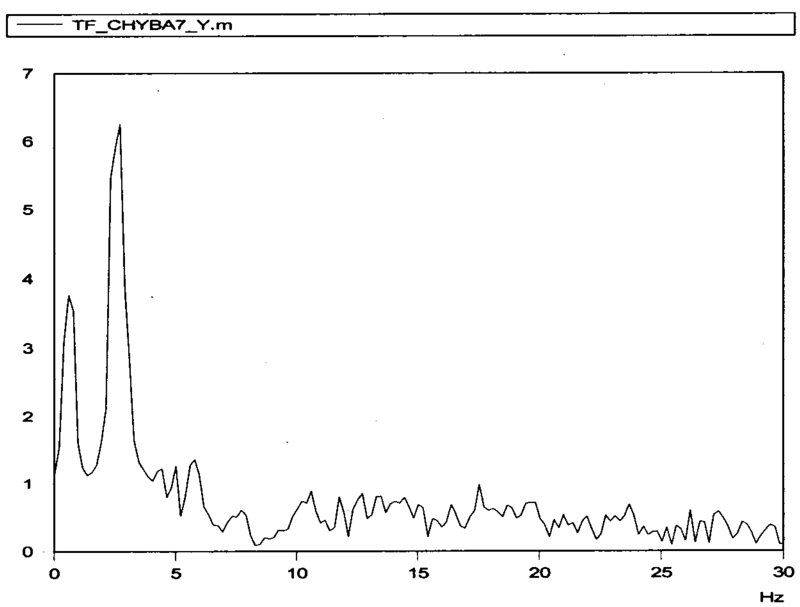

(b)

Figure B-10 Transfer functions for the CHYBA7 building

(a) X - direction (b) Y - direction

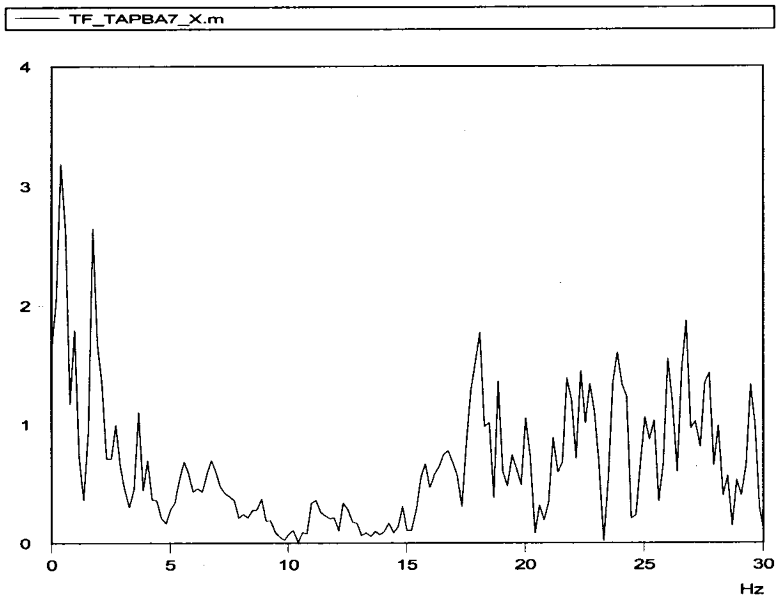

(a)

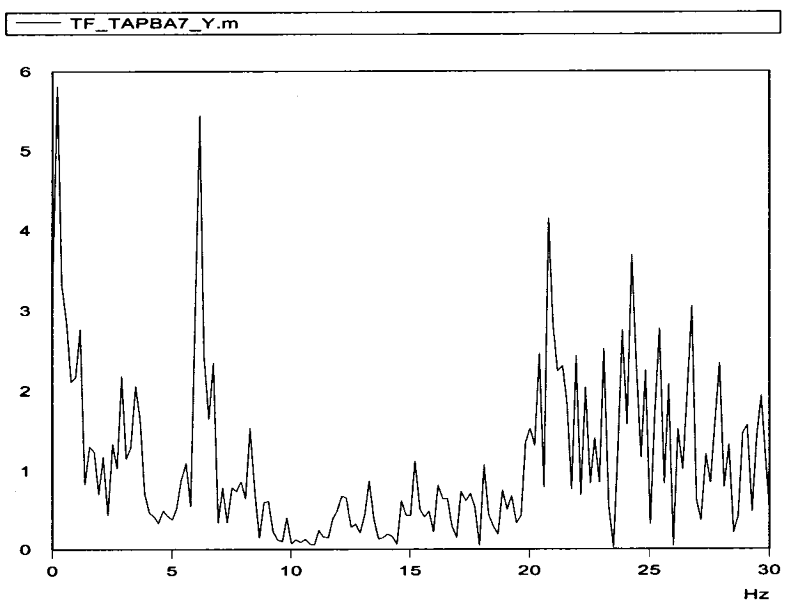

(b)

Figure B-11 Transfer functions for the TAPBA7 building

(a) X - direction (b) Y - direction

Appendix C

Mode Shapes and Natural Frequencies of the Buildings and Towers Modeled in SAP 2000

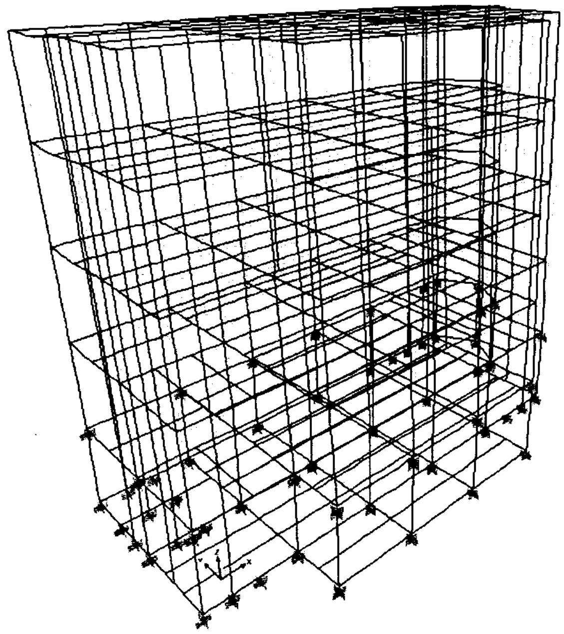

(a) Mode 1: Translation in the Y direction

(b) Mode 2: Translation in the X direction

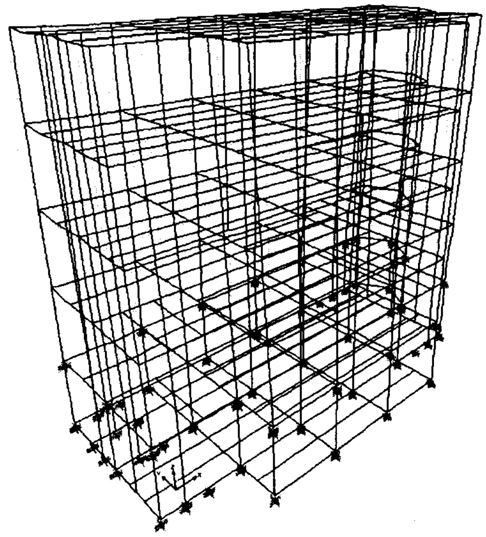

(c) Mode 3: Torsion

Figure C-1 Mode shapes of the CHYBA9 building

Table C-1 Natural periods and frequencies of the CHYBA9 building

Modes of vibration	Period (s)	Frequency (cycle/s)
Mode 1	0.30	3.34
Mode 2	0.26	3.85
Mode 3	0.17	5.76
Mode 4	0.14	7.27
Mode 5	0.14	7.40
Mode 6	0.09	10.54
Mode 7	0.09	10.57
Mode 8	0.09	10.61
Mode 9	0.09	10.63
Mode 10	0.08	12.05
Mode 11	0.08	12.27
Mode 12	0.07	13.47
Mode 13	0.07	14.95
Mode 14	0.06	15.64
Mode 15	0.06	16.00
Mode 16	0.06	16.35
Mode 17	0.06	16.53
Mode 18	0.06	17.74
Mode 19	0.05	19.68
Mode 20	0.05	20.06

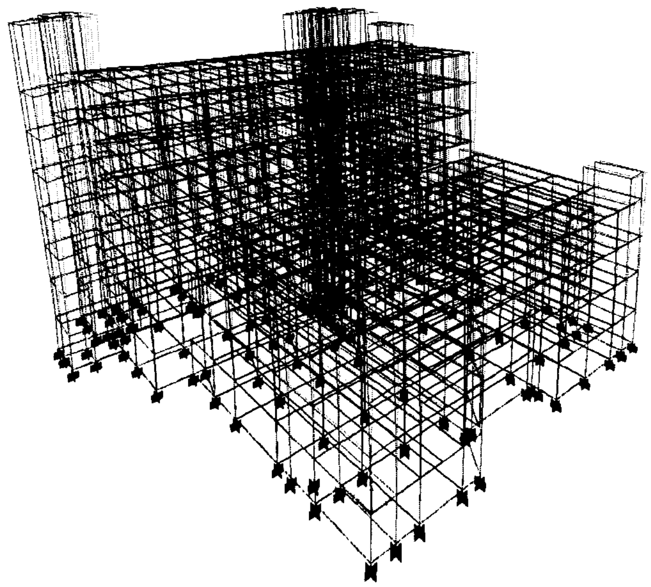

(a) Mode 1: Translation in the X direction

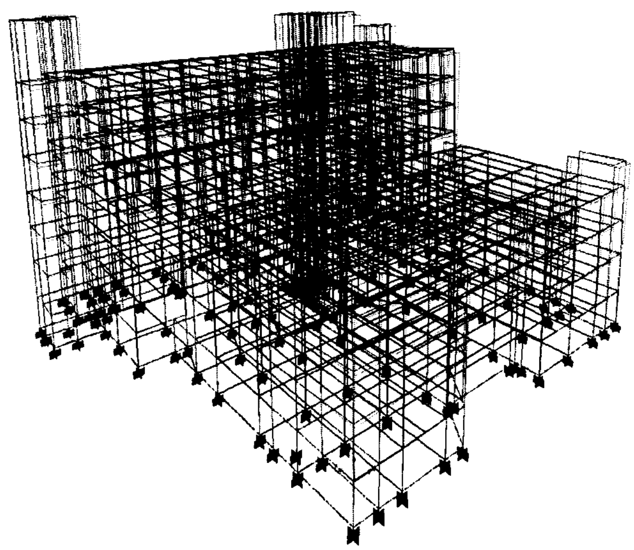

(b) Mode 2: Translation in the Y direction

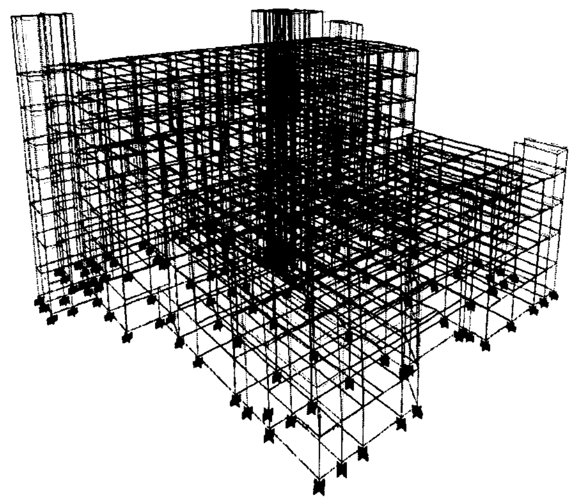

(c) Mode 3: Torsion

Figure C-2 .Mode shapes of the CHYBA4 building

Table C-2 Natural periods and frequencies of the CHYBA4 building

Modes of vibration	Period (s)	Frequency (cycle/s)
Mode 1	0.41	2.45
Mode 2	0.31	3.25
Mode 3	0.23	4.26
Mode 4	0.14	7.20
Mode 5	0.14	7.39
Mode 6	0.12	8.05
Mode 7	0.12	8.32
Mode 8	0.12	8.46
Mode 9	0.12	8.56
Mode 10	0.12	8.68
Mode 11	0.11	8.98
Mode 12	0.11	9.24
Mode 13	0.11	9.47
Mode 14	0.10	9.59
Mode 15	0.10	9.66
Mode 16	0.10	9.69
Mode 17	0.10	9.81
Mode 18	0.10	9.98
Mode 19	0.10	10.02
Mode 20	0.10	10.17

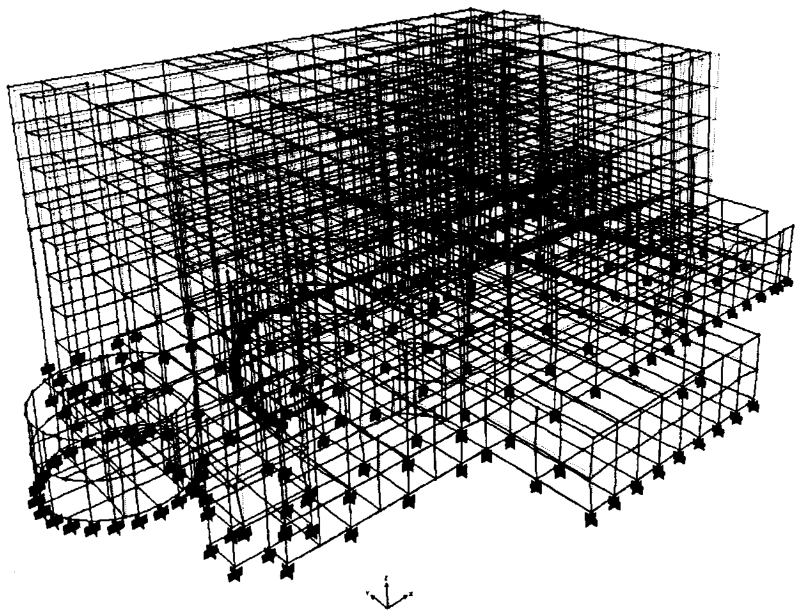

(a) Mode 1: Translation in the Y direction

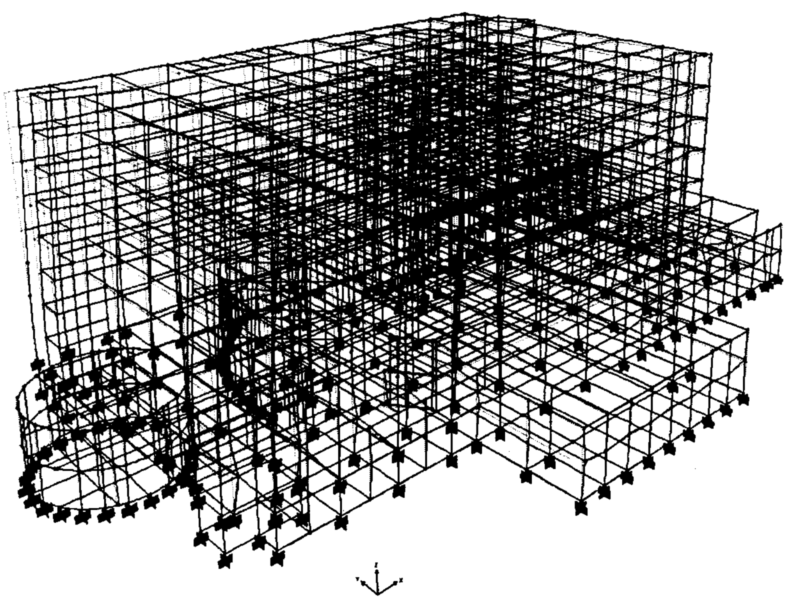

(b) Mode 2: Translation in the X direction

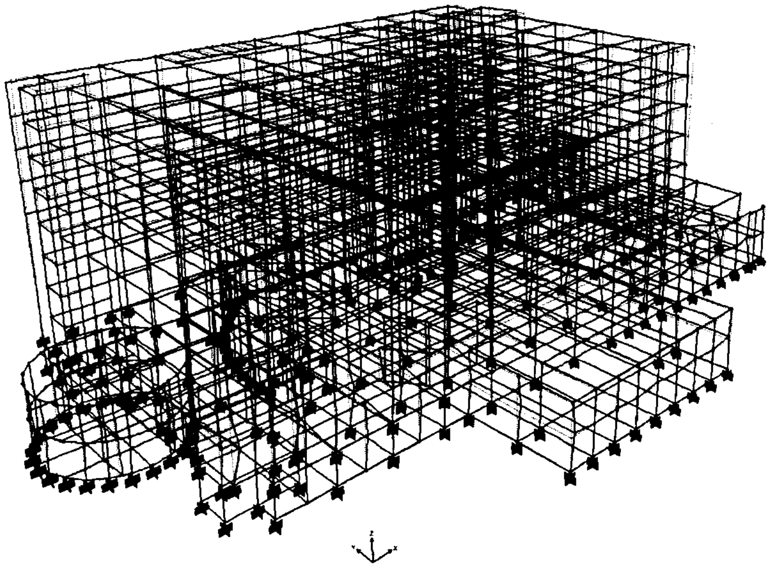

(c) Mode 3: Torsion

Figure C-3 Mode shapes of the TCUBAA building

Table C-3 Natural periods and frequencies of the TCUBAA building

Modes of vibration	Period (s)	Frequency (cycle/s)
Mode 1	0.74	1.34
Mode 2	0.69	1.45
Mode 3	0.62	1.62
Mode 4	0.21	4.82
Mode 5	0.20	5.09
Mode 6	0.18	5.60
Mode 7	0.17	5.75
Mode 8	0.17	5.88
Mode 9	0.16	6.16
Mode 10	0.16	6.35
Mode 11	0.15	6.52
Mode 12	0.15	6.67
Mode 13	0.15	6.83
Mode 14	0.14	6.90
Mode 15	0.14	6.99
Mode 16	0.14	7.04
Mode 17	0.14	7.09
Mode 18	0.14	7.18
Mode 19	0.14	7.25
Mode 20	0.14	7.30

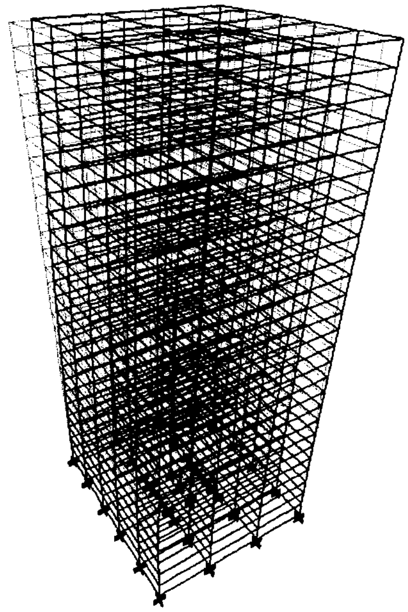

(a) Mode 1: Translation in the X direction

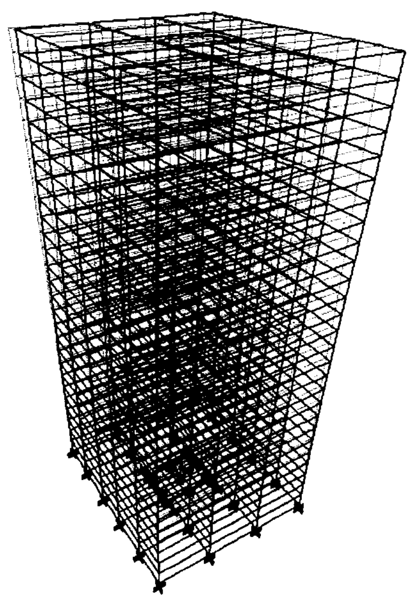

(b) Mode 2: Translation in the Y direction

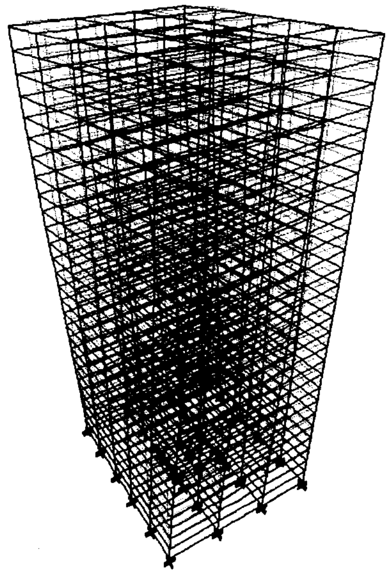

(c) Mode 3: Torsion

Figure C-4 Mode shapes of the 2020 University building

Table C-4 Natural periods and frequencies of the 2020 University building

Modes of vibration	Period (s)	Frequency (cycle/s)
Mode 1	2.01	0.50
Mode 2	1.88	0.53
Mode 3	1.36	0.73
Mode 4	0.63	1.60
Mode 5	0.52	1.91
Mode 6	0.48	2.07
Mode 7	0.30	3.33
Mode 8	0.29	3.46
Mode 9	0.23	4.44
Mode 10	0.20	5.08
Mode 11	0.19	5.24
Mode 12	0.16	6.09
Mode 13	0.13	7.49
Mode 14	0.13	7.75
Mode 15	0.13	7.98
Mode 16	0.11	8.91
Mode 17	0.10	10.22
Mode 18	0.09	10.56
Mode 19	0.09	11.31
Mode 20	0.08	12.00

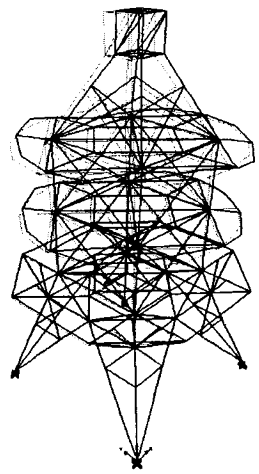

(a) Mode 1: Translation in the X direction

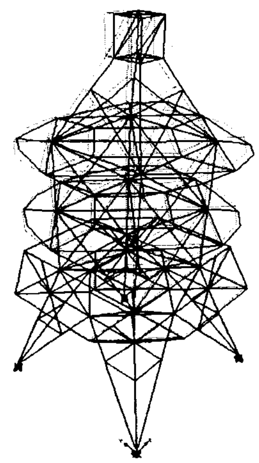

(b) Mode 2: Translation in the Y direction

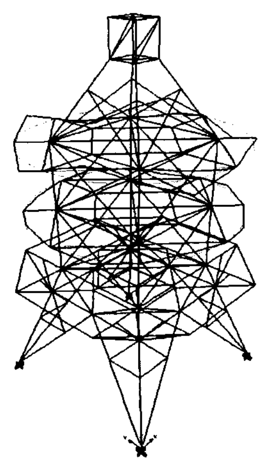

(b) Mode 3: Torsion

Figure C-5 Mode shapes of the TC1 tower

Table C-5 Natural periods and frequencies of the TC1 tower

Modes of vibration	Period (s)	Frequency (cycle/s)
Mode 1	0.14	7.27
Mode 2	0.14	7.40
Mode 3	0.09	10.55
Mode 4	0.09	10.58
Mode 5	0.09	10.61
Mode 6	0.09	10.64
Mode 7	0.08	12.28
Mode 8	0.06	15.98
Mode 9	0.06	16.30
Mode 10	0.05	19.87
Mode 11	0.05	19.99
Mode 12	0.05	20.73
Mode 13	0.05	20.75
Mode 14	0.05	21.02
Mode 15	0.04	23.62
Mode 16	0.04	23.79
Mode 17	0.04	24.32
Mode 18	0.04	24.47
Mode 19	0.04	24.71
Mode 20	0.04	25.36

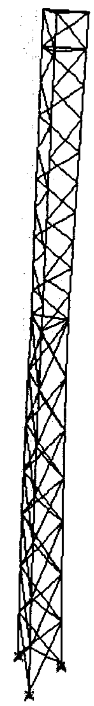

(a) Mode 1: Translation in the X direction

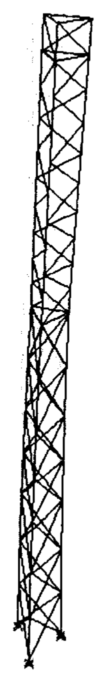

(b) Mode 1: Translation in the Y direction

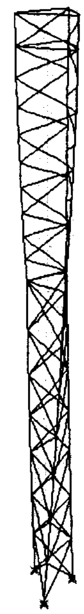

(c) Mode 3: Torsion

Figure C-6 Mode shapes of the TC2 tower

Table C-6 Natural periods and frequencies of the TC2 tower

Modes of vibration	Period (s)	Frequency (cycle/s)
Mode 1	0.37	2.69
Mode 2	0.37	2.69
Mode 3	0.11	9.18
Mode 4	0.10	10.11
Mode 5	0.10	10.11
Mode 6	0.05	18.36
Mode 7	0.04	22.27
Mode 8	0.04	22.27
Mode 9	0.03	29.83
Mode 10	0.03	30.05
Mode 11	0.03	30.05
Mode 12	0.03	36.43
Mode 13	0.03	36.43
Mode 14	0.03	36.54
Mode 15	0.03	38.03
Mode 16	0.03	38.66
Mode 17	0.02	40.40
Mode 18	0.02	41.10
Mode 19	0.02	41.10
Mode 20	0.02	41.39

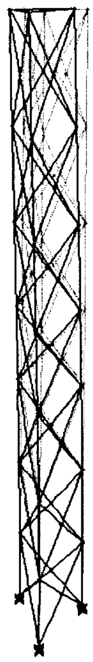

(a) Mode 1: Translation in the X direction

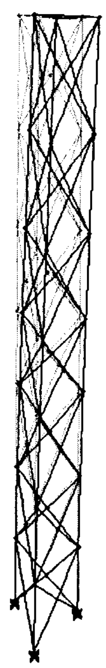

(b) Mode 2: Translation in the Y direction

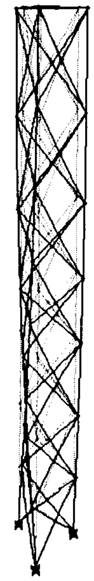

(c) Mode 3: Torsion

Figure C-7 Mode shapes of the TC3 tower

Table C-7 Modal periods and frequencies of the TC3 tower

Modes of vibration	Period (s)	Frequency (cycle/s)
Mode 1	0.19	5.37
Mode 2	0.19	5.37
Mode 3	0.08	12.33
Mode 4	0.05	20.39
Mode 5	0.05	20.39
Mode 6	0.04	28.02
Mode 7	0.03	30.03
Mode 8	0.03	30.03
Mode 9	0.03	36.63
Mode 10	0.02	40.86
Mode 11	0.02	40.87
Mode 12	0.02	42.18
Mode 13	0.02	42.19
Mode 14	0.02	43.90
Mode 15	0.02	51.26
Mode 16	0.02	51.28
Mode 17	0.02	51.29
Mode 18	0.02	57.89
Mode 19	0.02	58.85
Mode 20	0.02	60.87

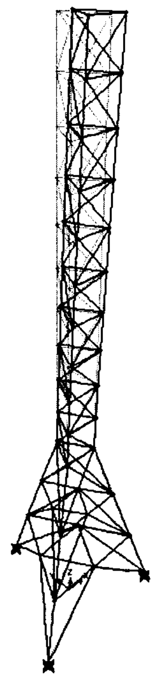

(a) Mode 1: Biaxial in the X and Y directions

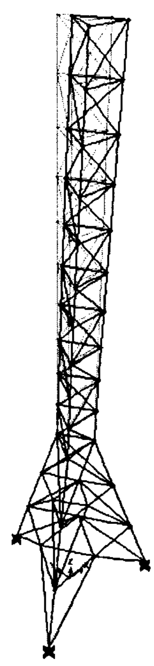

(b) Mode 2: Biaxial in the X and Y directions

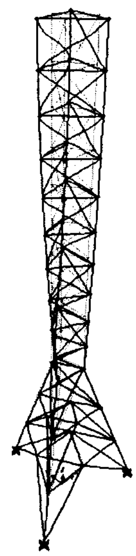

(c) Mode 3: Torsion

Figure C-8 Mode shapes of the TC4 tower

Table C-8 Natural periods and frequencies of the TC4 tower

Modes of vibration	Period (s)	Frequency (cycle/s)
Mode 1	0.25	3.94
Mode 2	0.25	3.94
Mode 3	0.08	11.92
Mode 4	0.05	20.80
Mode 5	0.05	20.80
Mode 6	0.04	27.79
Mode 7	0.03	34.13
Mode 8	0.03	34.19
Mode 9	0.03	38.13
Mode 10	0.02	40.60
Mode 11	0.02	49.31
Mode 12	0.02	49.33
Mode 13	0.02	51.28
Mode 14	0.02	61.27
Mode 15	0.02	63.08
Mode 16	0.02	63.23
Mode 17	0.01	79.43
Mode 18	0.01	82.33
Mode 19	0.01	82.42
Mode 20	0.01	95.05

Appendix D

Detailed Calculation of Efforts (V, M) at the Bases of the TC2, TC3, and TC4 Towers Mounted on the CHYBA9 Building

Loading Cases – UHS 2%/50 Years

I) From the numerical simulations in SAP 2000

II) From the proposed simplified method

Table D-1 Forces at the base of the TC2 tower mounted on the CHYB9 building calculated in SAP 2000
(a) U1 - direction (b) U2 - direction

(a)	P (N)			M_{demand} (N-m)	V_{demand} (N)	M_{demand} / V_{demand}
Loading cases - 2% - U1	1st Leg	2nd Leg	3rd Leg			
1	77.55	99.41	25.26	22120.00	935	23.7
2	84.99	112.21	29.05	24650.00	1122	22.0
3	94.13	115.79	22.67	26240.00	1577	16.6
4	76.37	91.99	16.57	21045.00	1028	20.5
5	125.74	152.11	27.28	34731.25	1649	21.1
6	133.15	141.4	19.2	34318.75	1933	17.8
7	97.87	117.63	22.66	26937.50	1421	19.0
8	82.56	92.99	21.59	21943.75	1102	19.9
9	81.5	96.03	16.75	22191.25	1136	19.5
10	125.86	137.49	27.19	32918.75	1572	20.9

(b)	P (N)			M_{demand} (N-m)	V_{demand} (N)	M_{demand} / V_{demand}
Loading cases - 2% - U2	1st Leg	2nd Leg	3rd Leg			
1	57.44	48.65	104.31	22659.12	1278	17.7
2	98.98	78.31	175.97	38104.56	1833	20.8
3	120.77	101.25	221.33	47856.96	2117	22.6
4	75.63	66.48	142.11	30695.76	1403	21.9
5	101.44	87.63	188.33	40732.56	2023	20.1
6	123.21	108.82	231.62	50059.44	2684	18.7
7	103.44	86.91	190.34	41114.16	1831	22.5
8	110.26	94.57	204.48	44192.88	1918	23.0
9	93.3	74.2	166.82	36082.08	1563	23.1
10	115.29	96.67	211.5	45717.12	2138	21.4

Table D-2 Forces at the base of the TC3 tower mounted on the CHYB9 building calculated in SAP 2000
(a) U1 - direction (b) U2 - direction

(a)	P (N)			M_{demand} (N-m)	V_{demand} (N)	M_{demand} / V_{demand}
Loading cases - 2% - U1	1st Leg	2nd Leg	3rd Leg			
1	219.09	304.53	85.27	65452.50	5347	12.2
2	330.28	438.39	107.81	96083.75	7675	12.5
3	223.41	309.25	90.25	66582.50	5298	12.6
4	215.75	281.11	65.65	62107.50	4968	12.5
5	199.78	264.65	70.99	58053.75	4739	12.3
6	293.64	383.74	90.59	84672.50	6637	12.8
7	244.79	329.93	89.23	71840.00	5936	12.1
8	219.98	299.49	80.74	64933.75	5293	12.3
9	272.19	367.06	94.06	79906.25	6368	12.5
10	274.25	362.37	87.16	79577.50	6416	12.4

(b)	P (N)			M_{demand} (N-m)	V_{demand} (N)	M_{demand} / V_{demand}
Loading cases - 2% - U2	1st Leg	2nd Leg	3rd Leg			
1	76.81	87.84	161.21	35150.22	2839	12.4
2	139.63	133.45	268.49	58459.33	4784	12.2
3	98.59	85.85	184.19	39895.18	3214	12.4
4	71.73	80.11	151.19	32779.54	2562	12.8
5	97.74	74.73	163.05	35980.14	2976	12.1
6	125.93	128.43	246.44	53925.82	4392	12.3
7	96.03	86.37	180.41	39202.38	3252	12.1
8	93.05	83.78	157.6	35508.17	2810	12.6
9	101.06	79.82	173.3	38066.47	3080	12.4
10	104.15	104.26	177.14	40607.46	3250	12.5

Table D-3 Forces at the base of the TC4 tower mounted on the CHYB9 building calculated in SAP 2000
(a) U1 - direction (b) U2 - direction

(a)	P (N)			M_{demand} (N-m)	V_{demand} (N)	M_{demand} / V_{demand}
Loading cases - 2% - U1	1st Leg	2nd Leg	3rd Leg			
1	352.37	324.86	31.47	186238.25	14461	12.9
2	318.35	287.21	33.1	166529.00	12969	12.8
3	240.11	222.06	23.97	127096.75	9599	13.2
4	251.12	227.18	27.24	131532.50	10629	12.4
5	343.48	309.73	36.08	179632.75	14696	12.2
6	231.39	208.51	26.58	120972.50	9805	12.3
7	323.93	300.42	30.47	171696.25	13688	12.5
8	341.12	316.35	34.95	180804.25	14121	12.8
9	224.14	207.61	25.47	118731.25	9874	12.0
10	266.47	241.83	29.68	139782.50	11258	12.4

(b)	P (N)			M_{demand} (N-m)	V_{demand} (N)	M_{demand} / V_{demand}
Loading cases - 2% - U2	1st Leg	2nd Leg	3rd Leg			
1	57.09	82.38	130.54	63553.93	4854	13.1
2	84.76	109.29	194.61	92545.51	7384	12.5
3	61.8	75.78	121.4	60353.63	5002	12.1
4	48.84	77.38	118.68	57688.03	4513	12.8
5	73.09	111.66	172.39	84018.76	6315	13.3
6	53.84	91.45	131.33	64728.07	5164	12.5
7	63.12	97.86	138.95	69635.63	5880	11.8
8	82.95	112.72	172.15	85675.24	6980	12.3
9	65.69	95.81	150.73	73456.32	6079	12.1
10	57.8	110.78	155.21	76001.33	6145	12.4

Table D-4 Shear forces at the base of the TC2 tower mounted on the CHYBA9 building calculated according to the proposed simplified method – U1 direction

CHYBA9-TC2		Loading cases - 2% - U1									
Panel #	Mass (kg)	1	2	3	4	5	6	7	8	9	10
1	581	529.87	562.99	551.80	567.39	548.62	556.58	542.74	528.15	565.19	559.08
2	502	356.85	402.43	445.39	450.82	392.64	486.75	394.72	369.64	426.97	436.01
3	434	229.44	274.87	369.10	310.78	307.59	484.04	282.00	265.23	305.07	351.50
4	217	118.28	147.12	200.20	150.21	194.21	282.88	149.05	137.31	168.09	207.47
5	102	76.88	89.47	118.60	94.95	122.41	150.16	94.31	78.74	104.61	126.80
6	102	108.98	114.31	147.25	123.70	153.54	167.26	124.75	100.34	129.46	154.66
7	102	149.13	140.47	180.67	154.35	185.30	195.25	156.37	132.61	162.03	185.01
8	102	190.73	172.69	221.44	188.43	217.62	233.46	188.69	170.38	205.69	222.74
9	102	232.30	212.63	263.79	225.03	249.91	273.03	220.96	209.03	251.20	266.51
	$\Sigma=$	1992.44	2116.98	2498.24	2265.66	2371.84	2829.42	2153.58	1991.42	2318.32	2509.77
	Rooftop acceleration	1.21	1.22	0.95	0.94	1.18	0.94	1.19	1.13	0.83	1.05
	$\Sigma m(x)a(x) = V_{calculated}$	2413.23	2578.01	2370.83	2119.52	2802.71	2651.68	2569.61	2247.88	1934.63	2645.45
	V_{demand}	935	1122	1577	1028	1649	1933	1421	1102	1136	1572
	$V_{calculated}/V_{demand}$	2.58	2.30	1.50	2.06	1.70	1.37	1.81	2.04	1.70	1.68

Table D-5 Shear forces at the base of the TC2 tower mounted on the CHYBA9 building calculated according to the proposed simplified method – U2 direction

CHYBA9-TC2		Loading cases - 2% - U2									
Panel #	Mass (kg)	1	2	3	4	5	6	7	8	9	10
1	581	585.00	515.68	527.84	553.25	578.91	557.44	561.75	535.98	515.71	625.70
2	502	488.80	385.72	399.89	483.74	518.64	578.78	456.86	410.34	347.14	585.80
3	434	466.83	340.55	480.66	488.09	629.85	715.23	451.67	419.92	328.02	691.15
4	217	267.78	209.86	361.78	312.53	445.79	456.63	299.47	297.44	233.65	514.55
5	102	133.92	135.39	215.31	187.82	258.21	252.33	184.52	184.94	146.58	311.69
6	102	165.67	177.21	266.33	225.48	312.69	290.99	236.83	231.51	187.44	377.48
7	102	221.78	220.31	326.32	274.24	372.68	347.65	292.94	281.65	230.78	450.33
8	102	284.22	270.39	392.16	339.54	441.14	423.65	350.59	333.69	278.53	530.98
9	102	347.29	327.83	461.24	408.87	515.71	503.90	411.41	386.32	332.06	613.42
	$\Sigma=$	2961.30	2582.93	3431.52	3273.56	4073.61	4126.60	3246.02	3081.79	2599.90	4701.11
	Rooftop acceleration	0.67	1.17	1.20	0.65	0.86	0.79	0.85	0.90	1.08	0.69
	$\sum m(x)a(x) = V_{calculated}$	1989.31	3012.94	4112.96	2142.54	3523.19	3275.82	2760.68	2766.59	2805.60	3253.78
	V_{demand}	1278	1833	2117	1403	2588	2684	1831	1918	1563	2138
	$V_{calculated}/V_{demand}$	1.56	1.64	1.94	1.53	1.36	1.22	1.51	1.44	1.80	1.52

Table D-6 Overturning moments at the base of the TC2 tower mounted on the CHYBA9 building calculated according to the proposed simplified method – U1 direction

CHYBA9-TC2			Loading cases - 2% - U1									
Panel #	Mass (kg)	x	1	2	3	4	5	6	7	8	9	10
1	581	3.34	1772.07	1882.83	1845.39	1897.53	1834.76	1861.38	1815.10	1766.32	1890.17	1869.76
2	502	9.61	3427.67	3865.50	4278.16	4330.23	3771.43	4675.42	3791.37	3550.47	4101.23	4187.98
3	434	15.02	3446.64	4129.12	5544.57	4668.57	4620.56	7271.27	4236.14	3984.28	4582.82	5280.22
4	217	18.77	2220.29	2761.70	3758.20	2819.75	3645.78	5310.26	2797.93	2577.59	3155.41	3894.59
5	102	21.02	1616.12	1880.80	2493.22	1995.93	2573.40	3156.76	1982.58	1655.30	2199.12	2665.69
6	102	23.02	2508.85	2631.53	3389.96	2847.81	3534.86	3850.72	2872.08	2309.99	2980.41	3560.70
7	102	25.02	3731.45	3514.76	4520.69	3862.25	4636.50	4885.51	3912.65	3318.20	4054.29	4629.26
8	102	27.02	5153.85	4666.45	5983.63	5091.85	5880.65	6308.51	5098.78	4603.87	5558.28	6018.79
9	102	29.02	6741.70	6170.99	7655.82	6530.89	7252.83	7923.92	6412.76	6066.42	7290.25	7734.53
		$\Sigma=$	30618.65	31503.70	39469.64	34044.81	37750.77	45243.76	32919.40	29832.45	35811.98	39841.52
		Rooftop acceleration	1.21	1.22	0.95	0.94	1.18	0.94	1.19	1.13	0.83	1.05
		$M_{calculated} = \sum m(x)a(x)x$	37085.00	38364.57	37456.69	31848.92	44608.57	42401.54	39278.77	33674.27	29885.10	41995.36
		M_{demand}	22119	22120	24650	26240	30632.5	34731.25	34318.75	26937.5	21943.75	22191.25
		$M_{calculated}/M_{demand}$	1.68	1.73	1.52	1.21	1.46	1.22	1.14	1.25	1.36	1.89

Table D-7 Overturning moments at the base of the TC2 tower mounted on the CHYBA9 building calculated according to the proposed simplified method – U2 direction

CHYBA9-TC2			Loading cases - 2% - U2									
Panel #	Mass (kg)	x	1	2	3	4	5	6	7	8	9	10
1	581	3.34	1956.45	1724.60	1765.26	1850.25	1936.06	1864.25	1878.67	1792.51	1724.69	2092.55
2	502	9.61	4695.08	3704.97	3841.11	4646.46	4981.75	5559.35	4388.32	3941.48	3334.39	5626.78
3	434	15.02	7012.76	5115.68	7220.44	7332.13	9461.59	10744.12	6784.97	6308.00	4927.54	10382.41
4	217	18.77	5026.73	3939.48	6791.25	5866.84	8368.34	8571.91	5621.64	5583.53	4385.99	9659.15
5	102	21.02	2815.19	2846.22	4526.29	3948.29	5428.08	5304.52	3878.88	3887.88	3081.45	6552.44
6	102	23.02	3814.13	4079.65	6131.37	5190.91	7198.77	6699.12	5452.22	5329.76	4315.25	8690.43
7	102	25.02	5549.40	5512.48	8165.20	6862.01	9325.13	8699.00	7329.84	7047.34	5774.47	11268.12
8	102	27.02	7680.27	7306.56	10596.92	9175.09	11920.35	11447.93	9473.65	9017.06	7526.31	14348.25
9	102	29.02	10079.16	9514.40	13386.19	11866.28	14966.97	14624.18	11939.91	11211.74	9637.13	17802.74
		$\Sigma=$	48629.17	43744.04	62424.03	56738.27	73587.05	73514.38	56748.11	54119.31	44707.22	86422.87
		Rooftop acceleration	0.67	1.17	1.20	0.65	0.86	0.79	0.85	0.90	1.08	0.69
		$\Sigma m(x)a(x)\,x = M_{calculated}$	32667.61	51026.55	74820.19	37135.20	63643.96	58357.92	48263.13	48583.99	48244.45	59815.86
		M_{demand}	22659.12	38104.56	47856.96	30695.76	57551.04	50059.44	41114.16	44192.88	36082.08	45717.12
		$M_{calculated}/M_{demand}$	1.44	1.34	1.56	1.21	1.11	1.17	1.17	1.10	1.34	1.31

Table D-8 Shear forces at the base of the TC3 tower mounted on the CHYBA9 building calculated according to the proposed simplified method – U1 direction

CHYBA9-TC3		Loading cases - 2% - U1									
Panel #	Mass (kg)	1	2	3	4	5	6	7	8	9	10
1	581	767.48	930.54	826.08	826.75	833.45	880.36	840.82	889.78	865.09	959.96
2	502	1107.15	1566.33	1379.17	1320.36	1265.61	1425.32	1347.23	1442.52	1384.15	1576.89
3	434	1490.73	2188.84	1953.93	1821.41	1671.43	1908.67	1889.06	1971.75	2017.79	2149.22
4	217	963.64	1425.43	1273.24	1166.45	1060.31	1217.88	1238.12	1268.04	1375.37	1407.09
	$\Sigma=$	4329.00	6111.14	5432.43	5134.97	4830.80	5432.24	5315.22	5572.09	5642.40	6093.16
	Rooftop acceleration	1.20	1.19	0.95	0.93	1.18	0.93	1.18	1.10	0.83	1.03
	$\sum m(x)a(x) = V_{calculated}$	5207.83	7271.95	5149.35	4768.69	5705.37	5077.62	6250.86	6126.96	4671.90	6283.75
	V_{demand}	5347	7675	5298	4968	5936	5293	6368	6416	4527	6359
	$V_{calculated}/V_{demand}$	0.97	0.95	0.97	0.96	0.96	0.96	0.98	0.95	1.03	0.99

Table D-9 Shear forces at the base of the TC3 tower mounted on the CHYBA9 building calculated according to the proposed simplified method – U2 direction

CHYBA9-TC3		Loading cases - 2% - U2									
Panel #	Mass (kg)	1	2	3	4	5	6	7	8	9	10
Panel 1	581	750.64	756.76	690.86	692.55	746.07	663.85	700.74	689.10	688.81	705.61
Panel 2	502	1068.42	1056.01	932.13	958.18	1003.12	868.65	931.94	895.26	826.15	902.46
Panel 3	434	1416.35	1355.38	1237.50	1356.06	1229.52	1159.56	1191.66	1169.51	987.41	1106.65
Panel 4	217	906.63	859.00	798.85	905.25	757.08	752.01	738.99	748.01	608.87	677.77
	$\sum=$	4142.03	4027.16	3659.35	3912.03	3735.79	3444.07	3563.32	3501.88	3111.25	3392.48
	Rooftop acceleration	0.67	1.15	0.90	0.66	0.87	0.80	0.86	0.89	0.98	0.98
	$\sum m(x)a(x) = V_{calculated}$	2762.86	4615.61	3280.42	2570.13	3264.34	2760.15	3053.16	3132.92	3046.41	3320.83
	V_{demand}	2839	4784	3214	2562	3252	2810	3080	3250	3043	3461
	$V_{calculated}/V_{demand}$	0.97	0.96	1.02	1.00	1.00	0.98	0.99	0.96	1.00	0.96

Table D-10 Overturning moments at the base of the TC3 tower mounted on the CHYBA9 building calculated according to the proposed simplified method – U1 direction

CHYBA9-TC3			Loading cases - 2% - U1									
Panel #	Mass (kg)	x	1	2	3	4	5	6	7	8	9	10
1	581	3.34	2566.71	3112.04	2762.70	2764.94	2787.35	2944.22	2811.97	2975.73	2893.14	3210.42
2	502	9.61	10634.56	15045.14	13247.43	12682.52	12156.60	13690.68	12940.59	13855.85	13295.22	15146.57
3	434	15.02	22393.70	32880.72	29351.89	27361.19	25108.24	28672.11	28377.41	29619.57	30311.17	32285.60
4	217	18.78	18089.43	26758.12	23901.32	21896.57	19904.06	22862.10	23241.93	23803.71	25818.52	26413.84
		$\sum=$	53684.39	77796.01	69263.35	64705.21	59956.25	68169.11	67371.90	70254.86	72318.05	77056.43
		Rooftop acceleration	1.20	1.19	0.95	0.93	1.18	0.93	1.18	1.10	0.83	1.03
		$M_{calculated} = \sum m(x)a(x)x$	64582.86	92573.37	65654.04	60089.78	70810.73	63719.03	79231.37	77250.84	59879.35	79466.76
		M_{demand}	65452.5	96083.75	66582.5	62107.5	71840	64933.75	79906.25	79577.5	60258.75	80038.75
		$M_{calculated}/M_{demand}$	0.99	0.96	0.99	0.97	0.99	0.98	0.99	0.97	0.99	0.99

Table D-11 Overturning moments at the base of the TC3 tower mounted on the CHYBA9 building calculated according to the proposed simplified method – U2 direction

CHYBA9-TC3			Loading cases - 2% - U2									
Panel #	Mass (kg)	x	1	2	3	4	5	6	7	8	9	10
1	581	3.34	2510.38	2530.87	2310.48	2316.13	2495.11	2220.13	2343.49	2304.59	2303.63	2359.80
2	502	9.61	10262.51	10143.31	8953.38	9203.61	9635.29	8343.64	8951.62	8599.25	7935.45	8668.40
3	434	15.02	21276.37	20360.59	18589.78	20370.68	18469.91	17418.98	17901.04	17568.40	14832.88	16624.05
4	217	18.78	17019.30	16125.17	14996.04	16993.34	14211.90	14116.77	13872.29	14041.67	11429.76	12723.10
		$\sum=$	51068.56	49159.94	44849.69	48883.76	44812.22	42099.52	43068.45	42513.91	36501.70	40375.36
		Rooftop acceleration	0.67	1.15	0.90	0.66	0.87	0.80	0.86	0.89	0.98	0.98
		$M_{calculated} = \sum m(x)a(x)x$	34064.26	56343.19	40205.50	32115.65	39156.91	33739.40	36902.34	38034.64	35741.01	39522.63
		M_{demand}	35150.22	58459.33	39895.18	32779.54	39202.38	35508.17	38066.47	40607.46	36864.90	41368.10
		$M_{calculated}/M_{demand}$	0.97	0.96	1.01	0.98	1.00	0.95	0.97	0.94	0.97	0.96

Table D-12 Shear forces at the base of the TC4 tower mounted on the CHYBA9 building calculated according to the proposed simplified method – U1 direction

CHYBA9-TC4		Loading cases - 2% - U1									
Panel #	Mass (kg)	1	2	3	4	5	6	7	8	9	10
1	890	922.62	910.76	919.40	917.16	928.25	916.06	908.13	915.61	926.44	934.45
2	440	484.44	460.88	475.76	469.93	478.30	475.63	449.72	470.97	474.78	482.47
3	315	392.98	347.82	352.02	396.28	386.70	373.29	342.33	371.77	405.98	406.29
4	255	558.77	478.12	467.96	569.63	583.45	515.41	542.58	584.21	588.21	611.71
5	255	1119.27	960.77	933.56	1043.32	1138.53	984.65	1106.85	1248.93	1086.69	1193.16
6	255	1865.54	1617.29	1602.18	1656.88	1822.02	1567.64	1788.91	2128.43	1720.12	1947.13
7	255	2690.73	2366.06	2419.06	2358.75	2565.41	2191.59	2553.46	3102.64	2422.26	2783.07
8	255	3564.82	3156.56	3299.25	3086.01	3338.15	2869.28	3361.27	4108.46	3149.46	3648.60
	$\Sigma=$	11599.18	10298.26	10469.21	10497.96	11240.81	9893.56	11053.24	12931.03	10773.94	12006.87
	Rooftop acceleration	1.20	1.21	0.93	0.94	1.18	0.93	1.15	1.01	0.82	0.85
	$\sum m(x)a(x) = V_{calculated}$	13893.15	12461.93	9733.33	9872.07	13273.71	9219.11	12680.50	13009.13	8828.92	10156.01
	V_{demand}	14461	12969	9599	10629	14696	9805	13688	14121	9874	11258
	$V_{calculated}/V_{demand}$	0.96	0.96	1.01	0.93	0.90	0.94	0.93	0.92	0.89	0.90

Table D-13 Shear forces at the base of the TC4 tower mounted on the CHYBA9 building calculated according to the proposed simplified method – U2 direction

CHYBA9-TC4		Loading cases - 2% - U2									
Panel #	Mass (kg)	1	2	3	4	5	6	7	8	9	10
1	890	885.30	907.48	889.81	875.85	892.84	888.73	895.95	890.37	894.68	886.11
2	440	464.86	478.95	454.69	427.61	457.57	445.18	463.24	452.49	456.33	448.23
3	315	399.03	394.43	362.07	354.26	374.36	363.41	392.89	387.36	365.21	381.50
4	255	468.01	453.19	381.95	431.37	464.44	416.12	458.60	490.60	398.88	478.56
5	255	741.64	703.94	547.95	699.55	771.17	630.22	681.07	785.47	602.39	769.94
6	255	1114.18	1012.66	766.10	1043.10	1123.69	907.83	928.83	1123.26	875.66	1115.46
7	255	1545.20	1368.05	1030.12	1414.77	1535.36	1217.55	1198.54	1502.63	1182.10	1484.82
8	255	2038.25	1792.62	1358.89	1815.74	2016.06	1545.08	1510.72	1912.09	1500.98	1859.89
	$\sum=$	7656.46	7111.33	5791.57	7062.26	7635.49	6414.12	6529.83	7544.28	6276.23	7424.51
	Rooftop acceleration	0.66	1.08	0.93	0.65	0.88	0.82	0.86	0.86	0.96	0.79
	$\sum m(x)a(x) = V_{calculated}$	5024.40	7699.15	5373.07	4605.09	6745.57	5245.60	5628.52	6498.87	6036.98	5841.53
	V_{demand}	4854	7384	5002	4513	6315	5164	5880	6980	6079	6145
	$V_{calculated}/V_{demand}$	1.04	1.04	1.07	1.02	1.07	1.02	0.96	0.93	0.99	0.95

Table D-14 Overturning moments at the base of the TC4 tower mounted on the CHYBA9 building calculated according to the proposed simplified method – U1 direction

CHYBA9-TC4			Loading cases - 2% - U1									
Panel #	Mass (kg)	x	1	2	3	4	5	6	7	8	9	10
1	890	1.3	1199.4	1184.0	1195.2	1192.3	1206.7	1190.9	1180.6	1190.3	1204.4	1214.8
2	440	3.8	1840.9	1751.3	1807.9	1785.7	1817.6	1807.4	1708.9	1789.7	1804.2	1833.4
3	315	6.2	2436.5	2156.5	2182.5	2457.0	2397.6	2314.4	2122.4	2305.0	2517.1	2519.0
4	255	8.3	4637.8	3968.4	3884.1	4727.9	4842.7	4277.9	4503.4	4848.9	4882.1	5077.2
5	255	11.3	12647.8	10856.7	10549.3	11789.5	12865.3	11126.6	12507.4	14112.9	12279.6	13482.7
6	255	13.9	25931.0	22480.3	22270.4	23030.6	25326.1	21790.2	24865.8	29585.1	23909.6	27065.1
7	255	16.5	44397.0	39040.0	39914.4	38919.4	42329.2	36161.3	42132.1	51193.6	39967.3	45920.6
8	255	19.1	68088.1	60290.2	63015.7	58942.9	63758.6	54803.3	64200.2	78471.6	60154.6	69688.2
		$\sum=$	161178.5	141727.50	144819.55	142845.26	154543.78	133471.91	153220.93	183497.21	146718.91	166800.95
		Rooftop acceleration	1.20	1.21	0.93	0.94	1.18	0.93	1.15	1.01	0.82	0.85
		$M_{calculated} = \sum m(x)a(x)x$	193054.8	171504.4	134640.2	134328.8	182493.0	124373.1	175778.1	184605.5	120231.7	141088.6
		M_{demand}	186238.3	166529.0	127096.8	131532.5	179632.8	120972.5	171696.3	180804.3	118731.3	139782.5
		$M_{calculated}/M_{demand}$	1.04	1.03	1.06	1.02	1.02	1.03	1.02	1.02	1.01	1.01

Table D-15 Overturning moments at the base of the TC4 tower mounted on the CHYBA9 building calculated according to the proposed simplified method – U2 direction

CHYBA9-TC4			Loading cases - 2% - U2									
Panel #	Mass (kg)	x	1	2	3	4	5	6	7	8	9	10
1	890	1.3	1150.9	1179.7	1156.8	1138.6	1160.7	1155.4	1164.7	1157.5	1163.1	1151.9
2	440	3.8	1766.5	1820.0	1727.8	1624.9	1738.8	1691.7	1760.3	1719.5	1734.0	1703.3
3	315	6.2	2474.0	2445.5	2244.8	2196.4	2321.0	2253.1	2435.9	2401.6	2264.3	2365.3
4	255	8.3	3884.4	3761.4	3170.2	3580.4	3854.8	3453.8	3806.4	4072.0	3310.7	3972.1
5	255	11.3	8380.5	7954.6	6191.8	7905.0	8714.3	7121.5	7696.1	8875.8	6807.0	8700.4
6	255	13.9	15487.2	14076.0	10648.7	14499.0	15619.4	12618.9	12910.7	15613.4	12171.6	15505.0
7	255	16.5	25495.8	22572.8	16997.0	23343.8	25333.4	20089.6	19775.9	24793.5	19504.7	24499.5
8	255	19.1	38930.6	34239.1	25954.9	34680.7	38506.7	29510.9	28854.7	36520.8	28668.7	35523.8
		$\sum=$	97569.82	88049.17	68091.94	88968.8	97249.06	77894.88	78404.72	95154.05	75624.17	93421.15
		Rooftop acceleration	0.66	1.08	0.93	0.65	0.88	0.82	0.86	0.86	0.96	0.79
		$M_{calculated} = \sum m(x)a(x)x$	64028.2	95327.3	63171.6	58013.9	85914.7	63704.0	67582.5	81968.6	72741.4	73502.8
		M_{demand}	63553.9	92545.5	60353.6	57688.0	84018.8	64728.1	69635.6	85675.2	73456.3	76001.3
		$M_{calculated}/M_{demand}$	1.01	1.03	1.05	1.01	1.02	0.98	0.97	0.96	0.99	0.97

Appendix E

Acceleration Amplification along the TC2, TC3, and TC4 Towers Mounted on the CHYBA9 Building

I) Detailed calculations from the numerical simulations

II) Profiles

Table E-1 Acceleration amplification along the TC2 tower mounted on the CHYBA9 building - set high a/v - U1

CHYBA9-TC2	Acceleration amplification													
Distance from the tower base (m)	Loading cases - high a/v - U1													
	1	2	3	4	5	6	7	8	9	10	11	12	13	14
0.00	1.00	1.00	1.00	1.00	1.00	1.00	1.00	1.00	1.00	1.00	1.00	1.00	1.00	1.00
6.69	0.80	1.06	0.99	0.83	0.88	0.88	1.12	0.93	0.88	1.01	1.01	0.84	0.86	0.90
12.52	0.67	1.09	0.78	0.58	0.93	0.85	1.03	1.07	0.96	0.92	0.92	0.50	0.79	0.79
17.52	0.64	1.27	0.60	0.37	1.18	0.79	0.80	1.20	0.99	0.72	0.72	0.45	0.53	0.55
20.02	0.94	1.66	0.75	0.67	1.38	1.00	0.92	1.46	1.12	0.84	0.84	0.79	0.77	0.73
22.02	1.30	2.06	1.00	0.98	1.60	1.36	1.13	1.76	1.53	0.93	0.93	1.09	1.07	0.88
24.02	1.68	2.49	1.27	1.34	2.15	1.86	1.38	2.15	2.01	1.25	1.25	1.40	1.46	1.09
26.02	2.09	2.94	1.56	1.73	2.76	2.41	1.75	2.56	2.53	1.77	1.77	1.72	1.91	1.51
28.02	2.50	3.41	1.97	2.12	3.39	2.96	2.18	2.98	3.05	2.31	2.31	2.11	2.38	1.95
30.00	2.94	3.95	2.36	2.51	4.01	3.51	2.61	3.40	3.57	2.83	2.83	2.52	2.84	2.38

Table E-2 Acceleration amplification along the TC2 tower mounted on the CHYBA9 building - set high a/v - U2

CHYBA9-TC2	Acceleration amplification													
Distance from the tower base (m)	Loading cases - high a/v - U2													
	1	2	3	4	5	6	7	8	9	10	11	12	13	14
0.00	1.00	1.00	1.00	1.00	1.00	1.00	1.00	1.00	1.00	1.00	1.00	1.00	1.00	1.00
6.69	0.82	0.97	0.96	0.84	1.08	0.76	0.81	0.91	1.01	1.14	1.14	0.75	1.19	0.83
12.52	0.75	0.87	0.84	0.50	1.63	0.79	0.83	1.00	1.09	1.07	1.07	0.36	1.12	0.72
17.52	1.28	1.80	1.19	0.69	2.16	1.16	1.03	1.79	1.60	0.77	0.77	0.80	1.38	0.88
20.02	1.90	2.41	1.49	1.11	2.84	1.45	1.49	2.35	1.98	1.13	1.13	1.28	1.73	1.11
22.02	2.44	2.94	1.77	1.51	3.55	1.90	2.01	2.83	2.32	1.45	1.45	1.70	2.02	1.49
24.02	3.02	3.54	2.05	1.94	4.31	2.37	2.59	3.34	2.82	1.79	1.79	2.14	2.38	1.96
26.02	3.62	4.20	2.34	2.39	5.10	2.87	3.19	3.87	3.35	2.13	2.13	2.61	2.80	2.46
28.02	4.23	4.86	2.69	2.85	5.89	3.37	3.80	4.41	3.90	2.47	2.47	3.07	3.22	3.06
30.00	4.84	5.52	3.08	3.30	6.69	3.86	4.41	4.94	4.46	2.80	2.80	3.56	3.64	3.68

Table E-3 Average values and standard deviations of acceleration amplification along the TC2 tower mounted on the CHYBA9 building - set high a/v - U1&U2 directions

CHYBA9-TC2	Acceleration amplification			
Distance from the tower base (m)	Loading cases - high a/v			
	U1		U2	
	μ	σ	μ	σ
0.00	1.00	0.00	1.00	0.00
6.69	0.93	0.09	0.94	0.15
12.52	0.85	0.18	0.90	0.30
17.52	0.77	0.29	1.24	0.46
20.02	0.99	0.30	1.67	0.55
22.02	1.26	0.36	2.10	0.64
24.02	1.63	0.43	2.57	0.75
26.02	2.07	0.47	3.07	0.87
28.02	2.55	0.51	3.59	0.99
30.00	3.02	0.57	4.11	1.11

Table E-4 Acceleration amplification along the TC2 tower mounted on the CHYBA9 building - set medium a/v - U1

CHYBA9-TC2	Acceleration amplification														
Distance from the tower base (m)	Loading cases - medium a/v - U1														
	1	2	3	4	5	6	7	8	9	10	11	12	13	14	15
0.00	1.00	1.00	1.00	1.00	1.00	1.00	1.00	1.00	1.00	1.00	1.00	1.00	1.00	1.00	1.00
6.69	0.79	0.95	0.88	0.82	0.96	0.86	0.81	0.93	0.93	0.82	0.82	0.98	0.83	0.82	1.07
12.52	0.66	1.13	0.81	0.60	0.90	0.58	0.65	0.69	0.84	0.73	0.73	0.90	0.56	0.82	1.20
17.52	0.59	1.26	0.93	0.44	1.39	0.38	0.63	0.57	0.77	0.77	0.77	0.95	0.46	1.02	1.67
20.02	0.76	1.59	1.25	0.65	1.84	0.53	0.86	0.76	0.98	1.16	1.16	1.18	0.62	1.20	1.94
22.02	1.04	1.92	1.61	0.97	2.26	0.78	1.21	1.03	1.37	1.60	1.60	1.43	0.82	1.39	2.29
24.02	1.43	2.28	2.00	1.30	2.69	1.06	1.58	1.32	1.78	2.08	2.08	1.77	1.08	1.65	2.75
26.02	1.85	2.66	2.41	1.65	3.14	1.36	1.98	1.67	2.21	2.59	2.59	2.13	1.43	2.01	3.23
28.02	2.27	3.04	2.82	2.00	3.59	1.68	2.37	2.04	2.66	3.11	3.11	2.49	1.79	2.40	3.72
30.00	2.68	3.42	3.23	2.35	4.04	2.00	2.76	2.40	3.10	3.62	3.62	2.85	2.15	2.79	4.21

Table E-5 Acceleration amplification along the TC2 tower mounted on the CHYBA9 building - set medium a/v - U2

CHYBA9-TC2	Acceleration amplification														
Distance from the tower base (m)	Loading cases - medium a/v - U2														
	1	2	3	4	5	6	7	8	9	10	11	12	13	14	15
0.00	1.00	1.00	1.00	1.00	1.00	1.00	1.00	1.00	1.00	1.00	1.00	1.00	1.00	1.00	1.00
6.69	0.88	0.99	0.92	0.73	0.76	0.88	0.96	0.83	0.81	0.81	0.81	0.80	0.77	0.70	0.90
12.52	0.86	0.93	1.15	0.45	0.82	0.57	0.76	0.47	0.53	0.59	0.59	0.77	0.50	0.74	1.05
17.52	1.33	1.50	1.89	0.91	1.76	0.68	1.30	0.81	0.89	1.25	1.25	0.96	0.80	0.92	1.63
20.02	1.91	1.89	2.60	1.44	2.50	1.12	1.89	1.15	1.30	1.81	1.81	1.50	1.20	1.42	1.98
22.02	2.43	2.32	3.23	1.93	3.14	1.52	2.41	1.45	1.67	2.33	2.33	1.97	1.58	1.86	2.42
24.02	3.00	2.85	3.90	2.47	3.83	1.94	3.01	1.94	2.08	2.90	2.90	2.49	1.98	2.33	2.93
26.02	3.59	3.40	4.60	3.04	4.55	2.39	3.68	2.48	2.53	3.50	3.50	3.03	2.41	2.84	3.46
28.02	4.19	3.95	5.38	3.62	5.29	2.84	4.36	3.03	2.99	4.11	4.11	3.58	2.84	3.34	4.00
30.00	4.78	4.51	6.16	4.19	6.01	3.29	5.03	3.58	3.45	4.72	4.72	4.12	3.27	3.85	4.53

Table E-6 Average values and standard deviations of acceleration amplification along the TC2 tower mounted on the CHYBA9 building - set medium a/v - U1&U2 directions

CHYBA9-TC2	Acceleration amplification			
Distance from the tower base (m)	Loading cases - medium a/v			
	U1		U2	
	μ	σ	μ	σ
0.00	1.00	0.00	1.00	0.00
6.69	0.89	0.08	0.84	0.08
12.52	0.79	0.19	0.72	0.21
17.52	0.84	0.37	1.19	0.38
20.02	1.10	0.43	1.70	0.46
22.02	1.42	0.47	2.17	0.54
24.02	1.79	0.53	2.70	0.62
26.02	2.19	0.57	3.27	0.70
28.02	2.61	0.62	3.84	0.79
30.00	3.01	0.67	4.41	0.88

Table E-7 Acceleration amplification along the TC2 tower mounted on the CHYBA9 building - set low a/v - U1

CHYBA9-TC2	Acceleration amplification														
Distance from the tower base (m)	Loading cases - low a/v - U1														
	1	2	3	4	5	6	7	8	9	10	11	12	13	14	15
0.00	1.00	1.00	1.00	1.00	1.00	1.00	1.00	1.00	1.00	1.00	1.00	1.00	1.00	1.00	1.00
6.69	0.95	0.91	0.89	0.89	0.85	0.76	0.86	0.96	0.89	0.91	0.91	0.91	0.93	0.99	1.06
12.52	0.97	0.91	0.61	0.75	0.64	0.64	0.58	0.82	0.67	0.74	0.74	0.87	0.73	0.90	1.14
17.52	1.27	1.06	0.47	0.89	0.57	0.68	0.67	1.00	0.53	0.79	0.79	1.15	1.11	1.02	1.63
20.02	1.44	1.33	0.66	1.13	0.83	0.93	0.87	1.12	0.74	0.86	0.86	1.41	1.33	1.26	1.95
22.02	1.62	1.60	0.84	1.35	1.16	1.27	1.06	1.29	1.04	1.14	1.14	1.67	1.56	1.48	2.35
24.02	1.95	1.88	1.05	1.73	1.52	1.68	1.33	1.54	1.39	1.45	1.45	2.02	1.91	1.77	2.77
26.02	2.29	2.19	1.29	2.13	1.91	2.11	1.66	1.88	1.75	1.78	1.78	2.42	2.29	2.10	3.21
28.02	2.64	2.50	1.54	2.55	2.30	2.55	1.99	2.26	2.12	2.11	2.11	2.82	2.68	2.48	3.69
30.00	2.98	2.82	1.83	2.95	2.68	2.98	2.32	2.64	2.49	2.44	2.44	3.22	3.06	2.87	4.17

Table E-8 Acceleration amplification along the TC2 tower mounted on the CHYBA9 building - set low a/v - U2

CHYBA9-TC2	Acceleration amplification														
Distance from the tower base (m)	Loading cases - low a/v - U2														
	1	2	3	4	5	6	7	8	9	10	11	12	13	14	15
0.00	1.00	1.00	1.00	1.00	1.00	1.00	1.00	1.00	1.00	1.00	1.00	1.00	1.00	1.00	1.00
6.69	1.08	0.83	0.82	0.95	0.74	0.72	0.82	1.07	0.95	0.82	0.82	0.91	0.78	0.88	0.97
12.52	1.64	0.89	0.66	0.80	0.62	0.65	0.53	1.27	0.86	0.67	0.67	0.78	0.67	0.62	1.22
17.52	2.87	1.53	1.06	1.01	1.20	1.11	1.05	2.18	1.03	0.96	0.96	1.16	1.43	0.84	2.09
20.02	3.84	1.97	1.34	1.33	1.72	1.68	1.50	2.71	1.55	1.34	1.34	1.56	1.93	1.27	2.74
22.02	4.68	2.34	1.74	1.68	2.17	2.21	1.90	3.17	2.00	1.67	1.67	1.90	2.40	1.65	3.37
24.02	5.57	2.78	2.26	2.10	2.66	2.79	2.33	3.64	2.50	2.02	2.02	2.28	2.90	2.06	4.06
26.02	6.48	3.24	2.82	2.57	3.18	3.40	2.77	4.14	3.03	2.50	2.50	2.67	3.42	2.49	4.78
28.02	7.39	3.78	3.39	3.05	3.70	4.02	3.22	4.79	3.56	2.99	2.99	3.06	3.94	2.93	5.51
30.00	8.29	4.33	3.96	3.51	4.21	4.64	3.66	5.47	4.09	3.48	3.48	3.45	4.46	3.36	6.24

Table E-9 Average values and standard deviations of acceleration amplification along the TC2 tower mounted on the CHYBA9 building - set low a/v - U1&U2 directions

CHYBA9-TC2	Acceleration amplification			
Distance from the tower base (m)	Loading cases - low a/v			
	U1		U2	
	μ	σ	μ	σ
0.00	1.00	0.00	1.00	0.00
6.69	0.91	0.07	0.88	0.11
12.52	0.78	0.15	0.84	0.31
17.52	0.91	0.31	1.36	0.58
20.02	1.12	0.34	1.85	0.72
22.02	1.37	0.36	2.30	0.84
24.02	1.70	0.40	2.80	0.97
26.02	2.05	0.43	3.33	1.08
28.02	2.42	0.48	3.89	1.21
30.00	2.79	0.52	4.44	1.34

Table E-10 Acceleration amplification along the TC2 tower mounted on the CHYBA9 building - set UHS 2%/50 years - U1

CHYBA9-TC2	Acceleration amplification									
Distance from the tower base (m)	Loading cases - 2% - U1									
	1	2	3	4	5	6	7	8	9	10
0.00	1.00	1.00	1.00	1.00	1.00	1.00	1.00	1.00	1.00	1.00
6.69	0.82	0.94	0.90	0.95	0.89	0.92	0.87	0.82	0.95	0.92
12.52	0.60	0.67	0.88	0.84	0.68	1.02	0.70	0.65	0.76	0.81
17.52	0.46	0.60	0.83	0.59	0.74	1.21	0.60	0.57	0.65	0.81
20.02	0.63	0.75	1.02	0.80	1.05	1.40	0.78	0.70	0.90	1.10
22.02	0.88	1.00	1.31	1.07	1.35	1.54	1.07	0.85	1.15	1.38
24.02	1.26	1.24	1.58	1.36	1.66	1.74	1.38	1.12	1.39	1.65
26.02	1.66	1.51	1.96	1.67	1.97	2.09	1.69	1.48	1.79	1.98
28.02	2.08	1.87	2.38	2.03	2.29	2.48	2.01	1.86	2.24	2.39
30.00	2.48	2.30	2.79	2.39	2.61	2.87	2.32	2.24	2.68	2.83

Table E-11 Acceleration amplification along the TC2 tower mounted on the CHYBA9 building - set UHS 2%/50 years - U2

CHYBA9-TC2	Acceleration amplification									
Distance from the tower base (m)	Loading cases - 2% - U2									
	1	2	3	4	5	6	7	8	9	10
0.00	1.00	1.00	1.00	1.00	1.00	1.00	1.00	1.00	1.00	1.00
6.69	1.01	0.78	0.82	0.90	0.99	0.92	0.93	0.85	0.78	1.15
12.52	0.93	0.76	0.78	1.02	1.07	1.39	0.89	0.79	0.61	1.18
17.52	1.22	0.81	1.44	1.23	1.83	1.91	1.19	1.15	0.90	2.01
20.02	1.25	1.13	1.90	1.65	2.28	2.30	1.57	1.60	1.25	2.74
22.02	1.38	1.53	2.33	2.03	2.78	2.65	2.05	2.03	1.62	3.37
24.02	1.87	1.95	2.90	2.39	3.35	3.06	2.59	2.51	2.05	4.03
26.02	2.48	2.37	3.50	2.98	3.96	3.76	3.15	3.01	2.47	4.80
28.02	3.10	2.93	4.19	3.67	4.69	4.55	3.72	3.53	2.99	5.61
30.00	3.71	3.50	4.86	4.34	5.42	5.33	4.35	4.05	3.52	6.42

Table E-12 Average values and standard deviations of acceleration amplification along the TC2 tower mounted on the CHYBA9 building - set UHS 2%/50 years - U1&U2 directions

CHYBA9-TC2	Acceleration amplification			
Distance from the tower base (m)	Loading cases - 2%			
	U1		U2	
	μ	σ	μ	σ
0.00	1.00	0.00	1.00	0.00
6.69	0.90	0.05	0.90	0.11
12.52	0.76	0.12	0.93	0.23
17.52	0.70	0.19	1.35	0.39
20.02	0.91	0.21	1.75	0.49
22.02	1.16	0.21	2.17	0.57
24.02	1.43	0.20	2.66	0.63
26.02	1.78	0.20	3.24	0.71
28.02	2.16	0.22	3.86	0.81
30.00	2.55	0.24	4.50	0.90

Table E-13 Acceleration amplification along the TC2 tower mounted on the CHYBA9 building - set UHS 10%/50 years - U1

CHYBA9-TC2	Acceleration amplification									
Distance from the tower base (m)	Loading cases - 10% - U1									
	1	2	3	4	5	6	7	8	9	10
0.00	1.00	1.00	1.00	1.00	1.00	1.00	1.00	1.00	1.00	1.00
6.69	0.89	0.94	0.90	0.95	0.96	0.92	0.90	0.92	0.82	0.90
12.52	0.69	0.83	0.88	0.84	0.81	0.81	0.72	0.77	0.69	0.67
17.52	0.39	0.59	0.83	0.59	0.97	0.77	0.62	0.80	0.59	0.67
20.02	0.50	0.85	1.02	0.79	1.16	0.99	0.82	1.13	0.89	0.85
22.02	0.76	1.12	1.31	1.07	1.47	1.34	1.08	1.55	1.27	1.08
24.02	1.03	1.48	1.58	1.36	1.79	1.70	1.35	1.99	1.67	1.34
26.02	1.40	1.87	1.96	1.67	2.18	2.10	1.63	2.45	2.10	1.64
28.02	1.77	2.26	2.38	2.03	2.58	2.50	1.91	2.92	2.54	1.94
30.00	2.14	2.64	2.79	2.39	2.97	2.90	2.19	3.38	2.97	2.23

Table E-14 Acceleration amplification along the TC2 tower mounted on the CHYBA9 building - set UHS 10%/50 years - U2

CHYBA9-TC2	Acceleration amplification									
Distance from the tower base (m)	Loading cases - 10% - U2									
	1	2	3	4	5	6	7	8	9	10
0.00	1.00	1.00	1.00	1.00	1.00	1.00	1.00	1.00	1.00	1.00
6.69	0.79	0.78	0.93	0.90	0.82	0.83	0.83	0.80	0.78	0.79
12.52	0.65	0.56	0.83	1.02	0.70	0.74	0.96	0.88	0.54	0.90
17.52	0.68	0.74	1.39	1.23	1.15	0.98	1.25	1.29	1.05	1.59
20.02	0.98	1.04	1.96	1.65	1.45	1.43	1.70	1.80	1.49	2.14
22.02	1.33	1.32	2.46	2.03	1.86	1.82	2.16	2.24	1.91	2.63
24.02	1.70	1.64	3.03	2.39	2.40	2.22	2.72	2.71	2.36	3.16
26.02	2.09	1.99	3.66	2.98	2.97	2.62	3.30	3.20	2.84	3.74
28.02	2.47	2.49	4.31	3.67	3.56	3.03	3.90	3.70	3.34	4.35
30.00	2.84	2.97	4.96	4.34	4.14	3.46	4.49	4.23	3.84	4.95

Table E-15 Average values and standard deviations of acceleration amplification along the TC2 tower mounted on the CHYBA9 building - set UHS 10%/50 years - U1&U2 directions

CHYBA9-TC2	Acceleration amplification			
Distance from the tower base (m)	Loading cases - 10%			
	U1		U2	
	μ	σ	μ	σ
0.00	1.00	0.00	1.00	0.00
6.69	0.91	0.04	0.83	0.05
12.52	0.77	0.07	0.78	0.17
17.52	0.68	0.16	1.13	0.28
20.02	0.90	0.19	1.56	0.37
22.02	1.20	0.23	1.98	0.43
24.02	1.53	0.28	2.43	0.50
26.02	1.90	0.32	2.94	0.59
28.02	2.28	0.36	3.48	0.66
30.00	2.66	0.41	4.02	0.74

Table E-16 Acceleration amplification along the TC2 tower mounted on the CHYBA9 building - set UHS 50%/50 years - U1

CHYBA9-TC2	Acceleration amplification									
Distance from the tower base (m)	Loading cases - 50 % - U1									
	1	2	3	4	5	6	7	8	9	10
0.00	1.00	1.00	1.00	1.00	1.00	1.00	1.00	1.00	1.00	1.00
6.69	0.93	0.79	0.87	0.99	0.83	0.85	0.90	0.92	0.82	0.90
12.52	0.71	0.78	0.64	0.82	0.52	0.68	0.72	0.77	0.69	0.67
17.52	0.45	0.78	0.77	0.76	0.42	0.66	0.62	0.80	0.59	0.67
20.02	0.67	1.00	0.87	1.05	0.49	0.83	0.82	1.13	0.89	0.85
22.02	0.93	1.38	0.91	1.31	0.68	1.08	1.08	1.55	1.27	1.08
24.02	1.22	1.78	1.19	1.61	0.95	1.48	1.35	1.99	1.67	1.34
26.02	1.57	2.20	1.49	1.95	1.24	1.96	1.63	2.45	2.10	1.64
28.02	1.95	2.62	1.79	2.42	1.57	2.45	1.91	2.92	2.54	1.94
30.00	2.33	3.09	2.14	2.92	1.91	2.94	2.19	3.38	2.97	2.23

Table E-17 Acceleration amplification along the TC2 tower mounted on the CHYBA9 building - set UHS 50%/50 years - U2

CHYBA9-TC2	Acceleration amplification									
Distance from the tower base (m)	Loading cases - 50% - U2									
	1	2	3	4	5	6	7	8	9	10
0.00	1.00	1.00	1.00	1.00	1.00	1.00	1.00	1.00	1.00	1.00
6.69	1.06	0.87	0.90	0.95	1.13	1.13	0.75	0.89	0.70	0.85
12.52	0.94	1.28	0.87	0.81	0.96	1.24	0.71	0.96	0.63	0.77
17.52	1.31	2.35	1.11	1.30	1.75	2.06	1.25	1.80	1.53	1.59
20.02	1.71	3.05	1.58	1.83	2.46	2.75	1.67	2.54	2.12	2.20
22.02	2.14	3.67	1.98	2.27	3.05	3.35	2.04	3.18	2.62	2.73
24.02	2.59	4.34	2.43	2.70	3.56	3.89	2.42	3.85	3.15	3.30
26.02	3.01	5.17	2.96	3.12	3.99	4.56	2.90	4.53	3.70	3.90
28.02	3.52	6.02	3.48	3.61	4.37	5.37	3.42	5.21	4.29	4.56
30.00	4.08	6.87	4.00	4.17	5.12	6.24	3.95	5.89	4.87	5.21

Table E-18 Average values and standard deviations of acceleration amplification along the TC2 tower mounted on the CHYBA9 building - set UHS 50%/50 years - U1&U2 directions

CHYBA9-TC2	Acceleration amplification			
Distance from the tower base (m)	Loading cases - 50%			
	U1		U2	
	μ	σ	μ	σ
0.00	1.00	0.00	1.00	0.00
6.69	0.88	0.06	0.92	0.14
12.52	0.70	0.08	0.92	0.21
17.52	0.65	0.13	1.61	0.39
20.02	0.86	0.18	2.19	0.50
22.02	1.13	0.25	2.70	0.59
24.02	1.46	0.31	3.22	0.68
26.02	1.82	0.37	3.78	0.79
28.02	2.21	0.43	4.38	0.91
30.00	2.61	0.50	5.04	1.03

Table E-19 Acceleration amplification along the TC3 tower mounted on the CHYBA9 building - set high a/v - U1

CHYBA9-TC3	Acceleration amplification													
Distance from the tower base (m)	Loading cases - high a/v - U1													
	1	2	3	4	5	6	7	8	9	10	11	12	13	14
0.00	1.00	1.00	1.00	1.00	1.00	1.00	1.00	1.00	1.00	1.00	1.00	1.00	1.00	1.00
6.69	1.87	1.91	2.35	2.03	1.69	1.82	2.09	1.63	1.51	1.26	1.26	2.21	1.60	1.77
12.52	3.52	3.27	4.70	3.50	3.01	3.18	4.10	2.99	3.43	2.30	2.30	4.11	2.86	3.20
17.52	5.26	4.78	7.15	5.15	4.47	4.61	6.43	4.43	5.71	3.50	3.50	6.15	4.16	4.74
20.00	6.15	5.58	8.40	6.00	5.30	5.35	7.64	5.16	6.88	4.12	4.12	7.19	4.83	5.60

Table E-20 Acceleration amplification along the TC3 tower mounted on the CHYBA9 building - set high a/v - U2

CHYBA9-TC3	Acceleration amplification													
Distance from the tower base (m)	Loading cases - high a/v - U2													
	1	2	3	4	5	6	7	8	9	10	11	12	13	14
0.00	1.00	1.00	1.00	1.00	1.00	1.00	1.00	1.00	1.00	1.00	1.00	1.00	1.00	1.00
6.69	1.58	1.36	1.54	1.38	1.58	1.49	1.46	1.37	1.51	1.40	1.40	1.51	1.51	1.58
12.52	2.63	1.95	2.74	1.99	2.49	2.22	2.67	2.14	2.94	1.92	1.92	2.35	2.34	2.38
17.52	3.74	2.59	4.16	2.62	3.44	2.96	4.10	2.95	4.55	2.92	2.92	3.25	3.32	3.50
20.00	4.31	2.91	4.89	2.94	3.92	3.37	4.83	3.36	5.37	3.43	3.43	3.71	3.87	4.07

Table E-21 Average values and standard deviations of acceleration amplification along the TC3 tower mounted on the CHYBA9 building - set high a/v - U1&U2 directions

CHYBA9-TC3	Acceleration amplification			
Distance from the tower base (m)	Loading cases - High a/v			
	U1		U2	
	μ	σ	μ	σ
0.00	1.00	0.00	1.00	0.00
6.69	1.78	0.32	1.48	0.08
12.52	3.32	0.66	2.34	0.33
17.52	5.00	1.06	3.36	0.60
20.00	5.88	1.27	3.89	0.74

Table E-22 Acceleration amplification along the TC2 tower mounted on the CHYBA9 building - set medium a/v - U1

CHYBA9-TC3	Acceleration amplification														
Distance from the tower base (m)	Loading cases - medium a/v - U1														
	1	2	3	4	5	6	7	8	9	10	11	12	13	14	15
0.00	1.00	1.00	1.00	1.00	1.00	1.00	1.00	1.00	1.00	1.00	1.00	1.00	1.00	1.00	1.00
6.69	1.58	1.97	1.84	2.17	1.48	1.84	1.77	1.73	2.33	1.72	1.72	1.73	1.75	1.43	1.54
12.52	2.67	3.69	3.28	3.87	2.50	3.22	2.97	2.93	4.46	2.82	2.82	3.13	3.32	2.47	2.45
17.52	4.02	5.69	5.09	5.74	3.79	4.76	4.29	4.19	6.81	3.99	3.99	4.81	5.02	3.65	3.41
20.00	4.71	6.71	6.04	6.70	4.45	5.55	4.96	4.83	8.02	4.59	4.59	5.66	5.89	4.26	3.95

Table E-23 Acceleration amplification along the TC3 tower mounted on the CHYBA9 building - set medium a/v - U2

CHYBA9-TC3	Acceleration amplification														
Distance from the tower base (m)	Loading cases - medium a/v - U2														
	1	2	3	4	5	6	7	8	9	10	11	12	13	14	15
0.00	1.00	1.00	1.00	1.00	1.00	1.00	1.00	1.00	1.00	1.00	1.00	1.00	1.00	1.00	1.00
6.69	1.59	1.55	1.34	1.39	1.31	1.52	1.48	1.10	1.50	1.27	1.27	1.54	1.60	1.31	1.17
12.52	2.55	2.47	2.14	2.02	1.99	2.38	2.19	1.53	2.27	1.77	1.77	2.58	2.57	1.92	1.67
17.52	3.57	3.55	3.11	2.83	2.75	3.27	2.93	2.30	3.09	2.32	2.32	3.76	3.60	2.60	2.26
20.00	4.08	4.14	3.61	3.25	3.14	3.73	3.30	2.69	3.50	2.60	2.60	4.36	4.12	2.95	2.57

Table E-24 Average values and standard deviations of acceleration amplification along the TC3 tower mounted on the CHYBA9 building - set medium a/v - U1&U2 directions

CHYBA9-TC3	Acceleration amplification			
Distance from the tower base (m)	Loading cases - medium a/v			
	U1		U2	
	μ	σ	μ	σ
0.00	1.00	0.00	1.00	0.00
6.69	1.77	0.24	1.40	0.16
12.52	3.11	0.56	2.12	0.35
17.52	4.62	0.93	2.95	0.52
20.00	5.39	1.12	3.38	0.62

Table E-25 Acceleration amplification along the TC3 tower mounted on the CHYBA9 building - set low a/v - U1

CHYBA9-TC3	Acceleration amplification														
Distance from the tower base (m)	Loading cases - low a/v - U1														
	1	2	3	4	5	6	7	8	9	10	11	12	13	14	15
0.00	1.00	1.00	1.00	1.00	1.00	1.00	1.00	1.00	1.00	1.00	1.00	1.00	1.00	1.00	1.00
6.69	1.81	1.61	2.06	2.31	1.85	1.94	1.68	1.87	1.97	1.75	1.75	1.73	1.67	1.68	1.84
12.52	3.06	2.77	3.61	4.43	3.09	3.30	2.66	3.11	3.53	3.20	3.20	2.87	2.74	2.69	3.17
17.52	4.38	3.96	5.35	6.64	4.40	4.74	3.70	4.44	5.28	4.73	4.73	4.22	3.87	3.87	4.56
20.00	5.05	4.56	6.24	7.77	5.07	5.47	4.23	5.12	6.17	5.51	5.51	4.91	4.51	4.54	5.28

Table E-26 Acceleration amplification along the TC3 tower mounted on the CHYBA9 building - set low a/v - U2

CHYBA9-TC3	Acceleration amplification														
Distance from the tower base (m)	Loading cases - low a/v - U2														
	1	2	3	4	5	6	7	8	9	10	11	12	13	14	15
0.00	1.00	1.00	1.00	1.00	1.00	1.00	1.00	1.00	1.00	1.00	1.00	1.00	1.00	1.00	1.00
6.69	1.49	1.33	1.45	1.33	1.30	1.26	1.33	1.44	1.32	1.44	1.44	1.19	1.26	1.34	1.37
12.52	2.54	1.86	2.38	1.95	1.98	1.90	1.95	2.37	2.13	2.27	2.27	1.85	1.72	1.85	1.95
17.52	3.61	2.50	3.46	2.74	2.73	2.57	2.66	3.62	2.96	3.20	3.20	2.57	2.28	2.45	2.60
20.00	4.18	2.84	4.02	3.19	3.12	2.92	3.04	4.25	3.39	3.67	3.67	2.93	2.56	2.78	3.01

Table E-27 Average values and standard deviations of acceleration amplification along the TC3 tower mounted on the CHYBA9 building - set low a/v - U1&U2 directions

CHYBA9-TC3	Acceleration amplification			
Distance from the tower base (m)	Loading cases - low a/v			
	U1		U2	
	μ	σ	μ	σ
0.00	1.00	0.00	1.00	0.00
6.69	1.83	0.18	1.35	0.08
12.52	3.16	0.45	2.06	0.24
17.52	4.59	0.75	2.88	0.44
20.00	5.33	0.89	3.30	0.53

Table E-28 Acceleration amplification along the TC3 tower mounted on the CHYBA9 building - set UHS 2%/50 years - U1

CHYBA9-TC3	Acceleration amplification									
Distance from the tower base (m)	Loading cases - 2% - U1									
	1	2	3	4	5	6	7	8	9	10
0.00	1.00	1.00	1.00	1.00	1.00	1.00	1.00	1.00	1.00	1.00
6.69	1.64	2.20	1.84	1.85	1.87	2.03	1.89	2.06	1.98	2.30
12.52	2.77	4.04	3.65	3.41	3.17	3.65	3.47	3.68	3.54	3.98
17.52	4.10	6.05	5.35	4.98	4.53	5.15	5.23	5.40	5.76	5.93
20.00	4.78	7.09	6.38	5.77	5.24	6.08	6.18	6.28	6.91	7.04

Table E-29 Acceleration amplification along the TC3 tower mounted on the CHYBA9 building - set UHS 2%/50 years - U2

CHYBA9-TC3	Acceleration amplification									
Distance from the tower base (m)	Loading cases - 2% - U2									
	1	2	3	4	5	6	7	8	9	10
0.00	1.00	1.00	1.00	1.00	1.00	1.00	1.00	1.00	1.00	1.00
6.69	1.58	1.61	1.38	1.38	1.57	1.29	1.41	1.37	1.37	1.43
12.52	2.67	2.60	2.34	2.43	2.43	2.18	2.30	2.19	1.92	2.17
17.52	3.85	3.64	3.37	3.82	3.24	3.17	3.19	3.19	2.63	2.93
20.00	4.50	4.27	4.00	4.53	3.74	3.76	3.62	3.70	2.98	3.31

Table E-30 Average values and standard deviations of acceleration amplification along the TC3 tower mounted on the CHYBA9 building - set UHS 2%/50 years - U1&U2

CHYBA9-TC3	Acceleration amplification			
Distance from the tower base (m)	Loading cases - 2%			
	U1		U2	
	μ	σ	μ	σ
0.00	1.00	0.00	1.00	0.00
6.69	1.97	0.19	1.46	0.13
12.52	3.57	0.43	2.34	0.23
17.52	5.29	0.69	3.31	0.35
20.00	6.23	0.85	3.83	0.45

Table E-31 Acceleration amplification along the TC3 tower mounted on the CHYBA9 building - set UHS 10%/50 years - U1

CHYBA9-TC3	Acceleration amplification									
Distance from the tower base (m)	Loading cases - 10% - U1									
	1	2	3	4	5	6	7	8	9	10
0.00	1.00	1.00	1.00	1.00	1.00	1.00	1.00	1.00	1.00	1.00
6.69	1.77	2.17	1.43	1.85	1.65	1.65	1.92	2.06	1.54	1.56
12.52	3.19	3.81	2.27	3.41	3.19	3.19	3.25	3.62	2.58	2.90
17.52	4.71	5.40	3.52	4.98	4.71	4.71	4.65	5.48	3.79	4.43
20.00	5.49	6.49	4.19	5.77	5.46	5.46	5.37	6.51	4.44	5.21

Table E-32 Acceleration amplification along the TC3 tower mounted on the CHYBA9 building - set UHS 10%/50years - U2

CHYBA9-TC3	Acceleration amplification									
Distance from the tower base (m)	Loading cases - 10% - U2									
	1	2	3	4	5	6	7	8	9	10
0.00	1.00	1.00	1.00	1.00	1.00	1.00	1.00	1.00	1.00	1.00
6.69	1.32	1.21	1.38	1.39	1.44	1.24	1.41	1.26	1.46	1.48
12.52	1.98	1.98	2.34	2.43	2.14	1.84	2.17	1.76	2.27	2.40
17.52	2.71	2.77	3.37	3.82	2.94	2.74	3.10	2.43	3.09	3.46
20.00	3.14	3.14	4.00	4.53	3.36	3.21	3.59	2.81	3.50	4.00

Table E-33 Average values and standard deviations of acceleration amplification along the TC3 tower mounted on the CHYBA9 building - set UHS 10%/50 years - U1&U2 directions

CHYBA9-TC3	Acceleration amplification			
Distance from the tower base (m)	Loading cases - 10%			
	U1		U2	
	μ	σ	μ	σ
0.00	1.00	0.00	1.00	0.00
6.69	1.76	0.24	1.36	0.10
12.52	3.14	0.46	2.13	0.23
17.52	4.64	0.62	3.04	0.41
20.00	5.44	0.74	3.53	0.52

Table E-34 Acceleration amplification along the TC3 tower mounted on the CHYBA9 building - set UHS 50%/50 years - U1

CHYBA9-TC3	Acceleration amplification									
Distance from the tower base (m)	Loading cases - 50% - U1									
	1	2	3	4	5	6	7	8	9	10
0.00	1.00	1.00	1.00	1.00	1.00	1.00	1.00	1.00	1.00	1.00
6.69	1.89	1.94	1.80	1.80	1.74	1.79	1.92	2.06	1.54	1.56
12.52	3.16	3.34	3.07	3.07	3.00	3.29	3.25	3.62	2.58	2.90
17.52	4.47	4.86	4.47	4.63	4.36	4.97	4.65	5.48	3.79	4.43
20.00	5.30	5.77	5.34	5.65	5.07	5.88	5.37	6.51	4.44	5.21

Table E-35 Acceleration amplification along the TC3 tower mounted on the CHYBA9 building - set UHS 50%/50 years - U2

CHYBA9-TC3	Acceleration amplification along the tower height									
Tower height from its base (m)	Loading cases - 50% - U2									
	1	2	3	4	5	6	7	8	9	10
0.00	1.00	1.00	1.00	1.00	1.00	1.00	1.00	1.00	1.00	1.00
6.69	1.53	1.44	1.35	1.45	1.58	1.54	1.41	1.26	1.46	1.49
12.52	2.59	2.23	2.18	2.47	2.65	2.59	2.17	1.76	2.27	2.40
17.52	3.75	3.22	3.18	3.75	3.64	3.64	3.10	2.43	3.09	3.46
20.00	4.38	3.88	3.68	4.41	4.11	4.17	3.59	2.81	3.50	4.00

Table E-36 Average values and standard deviations of acceleration amplification along the TC3 tower mounted on the CHYBA9 building - set UHS 50%/50 years - U1&U2 directions

CHYBA9-TC3	Acceleration amplification			
Distance from the tower base (m)	Loading cases - 50%			
	U1		U2	
	μ	σ	μ	σ
0.00	1.00	0.00	1.00	0.00
6.69	1.80	0.16	1.45	0.09
12.52	3.13	0.28	2.33	0.27
17.52	4.61	0.44	3.33	0.41
20.00	5.45	0.55	3.85	0.48

Table E-37 Acceleration amplification along the TC4 tower mounted on the CHYBA9 building - set high a/v - U1

CHYBA9-TC4	Acceleration amplification													
Distance from the tower base (m)	Loading cases - high a/v - U1													
	1	2	3	4	5	6	7	8	9	10	11	12	13	14
0.00	1.00	1.00	1.00	1.00	1.00	1.00	1.00	1.00	1.00	1.00	1.00	1.00	1.00	1.00
2.60	1.06	1.03	1.11	1.06	1.05	1.01	1.16	1.04	1.08	1.04	1.08	1.03	1.01	1.04
5.00	1.05	1.03	1.10	1.06	1.08	1.04	1.15	1.04	1.05	1.04	1.08	1.05	1.03	1.03
7.40	1.04	1.27	0.95	1.17	1.22	1.51	1.04	1.10	1.03	1.07	1.00	1.45	1.06	1.00
10.00	2.31	3.09	2.14	2.34	2.35	2.93	1.66	2.25	1.78	1.47	1.37	3.20	2.20	2.18
12.60	4.55	5.58	4.18	4.19	4.25	5.24	2.94	4.38	3.60	2.59	2.55	5.78	4.25	4.34
15.20	7.15	8.48	6.64	6.40	6.58	8.08	4.76	6.84	5.73	3.92	3.94	8.88	6.74	6.93
17.80	9.91	11.61	9.26	8.78	9.07	11.09	6.69	9.47	8.02	5.32	5.42	12.21	9.40	9.73
20.00	12.71	14.84	11.91	11.18	11.58	14.14	8.63	12.11	10.34	6.74	6.92	15.57	12.09	12.56

Table E-38 Acceleration amplification along the TC3 tower mounted on the CHYBA9 building - set high a/v - U2

CHYBA9-TC4	Acceleration amplification													
Distance from the tower base (m)	Loading cases - set of high a/v - U2													
	1	2	3	4	5	6	7	8	9	10	11	12	13	14
0.00	1.00	1.00	1.00	1.00	1.00	1.00	1.00	1.00	1.00	1.00	1.00	1.00	1.00	1.00
2.60	1.01	1.00	1.01	1.00	1.01	1.01	1.01	1.00	1.00	1.04	1.00	1.01	1.02	1.02
5.00	1.03	1.05	1.02	1.05	1.04	1.04	1.05	1.03	1.03	1.11	1.02	1.02	1.04	1.06
7.40	1.08	1.29	1.07	1.35	1.28	1.16	1.18	1.28	1.26	1.29	1.17	1.19	1.13	1.20
10.00	1.79	1.97	1.52	2.23	2.19	2.00	1.49	2.01	1.92	1.73	1.79	2.19	1.69	1.54
12.60	2.96	2.95	2.61	3.43	3.50	3.19	2.16	2.97	2.80	2.43	2.62	3.75	2.74	2.32
15.20	4.32	4.09	4.04	4.81	5.08	4.58	3.05	4.07	3.82	3.46	3.59	5.56	4.07	3.35
17.80	5.76	5.30	5.55	6.27	6.76	6.06	3.99	5.22	4.93	4.61	4.64	7.48	5.48	4.46
20.00	7.22	6.51	7.07	7.75	8.46	7.56	4.94	6.38	6.18	5.78	5.69	9.42	6.89	5.57

Table E-39 Average values and standard deviations of acceleration amplification along the TC4 tower mounted on the CHYBA9 building - set high a/v - U1&U2 directions

CHYBA9-TC4	Acceleration amplification			
Distance from the tower base (m)	Loading cases - high a/v			
	U1		U2	
	μ	σ	μ	σ
0.00	1.00	0.00	1.00	0.00
2.60	1.06	0.04	1.01	0.01
5.00	1.06	0.03	1.04	0.02
7.40	1.14	0.17	1.21	0.09
10.00	2.23	0.56	1.86	0.25
12.60	4.17	1.00	2.89	0.46
15.20	6.51	1.51	4.14	0.69
17.80	9.00	2.08	5.47	0.95
20.00	11.52	2.65	6.82	1.22

Table E-40 Acceleration amplification along the TC4 tower mounted on the CHYBA9 building - set medium a/v - U1

CHYBA9-TC4	Acceleration amplification														
Distance from the tower base (m)	Loading cases - medium a/v - U1														
	1	2	3	4	5	6	7	8	9	10	11	12	13	14	15
0.00	1.00	1.00	1.00	1.00	1.00	1.00	1.00	1.00	1.00	1.00	1.00	1.00	1.00	1.00	1.00
2.60	1.07	1.04	1.05	1.04	1.04	1.05	1.08	1.07	1.00	1.03	1.04	1.04	1.04	1.05	1.04
5.00	1.06	1.06	1.06	1.05	1.04	1.05	1.07	1.06	1.04	1.05	1.02	1.06	1.04	1.06	1.04
7.40	1.07	1.23	1.35	1.33	1.07	1.28	1.11	1.33	1.37	1.40	1.16	1.18	1.12	1.11	1.10
10.00	1.78	2.99	2.99	2.67	1.78	3.36	2.14	3.48	2.82	2.58	2.66	2.18	1.88	2.06	2.42
12.60	3.44	5.64	5.25	4.79	3.32	6.32	4.01	6.45	5.37	4.42	5.17	3.84	3.48	3.95	4.48
15.20	5.39	8.80	8.09	7.31	5.12	9.75	6.41	9.98	8.34	6.67	8.17	6.05	5.42	6.17	6.89
17.80	7.50	12.18	11.10	10.08	7.03	13.41	8.99	13.80	11.49	9.06	11.36	8.40	7.49	8.53	9.45
20.00	9.64	15.60	14.20	12.88	8.96	17.14	11.60	17.66	14.67	11.48	14.60	10.78	9.57	10.91	12.07

Table E-41 Acceleration amplification along the TC4 tower mounted on the CHYBA9 building - set medium a/v - U2

CHYBA9-TC4	Acceleration amplification														
Distance from the tower base (m)	Loading cases - medium a/v - U2														
	1	2	3	4	5	6	7	8	9	10	11	12	13	14	15
0.00	1.00	1.00	1.00	1.00	1.00	1.00	1.00	1.00	1.00	1.00	1.00	1.00	1.00	1.00	1.00
2.60	1.02	1.00	1.01	1.00	1.00	1.01	1.01	1.01	1.00	1.00	1.00	1.00	1.01	1.00	1.01
5.00	1.03	1.02	1.02	1.04	1.03	1.03	1.03	1.02	1.04	1.03	1.03	1.04	1.03	1.03	1.04
7.40	1.16	1.16	1.19	1.25	1.22	1.28	1.07	1.11	1.26	1.22	1.28	1.28	1.19	1.25	1.16
10.00	1.89	1.79	1.86	1.84	1.73	2.07	1.64	1.46	1.90	1.73	1.98	1.93	1.72	1.85	1.59
12.60	3.02	2.75	2.76	2.74	2.47	3.30	2.66	2.14	2.74	2.62	3.00	2.89	2.61	2.65	2.41
15.20	4.32	4.03	3.81	3.84	3.43	4.72	3.84	2.99	3.80	3.66	4.19	4.01	3.64	3.56	3.33
17.80	5.69	5.40	4.95	5.01	4.44	6.23	5.09	3.89	5.00	4.76	5.44	5.19	4.74	4.54	4.31
20.00	7.08	6.78	6.19	6.19	5.46	7.76	6.35	4.80	6.21	5.88	6.71	6.38	5.84	5.51	5.28

Table E-42 Average values and standard deviations of acceleration amplification along the TC4 tower mounted on the CHYBA9 building - set medium a/v - U1&U2 directions

CHYBA9-TC4	Acceleration amplification			
Distance from the tower base (m)	Loading cases - medium a/v			
	U1		U2	
	μ	σ	μ	σ
0.00	1.00	0.00	1.00	0.00
2.60	1.04	0.02	1.01	0.00
5.00	1.05	0.01	1.03	0.01
7.40	1.21	0.12	1.21	0.06
10.00	2.52	0.55	1.80	0.16
12.60	4.66	1.01	2.72	0.28
15.20	7.24	1.56	3.81	0.42
17.80	9.99	2.15	4.98	0.58
20.00	12.78	2.75	6.16	0.75

Table E-43 Acceleration amplification along the TC4 tower mounted on the CHYBA9 building - set low a/v - U1

CHYBA9-TC4	Acceleration amplification														
Distance from the tower base (m)	Loading cases - low a/v - U1														
	1	2	3	4	5	6	7	8	9	10	11	12	13	14	15
0.00	1.00	1.00	1.00	1.00	1.00	1.00	1.00	1.00	1.00	1.00	1.00	1.00	1.00	1.00	1.00
2.60	1.07	1.03	1.05	1.10	1.06	1.05	1.06	1.05	1.09	1.07	1.04	1.06	1.09	1.00	1.00
5.00	1.03	1.03	1.05	1.09	1.05	1.04	1.05	1.05	1.06	1.06	1.06	1.04	1.08	1.04	1.02
7.40	1.02	1.02	1.28	1.16	1.23	1.20	1.38	1.23	1.19	1.12	1.42	1.05	1.00	1.38	1.22
10.00	2.60	2.51	3.10	2.36	2.89	2.75	3.44	2.89	3.06	2.52	3.00	2.18	1.76	2.86	1.87
12.60	5.12	4.72	5.97	4.15	5.57	4.98	6.49	5.18	5.83	4.55	5.64	3.98	3.21	5.22	3.01
15.20	8.05	7.31	9.43	6.29	8.74	7.63	10.03	7.99	9.15	7.22	8.77	6.23	5.03	8.06	4.32
17.80	11.18	10.08	13.11	8.66	12.12	10.51	13.81	10.99	12.74	10.06	12.10	8.62	6.99	11.07	5.73
20.00	14.33	12.88	16.82	11.16	15.53	13.42	17.62	14.02	16.40	12.93	15.47	11.03	8.98	14.12	7.14

Table E-44 Acceleration amplification along the TC4 tower mounted on the CHYBA9 building - set low a/v - U2

CHYBA9-TC4	Acceleration amplification														
Distance from the tower base (m)	Loading cases - low a/v - U2														
	1	2	3	4	5	6	7	8	9	10	11	12	13	14	15
0.00	1.00	1.00	1.00	1.00	1.00	1.00	1.00	1.00	1.00	1.00	1.00	1.00	1.00	1.00	1.00
2.60	1.00	1.01	1.02	1.00	1.01	1.00	1.01	1.00	1.00	1.01	1.00	1.00	1.01	1.01	1.01
5.00	1.02	1.02	1.03	1.03	1.02	1.04	1.03	1.04	1.05	1.02	1.02	1.03	1.03	1.03	1.03
7.40	1.13	1.21	1.05	1.19	1.11	1.26	1.17	1.44	1.33	1.09	1.15	1.19	1.18	1.12	1.19
10.00	1.92	1.86	1.90	1.64	1.77	1.99	1.73	2.59	2.22	1.53	1.64	1.60	1.68	1.62	1.84
12.60	3.14	2.79	3.29	2.37	2.85	3.07	2.62	4.14	3.69	2.44	2.46	2.29	2.43	2.33	2.85
15.20	4.53	3.86	4.92	3.21	4.16	4.32	3.75	5.93	5.44	3.57	3.41	3.10	3.37	3.15	4.05
17.80	5.98	4.98	6.65	4.09	5.56	5.65	4.96	7.84	7.30	4.78	4.42	3.96	4.41	4.03	5.33
20.00	7.47	6.11	8.39	4.98	6.98	7.00	6.18	9.77	9.18	5.99	5.44	4.83	5.46	4.93	6.62

Table E-45 Average values and standard deviations of acceleration amplification along the TC4 tower mounted on the CHYBA9 building - set low a/v - U1&U2 directions

CHYBA9-TC4	Acceleration amplification			
Distance from the tower base (m)	Loading cases - low a/v			
	U1		U2	
	μ	σ	μ	σ
0.00	1.00	0.00	1.00	0.00
2.60	1.05	0.03	1.01	0.00
5.00	1.05	0.02	1.03	0.01
7.40	1.19	0.13	1.18	0.10
10.00	2.65	0.47	1.81	0.29
12.60	4.91	0.99	2.80	0.58
15.20	7.62	1.60	3.97	0.92
17.80	10.52	2.26	5.21	1.28
20.00	13.46	2.91	6.46	1.65

Table E-46 Acceleration amplification along the TC4 tower mounted on the CHYBA9 building - set UHS 2%/50 years - U1

CHYBA9-TC4	Acceleration amplification									
Distance from the tower base (m)	Loading cases - 2% - U1									
	1	2	3	4	5	6	7	8	9	10
0.00	1.00	1.00	1.00	1.00	1.00	1.00	1.00	1.00	1.00	1.00
2.60	1.07	1.05	1.07	1.06	1.09	1.06	1.04	1.06	1.08	1.10
5.00	1.13	1.05	1.10	1.06	1.09	1.10	1.00	1.08	1.08	1.09
7.40	1.37	1.16	1.14	0.99	1.37	1.27	1.17	1.28	1.50	1.49
10.00	3.02	2.59	2.53	2.11	3.21	2.78	3.09	3.30	3.11	3.31
12.60	5.76	4.95	4.79	3.89	5.72	4.95	5.60	6.49	5.41	6.05
15.20	8.87	7.74	7.78	6.16	8.57	7.35	8.43	10.20	8.08	9.22
17.80	12.23	10.82	11.20	8.75	11.55	9.84	11.59	14.13	10.92	12.60
20.00	15.72	13.94	14.68	11.38	14.63	12.66	14.77	18.09	13.78	16.01

Table E-47 Acceleration amplification along the TC4 tower mounted on the CHYBA9 building - set UHS 2%/50 years - U2

CHYBA9-TC4	Acceleration amplification									
Distance from the tower base (m)	Loading cases - 2% - U2									
	1	2	3	4	5	6	7	8	9	10
0.00	1.00	1.00	1.00	1.00	1.00	1.00	1.00	1.00	1.00	1.00
2.60	0.99	1.04	1.00	0.97	1.01	1.00	1.01	1.00	1.01	0.99
5.00	1.12	1.14	1.07	0.98	1.07	1.03	1.09	1.06	1.06	1.05
7.40	1.41	1.37	1.23	1.27	1.30	1.28	1.40	1.40	1.26	1.38
10.00	2.26	2.19	1.76	2.11	2.34	1.98	2.19	2.44	1.87	2.38
12.60	3.56	3.33	2.53	3.38	3.71	2.96	3.15	3.72	2.85	3.66
15.20	5.18	4.61	3.47	4.80	5.10	4.16	4.14	5.09	4.02	5.09
17.80	6.94	6.12	4.60	6.29	6.94	5.39	5.26	6.69	5.25	6.56
20.00	9.05	7.94	6.05	7.95	8.87	6.73	6.59	8.31	6.52	8.03

Table E-48 Average values and standard deviations of acceleration amplification along the TC4 tower mounted on the CHYBA9 building - set UHS 2%/50 years - U1&U2 directions

CHYBA9-TC4	Acceleration amplification			
Distance from the tower base (m)	Loading cases - 2%			
	U1		U2	
	μ	σ	μ	σ
0.00	1.00	0.00	1.00	0.00
2.60	1.06	0.02	1.00	0.02
5.00	1.08	0.03	1.07	0.05
7.40	1.31	0.17	1.35	0.09
10.00	2.95	0.37	2.18	0.27
12.60	5.38	0.68	3.29	0.47
15.20	8.24	1.01	4.55	0.69
17.80	11.36	1.37	5.99	0.99
20.00	14.57	1.73	7.57	1.29

Table E-49 Acceleration amplification along the TC4 tower mounted on the CHYBA9 building - set UHS 10%/50 years - U1

CHYBA9-TC4	Acceleration amplification									
Distance from the tower base (m)	Loading cases - 10% - U1									
	1	2	3	4	5	6	7	8	9	10
0.00	1.00	1.00	1.00	1.00	1.00	1.00	1.00	1.00	1.00	1.00
2.60	1.04	1.09	1.07	1.06	1.07	1.04	1.06	1.07	1.05	1.07
5.00	1.03	1.13	1.10	1.08	1.06	1.09	1.08	1.05	1.06	1.08
7.40	1.33	1.30	1.14	1.44	1.07	1.41	1.18	1.13	1.33	1.28
10.00	2.71	2.92	2.53	3.03	2.30	2.85	2.29	2.60	2.63	2.89
12.60	5.16	5.69	4.79	5.16	4.25	4.83	4.38	4.88	4.94	5.68
15.20	8.02	8.92	7.78	7.84	6.45	7.30	6.84	7.49	7.62	8.94
17.80	11.10	12.35	11.20	10.66	9.01	10.23	9.52	10.39	10.46	12.42
20.00	14.22	15.83	14.68	13.54	11.62	13.32	12.24	13.42	13.32	15.93

Table E-50 Acceleration amplification along the TC4 tower mounted on the CHYBA9 building - set UHS 10%/50 years - U2

CHYBA9-TC4	Acceleration amplification									
Distance from the tower base (m)	Loading cases - 10%-U2									
	1	2	3	4	5	6	7	8	9	10
0.00	1.00	1.00	1.00	1.00	1.00	1.00	1.00	1.00	1.00	1.00
2.60	1.00	1.02	1.00	0.97	0.99	0.99	1.01	1.01	1.00	1.01
5.00	1.09	1.10	1.07	0.98	0.99	1.04	1.02	1.05	1.06	1.04
7.40	1.23	1.31	1.23	1.27	1.17	1.29	1.29	1.27	1.37	1.24
10.00	2.19	1.87	1.76	2.11	1.86	2.08	2.02	1.88	2.27	1.84
12.60	3.36	2.65	2.53	3.38	2.78	3.11	3.00	2.68	3.52	2.88
15.20	4.50	3.52	3.47	4.80	3.88	4.26	4.22	3.62	4.95	4.07
17.80	5.88	4.41	4.60	6.29	5.01	5.57	5.51	4.63	6.47	5.37
20.00	7.40	5.55	6.05	7.95	6.15	6.95	6.80	5.85	8.01	6.68

Table E-51 Average values and standard deviations of acceleration amplification along the TC4 tower mounted on the CHYBA9 building - set UHS 10%/50 years - U1&U2 directions

CHYBA9-TC4	Acceleration amplification			
Distance from the tower base (m)	Loading cases - 10%			
	U1		U2	
	μ	σ	μ	σ
0.00	1.00	0.00	1.00	0.00
2.60	1.06	0.02	1.00	0.01
5.00	1.07	0.03	1.04	0.04
7.40	1.26	0.13	1.27	0.05
10.00	2.67	0.25	1.99	0.17
12.60	4.98	0.47	2.99	0.34
15.20	7.72	0.79	4.13	0.52
17.80	10.73	1.09	5.37	0.71
20.00	13.81	1.39	6.74	0.85

Table E-52 Acceleration amplification along the TC4 tower mounted on the CHYBA9 building - set UHS 50%/50 years - U1

CHYBA9-TC4	Acceleration amplification									
Distance from the tower base (m)	Loading cases - 50% - U1									
	1	2	3	4	5	6	7	8	9	10
0.00	1.00	1.00	1.00	1.00	1.00	1.00	1.00	1.00	1.00	1.00
2.60	1.05	1.09	1.12	1.02	1.04	1.05	1.06	1.07	1.05	1.07
5.00	1.04	1.08	1.16	1.07	1.06	1.10	1.08	1.05	1.06	1.08
7.40	1.03	1.15	1.24	1.51	1.28	1.37	1.18	1.13	1.33	1.28
10.00	2.29	2.53	2.87	3.55	2.84	2.57	2.29	2.60	2.63	2.89
12.60	4.35	4.78	5.28	6.37	5.08	4.60	4.38	4.88	4.94	5.68
15.20	6.59	7.33	8.09	9.69	7.87	7.07	6.84	7.49	7.62	8.94
17.80	9.29	10.01	11.30	13.67	10.84	9.93	9.52	10.39	10.46	12.42
20.00	12.25	12.85	14.73	17.71	13.84	12.82	12.24	13.42	13.32	15.93

Table E-53 Acceleration amplification along the TC4 tower mounted on the CHYBA9 building - set UHS 50%/50 years - U2

CHYBA9-TC4	Acceleration amplification									
Distance from the tower base (m)	Loading cases - 50% - U2									
	1	2	3	4	5	6	7	8	9	10
0.00	1.00	1.00	1.00	1.00	1.00	1.00	1.00	1.00	1.00	1.00
2.60	0.99	1.02	1.00	1.01	0.99	1.00	1.01	1.01	1.00	1.01
5.00	0.99	1.10	0.99	1.07	1.03	1.00	1.02	1.05	1.06	1.04
7.40	1.13	1.39	1.14	1.30	1.40	1.23	1.29	1.27	1.37	1.24
10.00	1.95	2.11	1.69	2.25	2.64	2.19	2.02	1.88	2.27	1.84
12.60	3.04	2.99	2.55	3.38	4.32	3.40	3.00	2.68	3.52	2.88
15.20	4.42	4.22	3.58	4.56	6.27	4.85	4.22	3.62	4.95	4.07
17.80	6.30	5.62	4.69	5.93	8.37	6.60	5.51	4.63	6.47	5.37
20.00	8.37	7.03	6.04	7.70	10.48	8.52	6.80	5.85	8.01	6.68

Table E-54 Average values and standard deviations of acceleration amplification along the TC4 tower mounted on the CHYBA9 building - set UHS 50%/50 years - U1&U2 directions

CHYBA9-TC4	Acceleration amplification			
Distance from the tower base (m)	Loading cases - 50%			
	U1		U2	
	μ	σ	μ	σ
0.00	1.00	0.00	1.00	0.00
2.60	1.06	0.03	1.00	0.01
5.00	1.08	0.04	1.04	0.04
7.40	1.25	0.14	1.28	0.10
10.00	2.71	0.37	2.08	0.27
12.60	5.03	0.62	3.17	0.51
15.20	7.75	0.96	4.48	0.78
17.80	10.78	1.36	5.95	1.09
20.00	13.91	1.75	7.55	1.38

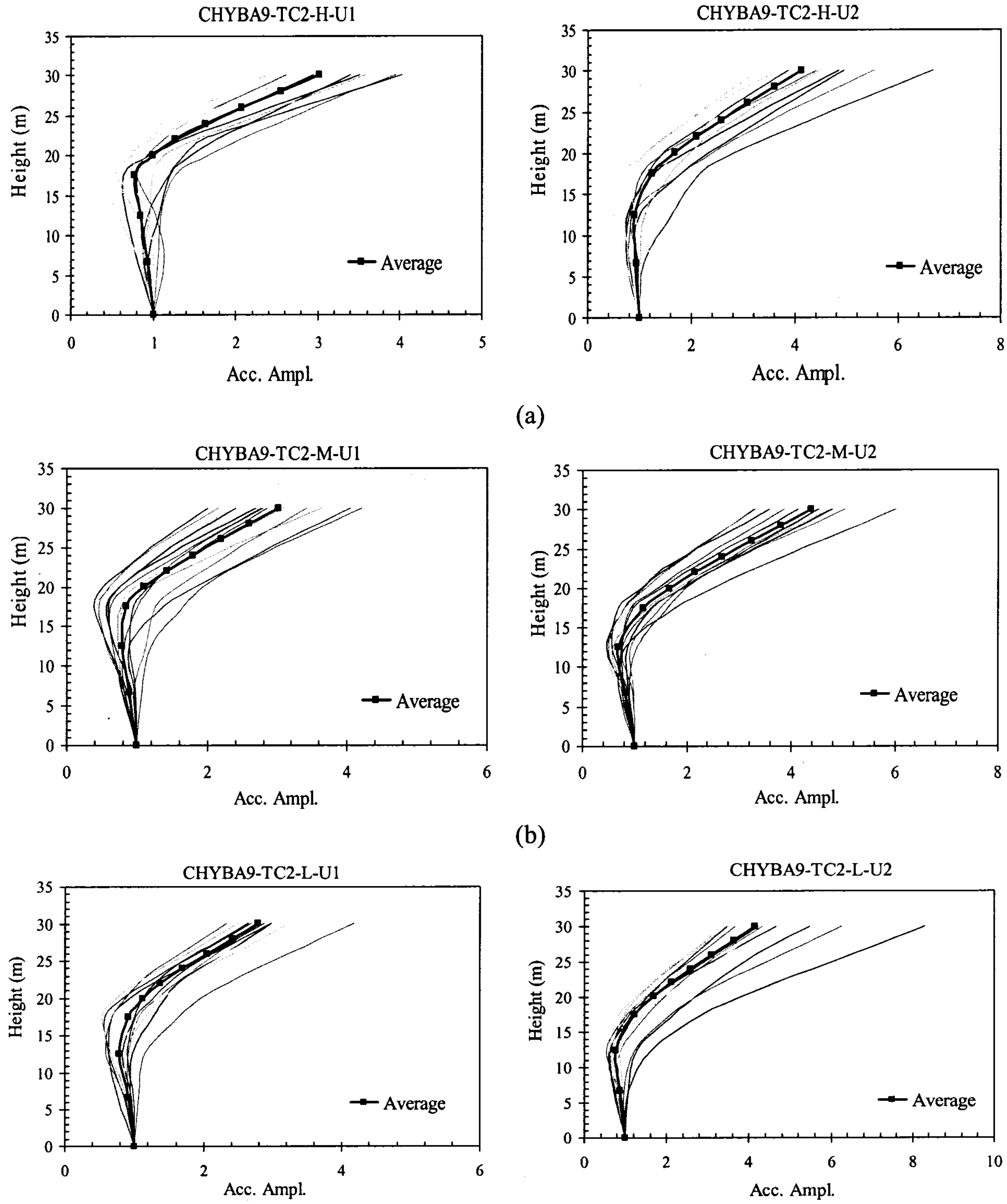

Figure E-1 Acceleration amplification profiles along the TC2 tower mounted on the CHYBA9 building for the sets: (a) high a/v, (b) medium a/v, (c) low a/v

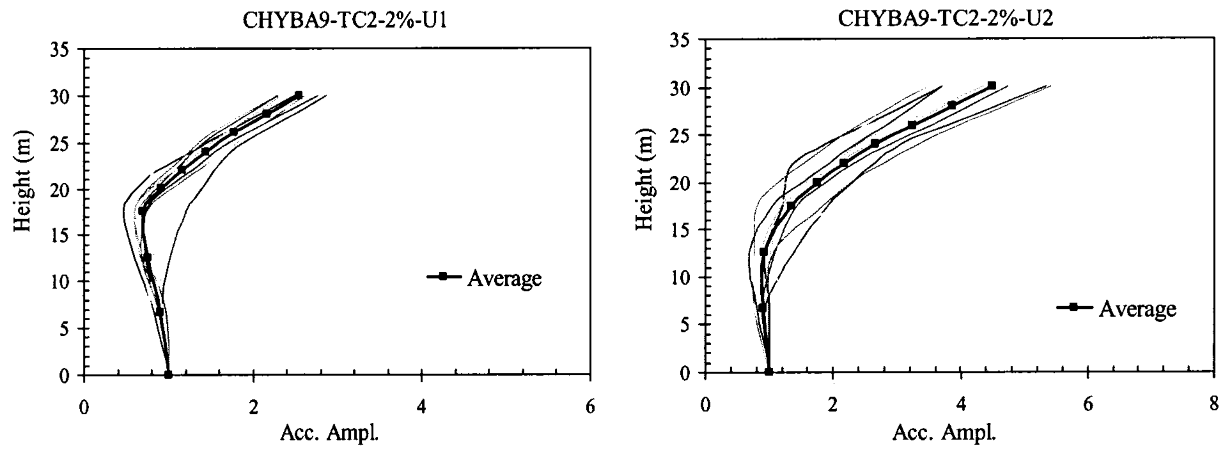

(a)

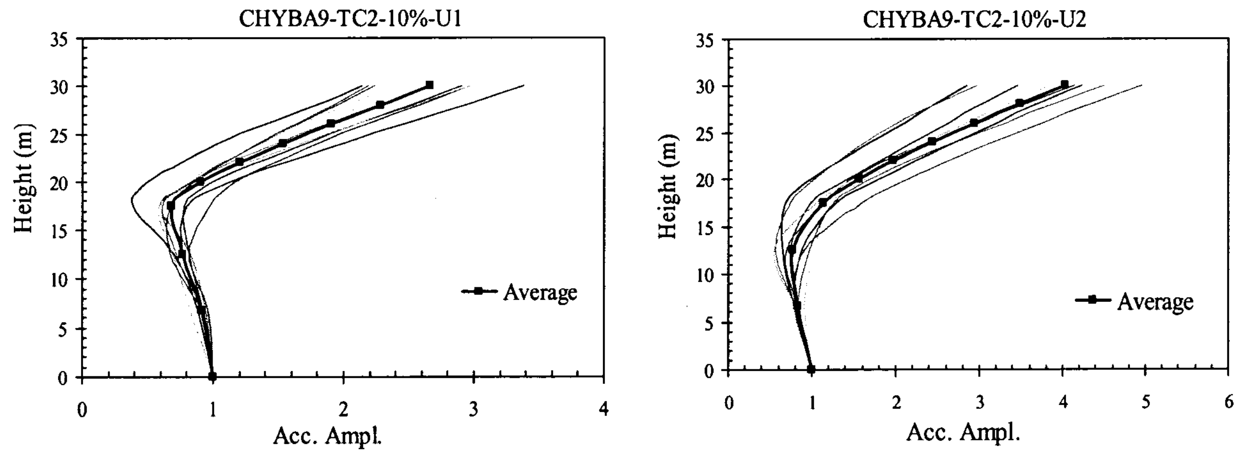

(b)

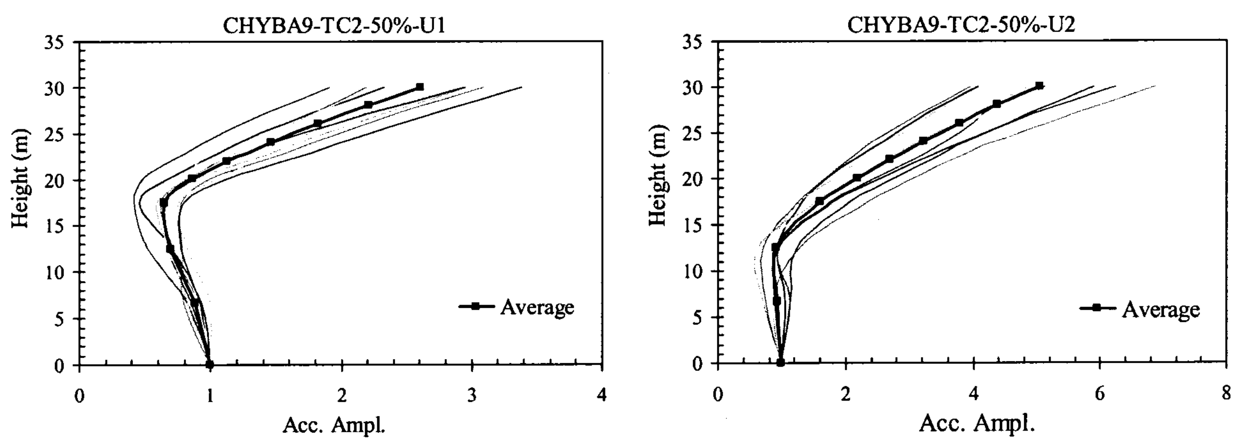

(c)

Figure E-2 Acceleration amplification profiles along the TC2 tower mounted on the CHYBA9 building for the sets: (a) UHS-2%, (b) UHS-10%, (c) UHS-50%

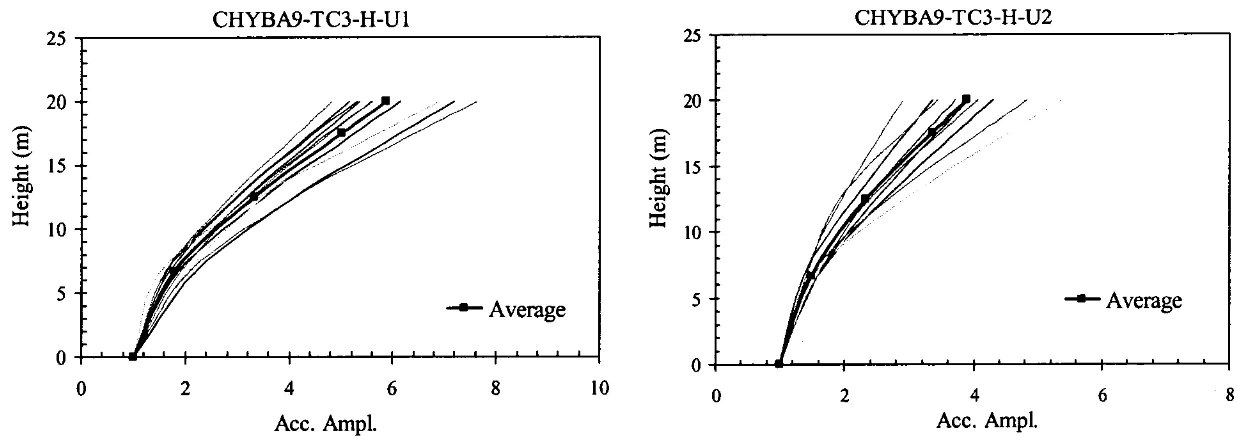

(a)

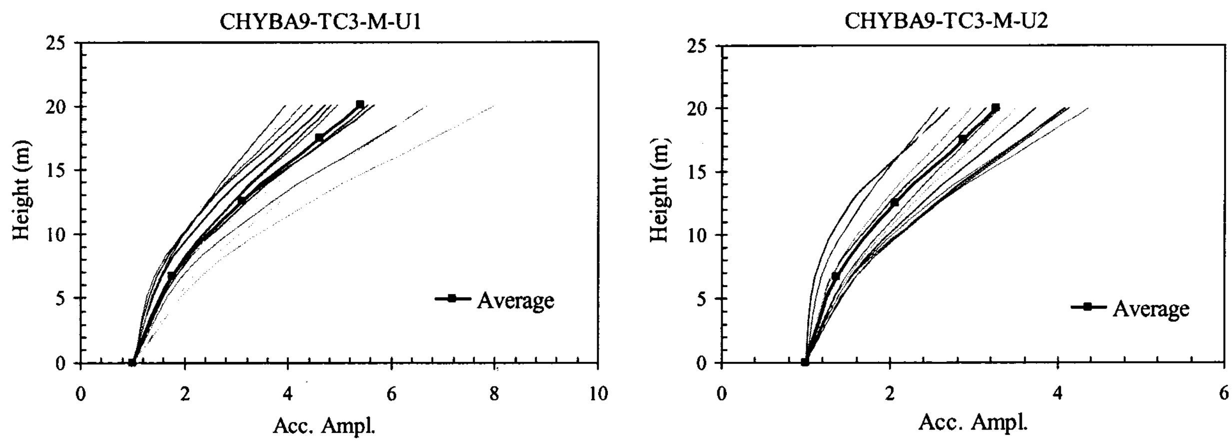

(b)

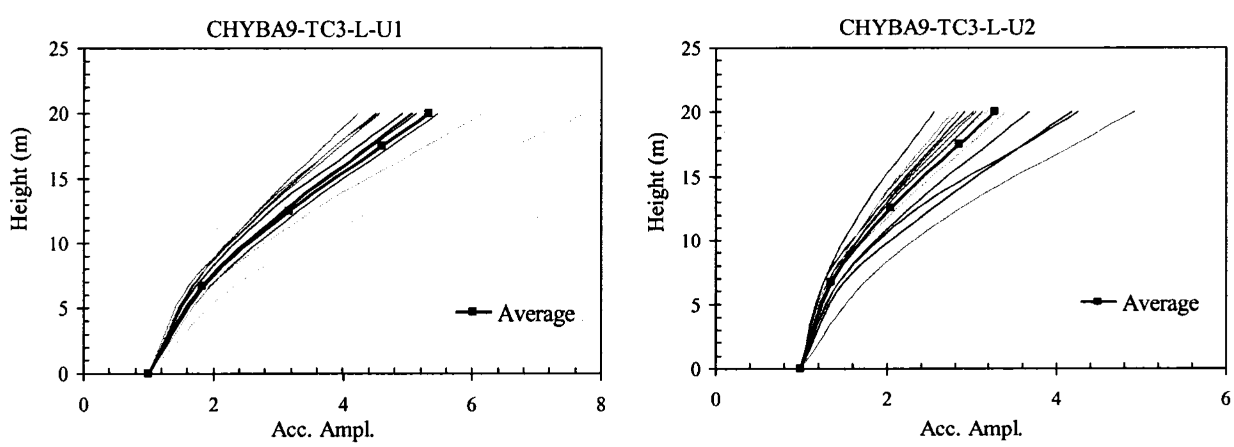

(c)

Figure E-3 Acceleration amplification profiles along the TC3 tower mounted on the CHYBA9 building for the sets: (a) high a/v, (b) medium a/v, (c) low a/v

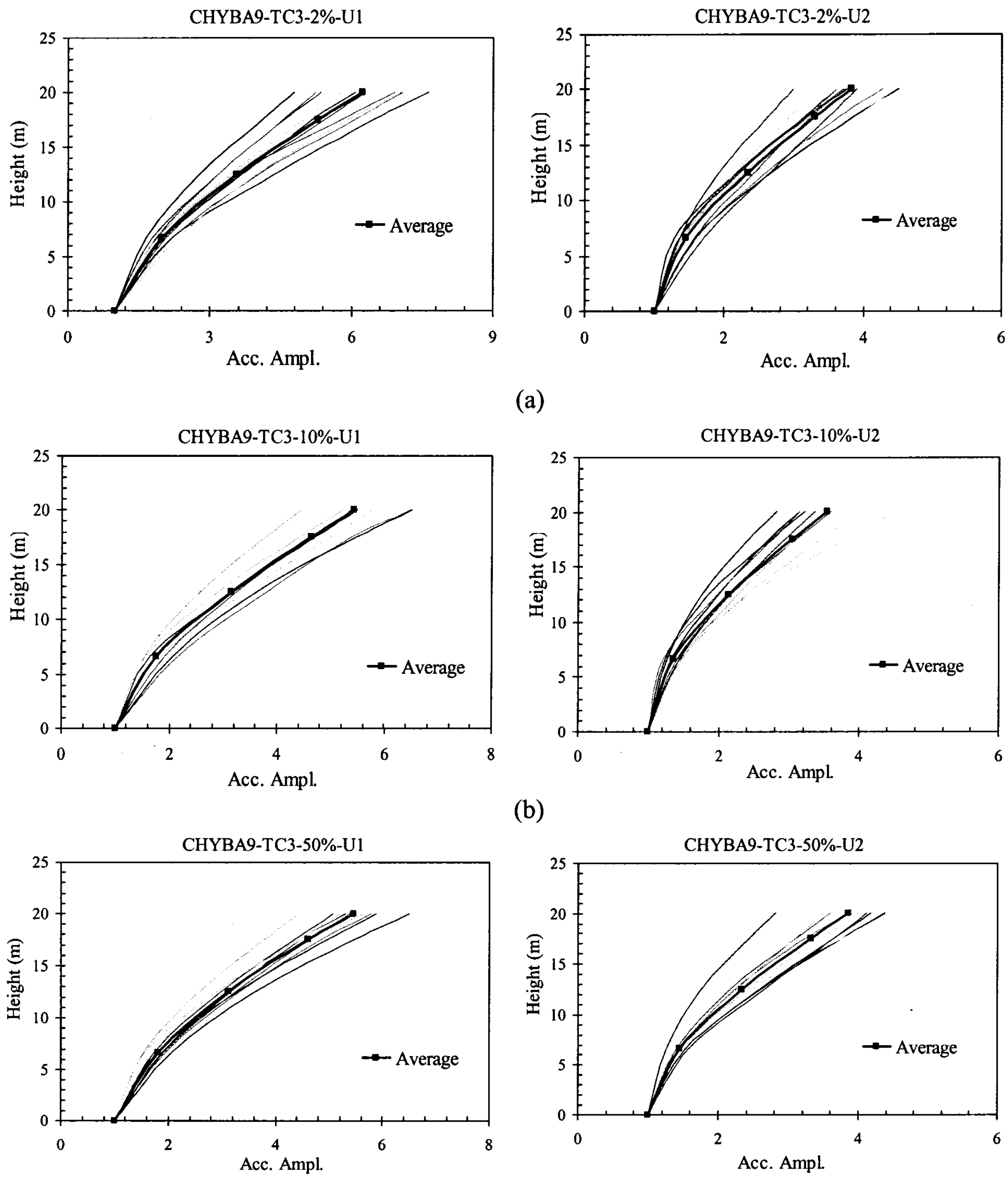

(c)

Figure E-4 Acceleration amplification profiles along the TC3 tower mounted on the CHYBA9 building for the sets: (a) UHS-2%, (b) UHS-10%, (c) UHS-50%

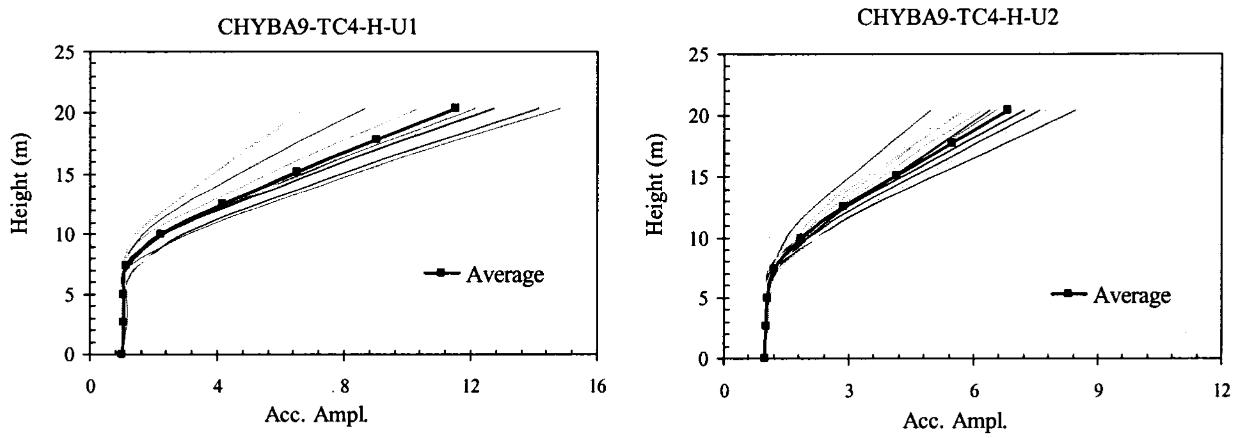

(a)

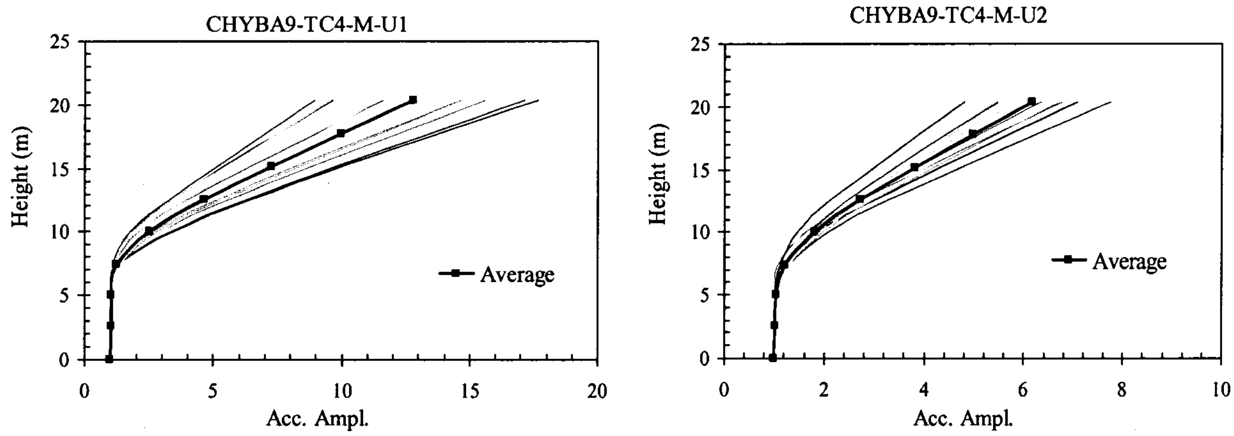

(b)

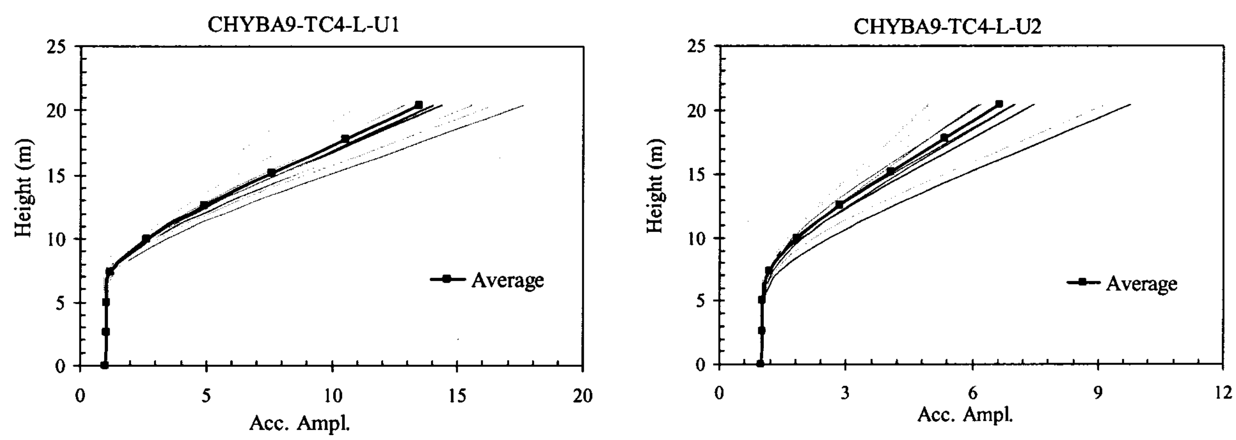

(c)

Figure E-5 Acceleration amplification profiles along the TC4 tower mounted on the CHYBA9 building for the sets: (a) high a/v, (b) medium a/v, (c) low a/v

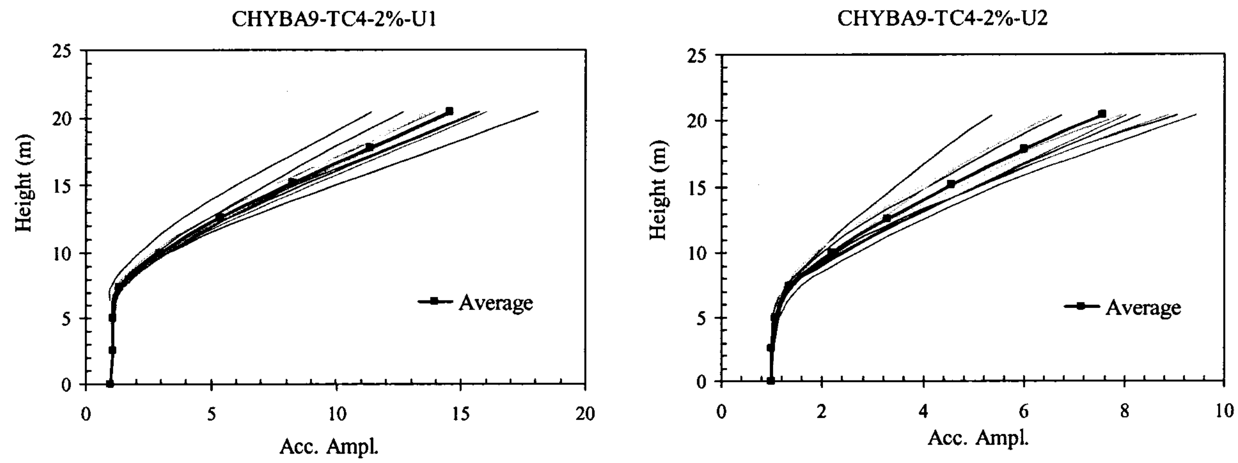

(a)

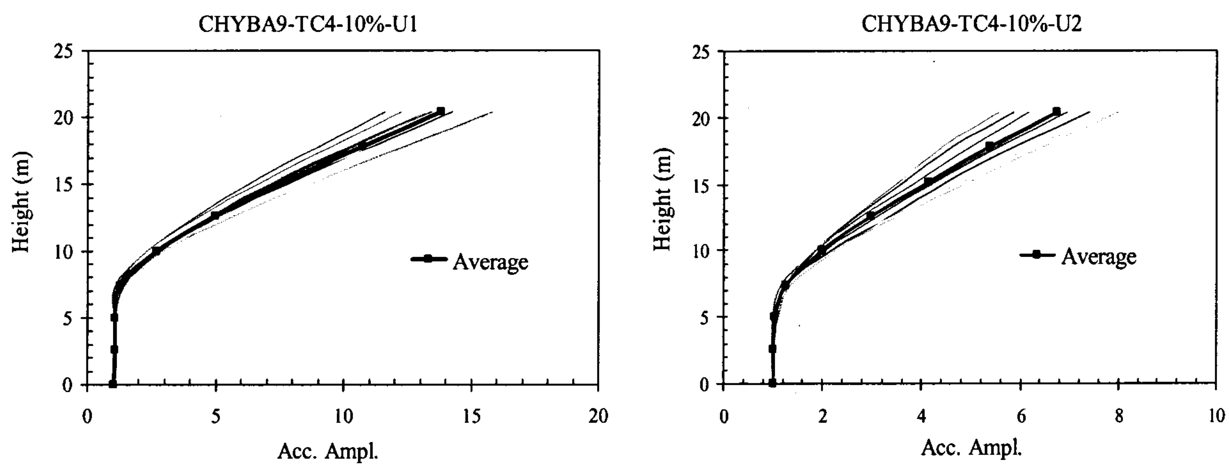

(b)

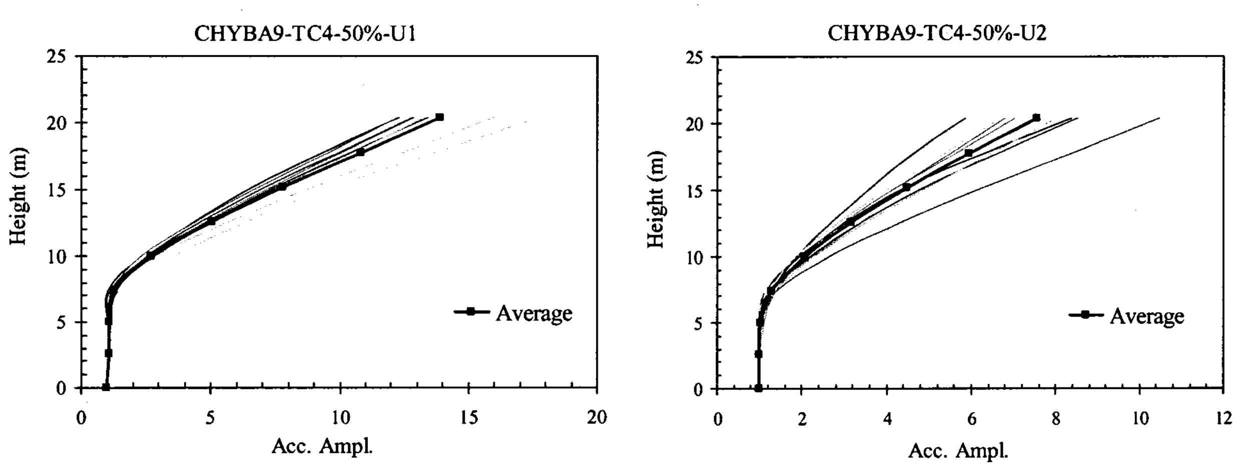

(c)

Figure E-6 Acceleration amplification profiles along the TC4 tower mounted on the CHYBA9 building for the sets: (a) UHS-2%, (b) UHS-10%, (c) UHS-50%